INFORMATION TO USERS

This manuscript has been reproduced from the microfilm master. UMI films the text directly from the original or copy submitted. Thus, some thesis and dissertation copies are in typewriter face, while others may be from any type of computer printer.

The quality of this reproduction is dependent upon the quality of the copy submitted. Broken or indistinct print, colored or poor quality illustrations and photographs, print bleedthrough, substandard margins, and improper alignment can adversely affect reproduction.

In the unlikely event that the author did not send UMI a complete manuscript and there are missing pages, these will be noted. Also, if unauthorized copyright material had to be removed, a note will indicate the deletion.

Oversize materials (e.g., maps, drawings, charts) are reproduced by sectioning the original, beginning at the upper left-hand corner and continuing from left to right in equal sections with small overlaps. Each original is also photographed in one exposure and is included in reduced form at the back of the book.

Photographs included in the original manuscript have been reproduced xerographically in this copy. Higher quality 6" x 9" black and white photographic prints are available for any photographs or illustrations appearing in this copy for an additional charge. Contact UMI directly to order.

UMI®

Bell & Howell Information and Learning
300 North Zeeb Road, Ann Arbor, MI 48106-1346 USA
800-521-0600

ENDOTHELIAL CELL INTERACTIONS WITH MODEL SURFACES: EFFECT OF SURFACE CHEMISTRY, SURFACE MOBILITY, AND THE ADSORBED PROTEIN LAYER

by

Caren Diana Tidwell

A dissertation submitted in partial fulfillment
of the requirements for the degree of

Doctor of Philosophy

University of Washington

1999

Program Authorized to Offer Degree: Bioengineering

Doctoral Dissertation

In presenting this thesis in partial fulfillment of the requirements for the Doctoral degree at the University of Washington, I agree that the Library shall make its copies freely available for inspection. I further agree that extensive copying of the dissertation is allowable only for scholarly purposes, consistent with "fair use" as prescribed in the U.S. Copyright Law. Requests for copying or reproduction of this dissertation may be referred to UMI Dissertation Services, 300 North Zeeb Road, P.O. Box 1346, Ann Arbor, MI 48106-1346, to whom the author has granted "the right to reproduce and sell (a) copies of the manuscript in microform and/or (b) printed copies of the manuscript made from microform."

Signature Karen Diana Tidwell

Date 6/4/99

University of Washington
Graduate School

This is to certify that I have examined this copy of a doctoral dissertation by

Caren Diana Tidwell

and have found that it is complete and satisfactory in all respects,
and that any and all revisions required by the final
examining committee have been made.

Chair of Supervisory Committee:

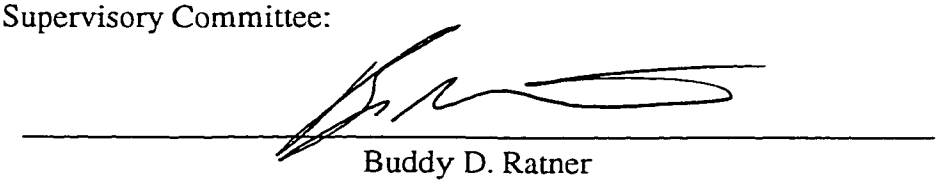

Buddy D. Ratner

Reading Committee:

Buddy D. Ratner

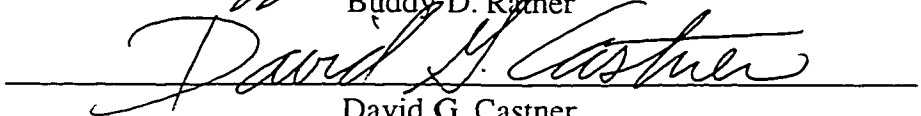

David G. Castner

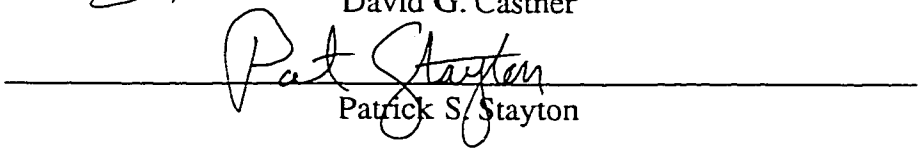

Patrick S. Stayton

Date: June 2, 1999

University of Washington

Abstract

ENDOTHELIAL CELL INTERACTIONS WITH MODEL SURFACES: EFFECT OF SURFACE CHEMISTRY, SURFACE MOBILITY, AND THE ADSORBED PROTEIN LAYER

by Caren Diana Tidwell

Chairperson of the Supervisory Committee: Professor Buddy D. Ratner
Department of Bioengineering

The clinical success of the small diameter vascular graft remains limited due to occlusion resulting from thrombus formation. Methods for promoting graft endothelialization have been investigated to improve graft healing. A common requirement of these methods is a substrate that will promote endothelial cell growth.

The effects of substrate surface properties on bovine aortic endothelial cell (BAEC) growth and protein adsorption were investigated using self-assembled monolayers (SAMs) of alkane thiols on gold. Surface properties studied were surface chemistry (type, concentration, and spatial arrangement of surface chemical functionalities) and surface molecular mobility. Adsorbed protein layers were characterized to determine the composition and binding strength (measured by SDS elutability) of three serum proteins.

BAEC growth varied with surface chemical functionality. BAEC growth was significantly higher on COOH SAMs than on CH_3 or OH-terminated SAMs. BAEC growth on binary composition SAMs varied significantly with functional group concentration. Cell growth increased with increasing COOH content, peaked at 50-60% COOH, then remained constant as COOH content increased. BAEC growth can be controlled by the surface concentration of growth-promoting

functional groups. The effect of functional group arrangement on cell growth was significant in the early phase of cell growth but diminished with increasing culture time. The effect of surface mobility on cell growth was limited.

Adsorbed protein layer composition varied significantly with binary SAM surface composition. Albumin and vitronectin adsorption levels were equivalent and were significantly higher than fibronectin adsorption. The elutability of albumin and fibronectin did not vary consistently with surface COOH content. Vitronectin elutability increased with increasing COOH content, peaked at 50-60% COOH, then remained constant with increasing COOH content. Comparing cell growth results with adsorbed protein layer characteristics, adhesive protein surface fraction (fibronectin and vitronectin) and vitronectin elutability varied with COOH content in a manner similar to cell growth. The promotion of BAEC growth was correlated with increased adhesive protein surface fraction and vitronectin elutability.

In this research, several substrate properties and adsorbed protein layer properties associated with the promotion of endothelial cell growth were identified. This information may aid in the design of implant surfaces that guide a specific biologic response.

TABLE OF CONTENTS

LIST OF FIGURES

LIST OF TABLES

Number *Page*

ACKNOWLEDGMENTS

There are many individuals that I would like to thank and acknowledge for providing me with support, encouragement, and assistance throughout my graduate studies. First, I would like to thank my thesis advisor, Professor Buddy Ratner, for his guidance and support through both my Master's research and my doctoral research. I would like to thank the other members of my supervisory committee, Professor Patrick Stayton, Professor Tom Horbett, Professor David Castner, and Professor Chad Oliver, for their encouragement and support through my studies.

This work represents the result of a wonderful collaborative effort between Battelle Pacific Northwest Laboratories who generously funded a significant portion of the research. My primary collaborator at Battelle was Barbara Tarasevich who provided me with an incredible amount of support, advice, and encouragement throughout this work and I would like to thank her for all that she has given to me over the last 6 years. It was truly a pleasure to collaborate with Barbara and her thesis advisor, Dr. David Allara and I am grateful for their involvement with my research.

The biomaterials group at the UW is a supportive group of students, postdocs, and staff who have provided me with a great deal of assistance during group discussions, in the lab, or during various other projects which I was involved in. There are several individuals in the biomaterials group who have been particularly helpful during my studies. I would like to thank Winston Ciridon for his cheerful assistance in the lab with many, many different projects. I would also like to thank Stephen Golledge and Dan Graham for collaborations on several surface analysis studies. Deborah-Leach Scampavia has provided me with a great deal of assistance, training, and support with surface analysis studies and I am very grateful to her. Many

thanks also go to Ann Schmierer and Laura Martinson for their assistance with the cell growth studies. I would also like to thank Mady Lund, Connie Payton, and Margaret Kramer for their help related to my research and their support during many other collaborative projects.

I have received financial support from several sources during the last 6 years. I would like to acknowledge and thank the following funding sources: Battelle Pacific Northwest Laboratories, the NIH Cardiovascular Training Grant, the NIH NESAC/BIO Grant (RR01296), and the National Science Foundation through the UWEB Engineering Research Center.

Many friends have provided constant support and encouragement during my studies. In particular, I would like to thank Ann Schmierer, Laura Martinson, Deborah Leach-Scampavia, Rita Jensen, Claire Haycox, Lynn Layman-Spillar, Kimberly Burton, and Dean Pettit. I am very thankful for their help and encouragement in all aspects of my life over the past years and feel lucky to have such wonderful friends. My family has also been a tremendous source of support through many long years of study and I am certain that I could not have completed my studies without them. I would like to thank my sister Kimberly Peterson and her husband Gene for their constant support and willingness to help. My parents, Wilfred and Christa Langhammer, have been incredibly supportive of all my efforts and I will always be grateful for all they have done for me. Finally, I would especially like to thank my daughters, Christina and Nicole, and my wonderful husband John, for their tremendous patience and support during these years. They provided me with endless support, encouragement, and love and made it possible for me to achieve this goal.

To John Tidwell

and

in loving memory of

Wilfred Langhammer

1928-1998

Chapter 1

Introduction and Literature Review

1.1 Introduction

The influence of surface phenomena on the biological response to synthetic materials is demonstrated by biochemical, cellular, and clinical responses to biomedical implants. The clinical success of a biomaterial is primarily dependent upon the ability of the surface to promote or inhibit specific protein and cellular responses. While clinically used implant materials are typically designed to achieve specific mechanical and permeability requirements, limited consideration is given to the interfacial reactions between these materials and the physiologic environment because it is not well understood why some biomaterials are, for example blood compatible, and other materials fail following implantation. These problems have been found difficult to solve due to the limited understanding of the fundamental phenomena controlling interfacial biology and the role of the surface in controlling the biological response.

When a biomaterial or biomedical device is placed into the body, a series of biological responses occurs at the surface of the material. The specific sequence of interactions or biological cascade that occurs is largely dependent upon the effect of the surface on the initial response that involves the adsorption of serum or plasma proteins onto the material surface. It is well established that proteins adsorb almost instantaneously onto the biomaterial surface and that the adsorbed protein layer subsequently mediates the biological response with the substrate. It has not yet been completely determined however, how the substrate affects the adsorbed protein layer and how the adsorbed protein layer, in turn, influences the biological response to the substrate. *In vitro* studies of biomaterials and biomedical devices have often yielded conflicting results because the interfaces involved are not well controlled and

characterized. The biocompatibility of many systems, therefore, has not been optimized and the development of new biomaterials has been limited because of an incomplete understanding of the interfacial biological interactions.

The clinical success of the small diameter vascular graft remains limited due to a high incidence of occlusion resulting from thrombus formation in the graft [1]. When endothelial cells, the natural antithrombotic surface contacting the blood in native vessels, are seeded onto synthetic grafts, improved graft healing is observed [2,3]. Therefore, methods for promoting graft endothelialization such as cell seeding at implantation [4], cell culture prior to implantation [5], and graft surface coating with specific plasma proteins [6,7] have been investigated to produce a thromboresistant surface. A common requirement of these methods is believed to be a substrate that will promote endothelial cell attachment and growth.

Anchorage-dependent cells, such as endothelial cells, require adhesion to a substrate in order for growth to occur. In addition, adhesion alone is not sufficient to ensure that cell growth will occur; cell spreading is a critical condition necessary for growth. The ability of polymer surfaces to support the attachment and growth of anchorage dependent cells varies significantly due to differences in polymer substrate properties. The attachment and growth of endothelial cells onto polymeric surfaces have been associated with various surface properties including wettability [8], electronegativity [9], and chemical composition [10,11]. There is evidence that hydrophilic surfaces such as TCPS promote endothelial cell growth but it is not known which features of the substrate promote growth and whether better substrates can be found.

Since plasma proteins rapidly adsorb to synthetic materials in a biological environment, material surface properties affect cellular interactions via the composition, structure, and conformation of the adsorbed protein layer [12-16]. The composition of

the adsorbed protein layer differs from the fluid phase composition, varies significantly with type of substrate, and has been demonstrated to undergo conformational and orientational changes with time [17-19]. Therefore, protein adsorption onto a substrate is important in controlling cellular interactions with synthetic surfaces *in vivo* and also *in vitro*, where serum is added to culture media to sustain cell growth. Few studies have addressed the effect of surface properties on cell behavior as mediated by the protein layer adsorbed from complex solutions such as plasma and serum.

The surface of a biomaterial is well known to influence the biological response. However, there is a limited understanding of the roles of many specific surface properties in controlling protein and cellular interactions with a substrate. Determining relationships between material surface properties and protein and/or cellular responses has been complicated by an inability to systematically control and vary the surface properties of polymer systems typically used in biointeraction studies. The primary objective of the research described in this thesis was to investigate the effect of substrate surface properties on endothelial cell growth as mediated by the adsorbed protein layer. Preliminary evidence suggests that specific surface properties such as chemical functional group concentration, spatial arrangement of surface chemical functionalities, and surface mobility may significantly affect protein and cellular interactions. However, the effects of these surface properties have not been well studied.

In this study, we investigated the roles of two important surface properties, surface chemistry and surface mobility, in serum protein adsorption and endothelial cell growth. The goals of this thesis project were first, to investigate the effects of surface chemistry (specifically functional group concentration and spatial arrangement) and surface mobility on endothelial cell growth using model surfaces composed of terminally functionalized self-assembled monolayers (SAMs) of alkane thiols on gold. Molecular self-assembly allows systematic control of film properties including surface chemistry

and structure. Second, we characterized protein layers adsorbed on homogeneous and heterogeneous SAM surfaces to investigate the effects of surface properties on the composition and binding strength of adsorbed protein layers. The final goal of this study was to establish correlations between surface properties, properties of the adsorbed protein layer, and endothelial cell growth. The central hypothesis of this thesis project is that endothelial cell growth on biomaterial surfaces is influenced by surface chemical composition (specifically functional group concentration and spatial arrangement) and surface molecular motions or surface mobility, as mediated by the adsorbed protein layer.

The study of biological interactions with terminally functionalized SAMs is of relevance towards understanding the effect of surface properties on protein adsorption and how the adsorbed protein layer consequently influences cell growth on biomaterial surfaces. Increased knowledge of how surfaces direct biological processes may lead to strategies for designing materials and implant surfaces that guide a specific biologic response, for example, the promotion or the inhibition of cell growth, therefore permitting more rational design of biomaterials. It is hoped that information gained through this research will allow the development of design strategies that will lead to biomimetic surface chemistries and structures for improved synthetic biomaterials.

1.2 Effect of Polymer Surface Chemistry on Protein Adsorption and Cell Growth

The influence of polymer surface chemistry on cell attachment and growth is demonstrated by the finding that hydrophobic polymers such as polystyrene or Teflon do not support cell attachment unless precoated with an adhesive protein such as Fn or vitronectin (Vn), while hydrophilic tissue culture polystyrene (TCPS) will support cell attachment without precoating with an adhesive serum protein [20,21]. In general,

hydrophobic surfaces, including currently available vascular graft materials such as expanded polytetrafluoroethylene (PTFE), are poor supports for the growth of endothelial cells [12,22] while hydrophilic surfaces are more supportive of cell attachment and growth. Very hydrophilic surfaces (i.e., hydrogels or agarose), however, are not supportive of cell attachment and growth, and maximal cell adhesion has been reported on surfaces of intermediate wettability [12]. Surface wettability, therefore, is not solely predictive of the cell growth characteristics of a substrate.

Surface oxidation has been demonstrated to promote cell adhesion and growth and surface modification by gas plasma (glow discharge) is a common method for fabricating surfaces with oxygen-containing functional groups. TCPS, the most commonly used cell culture substrate, is believed to be fabricated by a radiofrequency plasma modification of polystyrene (PS) which results in the incorporation of oxygen containing groups onto the PS surface. TCPS demonstrates an increased hydrophilicity and increased oxygen content compared with unmodified PS resulting in significantly improved cell attachment and growth characteristics. The improved cell growth characteristics of hydrophilic surfaces such as TCPS have been attributed to oxygen-containing functional groups. However, determination of the specific functionalities involved in cell growth is difficult, and contradictory results have been reported [23]. Surface sulfonate, hydroxyl, and carboxyl groups have all been proposed to promote cell attachment and growth [10,11]. Comparison between studies investigating the role of chemical functionalities in cell attachment and growth is complicated by the use of different cell lines and different cell interaction protocols.

The role of surface chemistry, specifically chemical functional groups, and the effect of adsorbed proteins in promoting endothelial cell growth was investigated by Ertel et al. [22,24,25]. It was observed that BAEC growth on radio-frequency plasma-deposited films increased with surface oxygen content and it was proposed that cell

growth was better correlated with a specific oxygen-containing functionality rather than with total oxygen concentration. A subsequent study demonstrated a correlation between BAEC growth on plasma-deposited films and surface carbonyl concentration but not with surface hydroxyl or carboxyl concentrations.

Surface carboxyl group content has been associated with the improved attachment and growth of various cell lines in several studies [26-28]. Ramsey et al. (Corning Glass Works) concluded that surface oxidation, primarily in the form of surface carboxyl groups, was responsible for improved cell growth and adhesiveness on plasma or oxidant treated hydrocarbon polymers [27]. McAuslan and Johnson studied the effects of introducing carboxyl groups onto poly(hydroxyethyl methacrylate), a hydroxyl-rich surface which does not support cell adherence and growth. Sulfuric acid etched polyHEMA surfaces (carboxyl-rich) supported cell growth at a rate approaching that attained with TCPS [28]. Carboxyl-rich substrates prepared by alkaline hydrolysis of cross-linked PMMA microspheres were found to support the growth of human skin fibroblasts, human heart, and lung cells [26]. Additionally, fibroblasts grown on the carboxyl-rich hydrogel surfaces were comparable to those grown on TCPS in terms of the uptake of ^{14}C amino acids and their incorporation into proteins.

Several groups have provided evidence of the importance of hydroxyl groups in cellular adhesion. Curtis et al., measuring short-term cellular adhesion, demonstrated that surface hydroxyl groups were supportive of cellular adhesion however, very high surface densities of hydroxyl groups diminished adhesion. Carboxyl groups were concluded to play a small role in cell adhesion as cell adhesion was slightly inhibited by surface carboxyl groups [11]. Hydroxylation of the PS surface resulting in increased cell adhesiveness is suggested to be the main feature provided by commercial treatments which renders PS suitable for cell culture. While enhanced cell adhesiveness on

hydroxyl containing surfaces has been reported [11,29], controversy exists as to whether or not the hydroxyl group, while promoting cell attachment, is also involved in enhancing the subsequent spreading and growth of cells. In a recent review, Horbett and Klumb [23] cite numerous studies demonstrating that cell adhesion and growth are not directly related and conclude that while anchorage-dependent cells require substrate attachment for growth to occur, adhesion alone is not sufficient to ensure cell growth. In support of this conclusion, Brandley observed a higher-short term fibroblast adhesion on hydroxyl group-derivatized polyacrylamide gels than on carboxylic-acid derivatized gels, however, carboxylic acid-derivatized surfaces supported more vigorous long-term cell growth than did the hydroxyl derivatized surfaces [29]. Growth of cells on carboxyl-derivatized surfaces resulted in cell attachment, growth, and morphology similar to that on TCPS. Hydroxyl derivatized surfaces supported long-term growth but at a much lower rate and extent. Ertel et al. [22,24] similarly observed the non-specific attachment of BAECs on a variety of oxygen-containing plasma-deposited film surfaces, including untreated PS, which was not necessarily followed by growth. Results of these studies suggest that surface functional groups may play different relative roles in cellular behaviors such as adhesion, growth, differentiation, and mobility.

Since protein adsorption from serum-containing culture medium occurs rapidly rendering direct recognition of the substrate by the cells virtually impossible, surface chemical functionalities are believed to affect cell growth indirectly via the adsorbed protein layer. Therefore, differences observed in cell growth on different surfaces are due to differences in the adsorption of proteins by the polymer surface [19,23]. Polymer surface properties can affect the amounts and types of proteins bound as well as the conformation, orientation, or binding strength of the adsorbed protein. Additionally, for cells which secrete and assemble an extracellular matrix (ECM), such as endothelial cells, polymer surface properties may affect the ability of the cell to

deposit its ECM by stabilizing the protein deposits or by affecting the orientation of cell-binding domains in the deposits [19,23].

Relatively few studies have been performed to investigate the effect of specific surface chemical functionalities on the adsorbed protein layer. Since most conventional polymer systems are chemically complex and contain a variety of chemical functionalities, self-assembled monolayers have more recently been used to investigate relationships between chemical functionality and protein adsorption. Lopez et al. used patterned SAMs of alkanethiols on gold [30] to evaluate the effect of terminal functionality on protein adsorption. Using ellipsometry, no protein adsorption was detected on oligo(ethylene glycol) terminated monolayers. However, CH_3 and COOH-terminated SAMs adsorbed a layer of protein 15-25 Å thick. In a similar study, SAMs containing mixtures of hydrophobic and hydrophilic alkanethiols were observed to adsorb increasing amounts of protein with increasing surface hydrophobicity [31]. Wojciechowski and Brash [32] observed higher levels of albumin (Alb) adsorption to a methyl-terminated silanized quartz surface than on unmodified quartz surface, which showed the lowest Alb affinity of any surface, tested. The hydroxyl groups present on quartz were believed to be associated with the low Alb affinity of this surface.

1.3 Effect of Polymer Surface Mobility on Protein Adsorption and Cell Growth

In general, polymer structures and properties are time and temperature dependent and therefore, can exhibit a variety of molecular motions and relaxations under normal conditions and in response to changing environments [33]. Transition and relaxation phenomena occurring in solid polymers, such as the glass transition, have significant effects on the physical and mechanical behavior of the polymer. In addition to polymer bulk relaxations and transitions, there is considerable evidence that polymer molecules

and segments at surfaces and interfaces also demonstrate motions and relaxations. Mobility of the polymer surface permits the interface to restructure or reorient in response to different environments. Polymer surface reorientation is especially pronounced in aqueous solutions where the polarity of the aqueous phase results in a high interfacial free energy driving force for the orientation of polar blocks, segments, or side chains of the polymer towards the aqueous phase in an attempt to minimize the interfacial free energy. In air and other nonpolar environments, the polymer will orient its apolar components toward the interface again in attempt to minimize the interfacial free energy.

The polymer structures responsible for the dynamic nature of the polymer surface range from blocks or domains to side chain functional groups. Molecular motions occurring along a polymer molecule can be defined in terms of primary molecular motions, such as large scale, main (backbone) motions, and of secondary molecular motions corresponding to the motion of pendant side chain groups [34]. The type and degree of molecular motions occurring in a polymer will be influenced by a number of factors including molecular weight, degree of crosslinking, crystallinity, chemical structure, steric factors, and other molecular parameters.

The role of side chain mobility in polymer surface dynamics and the effect of surface motions due to mobile side chains on protein and cellular interactions have received very limited attention. Merrill originally proposed that molecular motions at the blood-material interface might influence the initial deposition of plasma proteins [35]. He compared motions of the polymeric side chains to "a field of flowers blown by the wind" with flowers representing the side chains. Barenberg was one of the first to investigate the effects of restricted and unrestricted secondary molecular motion on the initial deposition of plasma proteins and cellular elements [34]. These studies concluded that there was a correlation between macromolecular motions and the initial adsorption

of blood elements and ultimately, thrombogenicity for the block copolymer system evaluated. In a subsequent study, Reichert and Barenberg evaluated the effect and interrelationship between primary (segmental backbone) and secondary (side chain) molecular motions on thrombogenesis, independent of morphological order, crystallinity, and/or associated water using a polyphosphazene (PNF) polymer [36]. When PNF side chain motions were restricted or partially restricted by irradiation, a substantial reduction in thrombus accumulation was observed relative to untreated control surfaces. The initial adsorption of plasma proteins and/or cellular elements onto the surface of the PNF polymers was mediated in part by the relative degrees of surface molecular mobility associated with the pendant fluoro side chains.

Maroudas proposed that the mechanical rigidity of a substrate might be a factor affecting cellular attachment [37,38]. It was suggested that rigid substrates are needed for cell attachment and that polymer chains that are stiff, on a molecular scale, would provide the required rigidity. Horbett investigated mouse 3T3 cell growth rates on a series of HEMA-EMA copolymers and observed a pronounced increase in cell growth rates at 30-50% EMA concentration [39]. It was proposed that the material parameter most likely to cause the significant increase in cell growth was surface chain mobility. Horbett suggested that HEMA chains in aqueous media would be flexible and would be a poor cell attachment substrate, while the stiffer EMA chains could form a good attachment substrate as proposed by Maroudas. The dividing point between good cell growth polymers and poor growth polymers was speculated to occur at the concentration of EMA units in the copolymer at which the stiff EMA chains would interfere with the mobility of the HEMA chains. Other factors including surface energetics, surface chemistry, and associated water were also noted as possibly having an effect on the observed cell growth results.

Numerous studies have demonstrated the ability of poly(ethylene oxide) (PEO) surfaces to resist the adsorption of plasma proteins and subsequent cellular adhesion [33,40]. The hydrophilicity and solubility properties of PEO results in surfaces that are in a liquid-like state with the polymer chain demonstrating significant flexibility or mobility [33]. Nagaoka et al. investigated the effects of PEO chain length on the adhesion of platelets and the adsorption of plasma proteins and observed a significant decrease in platelet adhesion and protein adsorption with increasing chain length [41]. Two mechanisms were proposed to account for the observed effect of the long PEO chain on the adsorption of blood components. First, it was suggested that the hydrated, long PEO chains on the surface of the hydrogel might exclude other hydrated biological polymers (such as plasma proteins or adhesive polysaccharide on the cell membrane of platelets) due to a volume restriction effect. The volume restriction effect is due to a repulsive force that is generated by the loss of possible chain conformations, as the volume available to the adsorbed chains is reduced between approaching surfaces. Secondly, it was proposed that the high mobility of the PEO surface chains prohibited blood component adsorption. It was thought that the rapid movements of the hydrated chains did not allow sufficient contact time between the blood components and the hydrogel surface, thereby suppressing adhesion.

Several studies have subsequently implicated surface mobility as an important parameter affecting protein adsorption and cellular interaction with biomaterials. In an evaluation of a series of plasma deposited (RFGD) films which exhibit low molecular mobility, Yeh et al. observed increased blood compatibility (as indicated by decreased platelet consumption) in baboon A-V shunt experiments [42]. Van Damme et al. investigated protein adsorption to a series of alkyl methacrylates with variable surface group mobility [43]. The most hydrophobic surface showed low levels of protein adsorption due to its ability to reorient after aqueous contact. In our laboratories, Lopez

and Ratner evaluated a series of plasma-deposited and model HEMA surfaces and observed decreased fibrinogen adsorption on surfaces with increased mobility [44].

1.4 Probing Polymer Surface Dynamics

Relatively few methods are available to probe interfacial motions or polymer surface dynamics. Polymer surface motions are not readily detectable by classical measurement of advancing contact angle or by other surface analysis techniques which primarily probe the solid-vacuum or solid-air interface. The most directly useful method for investigating polymer surface dynamics is the time-dependent Wilhelmy plate method for measuring contact angle dynamics and hysteresis [45]. In this method, the contact angle is not measured directly but is deduced from a force measurement as a function of the immersion depth in the liquid. The solid can either be immersed or emersed from the liquid to determine either the advancing contact angle of a liquid on a surface (Θ_A) or the receding contact angle (Θ_R). For many polymer systems, it is commonly observed that the contact angle deduced on immersion (advancing contact angle) is different from the contact angle calculated on emersion (receding contact angle). The difference between the advancing and receding contact angle is commonly called contact angle hysteresis. For an ideal system which meets all of the assumptions in classical contact angle experiments, the advancing and receding contact angle will be nearly identical and little or no hysteresis is observed. For most polymeric surfaces however, hysteretic behavior is observed [46].

There are two main classes of contact angle hysteresis: 1) thermodynamic hysteresis which results in stable, reproducible hysteresis loops that are independent of time and frequency; and 2) kinetic hysteresis which results in changes in the hysteresis curves which change as a function of rate measurement. Causes of thermodynamic

hysteresis include surface roughness and surface chemical heterogeneities. Surface roughness does not significantly contribute to hysteresis if surface asperities are in the range of 0.1-0.5 μ or below. The contribution of surface chemical heterogeneities to hysteresis is negligible for patches less than 0.1 μ in size [33].

Kinetic hysteresis can be caused by several factors including surface mobility and reorientation, surface deformation and/or penetration and swelling of the test surface by the liquid. Surface deformation has been demonstrated to cause only slight effects on hysteresis even on highly deformable polymers such as hydrogels [33]. Chen et al. recently studied molecular mechanisms associated with adhesion and contact angle hysteresis of monolayer surfaces [47]. Their findings questioned the traditional view that hysteresis is due to surface roughness effects or chemical heterogeneities and suggested that hysteresis effects were primarily due to molecular and segmental rearrangements. Reorientation of mobile hydrophilic or hydrophobic surface groups or segments at the polymer-water interface is a well-known cause of contact angle hysteresis [33]. In the case of mobile hydrophilic polymer surface groups that undergo reorientation, the advancing angle is measured on the surface with the hydrophilic groups directed inwards. During contact with water, the hydrophilic groups reorient to the aqueous phase to minimize interfacial free energy. During measurement of the receding contact angle, the altered, more hydrophilic surface is probed resulting in a lower receding contact angle. The hysteresis observed is considered to be indicative of short time scale surface transitions.

Other methods that are useful for measuring polymer surface dynamics include interfacial fluorescence and nuclear magnetic resonance (NMR) methods. A variety of fluorescent probes are available which are sensitive to various interfacial parameters such as pH, polarity, and interfacial motion. By covalently immobilizing a probe at the

substrate surface and monitoring the time course of fluorescence emission, stop-flow kinetic experiments can be performed to directly measure surface relaxation processes. Difficulties with this technique include low sensitivity and quenching [45].

NMR techniques provide the most direct information regarding surface mobility and dynamics. Pulsed Fourier transform ^{13}C methods with proton decoupling allow determination of spin-lattice (T1) and spin-spin (T2) relaxation times that permit conclusions regarding polymer surface chain and segment mobility [45,48]. However, high surface area particulate systems are typically required to obtain sufficient sensitivity. Therefore, to use NMR to measure relaxation times of surfaces, model systems with a high surface-to-volume must be developed. Nagaoka et al. evaluated the mobility of hydrogels containing methoxy poly(ethylene glycol) monomethacrylates with poly (oxyethylene) side chains of various chain lengths. Using proton decoupled ^{13}C NMR with small pieces of the hydrogel materials [41], POE chain mobility was evaluated by measuring the line width (T2) of the POE peak that was observed to decrease with increasing surface chain mobility.

Static SIMS is being applied to investigate a number of aspects of polymer and organic surface mobility in our laboratories. Static SIMS is particularly useful for the characterization of organic and polymeric surfaces due to its extremely high analytical sensitivity and ability to provide molecular information about substrate chemistry. With a sampling depth of approximately 10-15 Å, static SIMS allows investigation of the region of a polymer where interfacial interactions occur. Static SIMS analysis results in charged fragments that relate directly to specific molecular units comprising the surface region therefore providing a unique set of information useful for characterizing the surface.

The potential for static SIMS to probe molecular mobility was suggested by quadrupole SIMS studies of two crosslinked systems which demonstrated that polymer

crosslink density leads to changes in SIMS peak intensity ratios. In a study of conventionally prepared and RF plasma-deposited poly(2-hydroxyethyl methacrylate) films, it was observed in the negative ion SIMS that the total ion intensity and the ratio of molecular to atomic ions decreased significantly as the extent of molecular damage to the deposited film was increased [44]. Chilkoti and Ratner investigated the ability of SIMS to interrogate surface crosslinking using crosslinked gels of poly(2-hydroxyethyl methacrylate)(PHEMA) as model surfaces. The gels were characterized by swelling measurements to estimate the molecular weight of chains between crosslinks [49]. It was found that in the negative ion SIMS, the total ion intensity, and more significantly, the ratio of molecular ions to atomic ions, fell off sharply (by over an order of magnitude for total ion intensity) as crosslink density was increased.

In both of these studies, it was hypothesized that increasing crosslink density lead to the decreased intensity of the molecular ions relative to the atomic species. However, increased crosslink density also corresponds to reduced mobility for polymer chain segments. Ratner suggests that if mobility is important for the fragmentation process occurring on polymer surface during the SIMS analysis, especially where large segments of the surface need to be ejected to observe intact molecular units, perhaps SIMS can be used to empirically assess molecular mobility [50]. A number of polymeric and organic systems are currently being investigated by Ratner and Castner to relate crosslink density and mobility to static SIMS emission. The goal of these studies is to prove that increasing surface chain mobility results in an increase in total secondary ion yield and an increase in the ratio of the peak intensities of molecular ions to atomic ions.

1.5 Influence of the Adsorbed Protein Layer on Cell-Substrate Interactions

Upon exposure of a biomaterial to a physiologic environment, proteins and ions from the surrounding fluid phase rapidly adsorb to the material. The adsorbed protein layer influences subsequent cellular interactions with the biomaterial surface by mediating the response through the adsorbed protein-material interface. The chemical and morphological nature of the biomaterial surface directs the protein adsorption and the biological responses occurring in proximity to it. The nature of the rapidly adsorbed protein layer observed on all materials immersed in biological fluids might be the critical determinant dictating the success or failure of medical implants. Adsorbed proteins can retain a structure close to that in solution or may conformationally adjust in response to local environments.

Plasma and serum contain several proteins that have been demonstrated to facilitate cell attachment, spreading and growth such as Fn, Vn, von Willebrand factor, and thrombospondin. Serum and plasma also contain factors which act to decrease or prevent cell attachment either by blocking access of the cell to an adsorbed adhesive protein or, by competing with the adhesive protein for binding sites on the polymer surface. Cell attachment and growth is most likely directly affected by the balance of adhesion promoting versus the adhesion inhibiting proteins which adsorb to a surface [23]. In support of this, Steele demonstrated that cellular attachment to TCPS was dependent upon cell adhesive components of serum (Fn and Vn) overcoming the nonadhesive effect of other serum components [20].

The role of Fn in cell attachment, spreading, and growth is incompletely defined. Fn was initially identified as the serum protein primarily responsible for cell attachment and spreading during cell culture [8,51-54], however, contradictory results demonstrating poor correlations between Fn adsorption and cell attachment and growth

have been reported [20,21,25]. The decreased influence of Fn on cell attachment and growth is attributed to the adsorption behavior of Fn at serum concentrations used during typical cell culture conditions (i.e., 5-30% serum). When Fn is adsorbed from serum or plasma, a maximum, or Vroman peak, in adsorption is observed at a serum concentration of 0.1%, in contrast with Fn adsorption behavior from a single protein solution [55] and the behavior of other key cell adhesion proteins such as Vn which do not demonstrate a Vroman peak [19]. The adsorption of serum Fn to many surfaces decreases significantly or is completely blocked by other competing serum components such as Vn or Alb at serum concentrations greater than 1% [20]. Fn adsorption onto TCPS has been observed to be reduced by more than 90% in the presence of serum concentrations above 2%. Therefore, the amount of Fn that typically adsorbs onto surfaces at the serum concentrations typically used in cell culture (5-30%) is considered suboptimal or insufficient for cell attachment.

The relative importance of Fn in cell adhesion and growth has been demonstrated to be dependent upon substrate composition and cell type [55]. For oxygen-containing plasma surfaces such as TCPS, Steele [21] concluded that serum Fn was less important than Vn for initial attachment of fibroblasts and EC to TCPS and that Fn does not play an essential role in initial cell attachment. However, TCPS has been shown to adsorb more Fn from serum than does PS and it has been suggested that the increased Fn adsorption by TCPS contributes to the enhanced cell attachment and spreading observed on TCPS compared with PS [21].

While the amount of serum Fn adsorbed to a surface may not directly influence cellular interactions with a surface, several studies have suggested that the affinity of a substrate for Fn may be an important factor in the promotion of cellular attachment and growth. Following initial attachment and spreading, endothelial cells will secrete ECM components such as cellular Fn or collagen onto the substrate, which enhance cell

spreading and growth. Horbett [23] suggests that since anchorage-dependent cells will attempt to produce an ECM similar to that in vivo, the role of the substrate is to promote or at least not interfere with the formation of the ECM and that substrate properties which promote ECM matrix formation will most likely be good cell growth substrates. It has been proposed that substrates exhibiting a high affinity for Fn promote cell spreading and growth by permitting the deposition of cellular Fn onto the substrate surface [56,57]. Van Wachem demonstrated that TCPS adsorbed more Fn from dilute and undiluted serum medium than did hydrophobic polymers [12]. The enhanced adsorption of Fn onto TCPS is thought to be indicative of an increased affinity of TCPS for Fn and it has been suggested that the increased affinity of TCPS for Fn in the presence of other serum proteins, compared with other surfaces such as PS may promote cell attachment and growth by permitting or encouraging cellular deposition of endogenous Fn onto the polymer surface [56,57]. In support of this, endothelial cells deposit Fn onto TCPS as early as 30 minutes after seeding [58], but not onto PS [52]. The retraction and rounding up of EC on PS after 6 hours of spreading has been attributed to the inability of cells on PS to deposit cellular Fn.

Recent reports point to Vn, not Fn, as the critical adhesive protein mediating cellular interactions with polymer surfaces [20,21,58]. The depletion of Vn from 10% serum was shown to be more effective in reducing the spreading and attachment of cells on TCPS than was the depletion of Fn from serum [20]. The dominant effect of Vn on cell attachment and spreading compared with Fn is attributed to the adsorption behavior of these proteins at serum or plasma concentrations used during typical cell culture conditions (i.e., 5-30% serum). Fn adsorption displays a maximum in adsorption at intermediate serum dilutions (0.1%), therefore low amounts of Fn are observed to adsorb at serum concentrations used in cell culture. In contrast, Vn adsorption from serum does not exhibit a Vroman peak; instead, adsorption increases with increasing

plasma concentration. Therefore, Vn adsorption to surfaces at high serum concentrations (>1%) is typically significantly greater than Fn adsorption. A 28-fold increase in adsorbed surface Vn compared with adsorbed Fn was observed on TCPS exposed to 10% serum [20].

Serum also contains several proteins that have been demonstrated to decrease or inhibit cell attachment and growth such as Alb, IgG, alpha-1-antitrypsin, HDL, or alpha-2-macroglobulin [21]. Decreased attachment and spreading of several types of cells to TCPS was observed when serum containing culture medium was depleted of Fn and Vn [20]. The nonadhesive effect of the Vn and Fn depleted serum was thought to be due to "blocking" of protein binding sites by nonadhesive serum proteins. While the nonadhesive serum factors were not isolated, similar decreases in cell attachment were obtained by purified serum Alb. Since Alb comprises approximately 50% of the protein content of bovine serum, it could be expected to significantly contribute to the nonadhesive effect of serum [20]. Alb adsorption by a surface however, does not necessarily correlate with inhibition of cell growth. Vascular endothelial cells have also been observed to grow on TCPS surfaces preadsorbed with Alb by depositing relatively large amounts of cell derived Fn on the substrates in the process of conditioning it for growth [54]. Chinn observed similar amounts of Alb adsorption from 10% serum to poor growth surfaces as to surfaces that promoted growth [59]. Similarly, van Wachem [12] found that surfaces that promoted cell growth, such as TCPS, adsorbed more Alb and IgG from 10% serum than did poor growth substrates such as PET or fluorinated ethylene propylene polymers. Oxygen-rich plasma deposited surfaces that were found to promote cell growth, bound similar amounts of Alb and IgG from 10% serum as did surfaces that did not support cell growth [25].

While the type and amount of protein adsorbed on a substrate has been demonstrated to influence cell spreading and growth, the biological activity of the

adsorbed protein layer may have a more significant impact on cellular interactions with a substrate than does the composition of the protein layer. Numerous studies indicate that the ability of an adsorbed adhesion protein to influence cellular interactions is dependent on and modulated by the substrate on which the protein is adsorbed. Modulation of the biological activity of adsorbed proteins by the substrate may result from differences in conformation or orientation of the adsorbed protein which can affect the availability and potency of cell binding domains [19]. Studies suggest that proteins adsorbed to solid substrates undergo conformational changes in an attempt to minimize system energy. This typically includes a transition from a reversibly adsorbed state to a more tightly held state in which the protein is not completely denatured, but differs from its solution form [19].

Variations in the biological activity of adsorbed proteins may also be related to differences in the binding strength of an adsorbed protein which can affect cellular interactions with the protein or additionally, can affect the ability of an adsorbed protein to be displaced by other proteins [23]. Pettit demonstrated a good correlation between tightness of Fn binding (measured by resistance to elution with SDS) and epithelial cell outgrowth rates suggesting that variations in the biological activity of adsorbed Fn may be related to the resistance of Fn to removal by the cells [60]. It was concluded that one of the principal ways by which substrate properties influence cell behavior may be by affecting the binding strength of adhesion proteins which in turn modulates the ability of the protein to interact with cells. Ertel similarly observed a correlation between tightness of Alb and IgG binding and increased cell growth on oxygen-rich plasma deposited films [25]. The more tightly adsorbed protein layer on the oxygen-rich surfaces was thought to provide a more stable support for cell attachment and growth. The Alb and IgG bound to the oxygen-rich substrates was not displaceable by Fn and Fn adsorption to the oxygen-rich substrates preadsorbed with Alb or IgG was higher than on the

oxygen-poor substrates. Horbett suggests that the observation of Fn binding despite the presence of tightly bound Alb or IgG was possibly due to partial or complete denaturation of the adsorbed Alb or IgG which then allowed non-specific adsorption of the Fn onto the denatured protein layer [23]. It is suggested that surfaces which allow the initial tight binding of passivating proteins will be conditioned by further deposition by serum or cell-derived proteins to allow cell attachment, spreading and/or growth.

While some studies suggest that tight protein binding may be conducive to cell attachment and growth, other studies suggest that tight protein binding may not be desirable. Tight binding of a protein to a surface may indicate that conformational or orientational changes have taken place (i.e., partial denaturing of protein) during or after adsorption. Tightly bound proteins are also more resistant to displacement by serum or cell-derived proteins. It has been proposed that the role of the substrate is to promote cellular ECM formation. Thus, the substrate needs to provide sufficient amounts of serum-derived adsorbed adhesion factors to facilitate initial cell adhesion which subsequently allows the cell to deposit its own ECM [23,61]. In order for the substrate to facilitate ECM deposition by the cells, proteins initially adsorbed to the substrate from serum must be held loosely to allow displacement by cell-derived Fn. Also, cell deposited ECM materials must bind reasonably tightly to the substrate so that they are not easily exchanged for other proteins present in the culture medium [12]. Ertel has suggested [24] that the retraction and rounding up of EC on PS following an initial 6 hour period of spreading may result from tight binding of serum proteins on the hydrophobic PS surface preventing deposition of cell secreted proteins or their exchange with surface bound proteins. Van Wachem et al. demonstrated that HEC are able to deposit cellular Fn onto TCPS and concluded that the high affinity of TCPS for Fn and the nature of the adsorbed serum protein layer permits cells to deposit their own Fn onto the polymer surface [56]. Steele [21] similarly suggested that cell growth differences

observed on TCPS and PS may not be necessarily due to a difference in the initial adsorption of adhesive proteins but rather due to an enhanced resistance of adhesion proteins such as Vn on TCPS towards displacement by other proteins as has been observed in other studies [62]. Additionally, Steele suggested that there might be an enhanced displacement of other serum proteins from the surface of TCPS by Vn that results in the superior cell growth observed with TCPS.

Johnson [63] suggests that materials demonstrating poor cell growth characteristics do not allow deposition of sufficient ECM proteins because serum-derived passivating proteins such as Alb are held too tightly and can't be displaced by cell-derived proteins. Van Wachem proposed that cell spreading on good growth substrates such as TCPS begins after the desorption of proteins which inhibit cell adhesion, such as Alb, and the replacement of those proteins by cell derived Fn. The likelihood of the exchange of adsorbed proteins for serum and/or cellular Fn was suggested by findings that precoating of TCPS with Alb, IgG, or HDL delayed endothelial cell adhesion during the first hour after seeding but after 6 hours, the number of adherent cells was the same on protein-coated TCPS as on uncoated TCPS. The exchange of surface bound proteins for Fn was also suggested in an experiment by Grinnell who observed that more serum Fn adsorbed onto TCPS precoated with native Alb than onto TCPS precoated with denatured Alb [64]. Assuming that native Alb does not show large conformational changes during adsorption onto TCPS, native Alb would be expected to be more easily desorbed than denatured Alb. Desorption of the native Alb would allow exchange of the surface bound protein for Fn.

1.6 Self-Assembled Monolayers (SAMs) as Model Systems

Developing correlations between biomaterial surface properties and the response to a physiologic environment involves consideration of many factors that have been

shown to influence the bioresponse (i.e., surface chemistry, energy, charge, and organization). Elucidating relationships between surface properties and cellular responses is often difficult since the polymer systems typically used in biointeraction studies do not allow for systematic, controlled variations in material surface properties. For example, the type of surface often used in cell growth studies, the radio-frequency plasma-deposited film, is chemically complex and contains a broad spectrum of chemical functional groups rendering it difficult to determine the effect of any one chemical functionality on cell growth. In order to effectively determine the chemical functionalities or surface composition responsible for influencing protein adsorption and cell growth, a set of surfaces exhibiting systematic variations in surface chemistry which exhibit stability in biological media is required. Molecular self-assembly techniques provide an effective means of fabricating organic surfaces with well-defined structure and chemistry. Self-assembled monolayers are prepared by the spontaneous adsorption of amphiphilic molecules, from an organic fluid, onto polar substrates. These monolayers are comprised of a slightly tilted, crystalline-like structure of densely packed alkyl chains in an almost perfect all-trans (zig-zag) conformation. Silica and gold are the most commonly used substrates however; other materials such as aluminum and titanium have been investigated. The chemisorption of amphiphiles onto silica and titanium leads to the formation of a covalent bond between surface hydroxyl groups and a silane-end group while adsorption on gold, silver, and aluminum involves strong, non-covalent bonding such as the gold-thiolate bond between alkanethiolates and gold. Self-assembled monolayers of alkane thiols on gold are stable in a variety of organic and aqueous media, making them particularly suitable for biointeraction studies.

Self-assembled films offer many advantages such as ease of preparation, chemical and physical robustness, and allow synthesis of a wide range of structures demonstrating specific interactions. Self-assembly offers control over film thickness,

surface chemistry and surface structure. By varying the length of the amphiphilic molecule, film thickness can be controlled. The chemical structure of the solid-liquid interface can be controlled by the varying the terminal group of the amphiphile [65,66]. More complex systems can be constructed by coadsorbing two or more thiols with different terminal functional groups of with different chain lengths onto a common gold substrate. By mixing amphiphiles with differing terminal groups, surfaces with randomly distributed or phase separated functional groups can be created. The surface concentration of a particular surface functionality can be controlled by varying the relative concentration of the thiols in the adsorbing solution.

Model SAMs differ from many real surfaces in an important aspect. The chains and tail groups in the densely packed, oriented monolayers described above do not have the degrees of freedom available in an amorphous polymer or a fluid biological surface. Therefore, the monolayer cannot reconstruct in response to environmental changes. In 1989, the preparation and characterization of mixed self-assembled monolayers formed by the coadsorption of two thiols that differed in the length of the polymethlyene chain was described [67]. By coadsorbing thiols with different chain lengths, free volume and conformational freedom can be introduced into the outer portion of the monolayer. The structural model of the mixed monolayers of thiols with different chain lengths proposed by Bain et al. is comprised of two distinct phases: an oriented, densely packed inner phase (adjacent to the gold surface) surmounted by a disordered, liquid-like outer phase, as shown in Figure 1.1. The outer region is flexible and mobile relative to the quasi-crystalline inner region and can exist in a higher degree of conformational states. The free volume introduced into the outer region of the monolayer by the presence of the shorter chains results in gauche bonds and a loss of lateral and orientational order in the outer region of the monolayer. By varying the relative concentrations of the two thiols in the adsorbing solution, the surface concentration of disordered, mobile long chain

component can be varied. Measurement of advancing contact angles of water and dispersive liquids such as hexadecane have been used to probe mixed SAM monolayer structure. Large deviations in contact angle were observed for the mixed length SAMs compared with values obtained for homogeneous monolayers of either component due to the exposure of the nonpolar methylene groups at the surface of the SAM. These results supported the model of a disordered, liquid-like outer region at the monolayer-liquid interface.

Several studies have demonstrated the utility of self-assembled monolayer films in investigating the effect of surface chemistry on protein and cellular interactions. Lewandowska et al. investigated the growth of fibroblasts and neuroblastoma cells on glass modified with self-assembled monolayers of terminally functionalized alkylsilanes [68]. Each cell line acted in a unique manner corresponding to the conformation of fibronectin (Fn) adsorbed on the surface that was mediated by the surface chemical functionality. Neural and endothelial cell growth on patterned, assembled amino and perfluoroalkyl silanes was studied by Stenger et al. [69,70]. Attachment and growth was observed on the amino, but not on fluoro surfaces. Prime and Whitesides [31] concluded that SAMs of alkanethiolates on gold were useful model systems for investigating mechanisms of protein adsorption in their study of monolayers containing mixtures of hydrophobic and hydrophilic alkanethiols. Protein adsorption was correlated to monolayer composition and in general, increased with increasing surface hydrophobicity. Lopez et al. recently described methods for controlling the attachment and spreading of mammalian cells on surfaces using patterned SAMs of alkanethiols on gold [30]. SAMs terminated with an oligo(ethylene glycol) group uniformly prevented cell and protein attachment while other functional groups including CH_3 and CO_2H promoted protein adsorption and cell attachment to varying degrees. Di Milla et al.

similarly investigated the attachment and growth of osteosarcoma cells on patterned SAMs and observed cell attachment and growth on hydroxyl-terminated SAMs but not on methyl-terminated SAMs [71].

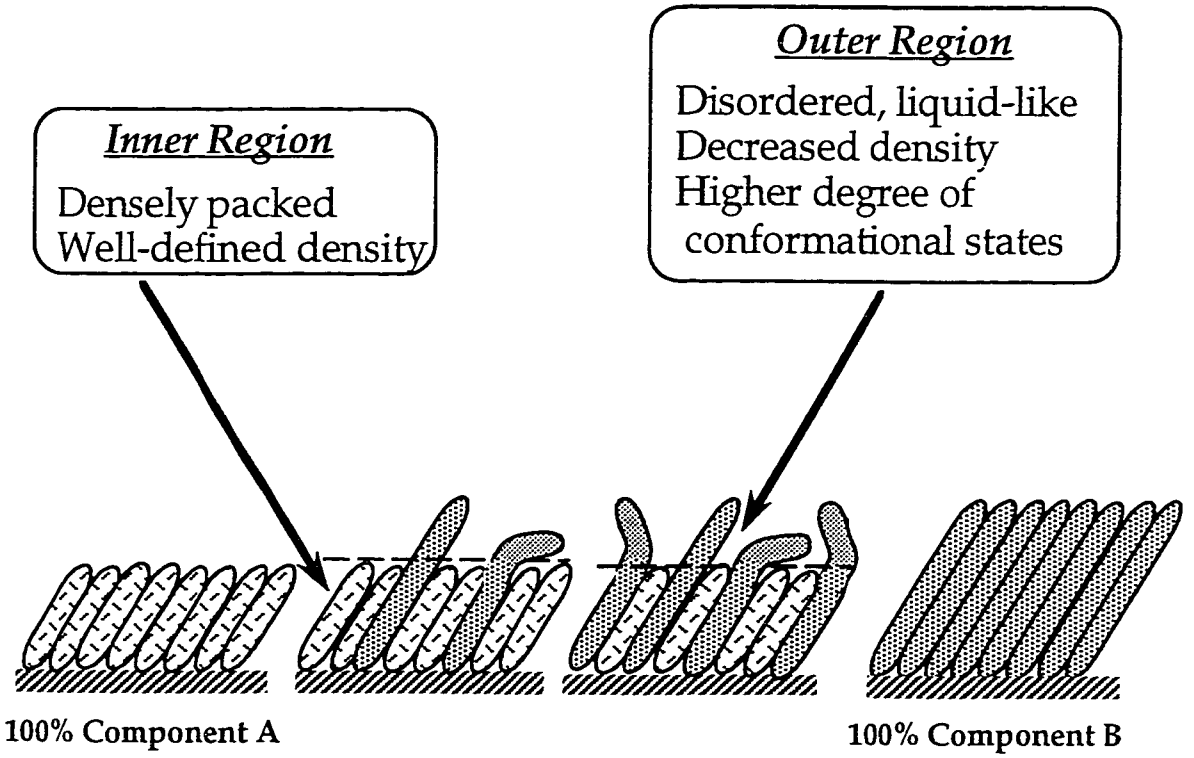

Figure 1.1 Schematic illustration of mixed self-assembled monolayers of alkylthiols with different polymethylene chain lengths. Mixed length SAMs demonstrate two structural regions: 1) the densely packed, inner region and, 2) the disordered, liquid-like outer region.

Chapter 2

Experimental Methods

2.1 SAM Fabrication for Biointeraction Studies

While SAMs have recently been utilized in biointeraction studies, SAMs are typically fabricated primarily for use in surface characterization studies. The requirements for utilizing SAMs in surface characterization studies are relatively straightforward. However, when utilizing SAMs in the types of biointeraction studies described in this work, several additional criteria must be satisfied. A discussion of the methods and techniques developed to satisfy these requirements is presented below.

2.1.1 Selection of SAM Substrate Material

The alkanethiol-gold based SAM system was selected for use in this project due to the good stability of this type of SAM, the variety of options for surface chemistry and structure, and the relative ease of preparation. Prior to selecting a substrate material and investigating gold deposition and SAM formation methods, criteria for the utilization of SAMs in protein and cellular interaction studies were established. Of primary importance was SAM stability throughout the protein and cell interaction studies. To use SAMs in protein adsorption studies and in dynamic contact angle studies, double-sided, 10 mm square SAMs were required. To use SAMs in cell proliferation experiments, 15 mm diameter one-sided SAMs were required. In addition, large numbers of samples are typically required in the biointeraction studies. Therefore, gold deposition and SAM adsorption methods were required to facilitate the preparation of a large number of samples at one time.

Several types of substrate material were investigated for use: glass, quartz, and silicon. Silicon was selected due to its availability, cost, and ability to be machined into

required sample geometries. To obtain samples of the required geometry, Si wafers were laser cut using a CNC mill. To avoid sintering of burrs to the Si surface during the machining procedure, a protective coating is applied to the wafer that is removed after cutting by soaking in ethanol.

The stability requirement necessitated the use of a chrome priming layer on the Si samples. After considerable experimentation with various deposition techniques and gold sources, gold coatings of acceptable surface composition and roughness were achieved on Cr-primed Si samples using an electron beam evaporator. To prepare double-sided samples, a fixture was designed which allows for sample rotation and coating of both sides of the samples without breaking vacuum. The fixture also allows for coating of an adequate number of samples (40) per deposition.

2.1.2 Procedure for SAM Formation

Upon initiation of this project, our laboratory had limited experience with the preparation of SAMs. Thus, we entered into collaboration with Professor David Allara's group at Pennsylvania State University and consulted with this group for guidance in SAM preparation techniques. In conjunction with Dr. Barbara Tarasevich at Penn State (and more recently at Battelle Pacific Northwest Laboratories), a protocol was developed for SAM preparation that incorporated requirements specific for our types of studies (i.e., double-sided samples, specific sample geometries, and increased sample number). Utilizing this protocol, SAMs were fabricated in our lab, analyzed with ESCA and results were compared with ESCA results obtained on SAMs prepared at Penn State under identical preparation conditions. Other than observing occasional contaminants, SAMs fabricated in our laboratory using this protocol are similar in surface composition and structure to SAMs fabricated at Penn State.

2.1.3 Evaluation of SAM Stability

The most critical requirement for utilizing SAMs in protein interaction and cell growth studies is the maintenance of SAM stability throughout the experimental procedure. Protein adsorption/elution and cell growth studies involve the exposure of the SAM to a variety of different solutions for varying time periods. A stability study was performed to assess SAM integrity following exposure to each type of solution used in the protein adsorption/elution and cell growth studies. To assess the effect of solution exposure, the SAMs were evaluated by ESCA, ellipsometry and FTIR before and after exposure to various solutions. To test SAM stability after exposure to solutions used in protein adsorption/elution and cell growth experiments, SAMs were exposed to a phosphate-buffered saline solution (24 hours, 37°C), Iscove's modified Dulbecco's medium (IMDM) (24 hours, 37°C), and a 3% (w/v) sodium dodecyl sulfate (SDS) solution (24 hours, 22°C). In addition, SAMs were subjected to the normal protein adsorption and cell growth experiment (i.e., sequential exposure to solutions) and evaluated by ESCA, ellipsometry, and FTIR. In all stability experiments, no changes in surface composition, film thickness, or IR spectral features indicative of SAM delamination or degradation were observed. The results of stability studies indicate that the methods developed for SAM fabrication allow for the preparation of SAMs suitable for use in biointeraction studies.

2.2 Preparation of Homogeneous and Binary Composition SAMs of Alkanethiolates on Gold

Si(100) wafers (Silicon Quest International, Santa Clara, CA; single-side polish, 3" diameter, ~ 0.35 mm thick) were laser cut (EBTEC Radcliffe, Pasadena, CA) into 15 mm diameter circles (for use in cell growth studies) or 10 x10 mm squares (to be used for surface characterization studies). Double-side polished Si (100) wafers were laser

cut into 10x10 mm squares (to be used for protein adsorption studies). 15 mm glass discs (Carolina Biological) were also used for cell growth studies. Substrates were cleaned by immersion in 1:4 H_2O_2/H_2SO_4 mixtures at 85°C for 10 minutes (Caution: this solution reacts strongly with organic compounds and should not be stored in closed containers. It must be handled with extreme caution.), followed by rinses in deionized water and absolute ethanol. Substrates for surface characterization and protein adsorption studies were coated by resistive evaporation of a 100 Å chromium adhesion layer followed by a 2000 Å gold layer (99.99%). Substrates for cell growth studies were coated by resistive evaporation of a 100 Å chromium adhesion layer followed by a 500 Å gold layer (99.99%). The thinner gold layer was transparent and thus allowed for direct visualization of cells on the SAM surfaces during the cell growth study. Deposition of gold occurred at $< 4 \times 10^{-7}$ torr base pressure at ~20-25 Å/s. The double-side polished wafers were attached by clips to a shaft which could be rotated 180° by a DC micromotor. This allowed coating of both sides of each sample in the same deposition batch.

To prepare chemically homogeneous SAMs, gold-coated Si substrates were immersed for approximately 48 hours into a 1 mM ethanolic solution of the n-alkanethiol terminated with the desired functionality. To prepare binary composition SAMs, gold-coated Si substrates were immersed for approximately 48 hours into binary ethanolic solutions of n-alkanethiols (1 mM total concentration) terminated with the desired functionality. Binary solution mixture ratios were chosen to achieve the desired surface composition in accordance either with values published in the literature or with solution ratio/surface composition curves generated for each binary pair as described in Chapter 5. All alkanethiols were synthesized at the University of Washington or at Pennsylvania State University as previously described [72].

Following the 48 hour adsorption period, samples were removed from the thiol solution and sonicated twice in ethanol for 5 minutes. In addition, SAMs containing a carboxylic acid terminated alkanethiol were rinsed several times in 0.1 M HCl followed by deionized water in order to remove adsorbed contaminants. All samples were stored in 100% ethanol for up to 1 week prior to use. Upon removal from storage solution, the samples were rinsed in ethanol and blown dry with a stream of pure nitrogen. The carboxylic acid-terminated SAMs were rinsed again with dilute HCl and distilled water.

2.3 Surface Analysis

2.3.1 Ellipsometry

Ellipsometry measurements were obtained using a single-wavelength (632.8 nm) ellipsometer (Rudolph Auto El) at 70° angle of incidence. Values of ellipsometric angles, Δ and Ψ, were translated into equivalent optical thicknesses using a 3-medium model [73-75]. A value of 1.50 + 0i was assigned to the refractive index of the thiolate films [28].

2.3.2 External Reflection Infrared Spectroscopy

Infrared external reflection spectra were obtained using a custom-modified BioRad-Digilab Fourier transform instrument with f/11 optics. Spectra were obtained at 2 cm^{-1} resolution using p-polarized light at an 86° angle of incidence as described elsewhere [65].

2.3.3 Contact Angle

Water contact angles (static) were obtained using deionized water and a Rame Hart contact angle goniometer maintained at 100% humidity. At least three spots were examined for each substrate surface.

2.3.4 X-Ray Photoelectron Spectroscopy (XPS)

Analyses were performed on an SSX-100 spectrometer (Surface Science Instruments, Mountain View, CA) using a monochromatic Al Kα source, a detection system with a 30° solid angle acceptance lens, a hemispherical analyzer, and a position sensitive detector. Surfaces were typically analyzed at a 55° take off angle, defined as the angle between the surface normal and the axis of the analyzer lens. Survey scans (0-1000 eV) were performed at a 150 eV analyzer pass energy using a 1000 μm x-ray spot size to determine surface composition. High-resolution O1s and C1s spectra were obtained at 25 eV pass energy over a 20 eV binding energy range. High-resolution spectra were resolved into individual Gaussian peaks using a least-squares fitting program. All binding energies (BE) were referenced by setting the lowest BE component of the resolved C1s peak (corresponding to carbon in a hydrocarbon environment) to 285.0 eV. Survey (0-1000 eV) and detailed elemental scans were used to determine surface elemental composition. High resolution scans were analyzed for quantitation of functional group content according to chemical shift data by Dilks et al. [76].

2.3.5 Time-of-Flight Secondary Ion Mass Spectroscopy (TOF-SIMS)

TOF-SIMS experiments were performed on a model 7200 Physical Electronics PHI instrument (Eden Prairie, MN) using triplicate samples of each SAM. The 8 keV

Cs^+ ion source was operated with a current of 1.5 pA, a pulse width of 9 ns, and a repetition rate of 5000 Hz. The resulting ion dose was maintained below 10^{13} ions/cm^2, with an area of analysis of 0.01 mm^2. A pulsed electron flood gun operated with an energy of 70 eV was used for charge neutralization. The secondary ions were extracted into a two-stage reflectron time-of-flight mass analyzer with a potential of 3 kV. A secondary ion focusing lens between the analyzer entrance and drift region was held at 1 kV, promoting high angular acceptance and good transmission of ions. The band pass of the analyzer is 100 eV, and an independent adjustable grid voltage (deceleration) allows energy focusing to be performed. The ions were post-accelerated to 10 kV and converted to charge pulses by a stacked pair of chevron-type multichannel plates (MCP). The signals were detected using a 256 stop time-to-digital converter (TDC) with 156 ps time resolution. The relative areas of the signals were measured by integrating the intensity of the signals over a one unit mass range.

2.4 Bovine Aortic Endothelial (BAE) Cell Culture

BAEC, a gift of Dr. Steven Schwartz (University of Washington), were maintained in continuous growth at 37°C, in a humidified atmosphere containing 7% CO_2 on TCPS dishes. Bovine cell growth medium consisted of Iscove's modified Dulbecco's medium (IMDM) (#12200-036, Gibco, Gaithersburg, MD) to which 10% heat-inactivated calf serum (#26170-019, Gibco), 1% sodium pyruvate (#320-1360), 1% nonessential amino acids (#320-1140), and 1% penicillin-streptomycin solution (#600-5070) were added. BAE cells were shown to be mycoplasma-free by the DAPI fluorochrome method [77]. Their identity was ascertained, in the laboratory of Dr. S. Schwartz, by the presence of von Willebrand factor [78] and the uptake of acetylated LDL [79]. BAEC were removed from growth surfaces (for passage or use in an assay) by first washing twice with 5 ml of PBS followed by an incubation in 2 ml of light

trypsin/EDTA (0.05%/0.53 mM; Gibco) for digestion. After cells had detached, serum-containing medium was added to inactivate the trypsin. Cells were counted by trypan blue exclusion. Cells were then resuspended in medium and replated to restimulate growth. Cells were passaged every 3-4 days and discarded after 12-14 passages.

Conditioned medium was prepared by seeding TCPS dishes (Falcon, #3003) at approximately 50% confluency in growth medium and harvesting after 4-5 days. Culture and conditioned media were 0.22 μm filtered before use. Conditioned medium was aliquoted and frozen at -20°C until needed.

2.5 Measurement of BAEC Attachment and Growth

2.5.1 Measurement of Cell Number by Giemsa Staining

In preliminary studies of cell growth on homogeneous and binary SAMs (Chapters 3 and 4), two types of cell growth studies were performed. The first type of study, a clonal growth assay, was performed by seeding BAE cells at low density onto the SAM substrates. After a 3 day culture period, the cells were fixed, stained, and counted to determine cell number. The second type of study involved seeding BAE cells at high density onto SAM substrates. After culture periods of 3, 5, or 7 days, cells were fixed, stained and evaluated qualitatively using reflectance microscopy.

For both types of studies, SAM substrates were placed in TCPS multiwells (Falcon, #3047), sterilized by incubation in 70% ethanol (15 minutes), and subsequently dried in a laminar flow hood prior to use in the cell growth assays. Prior to cell seeding, SAMs were incubated in two 1 ml volumes of sterile PBS at 37°C for several hours. The growth assay was performed by applying equal volumes of BAE cell suspension (in 10% bovine serum cell growth medium) and conditioned medium to the SAM substrates contained in the multiwell plate. A clonal growth assay (quantitative evaluation of cell

number following seeding at low cell density), was performed by seeding cells onto SAM substrates at a density of 53 cells/cm^2 (100 cells/well) and culturing for a period of 3 days. The qualitative evaluation of cell number was performed by seeding cells onto the SAM substrates at an initial density of 1330 cells/cm^2 (2500 cells/well) and culturing the cells for 3, 5, or 7 day periods. Following the designated culture period, cells were rinsed with PBS and fixed using cold (-20°C) 95% ethanol. The cells were stained with a Giemsa stain solution (prepared by diluting Giemsa stock solution with DI water (1:20) and filtering the solution through glass wool) for approximately 10 minutes, washed with DI water, and allowed to dry before counting. The number of cells on each SAM substrate seeded at the lower density (100 cells/well) was determined by counting the total surface area using reflected light microscopy. Substrates on which cells were seeded at the higher density were photographed under reflectance light microscopy and a qualitative evaluation of cell density was made.

2.5.2 Measurement of Cell Number by the MTT Cell Proliferation Assay

To quantitatively assess cell proliferation after multiple culture period time points, the MTT assay (Sigma Corp., #M5655) was used to measure the effect of substrate properties on endothelial cell proliferation. The MTT assay is a colorimetric method for determining the number of viable cells in a proliferation experiment. MTT is a water soluble tetrazolium salt that is converted to an insoluble purple formazan by cleavage of the tetrazolium ring. Cellular reduction of MTT is associated with enzymes of the endoplasmic reticulum. MTT is metabolically reduced by all viable cells. The water insoluble formazan can be solubilized and measured spectrophotometrically to obtain absorbance values as a function of concentration of converted dye. Tetrazolium salts have been developed as an alternative to the ^{3}H-thymidine uptake assay and have been used extensively in cell proliferation and cytotoxicity assays, enzyme assays and other

assay procedures [80]. The MTT assay is performed by adding MTT stock solution to each culture being assayed and incubating for 3-4 hours. At the end of the incubation period, the medium is removed and the converted dye is solubilized with acidic isopropanol. Absorbance of the converted dye is then measured at a wavelength of 570 nm. The quantity of formazan product as measured by the amount of 570 nm absorbance is directly proportional to the number of living cells in culture.

To perform the cell growth assay, SAM substrates were placed in TCPS multiwell plates (Falcon, #3047), sterilized by incubation in 70% ethanol (15 minutes), and dried in a laminar flow hood. Prior to cell seeding, SAMs were incubated in two 1 ml volumes of sterile PBS at 37°C for several hours. A BAE cell suspension was prepared for use in the assay as described in Section 2.4. The growth assay was performed by applying 0.5 ml of a BAE cell suspension (in 10% bovine serum cell growth medium) at a concentration of 1.0×10^5 cells/ml to the SAM substrates resulting in 5×10^4 cells per sample. Samples were then incubated at 37°C for the designated time period.

Cell morphology was evaluated throughout the culture period using light microscopy. Cell number was measured using the MTT assay system after 3 culture time periods: 4 hours, 1 day, and 3 days. MTT stock solution was prepared at a concentration of 5 mg/ml by dissolving MTT powder (Sigma, #M5655) in RPMI 1640 media (without phenol red). The MTT stock solution was filtered through a 0.2μ filter and stored at 2-8 °C, or frozen for use over extended periods. Three hours prior to the designated culture time period (i.e., 1 hour, 21 hours, and 69 hours of culture), 50 μl of MTT stock solution was added to each sample well and incubated for 3-4 hours. After the incubation period, the MTT reagent and media present in the sample well was removed and the converted dye was solubilized by adding 200 μl of 0.04 N acidic

isopropanol to each well. Multiwell plates were gently agitated on a shaker table to facilitate crystal dissolution. To measure the absorbance of the formazan solution, a 100 µl sample was taken from each substrate well and transferred to an ELISA plate. Absorbance of the converted dye was measured at a wavelength of 570 nm with background subtraction at 630-690 nm using an ELISA plate reader.

Prior to performing the cell proliferation experiments with the MTT assay system, a calibration curve of formazan solution absorbance versus cell number for the MTT assay was developed for the BAE cell line. To construct a calibration curve, a series of BAE cell suspensions (in 10% bovine serum cell growth medium) varying in cell concentration from approximately 1×10^4 to 1×10^6 cells/ml were prepared. The concentration of each cell suspension was determined (using multiple aliquots per cell suspension) using the trypan blue exclusion method described in Section 2.4. Cells were then applied to TCPS multiwell dishes and allowed to adhere for 2 hours. After cell adherence, 50 µl of the MTT stock solution was added to each sample well and incubated for a 3 or 4 hour period. The converted dye was then solubilized with 0.04N acidic isopropanol and absorbance was measured using an ELISA plate reader.

Figure 2.1 illustrates the relationship between formazan solution absorbance and BAE cell number for a MTT incubation period of 3 hours. The upper curve shown in Figure 2.1 was obtained using a 100 µl sample volume for the absorbance measurement while the lower curve was obtained with a 50 µl sample volume. Each curve includes data obtained during 5 separate experiments (average of quadruplicate samples for each data point) using BAE cells at various passage number (i.e., P7-P12). Calibration curves were generated using the KaleidaGraph (Synergy Software, Reading, PA) curve-fitting program. A fourth order polynomial was used to fit the absorbance data. Figure 2.2 similarly illustrates the relationship between formazan solution absorbance and BAE

cell number for a 4 hour MTT incubation period. Again, curves representing the use of a 100 µl and 50 µl sample volume are shown.

As shown in Figures 2.1 and 2.2, the relationship between absorbance and cell number is not linear, in agreement with data developed for other adherent cell lines by Sigma Corp. The use of a 100 µl sample volume for the absorbance measurement results in a greater sensitivity to cell number than does the 50 µl sample volume. Therefore, a 100 µl sample volume was chosen for use in all MTT assay experiments. Calibration curves obtained for the 3 hour incubation period did not differ significantly from data obtained with the 4 hour incubation period. Thus, a 3 hour MTT incubation period was chosen for use in MTT assay experiments. As illustrated in Figures 2.1 and 2.2, the MTT assay system provides an accurate measurement of differences in cell number over a wide range of cell concentrations (2 orders of magnitude). The lower limit of detection was approximately 10,000 cells. The upper limit of detection was not definitively determined however, 1 x 10^6 cells were easily detected with the assay. Since the cell growth experiments on SAM substrates of various surface chemistries results in a broad range of responses (i.e., cell death to confluent cell monolayers), it is essential that the cell assay system allow for evaluation of a wide range of cell response.

2.6 Protein Radiolabeling

An isotonic citrate-phosphate buffered saline (CPBSz) solution containing sodium azide was used in protein iodination (0.01 M sodium citrate, 0.01 M sodium phosphate, 0.12 M sodium chloride, and 0.02% (w/v) sodium azide, pH 7.4). Iodine-125 NaI used for labeling bovine Alb and Vn was obtained from Amersham, Arlington Heights, IL (# IMS-30). A 10 mg/ml solution of bovine serum Alb (#A7638, Sigma, St. Louis, MO) prepared in borate buffer (0.16 M NaCl and 0.20 M H_3BO_3, pH 8.0) was used in protein iodination. A 0.5 mg/ml solution of bovine serum vitronectin

(Sigma, St. Louis, MO) prepared in borate buffer was used in protein iodination ^{125}I-labeled Fn was purchased from ICN (#68066, ICN, Costa Mesa, CA).

Bovine Alb and Vn were radiolabeled with ^{125}I by the iodine monochloride (ICl) technique of MacFarlane [81] as modified by Helmkemp [82] and Horbett [39]. A twofold molar excess of ICl to protein was used. Iodination was performed at 0°C using 0.5 ml of each of the following solutions. Approximately 1 mCi of ^{125}I was added to 0.4 M borate and 0.32 M NaCl, pH 7.75. This mixture was added to ICl in 2M NaCl, and the resultant mixture was added to the protein solution. The mixture was allowed to react for 20 minutes. Unincorporated ^{125}I was separated from the iodinated protein by gel exclusion chromatography (#732-2010, BioRad). Radiolabeled protein solutions were stored at -70°C and used within 2 weeks of preparation. A small volume of the ^{125}I-labeled protein solution (Alb, Fn, or Vn) was added to the bovine serum solution to obtain a specific activity of 10^7 cpm/mg for Fn and Vn and 10^6 cpm/mg for Alb.

2.7 Protein Adsorption

The adsorption of ^{125}I-labeled Alb, Fn, and Vn from 10% bovine serum solution to SAMs was measured to determine the amount of each protein (ng/cm^2) adsorbed to the substrate from the same serum solution used in cell growth experiments. SAMs were placed in 2 ml polystyrene cups (Evergreen Scientific, Los Angeles, CA) containing degassed, sterile PBS buffer and hydrated for 2 hours at 37°C. Buffer was aspirated from each sample, and fresh, degassed IMDM buffer (0.75 ml) was added to each sample. Samples were allowed to equilibrate at 37°C for 1 hr. Protein adsorption was initiated by rapidly pipetting an equal volume (0.75 ml) of radiolabeled 20% bovine serum solution onto the sample immersed in buffer to achieve a final concentration of 10% serum. Serum (20%) used for protein adsorption was prepared by diluting calf

serum in HEPES-buffered IMDM. Complete mixing of the adsorbing solution was achieved by gentle pipetting. Adsorption was conducted for 2 hours at 37°C using quadruplicates of each type of SAM. Adsorption was terminated by dilution-displacement of the protein solution with buffer.

The dilution-displacement technique was performed by flowing approximately 20 volumes of IMDM buffer at a flow rate of approximately 400-600 ml/min from an overhead reservoir through the cup containing the sample and the radioactive protein solution. The protein solution was thus rapidly displaced, and exposure of the sample to an air-water interface was avoided. During sample rinsing, the sample was dislodged and caused to "flutter" in the buffer stream to ensure thorough rinsing.

The rinsed samples were then placed in sample-counting tubes containing IMDM buffer, and retained radioactivity on the sample was measured using a gamma counting system (Model #1185R, TM Analytic, Elk Grove, IL). Sample radioactivity was corrected for decay and background. The amount of adsorbed protein was calculated from the radioactivity retained by the surface, the specific activity of the adsorbing solution, and the planar equivalent surface area of the sample.

2.8 SDS Elution of Adsorbed Proteins

The elutability of Alb, Fn, and Vn adsorbed to SAM surfaces by a surfactant, sodium dodecyl sulfate (SDS), was evaluated to determine the strength of protein-surface interactions. Following protein adsorption (described in Section 2.7) and sample rinsing, samples were placed in 1.5 ml of a SDS solution for elution. A solution of 3% (w/v) sodium dodecyl sulfate (SDS) (BioRad, Richmond, CA) and 2.5% (v/v) gel buffer (0.4 M tri(hydroxylmethyl)aminomethane and 0.219 M H_3PO_4, pH 6.8) was used to elute adsorbed proteins.

After a 24 hour storage period in SDS, samples were serially dip-rinsed in IMDM buffer and placed immediately in counting tubes containing 1.5 ml of IMDM buffer. The retained radioactivity following elution with SDS was measured, and the surface protein after elution was determined from the retained radioactivity, the specific activity of the solution, and the planar equivalent surface area of the sample. The percent elutability is defined as the percent of adsorbed protein that is removed by SDS.

2.9 Statistical Analysis

The effect of SAM surface property on cell growth, protein adsorption, and protein elutability was compared statistically with a one-way analysis of variance (ANOVA). Significant differences were determined by ANOVA F-tests with an acceptable α level set at 0.05. If probability values for a set of data were calculated to be less than 0.05 ($p<0.05$), differences observed in the data were considered statistically significant. Statistical analyses were performed using EXCEL software, version 5.0 (Microsoft Corp., Redmond, WA).

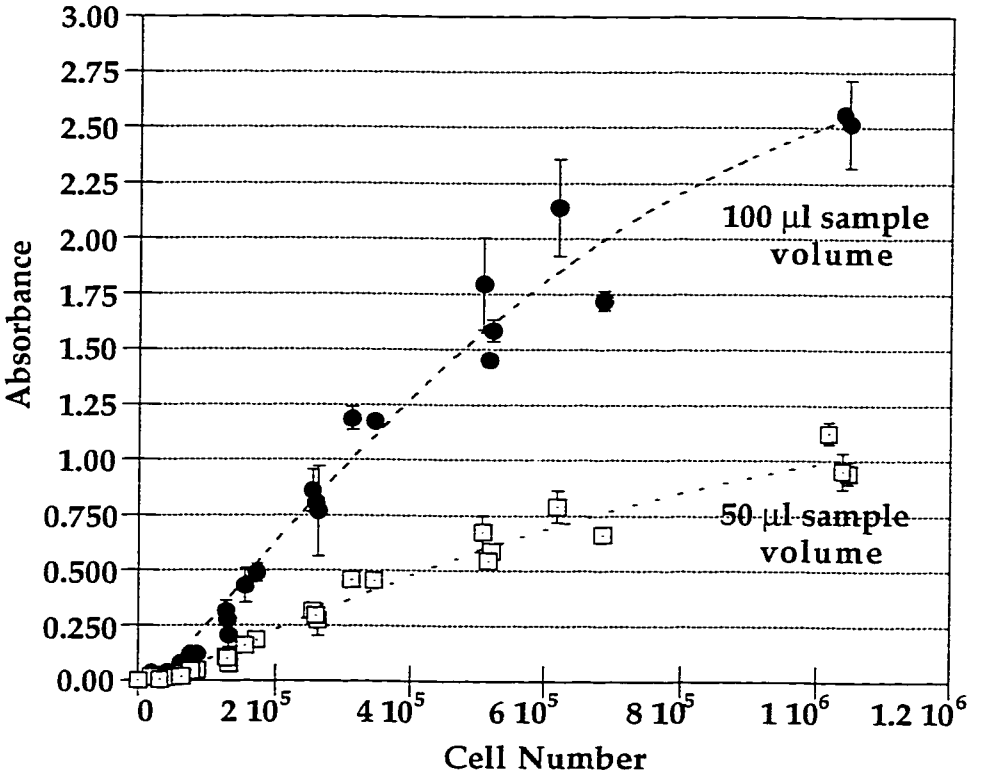

Figure 2.1 MTT conversion by bovine aortic endothelial cells on TCPS after a 3 hour incubation period. Cells were plated onto substrates in 10% bovine serum growth medium and allowed to adhere for 2 hours prior to addition of the MTT solution. Absorbance measurements were made with 50 and 100 µl sample volumes. Data represent the mean ± standard deviation for quadruplicate samples.

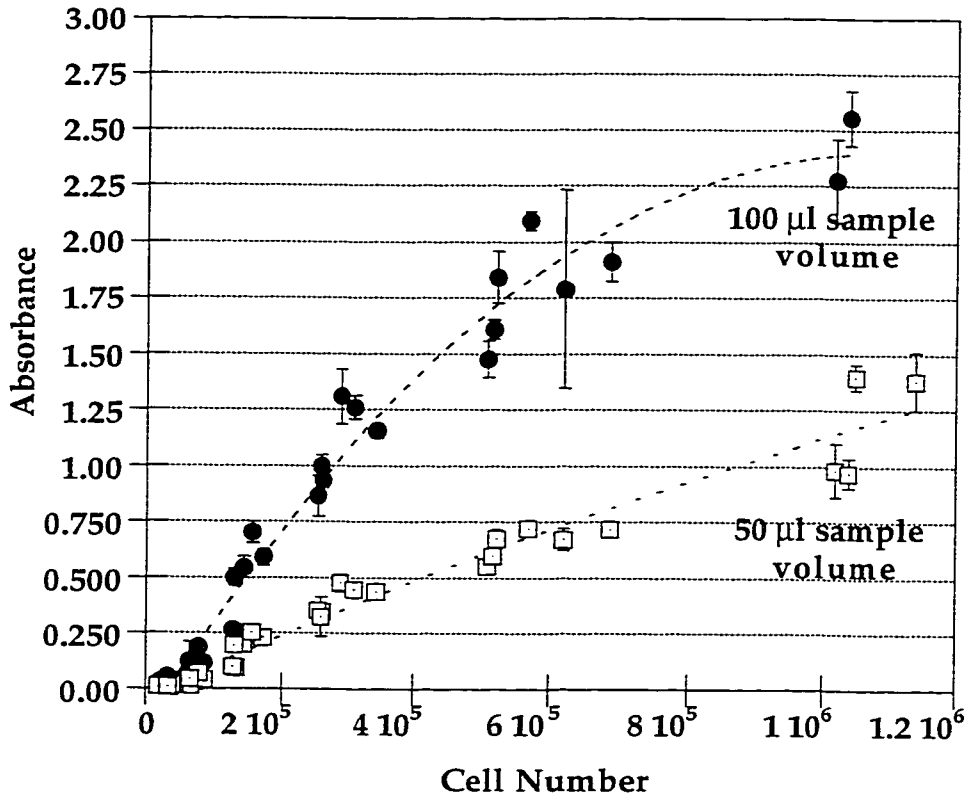

Figure 2.2 MTT conversion by bovine aortic endothelial cells on TCPS after a 4 hour incubation period. Cells were plated onto substrates in 10% bovine serum growth medium and allowed to adhere for 2 hours prior to addition of the MTT solution. Absorbance measurements were made with 50 and 100 µl sample volumes. Data represent the mean ± standard deviation for quadruplicate samples.

Chapter 3

Endothelial Cell Growth and Serum Protein Adsorption on Chemically Homogeneous SAMs

Note: This work, in a similar form, was published by C.D. Tidwell, S.I. Ertel, B.D. Ratner, B.J. Tarasevich, S. Atre, and D.L. Allara, *Langmuir* 1997, 13, 3404-3413.

3.1 Introduction

To investigate the role of specific chemical functionalities in endothelial cell growth, a series of chemically functionalized surfaces prepared by self-assembly of alkanethiolate monolayers on gold surfaces using the molecules $X(CH_2)_{15}SH$ with X = -CH_3, -CH_2OH, -CO_2CH_3, and -CO_2H were used as substrates for bovine aortic endothelial cell (BAEC) growth. Since cells seeded on a substrate in serum-containing culture medium interact with the adsorbed protein layer rather than with the substrate itself, the effect of chemical functionality on the adsorbed protein layer was investigated in conjunction with cell growth. The role of two serum proteins, Alb (a nonadhesive or blocking protein) and Fn (an adhesive protein), in cell growth was evaluated by measuring the amount of each protein bound and the tightness of binding (determined by resistance to SDS solubilization) on the SAM substrates. We hypothesized that the adsorbed protein layer characteristics (amount and binding strength of adsorbed protein) and cell growth would differ in response to specific surface chemical functional groups.

This is the first report in which protein/surface interactions (adsorption and binding strength) have been quantified and related to endothelial cell growth on well-characterized SAM surfaces. We determined that protein adsorption, protein elutability, and BAEC growth on the terminally functionalized surfaces differed in response to the

presence of specific surface functional groups. Correlations between cell growth and adsorbed protein layer characteristics were observed. We found that BAEC growth varied significantly with surface functionality. Cell growth increased in the following order: $-CH_2OH < -CO_2CH_3 < -CH_3 << -CO_2H$, illustrating the effect of specific surface functional groups. The significant differences in cell growth performance between different surfaces and the strong response to the carboxyl functionality are important observations.

3.2 Materials and Methods

Terminally functionalized self-assembled monolayers (SAMs) were prepared by adsorption of 1 mM ethanolic solutions of $X(CH_2)_{15}SH$ with X = $-CH_3$, $-CH_2OH$, $-CO_2CH_3$ and $-CO_2H$ onto evaporated gold substrates as described in Section 2.2. Triplicate samples of each type of SAM were characterized by ellipsometry, IR, contact angle, and XPS to confirm the presence of the expected functionality at the SAM surface (Section 2.3). The growth of BAEC (in 10% bovine serum medium) seeded at low density (53 cells/cm^2) and high density (1330 cells/cm^2) onto functionalized SAMs was evaluated after 3 days of growth and 5 days of growth respectively as described in Sections 2.4 and 2.5.1. Alb and Fn adsorption to the functionalized SAMs was determined by measuring the adsorption of ^{125}I labeled Alb and Fn from 10% bovine serum for 2 hours at 37°C. The binding strength of adsorbed Alb and Fn was evaluated by measuring protein retention after elution with a 3% sodium dodecyl sulfate (SDS) solution for 24 hours (Sections 2.6-2.8).

3.3 Results

3.3.1 Surface Characterization

The chemically homogeneous SAMs were prepared by the self-assembly of alkyl thiols terminally substituted with hydroxyl, methyl, methyl ester and carboxyl groups. The use of these functionalities provides a series of surfaces which exhibit a wide range in surface hydrophobicity and allows for investigation of the role of oxygen-containing functional groups in cell growth and protein adsorption.

The results of contact angle studies and XPS analysis are summarized in Table 3.1. Contact angle studies confirmed the presence of the expected functional group at the surface of the SAM and were in agreement with expected values. Contact angles ranged from 17° for the hydrophilic hydroxyl SAM surface to 109° for the hydrophobic methyl-terminated surface. XPS results were in agreement with compositions predicted from the structure of the alkyl thiol molecule used to form the SAM. XPS of the four types of SAMs showed surface compositions consistent with results obtained previously [65,83] and indicated the presence of the underlying gold substrate and the attached sulfur atoms. The methyl surface showed a 2.7% oxygen content due most likely to oxidation after removal form the ethanol storage solution.

All monolayers exhibited the functionality expected from the terminally substituted alkanethiol used, as indicated by the XPS high resolution C1s envelopes shown in Figure 3.1. An almost symmetrical single carbon peak was observed for the methyl-terminated monolayer. The C1s envelope of the hydroxyl-terminated monolayer showed 2 peaks with binding energies consistent with hydrocarbon and alcohol/ether (286.5 eV) functionalities. Two peaks were observed in the C1s envelope of the carboxyl-terminated monolayer with binding energies consistent with hydrocarbon and carboxyl/ester (288.8 eV) groups. The C1s envelope of the methyl ester surface demonstrated 3 peaks with binding energies consistent with hydrocarbon, ether, and

ester functionalities. Other minor peaks attributable to oxygen-containing species were noted in the spectra of the four SAMs presumably due to small amounts of air-oxidation which occurred prior to XPS analysis.

SIMS analysis of the homogeneous OH, COOH, and CH_3-terminated SAMs is discussed in Chapter 5.

3.3.2 BAEC Growth on Chemically Homogeneous SAMs

BAEC were seeded at low density onto OH, CH_3, CO_2CH_3, and COOH-terminated SAMs and TCPS and cultured for 3 days. Cell response was characterized by determining the total number of cells on each type of surface (total surface area = 1.81 cm^2) after the 3 day growth period (Figure 3.2). Cell growth on TCPS, a standard cell growth substrate, was significantly higher than that on any of the SAMs. Of the functionalized surfaces, cell growth on the COOH SAM was significantly higher than that on any of the other SAMs. The CH_3, CO_2CH_3, and OH SAMs exhibited poor growth characteristics. Very few cells were observed on the CO_2CH_3 or OH SAMs, while the CH_3 SAM supported the growth of a slightly increased number of cells. Areas of clonal growth were observed on the COOH SAM and TCPS. Cell spreading was observed in the majority of cells on the TCPS and COOH SAM. The few cells that were observed on the CH_3, OH, and CO_2CH_3 SAMs appeared well attached as evidenced by their spreading.

BAEC density and morphology on the functionalized SAMs and TCPS following seeding at higher density and a 5 day culture period were evaluated qualitatively (Figure 3.3). The OH SAM demonstrated the lowest cell density, and the majority of cells observed on this surface did not show evidence of spreading. The CO_2CH_3 SAM also exhibited a low cell density; however, spreading was observed in a greater number of cells on this surface. On the CH_3 SAM, a higher cell density was observed relative to the

OH and CO_2CH_3 SAMs, as well as evidence of cell spreading. A significant increase in cell number was observed on the COOH SAM with cell spreading observed in the majority of cells on this surface. A nearly confluent monolayer was achieved after 5 days of culture on the COOH surface. Cell density was highest on the TCPS surface, and the cell monolayer was nearly confluent after the 5 day growth period.

3.3.3 Albumin and Fibronectin Adsorption from 10% Serum

The amount of Alb and Fn adsorbed from 10% serum to the functionalized SAM surfaces is shown in Figures 3.4 and 3.5. Slight differences were observed in the amount of Alb adsorbed in response to the chemical functionality present on the SAM surface however, the differences were not significant (Figure 3.4). Alb surface density ranged from 23 ng/cm^2 on the CO_2CH_3 SAM to 33 ng/cm^2 on the COOH SAM. Alb adsorption does not appear to correlate with surface cell growth characteristics as similar Alb surface densities were observed on SAMs exhibiting significant differences in cell growth.

Fn adsorption from 10% serum varied significantly with surface functionality (Figure 3.5). Fn surface density ranged from approximately 2.5 ng/cm^2 on the COOH SAM to 0.8 ng/cm^2 on the OH and CO_2CH_3 SAMs. Adsorption to the COOH SAM was significantly higher than Fn adsorption to the OH and CO_2CH_3 SAMs. Fn adsorption to the CH_3 SAM was slightly higher than on the OH and CO_2CH_3 SAMs yet less than one-half the value of Fn adsorption to the COOH SAM. The amount of Fn adsorbed to the monolayer surfaces from 10% serum was significantly lower than the amount of Alb adsorbed. At least 25 times as much Alb as Fn adsorbed to the OH, CH_3, and CO_2CH_3 SAMs, while the COOH SAM adsorbed only 13 times as much Alb as Fn.

The low levels of Fn adsorption observed from 10% serum are in agreement with previous studies of Fn adsorption [20]. When Fn is adsorbed from serum or plasma, a

maximum, or Vroman peak, in adsorption is observed at a serum concentration of 0.1%. The adsorption of serum Fn to many surfaces decreases significantly or is completely blocked by other competing serum components (i.e., Vn or Alb) at serum concentrations greater than 1% [20]. Fn adsorption onto TCPS is reduced by more than 90% in the presence of serum concentrations above 2%. Therefore, small amounts of Fn are expected to adsorb onto surfaces at the serum concentrations (5-30%) typically used in cell culture. The lower levels of Fn adsorption relative to Alb observed on all monolayers are expected since serum contains a 175-fold excess of Alb compared with Fn, yet its competitive effectiveness for adsorption relative to other proteins is similar to that of Alb [62].

3.3.4 Albumin and Fibronectin Elutability after Adsorption from 10% Serum

The elutability of Alb and Fn adsorbed to the functionalized SAM surfaces following a 24 hour exposure to 3% SDS solution is shown in Figures 3.6 and 3.7. Alb elutability varied significantly with surface functional group. Alb elutability on the COOH and CH_3 SAMs was significantly higher than on the CO_2CH_3 and OH SAMs. Slight differences were observed in Fn elutability in response to SAM terminal functionality; however, the differences were not significant.

3.4 Discussion

3.4.1 Effect of Functional Group on Cell Growth

A wide range of cell responses is observed (from cell death to confluency) for the various surfaces made by adsorption of alkanethiols terminally substituted with hydroxyl, methyl, methyl ester, or carboxyl groups. The COOH functionality resulted in maximum cell growth promotion, while the OH and CO_2CH_3 functionalities

demonstrated poor cell growth characteristics. The CH_3 SAM was moderately supportive of cell growth in the high-density study however; it showed low cell growth in the low-density study. Since these surfaces exhibit similar structural properties (high packing density, constant average alkyl chain orientation) and differ principally in the nature of the terminal substituent [65,84], the cells are responding to the presence of specific surface functional groups, mediated by the adsorbed serum protein layer. While this idea is widely accepted [10,11,26,29,85], the identity of the functional group(s) promoting cell attachment and growth remains controversial.

Surface carboxyl groups promoted BAEC growth to a significantly greater extent than did the methyl, methyl ester, or hydroxyl groups. In agreement with this finding, carboxyl group content has been associated with improved attachment and growth of various cell lines in several studies [26-28]. Results of the present study and a previous study of BAEC growth on oxygen-containing plasma-deposited films demonstrate little correlation between hydroxyl group content and cell growth. While enhanced cell adhesiveness on hydroxyl-containing surfaces has been reported [11,29], controversy exists as to whether the hydroxyl group, while promoting cell attachment, is also involved in enhancing the subsequent spreading and growth of cells. In a recent review, Horbett and Klumb cite numerous studies demonstrating that cell adhesion and growth are not directly related and conclude that while anchorage-dependent cells require substrate attachment for growth to occur, adhesion alone is not sufficient to ensure cell growth [23].

TCPS and SAMs also differ in surface roughness or surface morphology (TCPS roughness ~5 nm, SAM roughness ~ 1 nm). While the effect of surface roughness on cell growth was not evaluated in this study, it is unlikely that the differences observed between TCPS and the SAMs in cell growth could be attributed solely to morphological differences. While surface roughness of the COOH SAM and TCPS differs by a factor

of 5, cell growth on the COOH SAM in the high-density study approached growth observed on TCPS. Similarly, cell growth differed significantly on the homogeneous SAM substrates, yet their surface roughness is equivalent. If surface morphology or roughness were significantly affecting cell growth, equivalent levels of growth might be expected on substrates of equivalent roughness.

Differences in cell growth response to SAM surface functionality were observed for the two types of cell growth studies performed. In the clonal growth assay, only the COOH SAM was supportive of cell growth, while all SAMs supported cell growth to some extent in the high-density study. The differences observed in cell growth patterns between the two studies are attributed to the initial cell-seeding density. It has been reported that increased cellular Fn deposition occurs at higher cell-seeding density [56]. For the COOH SAM, cellular Fn deposition from cells seeded at low density appears to be sufficient to promote cell attachment and growth due to either the increased affinity of this surface for cellular Fn or the increased amount of initially adsorbed Fn which allows attachment of cells such that cellular Fn can be produced and deposited on this surface. On the OH, CH_3, and CO_2CH_3 SAMs, cellular Fn production from cells seeded at low density appears insufficient to support cell proliferation. At higher seeding densities, increased levels of cellular Fn are probably produced which are above a critical threshold level that allows attachment and growth to occur on these surfaces.

3.4.2 Relating Protein Adsorption to Cell Growth

Alb adsorption to the functionalized SAMs did not differ significantly with surface functionality. The ability of a substrate to support cell growth does not appear to be negatively affected by the adsorption of Alb as evidenced by the superior cell growth observed on the COOH surface which demonstrated the highest level of Alb adsorption. In agreement with this result, other groups have similarly reported that the ability of a

substrate to support cell proliferation does not correlate with a lack of affinity for growth-inhibiting proteins such as Alb [25].

The relative importance of Fn in cell adhesion and growth has been demonstrated to be dependent upon substrate composition and cell type [55]. For oxygen-containing plasma surfaces such as TCPS, Fn does not play an essential role in initial cell attachment. However, TCPS has been shown to adsorb more Fn from serum than does PS, and it has been suggested that the increased Fn adsorption by TCPS contributes to the enhanced cell attachment and spreading observed on TCPS compared with PS [21]. In this study, all SAMs adsorbed levels of Fn typically considered insufficient for cell attachment [86]. However, Fn adsorption was highest on the SAM demonstrating maximal cell growth (COOH) and lowest on SAMs demonstrating poor cell growth (CO_2CH_3 and OH). The CH_3 SAM demonstrated slightly higher Fn adsorption levels than did the CO_2CH_3 and OH SAMs. As was observed for TCPS, the increased amount of Fn adsorbed on the COOH surface relative to the other SAMs may have contributed to an enhanced cell attachment and spreading. While cell attachment and spreading were not directly measured in this study, an increased level of cell attachment and spreading would be expected to result in increased cell growth.

Following initial attachment and spreading, endothelial cells will secrete ECM components such as cellular Fn or collagen onto the substrate, which enhance cell spreading and growth. In addition, the composition of the ECM secreted by endothelial cells has been shown to vary depending on adhesive molecules adsorbed onto the polymer surface with reduced levels of ECM components observed on Vn-coated TCPS compared with Fn-coated TCPS [86]. It has been proposed that substrates exhibiting a high affinity for Fn promote cell spreading and growth by permitting the deposition of cellular Fn onto the substrate surface [56,57]. The enhanced adsorption of Fn onto TCPS is thought to be indicative of an increased affinity of TCPS for Fn, and it has been

suggested that the high Fn affinity of TCPS permits cellular deposition of Fn. Cellular Fn deposition has been demonstrated to occur on TCPS as early as 30 minutes after seeding. In contrast, the retraction and rounding up of EC on PS after 6 hours of spreading have been attributed to an inability of cells on PS to deposit cellular Fn.

The increased Fn adsorption observed on the COOH SAM from a complex solution containing other proteins competing for adsorption sites suggests that the COOH SAM may have a higher affinity for Fn than the other SAM surfaces. In support of this, the COOH surface adsorbed only 13 times as much Alb as Fn, while the OH and CO_2CH_3 SAMs adsorbed at least 30 times as much Alb as Fn. If the Fn affinity of the COOH SAM is higher than that of the other SAMs, cellular Fn deposition may occur to a greater extent on this SAM. As discussed previously, cell growth after seeding at low density was observed on the COOH SAM only. It appears that only the COOH SAM supported the deposition of cellular Fn at a level sufficient to promote cell attachment, spreading, and growth of cells seeded at low density. On poor growth surfaces, the decreased Fn adsorption levels may be indicative of low Fn affinities. Additionally, since ECM component secretion levels have been shown to be dependent upon adsorbed adhesive proteins [86], the poor growth observed on surfaces with a higher Alb/Fn ratio (lower level of adsorbed adhesive molecules) may be indicative of a decreased level of ECM components secreted onto these surfaces which contain a higher surface fraction of nonadhesive molecules.

3.4.3 Relating Protein Elutability to Cell Growth

While the type and amount of protein adsorbed on a substrate will influence cell spreading and growth, the biological activity of the adsorbed proteins may have a more significant impact on cellular interactions. Numerous studies indicate that the ability of an adhesion protein to influence cellular interactions is modulated by the substrate on

which the protein is adsorbed. Modulation of the biological activity of adsorbed proteins by the substrate may result from differences in protein conformation or orientation which can affect the availability and potency of cell-binding domains [19]. Variations in the biological activity of adsorbed proteins may also be related to differences in the binding strength of an adsorbed protein that can affect cellular interactions with the protein or, additionally, can affect the ability of an adsorbed protein to be displaced by other proteins [23]. While some studies suggest that tight protein binding may be conducive to cell attachment and growth [22,60], other studies offer evidence that tight protein binding may not be desirable. Tight binding of a protein to a surface may indicate that conformational or orientational changes have taken place (i.e., partial denaturing of protein) during or after adsorption. Tightly bound proteins are also more resistant to displacement by other serum- or cell-derived proteins.

The removal or elution of adsorbed proteins by SDS was developed as a technique for examining the strength of protein-surface interactions [87]. In the present study, Alb elutability varied significantly with surface functional group. Alb elutability was significantly lower on surfaces exhibiting poor cell growth characteristics, the CO_2CH_3 and OH SAMs, than on the best cell growth surface, the COOH SAM. Alb elutability of the CH_3 SAM was lower than that of the COOH SAM yet higher than that of the CO_2CH_3 and OH SAMs. The low elutability (tight binding) of Alb on the CO_2CH_3 and OH SAMs suggests that Alb bound on these SAMs is resistant to displacement by other serum- or cell-derived proteins during initial cell attachment periods and later during cell spreading and growth phases. The poor growth observed on these SAMs might result from an inability of adsorbed Alb to be displaced by other proteins which facilitate growth. In contrast, Alb adsorbed to the COOH SAM is weakly held (high elutability) and therefore would likely be more easily displaced by other proteins promoting cell growth. While the OH and COOH SAMs adsorb similar

amounts of Alb, their cell growth characteristics differ significantly, which may result, in part, from the increased displaceability of Alb bound to the COOH SAM.

The elutability of Fn also varied with SAM surface functionality; however, the differences were not significant. As was observed for Alb, Fn elutability was higher on the COOH and CH_3 SAMs than on the CO_2CH_3 and OH SAMs. The low elutability (tight binding) of Fn on the CO_2CH_3 and OH SAMs suggests that Fn bound on these SAMs is more resistant to displacement by cell-derived proteins and/or other growth-promoting serum proteins such as Vn. Low elutabilities may also suggest that conformational or orientational changes have taken place (i.e., partial denaturing of protein) during or after adsorption. Since endothelial cell adhesion would be affected by conformational changes in adsorbed Fn, the poor growth observed on the CO_2CH_3 and OH SAMs may partially result from conformational changes occurring in Fn adsorbed to these surfaces which act to decrease cell adhesion and/or growth. In support of this, specific chemical functionalities have been demonstrated to modulate Fn functions for cell adhesion by affecting the conformation of bound Fn [68].

3.5 Conclusions

BAEC growth varied significantly in response to the presence of different chemical functionalities present on the monolayer surfaces. Surface COOH groups promoted BAEC spreading and growth to a significantly greater extent than did the CH_3, CO_2CH_3, or OH groups. Protein interaction studies demonstrated variations in Alb and Fn adsorption and elutability in response to SAM terminal functional group. Alb adsorption and Fn elutability did not differ significantly with terminal functional group. The best cell growth substrate (COOH SAM) demonstrated significantly higher Fn adsorption and Alb elutability than did the poor growth substrates (CO_2CH_3 and OH SAMs). The CH_3 SAM exhibited high Alb elutability and low Fn adsorption.

Substrates adsorbing higher levels of Fn and demonstrating high Alb elutabilities (i.e., the COOH SAM) may encourage cell growth by permitting the subsequent adsorption of cell-derived ECM proteins or other serum proteins which promote cell spreading and growth onto, or after displacement of, the initially adsorbed protein layer. The poor cell growth characteristics observed on the CO_2CH_3 and OH SAMs may result from the combined effect of reduced Fn adsorption and decreased elutability of adsorbed Alb. While Alb elutability was high on the CH_3 SAM, lower Fn adsorption levels may have contributed to the decreased cell growth observed on this surface relative to the COOH SAM.

This study makes important contributions to the understanding of cell growth on solid surfaces in that the protein layer adsorbed from a complex solution is quantitatively assessed and related to endothelial cell growth on well-characterized SAMs to evaluate the effect of surface chemistry on biological interactions. Cell growth cannot be correlated with any one aspect of the adsorbed protein layer. Rather, many factors contribute to the promotion or inhibition of cell growth, i.e., the amount and type of protein adsorbed, protein-binding strength, and the adsorbed protein conformation and/or orientation. To further correlate cell growth with adsorbed protein layer characteristics, additional factors must be evaluated such as the amount and binding strength of Vn and the conformation/orientation of adsorbed adhesive proteins such as Fn and Vn.

Table 3.1 XPS and Contact Angle Analysis of Chemically Homogeneous SAMs

		Elemental Composition (atom percent)[1]			
SAM Terminal Group	***Contact Angle***	***Carbon***	***Gold***	***Sulfur***	***Oxygen***
OH	17°	63.1 ± 2.5	26.9 ± 1.8	1.7 ± 0.5	8.4 ± 1.9
COOH	21°	64.2 ± 1.0	21.9 ± 1.5	1.4 ± 0.2	12.5 ± 0.7
CO_2CH_3	65°	63.8 ± 2.4	24.4 ± 0.5	1.4 ± 0.2	10.4 ± 0.4
CH_3	109°	68.8 ± 2.7	28.7 ± 1.9	1.7 ± 0.3	0.8 ± 0.6

[1] Data represent mean ± standard deviation for triplicate samples in duplicate experiments.

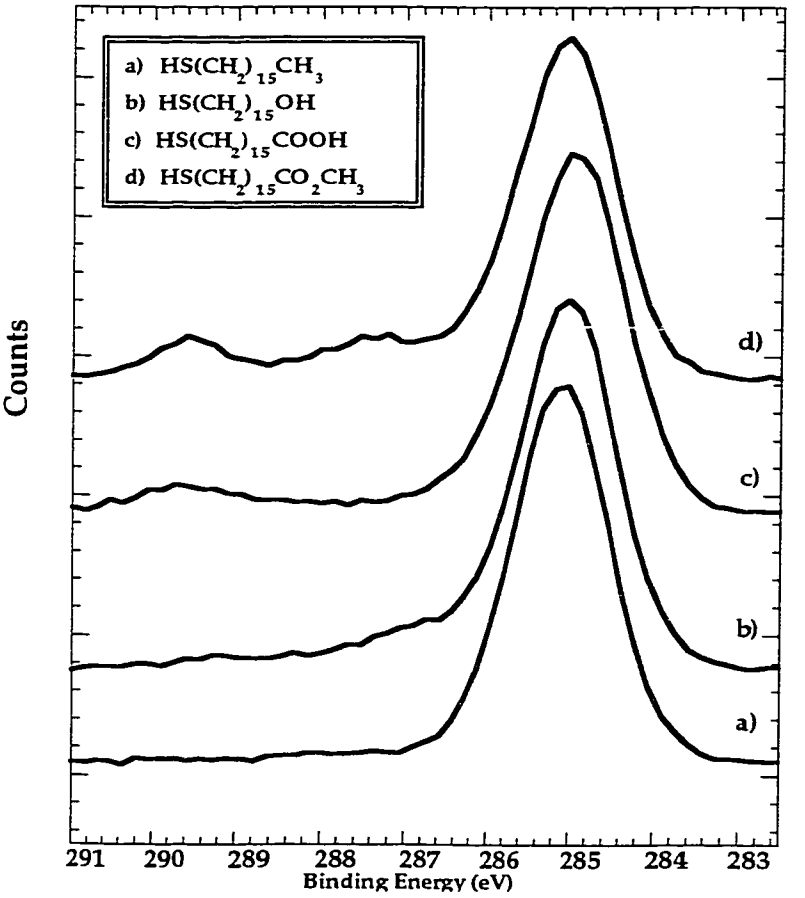

Figure 3.1 Representative XPS Carbon 1s spectra of a) methyl, b) hydroxyl, c) carboxyl, and d) methyl ester-terminated $HS(CH_2)_{15}X$ SAMs on gold obtained at a take-off angle of 55°.

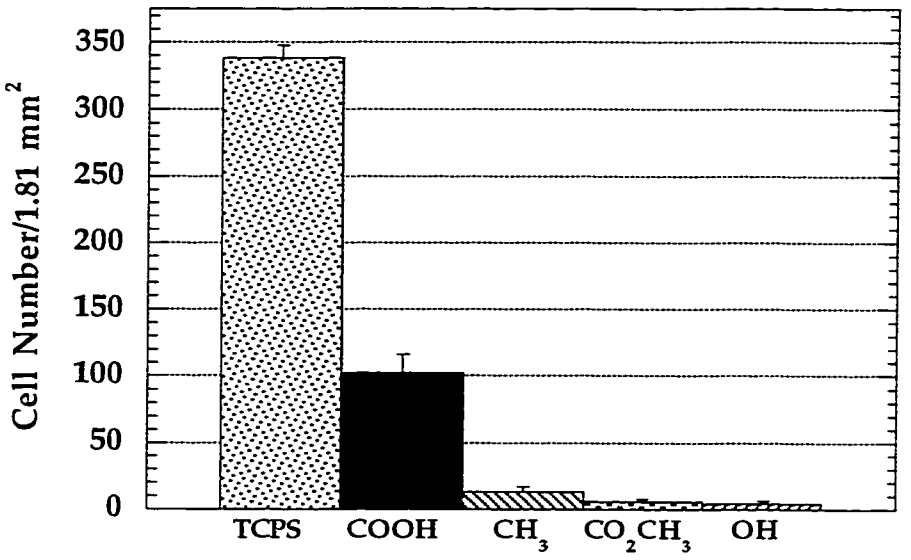

Figure 3.2 BAEC growth on COOH, CH_3, CO_2CH_3 and CH_2OH-terminated $X(CH_2)_{15}SH$ SAMs; and on TCPS. Cells were cultured for 3 days in medium containing 10% bovine serum. Cell number was determined by counting total number of cells on each 15 mm diameter sample (surface area = 1.81 cm^2). Data represent mean ± SEM for triplicate samples in duplicate experiments.

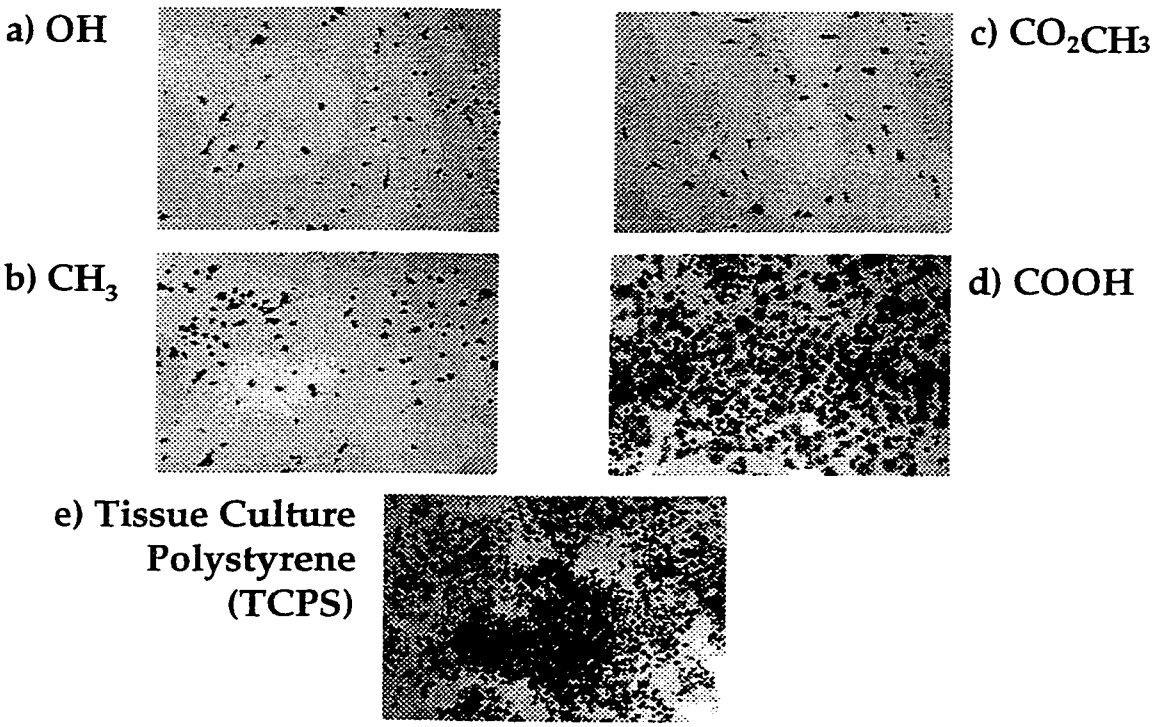

Figure 3.3 BAEC on a) CH_2OH, b) CO_2CH_3, c) CH_3, and d) COOH-terminated $X(CH_2)_{15}SH$ SAMs on gold, and e) TCPS after 5 days of culture. Cells were seeded at a density of 2500 cells/well or 1200 cells/cm^2 and cultured in medium containing 10% bovine serum.

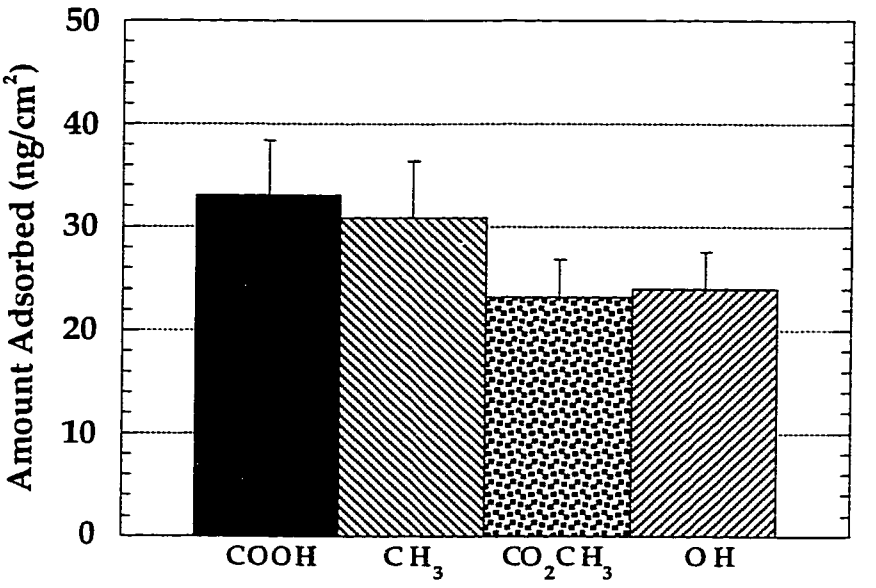

Figure 3.4 Effect of surface functional group on Alb adsorption to COOH, CH_3, CO_2CH_3 and CH_2OH-terminated $X(CH_2)_{15}SH$ SAMs. Alb was adsorbed from 10% bovine serum for 2 hours at 37°C. Data represent mean ± SEM for triplicate samples in duplicate experiments.

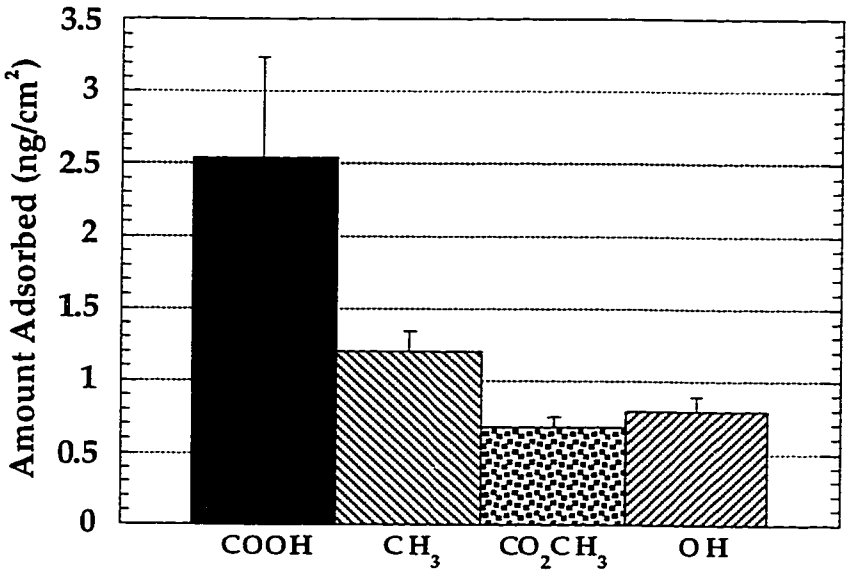

Figure 3.5 Effect of surface functional group on Fn adsorption to COOH, CH_3, CO_2CH_3 and CH_2OH-terminated $X(CH_2)_{15}SH$ SAMs. Fn was adsorbed from 10% bovine serum for 2 hours at 37°C. Data represent mean ± SEM for triplicate samples in duplicate experiments.

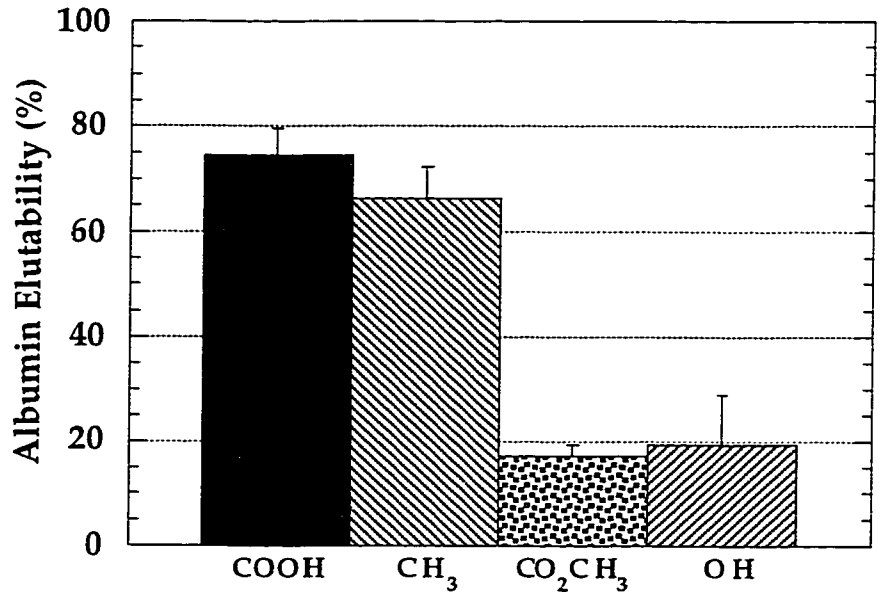

Figure 3.6 Effect of surface functional group on Alb elutability from COOH, CH_3, CO_2CH_3 and CH_2OH-terminated $X(CH_2)_{15}SH$ SAMs. Alb was adsorbed from 10% bovine serum for 2 hours at 37°C. Adsorbed Alb was eluted in a 3% SDS solution for 24 hours. Percent elutability is the fraction of initially adsorbed protein that is removed by SDS. Data represent mean ± SEM for triplicate samples in duplicate experiments.

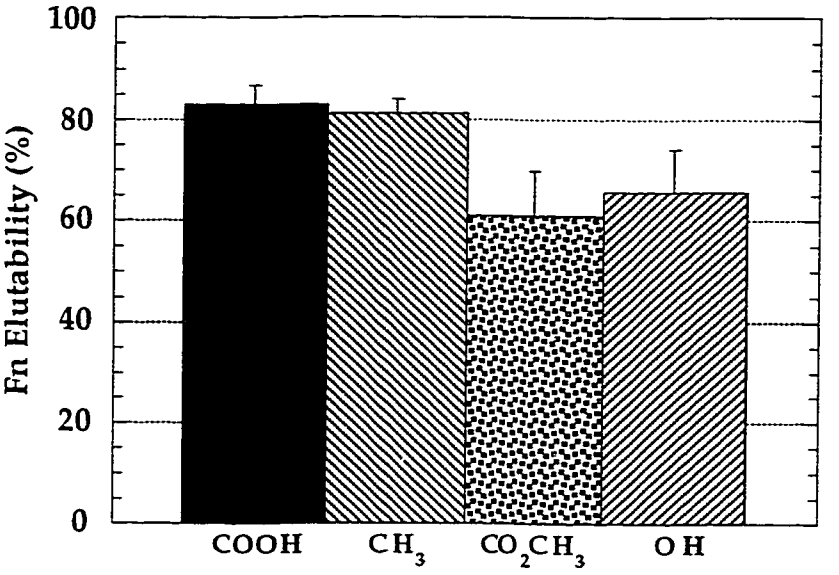

Figure 3.7 Effect of surface functional group on Fn elutability from COOH, CH_3, CO_2CH_3 and CH_2OH-terminated $X(CH_2)_{15}SH$ SAMs. Fn was adsorbed from 10% bovine serum for 2 hours at 37°C. Adsorbed Fn was eluted in a 3% SDS solution for 24 hours. Percent elutability is the fraction of initially adsorbed protein that is removed by SDS. Data represent mean ± SEM for triplicate samples in duplicate experiments.

Chapter 4

Preliminary Studies of Endothelial Cell Growth and Serum Protein Adsorption on Chemically Heterogeneous SAMs

4.1 Introduction

In studies of homogeneous SAMs (Chapter 3), it was observed that cell growth on the homogeneous SAMs was generally lower than cell growth on TCPS, particularly in the clonal growth study, and to a lesser extent in the high seeding density growth study. The increased cell growth observed on TCPS relative to the terminally functionalized monolayer surfaces is an important finding. Cell culture substrates (such as TCPS) are commonly fabricated by gas plasma (glow discharge) surface treatments or by plasma-polymerization of a monomer onto the substrate surface to achieve a desired surface chemistry that renders the substrate more conducive to cell attachment and growth. Polymer surfaces that promote cell growth are chemically complex and typically involve multiple chemical functionalities. Our observation of increased cell growth on TCPS relative to the homogenous SAM surfaces leads to the hypothesis that the presence of multiple chemical functionalities in certain proportions may be desirable for the promotion of cell attachment and growth. Several groups have similarly suggested the importance of substrate chemical complexity in biointeractions. Jozefonvicz et al. have introduced mixtures of chemical functional groups in various proportions into polymers and have obtained materials whose "bioactivity" approaches that of natural polymers such as heparin [88]. These polymers are believed to contain arrays of substituents that mimic chemical functional group arrays in natural biomolecules and therefore, behave as "bioactive" polymers. TCPS may act in this way also. Horbett has postulated that specific cell responses (i.e., adhesion, spreading and growth) occur more readily on some polymers than others due to the existence of an array of chemical functional groups

on the polymer which resembles the array of surface chemical groups present in the natural ECM of the cell *in vivo* [23].

To investigate the effect of increasing the chemical complexity of a surface on protein adsorption and cell growth, a preliminary study was performed utilizing two series of chemically heterogeneous or binary composition "mixed" SAMs. The first mixed SAMs series was prepared by the simultaneous adsorption of $CH_2OH(CH_2)_{15}SH$ and $CO_2H(CH_2)_{15}SH$ with target surface concentration ratios of 3:1, 1:1, and 1:3. The second mixed SAM series was prepared by the simultaneous adsorption of $CH_3(CH_2)_{15}SH$ and $CO_2H(CH_2)_{15}SH$ with target surface concentration ratios of 3:1, 1:1, and 1:3. The purposes of this preliminary study of chemically heterogeneous SAMs were: 1) to investigate methods for preparing binary SAMs that varied in surface functional group content, 2) to determine whether variations in functional group content would affect endothelial cell growth and. 3) to evaluate the effect of surface functional group content on the adsorbed protein layer.

4.2 Materials and Methods

Gold-coated Si wafers were prepared as substrates for SAM formation as described in Section 2.2. Gold-coated substrates were immersed into binary ethanolic solutions (1 mM total) of n-alkanethiols terminated with the desired functionality for approximately 48 hours. Alkanethiols were synthesized as previously described [72]. The binary SAMs were prepared as listed in Table 4.1. Binary solution mixture ratios were chosen in accordance with values published by Bain et al. to obtain surface molar fractions ranging from 0 to 1 [89]. The remainder of the SAM preparation procedure was performed as described in Section 2.2.

Binary SAMs were characterized by ellipsometry, contact angle, and XPS, and TOF-SIMS as described in Section 2.3. Cell culture and preparation for cell growth

studies was performed as described in Section 2.4. Triplicates of each mixed SAM were used in a clonal growth study that was performed as described in Section 2.5.1. The second type of cell growth study performed using the binary SAMs involved seeding at a higher density and culture for 3, 5, and 7 day periods followed by qualitative evaluation of cell density and morphology. In the high density study, cells were seeded at a density of 2660 cells/cm^2 (5000 cells/well) onto the binary SAM surfaces and cultured for 3, 5, or 7 days (n=1 for each type of substrate at each time point). TCPS was used as a control surface. Following the designated culture period, SAM substrates were rinsed, fixed and stained as described in Section 2.5.1. A representative area of each SAM was examined and photographed using reflected light microscopy.

4.3 Results and Discussion

4.3.1 Surface Analysis of COOH/OH and CH$_3$/COOH SAMs

Results of contact angle and XPS studies of COOH/OH and CH$_3$/COOH SAMs were consistent with expected surface composition values and are presented in Chapter 5 (Sections 5.3.1 and 5.3.3). To obtain quantitative information regarding the surface content of each thiol, the binary SAMs were analyzed by TOF-SIMS in collaboration with Dr. Anna Belu. The negative ion mode of TOF-SIMS has typically been used to characterize alkanethiols on gold due to the presence of molecular ion signals with significant intensities in the resulting spectra. The high mass range of the negative ion spectrum of an alkanethiol SAM on gold contains signals from the gold substrate (gold cluster ions and gold/sulfur cluster ions), the intact thiol, and clusters of gold atoms with thiol molecules. Figure 4.1 shows a select region in the high mass range of the negative TOF-SIMS spectra for the COOH/OH binary SAMs. The top spectrum shows results from the homogeneous HS(CH$_2$)$_{15}$CH$_2$OH SAM. The strongest molecular ion (M) signal is observed for the HS(CH$_2$)$_{15}$CH$_2$OH thiol with the loss of a proton and the

adduct of two gold atoms ($Au_2(M-H)^-$). The peak at 667 m/z indicates the $HS(CH_2)_{15}CH_2OH$ molecular ion cluster ($Au_2(M-H)^-$). The bottom spectrum shows results from the homogeneous carboxyl-terminated SAM with the $HS(CH_2)_{15}COOH$ molecular ion cluster indicated at 681 m/z. The three spectra in between show results from the COOH/OH binary SAMs with surface concentrations of 25%, 50%, and 75% COOH thiol. In these spectra, the $Au_2(M-H)^-$ ions for each of the thiols are observed. It is important to note however, that the intensity of the $Au_2(M-H)^-$ peak does not correspond directly to the quantity of molecules of the binary SAM surface.

The 50% COOH/50%OH SAM (center spectrum) has a 1:1 surface composition of the thiol molecules. However, the TOF-SIMS molecular ion cluster peak areas are not proportional. Since other methods (ellipsometry and XPS) have confirmed complete monolayer coverage for each of the binary SAMs, the differences in peak intensity of the molecular ions by TOF-SIMS is believed to result from differences in secondary ion yield. The different chemical composition of the thiols in the binary SAMs results in differing secondary ion yields in the TOF-SIMS experiment. To quantify thiol content on the binary SAM surface, a sensitivity factor must first be calculated for each thiol. The sensitivity factor is calculated from the homogeneous thiol sample by ratioing the molecular ion cluster signal to a gold substrate cluster signal. Once the sensitivity factor is taken into account for the differences in secondary ion yields of the molecular species, the thiol surface concentration can be calculated by ratioing the areas of the $Au_2(M-H)^-$ signals for each of the thiols.

After taking into consideration the sensitivity factors for each homogeneous thiol, the expected relative intensity as a function of surface composition can be modeled for the COOH/OH binary SAMs (Figure 4.2). Data obtained from the COOH/OH SAMs are in close agreement with expected results as indicated by the solid lines (Figure 4.2). The surface compositions of the CH_3/COOH SAMs were similarly evaluated by TOF-SIMS.

Figure 4.3 illustrates the expected relative intensity as a function of surface composition for the CH_3/COOH series. Data obtained for the CH_3/COOH SAM series is in close agreement with expected results as shown in Figure 4.3.

These results indicate that it is possible to quantify thiol mixtures comprised of differing terminal groups, with high accuracy once sensitivity factors from homogeneous SAMs are taken into consideration. The molecular specificity of TOF-SIMS is particularly important for the characterization of binary SAM systems. TOF-SIMS is especially advantageous for quantifying mixtures of molecules that do not have a distinct chemical species. Since molecular ions can be observed by TOF-SIMS, no distinct chemical functionality is necessary for quantification as is required with other methods such as XPS or FTIR. For example, quantification of the surface concentration of binary SAMs of similar composition but differing chain lengths (i.e., mixed length SAMs) is very difficult with methods such as XPS or FTIR but is relatively straightforward with TOF-SIMS.

4.3.2 BAEC Growth on COOH/OH Binary SAMs

BAEC were seeded at low density onto COOH/OH binary SAM substrates and TCPS and cultured for 3 days. Cell response was characterized by determining the total number of cells on each type of surface after the 3 day culture period (Figure 4.4). When seeded at low density, cell growth on TCPS was significantly higher than that on any of the binary COOH/OH SAMs (See Figure 3.2, TCPS not shown in Figure 4.4). As was observed in Chapter 3, the OH SAM exhibited poor cell growth. Cell growth improved significantly with the addition of the COOH functionality to the OH SAM. Cell number increased gradually with increasing COOH surface fraction. Cell growth was slightly higher on the 100% COOH SAM than on the 75% COOH SAM however,

the difference was not significant. Cell growth on the 100% COOH and the 75% COOH surfaces was significantly higher than that on the OH SAM.

BAEC density and morphology on the COOH/OH binary SAMs and TCPS following seeding at higher density were evaluated qualitatively after 3, 5, and 7 day culture periods. Figure 4.5 shows cell density after the 3 day culture period on the COOH/OH binary SAM surfaces. As was observed in Chapter 3, the OH SAM demonstrated the lowest cell density and the majority of cells on this surface did not show evidence of spreading. A significant increase in cell density was observed for the binary SAM surface containing 25% COOH groups. Given the poor cell growth performance of the homogeneous OH surface, it is remarkable that a 25% surface COOH concentration is sufficient to result in a significant improvement in cell growth. Cell density on the 50% COOH surface and the 75% COOH surfaces appeared to approach or exceed cell growth on the 100% COOH surface and on TCPS. Similar trends were observed for this series following 5 days (Figure 4.6) and 7 days (not shown) of growth. After 5 days of culture, all COOH-containing SAMs demonstrated an essentially confluent monolayer of cells. Comparing cell growth on the COOH-containing SAMs with cell growth on TCPS after 3 and 5 days of culture, a similar cell density and morphology was observed on the COOH-containing SAMs as on TCPS.

Results of both the 3 day clonal growth study and the higher density 3 and 5 day growth studies indicate a significant improvement in cell growth in response to the addition of the COOH functionality to the OH SAM. The results indicate that distinct differences in cell growth are observed in response to the SAM functional group concentration as well as functional group type. A COOH group surface concentration of as low as 25% resulted in a significant increase in cell growth. It appears that the addition of a small amount of a growth-promoting functional group can "rescue" the growth characteristics of a poor growth substrate. Results of this study suggest that a

surface COOH concentration much lower than 25% would be sufficient to promote cell growth on a binary COOH/OH surface. Further studies are needed to determine the minimum concentration of growth-promoting functional group required to promote a specific level of growth.

The purpose of this study was to investigate the effect of increasing the surface chemical complexity on cell growth. The binary COOH/OH SAMs demonstrated significantly improved cell growth compared to the homogeneous OH surface in both the low density and high density studies. In the clonal growth study, cell growth on the binary SAMs was lower than on the homogeneous COOH surface. However, in the high density study, growth on some of the binary SAMs approached or exceeded growth on the homogeneous COOH surface. While it appears that growth on chemically complex surfaces is superior to that on a homogeneous poor growth substrate, additional quantitative, high density studies are needed to determine if growth on chemically complex surfaces can exceed that on a growth-promoting homogeneous surface such as the COOH SAM. These results suggest however, that by varying surface chemical complexity, it is possible to promote or inhibit specific biological responses.

In the high density study, it was also observed that cell density on some of the COOH/OH mixtures appears to approach or exceed that on TCPS. This finding is significant in that growth levels on the majority of synthetic biomaterial surfaces are typically less than those observed on TCPS, a standard cell culture substrate. Results of this study suggest that it may be possible to create a surface which provides better cell growth characteristics than TCPS using binary or possibly tertiary SAMs containing an combination of functional groups which result in optimal cell growth. The ability to create a cell culture substrate with a well-defined substrate chemistry would be beneficial since the surface chemistry of most cell culture substrates is poorly defined and difficult to control.

4.3.3 BAEC Growth on CH_3/COOH Binary SAMs

BAEC were seeded at low density onto CH_3/COOH binary SAMs and TCPS, and cultured for 3 days. Cell response was characterized by determining the total number of cells on each type of surface after the 3 day growth period (Figure 4.7). Cell growth on TCPS, a standard cell growth substrate, was significantly higher than that on any of the CH_3/COOH SAMs (see Figure 3.2, TCPS not shown in Figure 4.7). For the binary SAMs, cell number increased with increasing surface COOH group concentration. Cell growth on the 75% COOH surface was slightly higher than that on the 100% COOH surface. As was observed in Chapter 3, the CH_3 SAM exhibited low cell growth, very few cells were observed on this surface. Cell growth improved with the addition of the COOH functionality to the CH_3 SAM. Cell growth on surfaces containing a surface COOH concentration of 50% or more were significantly higher than that on the homogeneous CH_3 SAM.

BAEC density and morphology on the CH_3/COOH binary SAMs and TCPS following seeding at higher density was evaluated qualitatively after 3, 5, and 7 day culture periods. Figure 4.8 shows cell density after the 3 day culture period on the CH_3/COOH SAMs. As was observed previously, the homogeneous CH_3 SAM demonstrated a lower cell density than did the homogeneous COOH surface. As the COOH surface content increased, cell density increased. After 3 days of culture, the 25% COOH surface showed a higher cell density than did the CH_3 surface. Cell density was significantly higher on surfaces containing a 50% or more surface COOH content. Similar trends were observed for this series following 5 days (Figure 4.9) and 7 days (not shown) of growth. Cell density on the 50% COOH surface and the 75% COOH surfaces appeared to approach or exceed cell growth on the 100% COOH surface and on TCPS. Results of both the 3 day clonal growth study and the higher density 3 and 5 day

growth studies indicate a significant improvement in cell growth in response to the addition of the COOH functionality to the CH_3 SAM.

Comparing the COOH/OH series to the CH_3/COOH series, cell density on the CH_3/COOH series in general, was lower than that observed on the COOH/OH series. For the COOH/OH series, a COOH surface concentration of only 25% was sufficient to promote cell growth to a level similar to that achieved on the 100% COOH surface. However, for the CH_3/COOH series, at least a 50% COOH content was required to promote cell growth to levels observed on the 100% COOH surface. After 5 days of culture, the 50% and 75% CH_3/COOH SAMs demonstrated an essentially confluent monolayer of cells, while the 25% CH_3/COOH SAM did not.

The differences observed in cell growth patterns between the COOH/OH SAMs and the CH_3/COOH SAMs are interesting. Since the CH_3 surface had demonstrated slightly better cell growth characteristics compared with the homogeneous OH surface in studies of homogeneous SAMs, it was anticipated that cell growth on the CH_3/COOH series would exceed that on the COOH/OH series. These results may reflect differences in the spatial arrangement of the functional groups for the two types of binary surfaces. It is possible that phase separation is occurring on the CH_3/COOH surfaces resulting in the formation of domains of each functional group. In the COOH/OH series, it is more likely that the functional groups would be randomly distributed on the surface of the binary SAM. The differences observed in cell growth between the CH_3/COOH SAMs and the COOH/OH SAMs may be due to an effect of functional group spatial arrangement on the adsorbed protein layer and consequently, on endothelial cell growth. Thus, both surface functional group concentration and functional group spatial arrangement may influence the endothelial cell growth characteristics of a substrate.

4.3.4 Albumin and Fibronectin Adsorption from 10% Serum to COOH/OH SAMs

The adsorption of albumin and fibronectin from 10% serum to the COOH/OH binary SAM substrates is shown in Figures 4.10 and 4.11. As was observed for the homogeneous SAMs, slight differences were observed in the amount of Alb adsorbed in response to the COOH surface concentration however, the differences were not significant (Figure 4.10). Alb surface density ranged from 17 ng/cm^2 on the 25% COOH SAM to 33 ng/cm^2 on the COOH SAM. Alb surface density did not correlate with surface COOH concentration. Consistent with previous results (Chapter 3), Alb adsorption does not appear to correlate with surface cell growth characteristics as similar Alb surface densities were observed on SAMs exhibiting significant differences in cell growth (i.e., the OH SAM and the 100% COOH SAM). As observed for the homogeneous SAMs, the ability of a substrate to support cell growth was not negatively affected by the amount of Alb adsorbed. Alb adsorption was highest on the COOH SAM and lowest on the 25% COOH SAM yet, both surfaces demonstrated good cell growth.

Fn adsorption from 10% serum varied significantly between the OH SAM and the COOH-containing SAMs (Figure 4.11). Fn surface density ranged from 2.7 ng/cm^2 on the 75% COOH SAM to 0.8 ng/cm^2 on the OH SAM. Fn adsorption was independent of COOH surface concentration as all COOH-containing SAMs adsorbed essentially equivalent amounts of Fn. As observed in Chapter 3, the amount of Fn adsorbed to the SAM surfaces from 10% serum was significantly lower than the amount of Alb adsorbed. Fn adsorption was significantly higher on the COOH and the binary OH/COOH surfaces than on the OH surface. As observed in Chapter 3, Fn adsorption results paralleled cell growth results, with good cell growth observed on the OH/COOH binary surfaces and the COOH surface. These results may further support the suggestion that higher Fn adsorption observed on good cell growth surfaces might

indicate an increased affinity of these surfaces for Fn or cellular Fn that promotes cell growth.

4.3.5 Albumin and Fibronectin Elutability after Adsorption from 10% Serum

The elutability of Alb adsorbed to the binary SAM surfaces following a 24 hour exposure to 3% SDS solution is shown in Figure 4.12. Alb elutability was highest on the 100% COOH SAM and lowest on the OH SAM. Alb elutability on the COOH/OH SAMs was moderate and did not vary significantly with COOH surface concentration. Alb elutabilities were higher on the COOH/OH SAMs than on the OH SAM. However, the differences were not significant.

In Chapter 3, it was observed that Alb elutability was significantly higher on growth-promoting surfaces than on poor growth surfaces. In the present study, cell growth on the COOH and the COOH/OH SAMs was high, yet Alb elutabilities on the COOH/OH SAMs were lower than on the COOH SAM and not significantly higher than on the OH SAM. These results may suggest that there is a minimum Alb elutability (i.e., a threshold level) above which growth is facilitated since sufficient Alb can be displaced from a substrate. For substrates with elutabilities below such a minimum Alb elutability, growth may be inhibited since enough adsorbed Alb cannot be displaced.

Higher Fn elutabilities were observed on the OH and COOH SAMs than on the COOH/OH binary SAMs (Figure 4.13). Fn elutability did not correlate with surface COOH concentration. As was observed for the homogeneous SAMs, there does not appear to be a correlation between cell growth and Fn elutability. Fn elutability was highest on the COOH SAM and lowest on the 50% COOH SAM, yet both surfaces demonstrated excellent cell growth.

4.4 Conclusions

Two chemically heterogeneous binary SAM series were prepared by the simultaneous adsorption of $HS(CH_2)_{15}CH_2OH$ and $HS(CH_2)_{15}CO_2H$ or $HS(CH_2)_{15}CH_3$ and $HS(CH_2)_{15}CO_2H$ alkanethiols on gold in varying proportions to achieve target surface concentration ratios of 3:1, 1:1, and 1:3. In clonal growth studies, endothelial cell growth increased with COOH surface concentration for both the COOH/OH series and the CH_3/COOH series. In high seeding density studies, cell density on binary SAMs with a surface COOH concentration of 50% or higher appeared to approach or exceed growth on the homogeneous COOH surfaces. These results suggest cell growth is influenced by surface functional group concentration and that chemically heterogeneous surfaces may result in improved cell growth characteristics compared with chemically homogeneous surfaces. Additional quantitative, high density studies are required to determine if growth on chemically heterogeneous surfaces can exceed that on a growth-promoting homogeneous surface such as the COOH SAM.

In high seeding density studies, we observed unexpected differences in cell growth between the COOH/OH series and the CH_3/COOH series. In general, cell growth was lower on the CH_3/COOH SAMs than on the COOH/OH SAMs at the same COOH surface concentration. As it is likely that the CH_3/COOH SAMs would exhibit more phase separation than would the COOH/OH SAMs, we propose that the observed differences may reflect differences in cellular response to the spatial arrangement of functional groups on the binary SAM surfaces. These results may suggest an effect of functional group spatial arrangement and degree of phase separation on endothelial cell growth in addition to the effect of functional group concentration.

Protein interaction studies with the COOH/OH SAMs demonstrated variations in Alb and Fn adsorption and elutability in response to SAM surface composition. Relationships between cell growth and adsorbed protein layer characteristics were

observed. Surfaces promoting cell growth (the COOH and the binary COOH/OH SAMs) demonstrated moderate to high albumin elutabilities and higher levels of Fn adsorption than did substrates inhibiting cell growth (the OH SAM). As discussed in Chapter 3, substrates adsorbing higher levels of Fn and demonstrating higher Alb elutabilities (decreased Alb binding strength) might encourage cell growth by permitting subsequent adsorption of cell derived or other adhesive proteins which promote cell spreading and growth onto, or after displacement of, the initially adsorbed protein layer.

Table 4.1

Composition of Thiol Solutions Used for Preparation of Binary SAMs

Thiol A	*Thiol B*	*Solution Fraction of Thiol A*	*Surface Fraction of Thiol A*
$HS(CH_2)_{15}CO_2H$	$HS(CH_2)_{15}CH_2OH$	0	0
$HS(CH_2)_{15}CO_2H$	$HS(CH_2)_{15}CH_2OH$	0.25	0.25
$HS(CH_2)_{15}CO_2H$	$HS(CH_2)_{15}CH_2OH$	0.50	0.50
$HS(CH_2)_{15}CO_2H$	$HS(CH_2)_{15}CH_2OH$	0.75	0.75
$HS(CH_2)_{15}CO_2H$	$HS(CH_2)_{15}CH_2OH$	1.0	1.0
$HS(CH_2)_{15}CO_2H$	$HS(CH_2)_{15}CH_3$	0	0
$HS(CH_2)_{15}CO_2H$	$HS(CH_2)_{15}CH_3$	0.50	0.25
$HS(CH_2)_{15}CO_2H$	$HS(CH_2)_{15}CH_3$	0.70	0.50
$HS(CH_2)_{15}CO_2H$	$HS(CH_2)_{15}CH_3$	0.90	0.75
$HS(CH_2)_{15}CO_2H$	$HS(CH_2)_{15}CH_3$	1.0	1.0

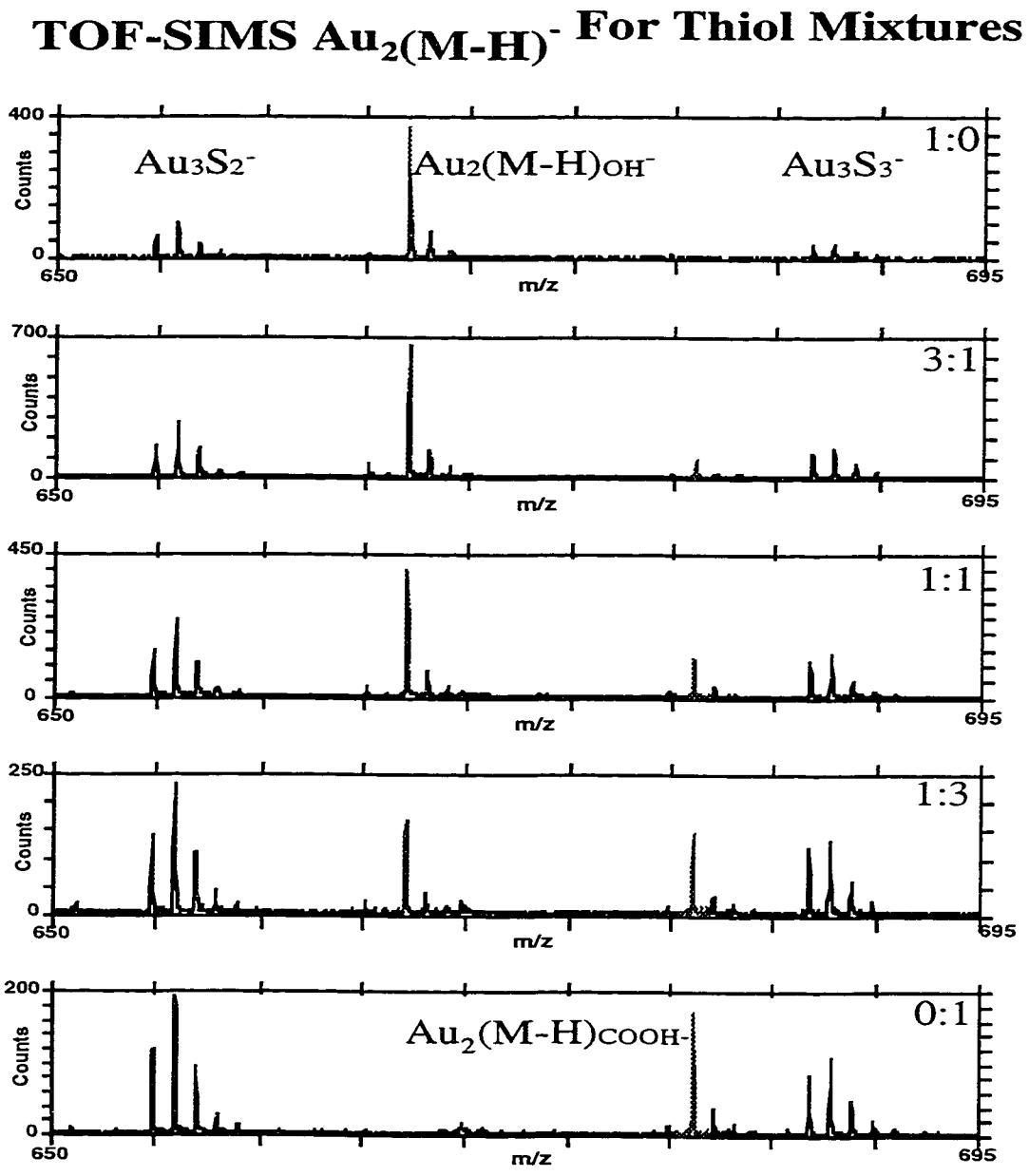

Figure 4.1 Negative ion static SIMS spectra of binary composition SAMs of $HS(CH_2)_{15}CH_2OH$ and $HS(CH_2)_{15}COOH$ containing a) 100% OH thiol, b) 75% OH/25% COOH, c) 50% OH/50% COOH, d) 25% OH/75% COOH, and e) 100% COOH thiol.

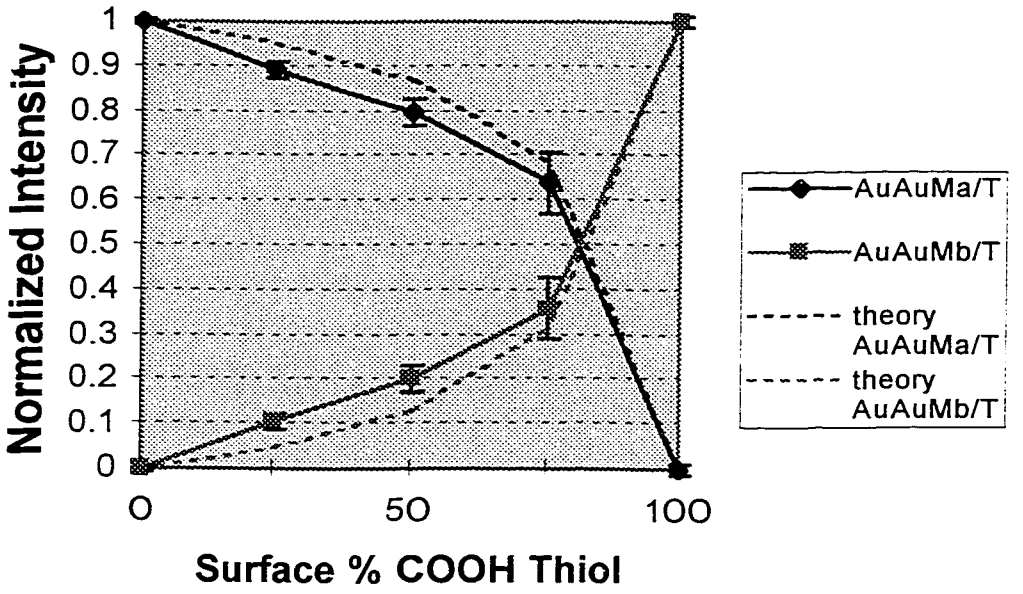

Figure 4.2 Normalized molecular ion cluster peak intensity of $HS(CH_2)_{15}CH_2OH$ (◆) and $HS(CH_2)_{15}COOH$ (■) for binary composition SAMs of $HS(CH_2)_{15}CH_2OH$ and $HS(CH_2)_{15}COOH$ as a function of surface COOH content. Dashed lines represent expected relative molecular ion cluster peak intensity. Data represent mean ± SEM for triplicate samples.

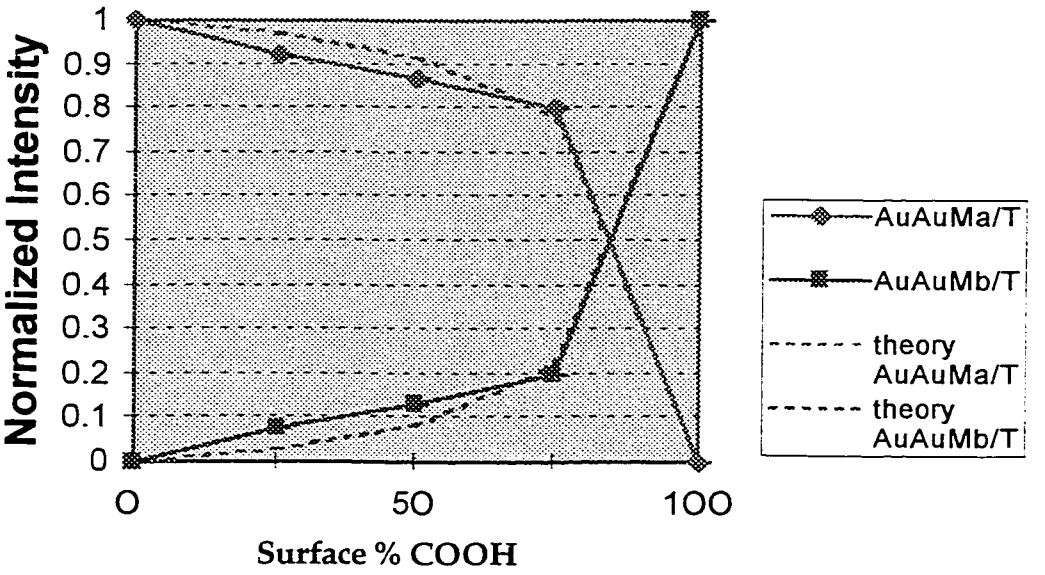

Figure 4.3 Normalized molecular ion cluster peak intensity of $HS(CH_2)_{15}CH_3$ (◆) and $HS(CH_2)_{15}COOH$ (■) for binary composition SAMs of $HS(CH_2)_{15}CH_3$ and $HS(CH_2)_{15}COOH$ as a function of surface COOH content. Dashed lines represent expected relative molecular ion cluster peak intensity. Data represent mean ± SEM for triplicate samples.

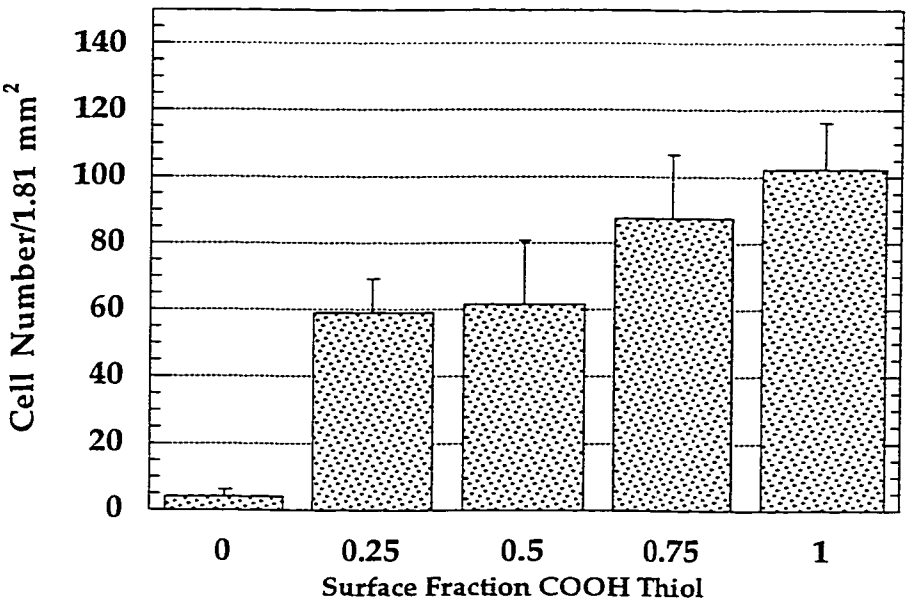

Figure 4.4 BAEC growth on binary composition SAMs of $HS(CH_2)_{15}CH_2OH$ and $HS(CH_2)_{15}COOH$. Cells were cultured for 3 days in medium containing 10% bovine serum. Cell number was determined by counting total number of cells on each 15 mm diameter sample (surface area = 1.81 cm^2). Data represent mean ± SEM for triplicate samples in duplicate experiments.

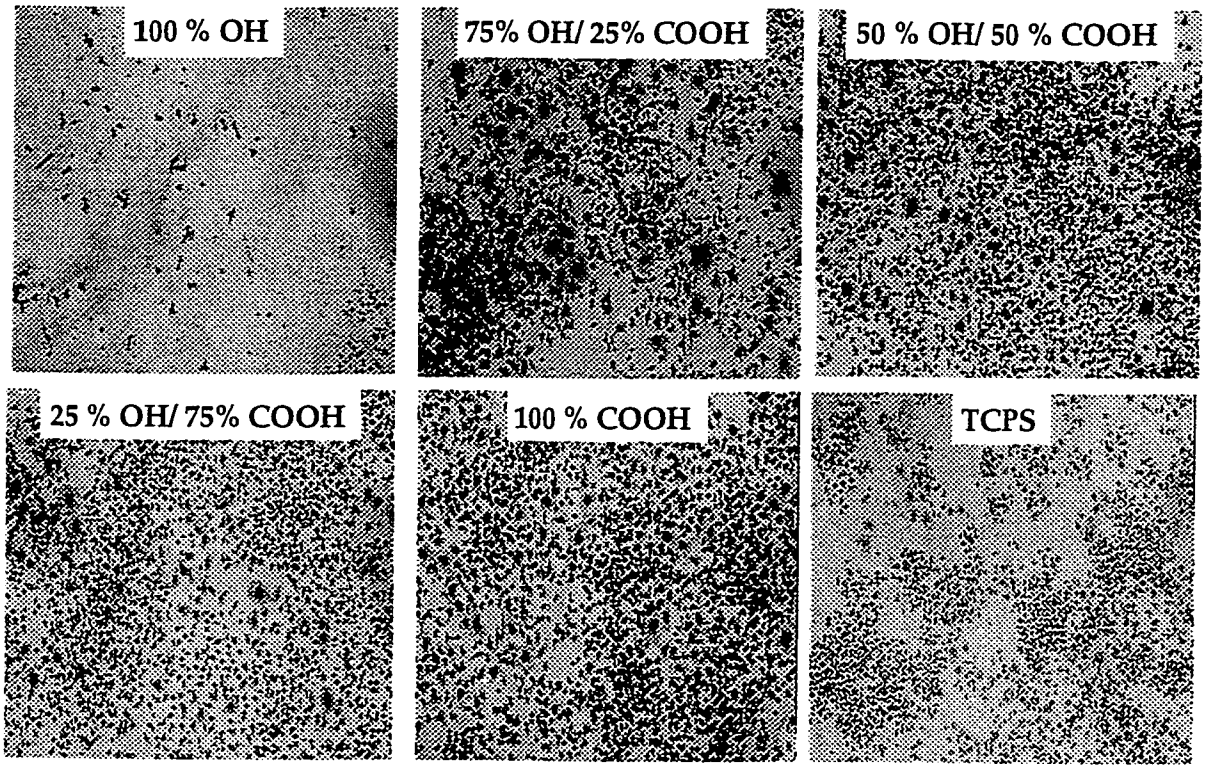

Figure 4.5 BAEC on binary composition SAMs of $HS(CH_2)_{15}CH_2OH$ and $HS(CH_2)_{15}COOH$ containing a) 100% OH thiol, b) 75% OH and 25% COOH thiols, c) 50% OH and 50% COOH thiols, d) 25% OH and 75% COOH thiols, and e) 100% COOH thiol. Cells were seeded at a density of 5000 cells/well or 2660 cells/cm^2 and cultured in medium containing 10% bovine serum for a 3 day period.

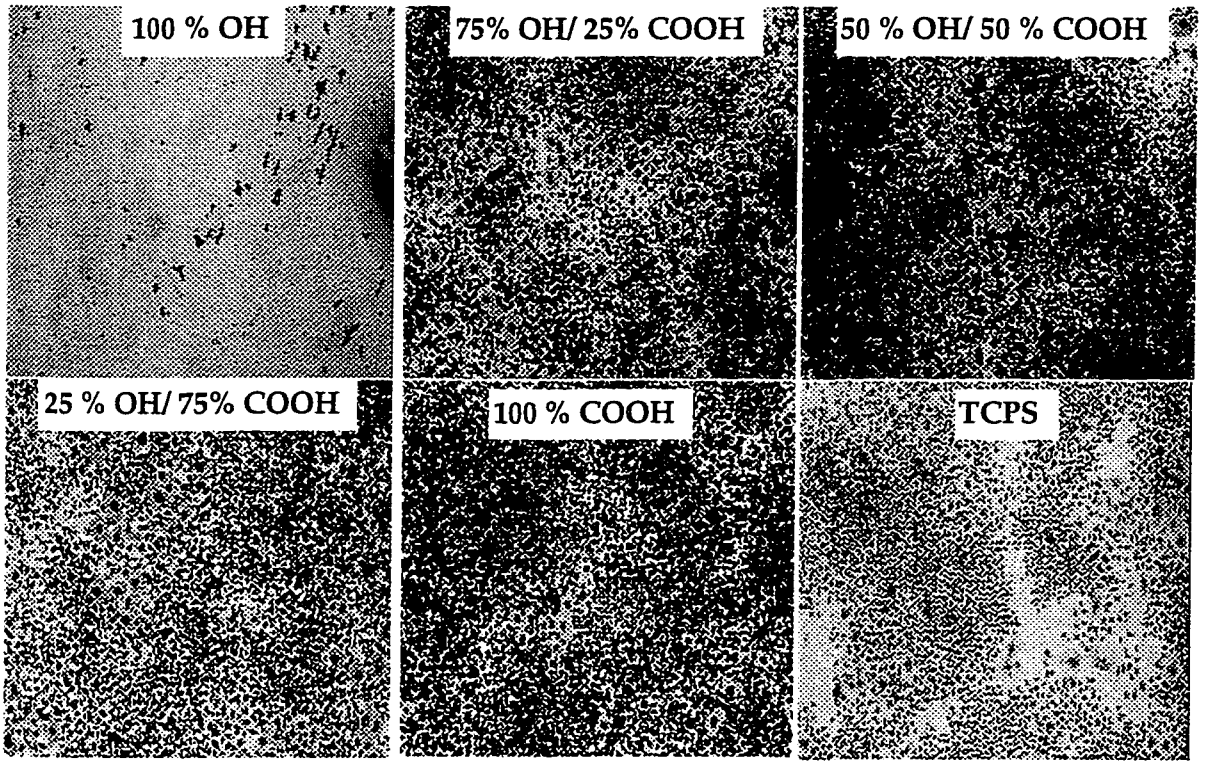

Figure 4.6 BAEC on binary composition SAMs of $HS(CH_2)_{15}CH_2OH$ and $HS(CH_2)_{15}COOH$ containing a) 100% OH thiol, b) 75% OH and 25% COOH thiols, c) 50% OH and 50% COOH thiols, d) 25% OH and 75% COOH thiols, and e) 100% COOH thiol. Cells were seeded at a density of 5000 cells/well or 2660 cells/cm^2 and cultured in medium containing 10% bovine serum for a 5 day period.

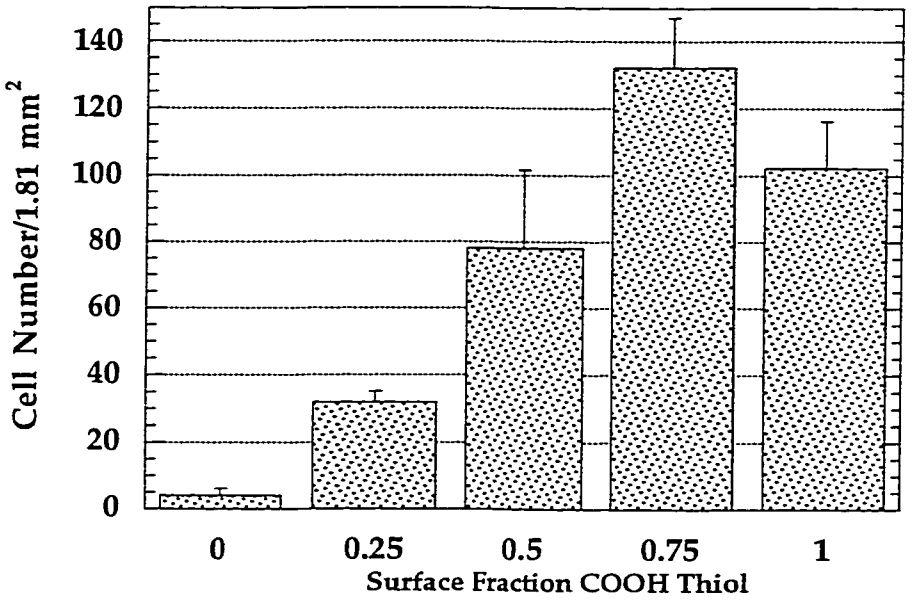

Figure 4.7 BAEC growth on binary composition SAMs of $HS(CH_2)_{15}CH_3$ and $HS(CH_2)_{15}COOH$. Cells were cultured for 3 days in medium containing 10% bovine serum. Cell number was determined by counting total number of cells on each 15 mm diameter sample (surface area = 1.81 cm^2). Data represent mean ± SEM for triplicate samples in duplicate experiments.

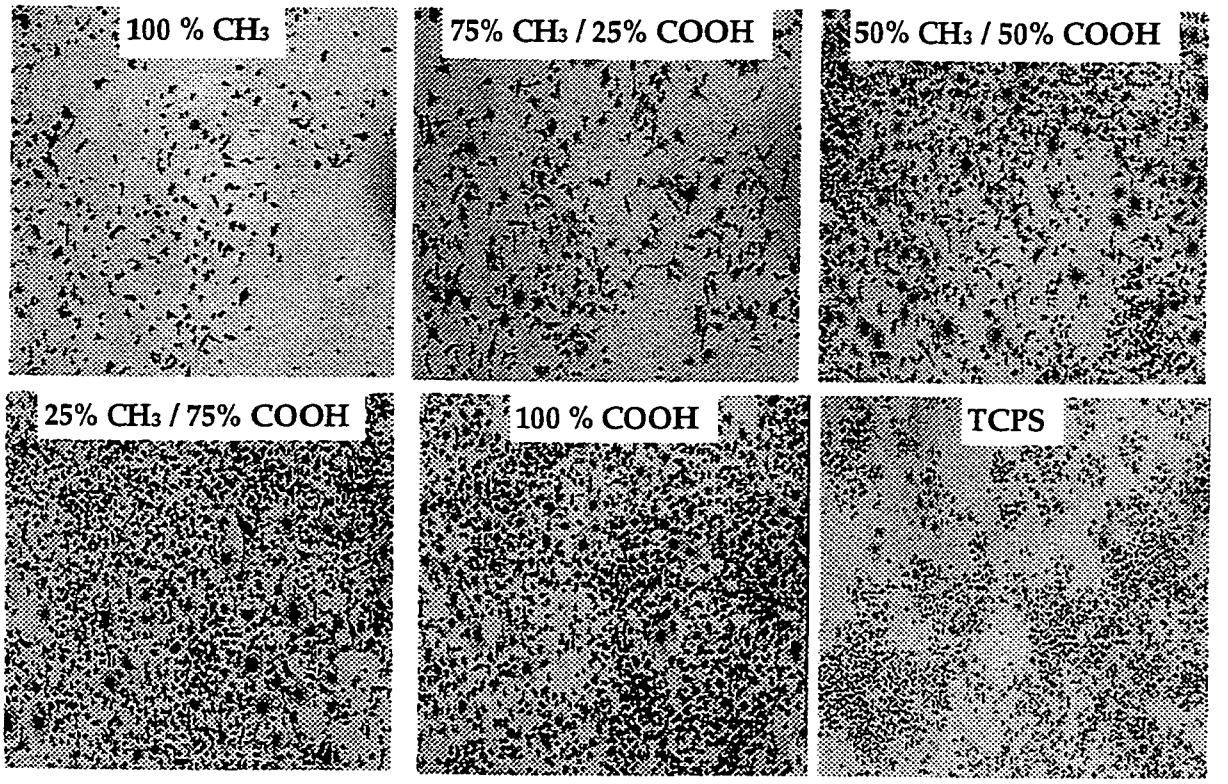

Figure 4.8 BAEC on binary composition SAMs of $HS(CH_2)_{15}CH_3$ and $HS(CH_2)_{15}COOH$ containing a) 100% CH_3 thiol, b) 75% CH_3 and 25% COOH thiols, c) 50% CH_3 and 50% COOH thiols, d) 25% CH_3 and 75% COOH thiols, and e) 100% COOH thiol. Cells were seeded at a density of 5000 cells/well or 2660 cells/cm^2 and cultured in medium containing 10% bovine serum for a 3 day period.

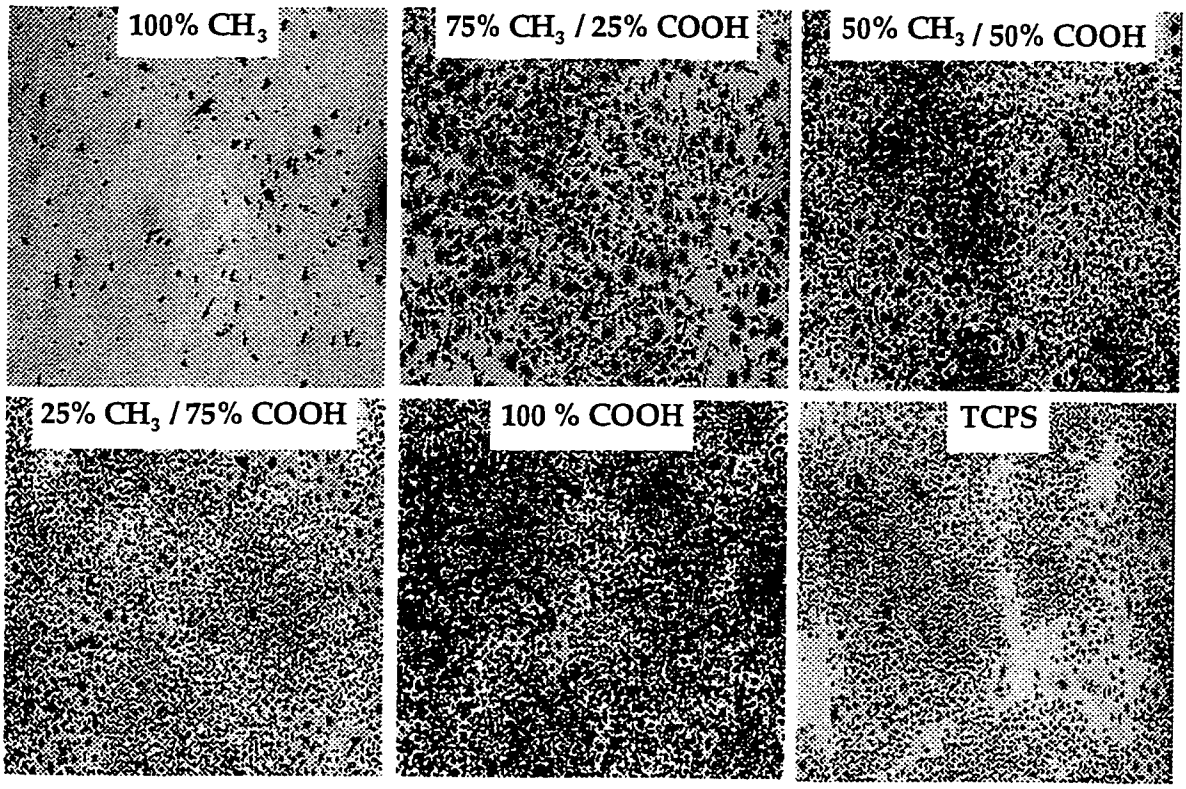

Figure 4.9 BAEC on binary composition SAMs of $HS(CH_2)_{15}CH_3$ and $HS(CH_2)_{15}COOH$ containing a) 100% CH_3 thiol, b) 75% CH_3 and 25% COOH thiols, c) 50% CH_3 and 50% COOH thiols, d) 25% CH_3 and 75% COOH thiols, and e) 100% COOH thiol. Cells were seeded at a density of 5000 cells/well or 2660 cells/cm^2 and cultured in medium containing 10% bovine serum for a 5 day period.

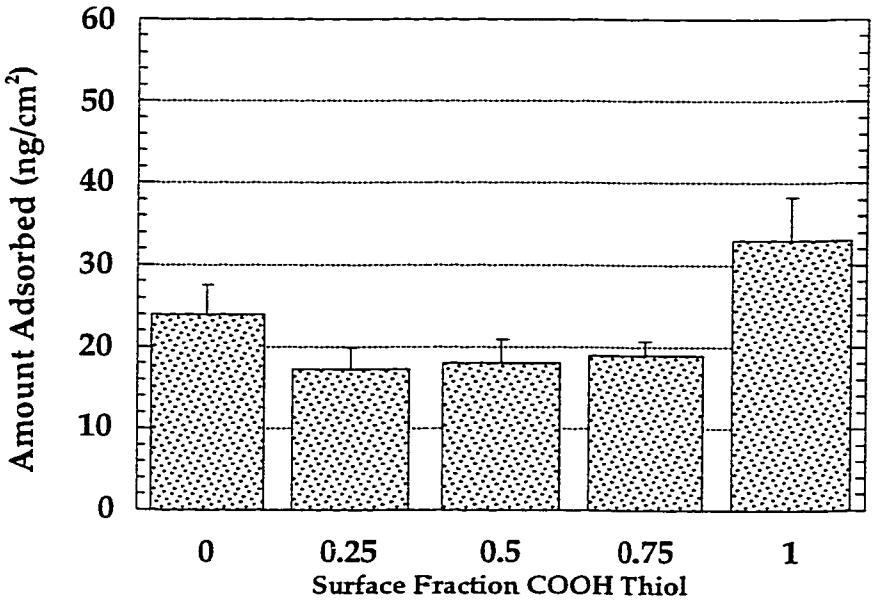

Figure 4.10 Effect of surface COOH content on Alb adsorption to binary composition SAMs of $HS(CH_2)_{15}CH_2OH$ and $HS(CH_2)_{15}COOH$. Alb was adsorbed from 10% bovine serum for 2 hours at 37°C. Data represent mean ± SEM for triplicate samples.

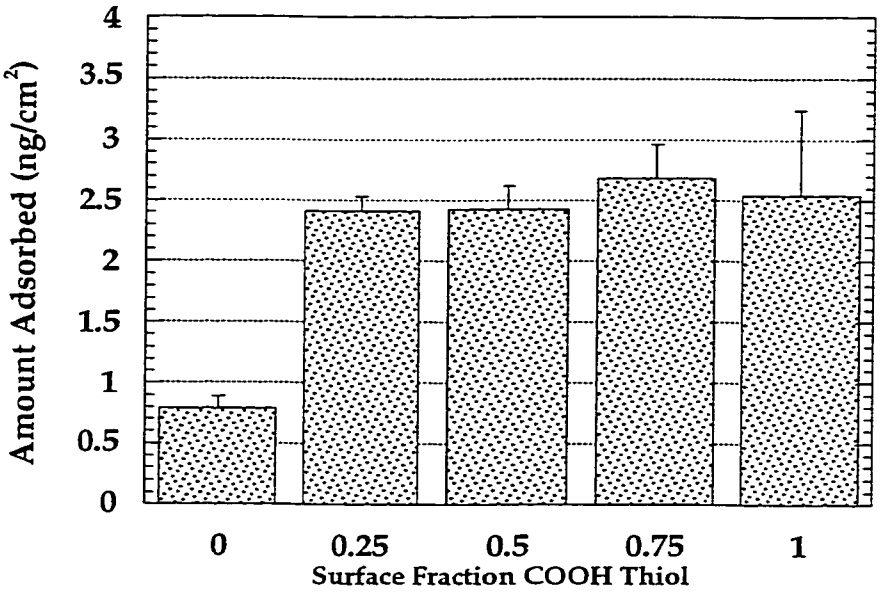

Figure 4.11 Effect of surface COOH content on Fn adsorption to binary composition SAMs of $HS(CH_2)_{15}CH_2OH$ and $HS(CH_2)_{15}COOH$. Fn was adsorbed from 10% bovine serum for 2 hours at 37°C. Data represent mean ± SEM for triplicate samples.

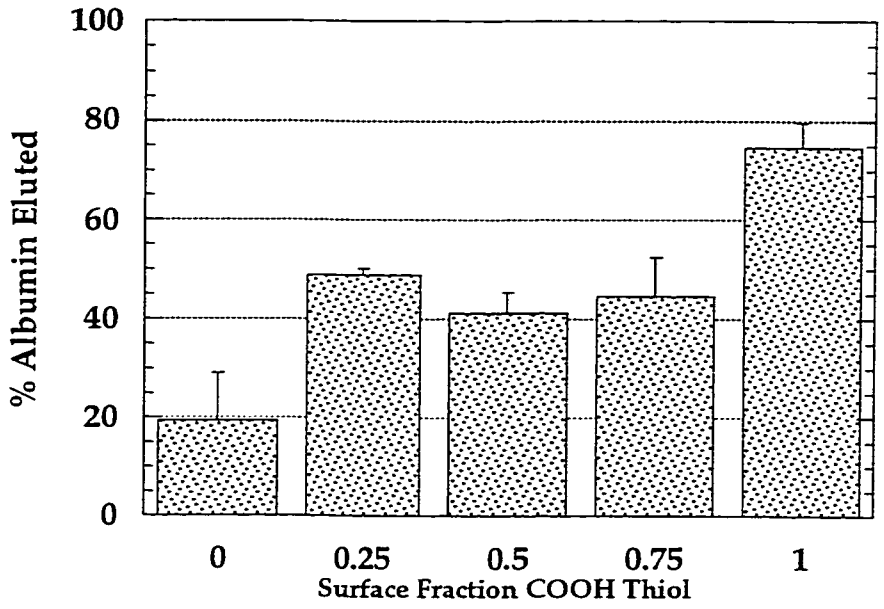

Figure 4.12 Effect of surface COOH content on Alb elutability from COOH/OH SAMs. Alb was adsorbed for 2 hours at 37°C and eluted in a 3% SDS solution for 24 hours. Percent elutability is the fraction of initially adsorbed protein which is removed by SDS. Data represent mean ± SEM for triplicate samples.

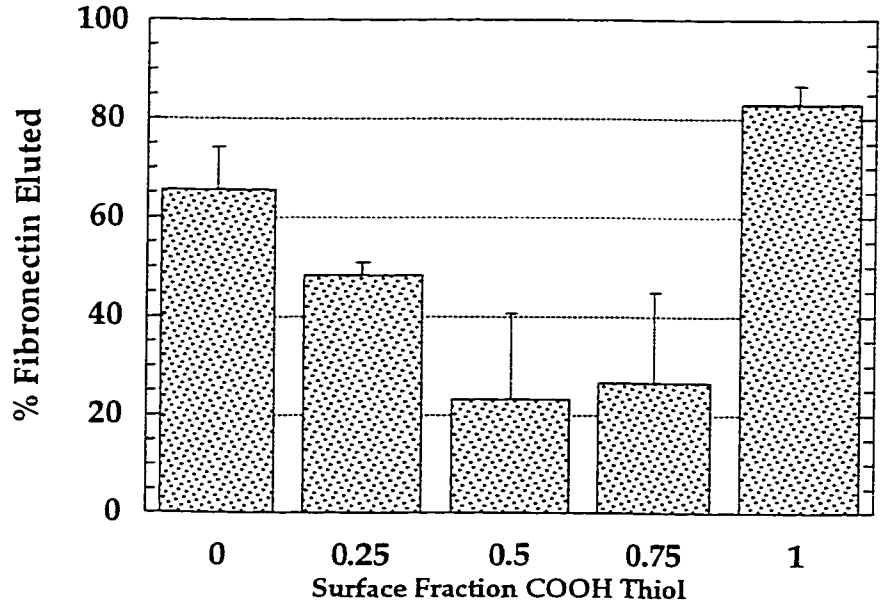

Figure 4.13 Effect of surface COOH content on Fn elutability from COOH/OH SAMs. Fn was adsorbed for 2 hours at 37°C and eluted in a 3% SDS solution for 24 hours. Percent elutability is the fraction of initially adsorbed protein which is removed by SDS. Data represent mean ± SEM for triplicate samples.

Chapter 5

Surface Analysis of Chemically Heterogeneous, Binary Composition SAMs

5.1 Introduction

Molecular self-assembly techniques provide an effective means of fabricating organic surfaces with a well-defined structure and chemistry. Self-assembled monolayers offer many advantages such as ease of preparation, stability in aqueous and organic environments, and most importantly, allow the synthesis of a variety of surfaces which differ systematically in structure and chemistry. Homogeneous SAMs, consisting of one chemical functionality, are useful as model systems however, many real surfaces, such as biological surfaces, differ from the model homogeneous SAMs in that they are quite often chemically and structurally complex. The complexity of the SAM surface can be increased in several ways to create more complex model systems. Chemically heterogeneous surfaces which vary systematically in functional group content can be formed by coadsorbing two or more thiols with different terminal functional groups onto a common gold surface. The distribution of chemical functionalities on a binary SAM surface can also be controlled to form random mixtures and phase separated domains of chosen surface functionalities. Structurally heterogeneous SAMs which vary systematically in the concentration of chains exhibiting molecular mobility at the interface can be formed using mixtures of thiols of different chain length.

Three types of SAMs were investigated in this work: 1) chemically homogeneous SAMs (Chapter 3), 2) chemically heterogeneous, binary composition SAMs (Chapters 4, 6 and 8) and, 3) structurally heterogeneous, binary composition SAMs (Chapter 7). Surface analysis of the chemically homogeneous SAMs was presented in Chapter 3 (Section 3.3.1). Surface analysis studies of chemically heterogeneous, binary

composition SAMs are presented in this chapter. The preliminary studies of chemically heterogeneous SAMs described in Chapter 4 included a limited TOF-SIMS study of 5 surface compositions of COOH/OH and COOH/CH_3 SAMs. In Chapter 5, surface characterization of a complete series of three binary SAM systems (COOH/OH, COOH/CH_3, and OH/CH_3 SAMs) is described. Surface characterization of structurally heterogeneous, binary composition SAMs is described in Chapter 7.

The chemically heterogeneous SAMs described in this chapter were prepared using mixtures of alkanethiols terminated with hydroxyl, methyl, and carboxyl functionalities to obtain substrates demonstrating a systematic variation in surface functional group content. Heterogeneous SAMs with a random distribution of chemical functionalities were prepared utilizing mixtures of functional groups in which random mixing was expected. Phase separated chemically heterogeneous SAMs were formed using combinations of functional groups which have previously demonstrated domain formation.

For many binary SAM systems (particularly systems containing a polar and a non-polar component), surface composition differs from the alkanethiol solution composition due to differences in relative solubility and affinities of the thiol components for the surface. Determination of the relationship between alkanethiol solution composition and binary SAM surface composition is crucial for obtaining binary SAMs with the desired surface functional group concentration. In preliminary studies of the COOH/OH and the COOH/CH_3 binary SAMs (Chapter 4), thiol solution compositions were chosen in accordance with published literature values. While the resulting surface compositions were in close agreement with targeted surface compositions as determined by TOF-SIMS, there was some deviation between predicted and actual surface compositions (see Figures 4.2 and 4.3). In the present chapter, surface composition/solution composition relationships were determined for the three binary

SAM systems investigated by evaluating surface composition as a function of thiol solution composition for a complete series of binary SAMs prepared from adsorbing thiol solutions ranging in composition from 0-100% of each thiol. These relationships were used to select alkanethiol solution ratios to prepare chemically heterogeneous SAMs for cell growth studies as described in Chapter 6.

Binary composition SAMs were characterized by several surface analysis techniques that provided complementary information about the structure and composition of the SAM. SAM wettability was assessed by measuring static contact angles of water using goniometry. Binary SAM surface composition was determined by XPS and TOF-SIMS. SAM surface structure was investigated by TOF-SIMS.

5.2 Materials and Methods

5.2.1 Preparation of Chemically Heterogeneous SAMs

Three binary SAM systems were prepared for surface characterization studies: 1) a series of mixtures of $HS(CH_2)_{15}COOH$ and $HS(CH_2)_{15}CH_2OH$, 2) a series of mixtures of $HS(CH_2)_{15}COOH$ and $HS(CH_2)_{15}CH_3$ and, 3) a series of mixtures of $HS(CH_2)_{15}OH$ and $HS(CH_2)_{15}CH_3$. Binary SAMs were prepared as described in Section 2.2. For the OH/CH_3 and $COOH/CH_3$ SAM systems, a set of 11 surface compositions was prepared (solution fraction of OH or COOH thiol: 0, 10, 20, 30, 40, 50, 60, 70, 80, 90, and 100%). For the COOH/OH SAM system, a set of 7 surface compositions was prepared (solution fraction of OH thiol: 0, 10, 20, 40, 60, 80, and 100%)

5.2.2 Surface Analysis of Chemically Heterogeneous SAMs

Binary SAMs were characterized by ellipsometry (Battelle PNL), contact angle (Battelle PNL), XPS (Battelle and UW), and TOF-SIMS (UW) as described in section 2.3. Triplicates of each surface composition were analyzed by ellipsometry and contact

angle. A minimum of two replicates of each surface composition were analyzed by SIMS (analysis on 2 spots per sample) and a minimum of two replicates of each surface composition were analyzed by XPS (analysis on 3 spots per sample).

5.3 Results and Discussion

5.3.1 XPS and Contact Angle Analysis of $COOH/CH_3$ and OH/CH_3 SAMs

The elemental surface compositions determined by XPS for a full series (11 surface compositions) of $COOH/CH_3$ binary SAMs are presented in Table 5.1. The elemental surface compositions determined by XPS of a full series (11 surface compositions) of OH/CH_3 binary SAMs are presented in Table 5.2. Elemental surface compositions for the $COOH/CH_3$ and OH/CH_3 systems are consistent with the theoretical elemental compositions predicted for each type of binary SAM from the chemical composition of the thiols used to form the monolayers.

Since the $COOH/CH_3$ and OH/CH_3 SAM systems contain a unique heteroatom in the thiol terminal functional group, SAM surface composition can be quantified using XPS elemental surface composition. SAM monolayer compositions were determined from the intensity of the photoelectron signal from the heteroatom in the tail group, normalized to the intensity from the monolayer composed only of the thiol with a polar tail group. To calculate binary SAM surface composition, the ratio of the O(1s) intensity to the intensity of the Au(4f7/2) photoelectrons from the substrate was normalized to the O(1s)/Au(4f7/2) ratio for the homogeneous COOH or OH-terminated SAM. In this calculation, the O/Au ratios were corrected for any oxygen signal measured on the homogeneous methyl-terminated monolayer.

The relationships between the thiol solution composition in the ethanolic adsorbing solutions and the surface composition of the heterogeneous monolayer for the $COOH/CH_3$ and OH/CH_3 SAM systems as determined by XPS are presented in Figure

5.1. The curves shown in Figure 5.1 were developed from XPS data collected at UW and at Battelle for each series of binary SAMs.

For both the $COOH/CH_3$ and OH/CH_3 SAM systems, SAM surface composition differs significantly from the solution concentration of the adsorbing thiol solution. For both systems, adsorption of the CH_3-terminated thiol is favored over adsorption of the OH or COOH-terminated thiol resulting in binary SAM surfaces which are methyl rich. For example, a SAM prepared from a 50% OH/50% CH_3 solution results in a surface composition of 30% OH and 70% CH_3. Therefore, to obtain a binary SAM surface with a 50%/50% surface composition, an adsorbing solution containing excess of the polar thiol component is required. Comparing the $COOH/CH_3$ and OH/CH_3 SAM systems, Figure 5.1 shows that at an equivalent solution concentration, the surface fraction of OH thiol in the SAM is higher than the surface fraction of COOH thiol in the monolayer. While adsorption of the CH_3 thiol is more strongly favored in both systems (over adsorption of the polar component), adsorption of the OH thiol is higher than adsorption of the COOH thiol given the same solution fraction of the polar thiol. This result is likely due to an increased solvation of the COOH thiol in ethanol relative to the OH thiol. For both systems, the preferential adsorption of the CH_3 component reflects better solvation of the polar component thiol in the ethanolic solution than at the surface of the monolayer. The results shown in Figure 5.1 are consistent with previously published XPS studies of binary SAM systems. Bain et al., reported similar SAM surface composition/solution composition relationships for binary SAM systems of $HS(CH_2)_{10}COOH$ and $HS(CH_2)_{10}CH_3$; and $HS(CH_2)_{10}CH_2OH$ and $HS(CH_2)_{10}CH_3$ [89,90]. For both systems, Bain observed preferential adsorption of the CH_3-terminated thiol relative to the polar terminated thiol, and preferential adsorption of the OH thiol relative to the COOH thiol for all but one of the solution concentrations investigated [89,90].

The advancing contact angle of water as a function of the surface fraction of the polar component in the binary SAM (as determined by XPS) is shown in Figure 5.2 for the $COOH/CH_3$ and OH/CH_3 SAM systems. An increase in surface hydrophilicity is observed for both systems with increasing surface fraction of polar component. If the thiol components in the binary SAM acted independently, the contact angle of the binary SAM would be given by Cassie's law [91] as follows,

$$\cos\theta = \chi_1 \cos\theta_1 + \chi_2 \cos\theta_2$$

where χ_1 and χ_2 are the mole fractions of the two components in the binary SAM and θ_1 and θ_2 are the contact angles of a homogeneous (pure) SAM of the two components. According to this equation, the relationship between the contact angle and the surface fraction of a component in the binary monolayer would be expected to be linear. The water contact angles shown in Figure 5.2 deviate significantly from linearity. For both SAM systems, we observed a lower contact angle at all surface compositions than would be predicted by Cassie's law. It has been suggested that poor hydrogen bonding between polar tail groups in the monolayer contributes to the increase in apparent hydrophilicity of the polar tail groups [92].

5.3.2 TOF-SIMS Analysis of $COOH/CH_3$ and OH/CH_3 SAMs

In Chapter 4, preliminary data was presented which demonstrated the ability of TOF-SIMS to obtain accurate, quantitative information regarding the surface content of each thiol in a binary SAM. In the preliminary evaluation of binary SAMs, the negative ion mode of TOF-SIMS was found to be useful for characterizing alkanethiols on gold due to the presence of molecular ion signals with significant intensities in the resulting spectra. The high mass range of the negative ion spectrum of an alkanethiol SAM on

gold was found to contain signals from the gold substrate (gold cluster ions and gold/sulfur cluster ions), the intact thiol, and clusters of gold atoms with thiol molecules.

To expand upon the TOF-SIMS analysis described in Chapter 4, a full series (11 surface compositions) of $COOH/CH_3$ and OH/CH_3 SAMs were evaluated by TOF-SIMS in order to determine the surface composition resulting from each thiol solution ratio. The relative intensity of the thiol molecular ion cluster ($Au_2(M-H)^-$) measured by negative-ion TOF-SIMS for the $COOH/CH_3$ and the OH/CH_3 binary SAMs was evaluated as a function of thiol solution composition. Figure 5.3 shows the normalized intensity of the $HS(CH_2)_{15}COOH$ molecular ion cluster (681 m/z) and the $HS(CH_2)_{15}CH_3$ molecular ion cluster (651 m/z) as a function of the adsorbing thiol solution composition. Figure 5.4 shows the normalized intensity of the $HS(CH_2)_{15}CH_2OH$ molecular ion cluster (667 m/z) and the $HS(CH_2)_{15}CH_3$ molecular ion cluster (651 m/z) as a function of the adsorbing thiol solution composition. Both Figure 5.3 and 5.4 show a decrease in intensity of the $HS(CH_2)_{15}CH_3$ molecular ion cluster (651 m/z) and an increase in intensity of the OH or COOH molecular ion cluster (667 m/z and 681 m/z respectively) with increasing solution fraction of polar component. In both binary SAM systems, a significant difference in the intensities of the thiol molecular ion clusters is observed. As discussed in Section 4.3.1, the differences observed in peak intensities of the molecular ions results from differences in secondary ion yield for the thiols in a binary pair. The CH_3 molecular ion cluster demonstrated the highest intensity in both binary SAM systems. Among the polar thiols, the intensity of the $HS(CH_2)_{15}CH_2OH$ molecular ion cluster was generally higher than that of the $HS(CH_2)_{15}COOH$ molecular ion cluster especially at solution fraction values greater than 50%. The $HS(CH_2)_{15}COOH$ molecular ion cluster intensity was relatively low over the entire range of solution ratios.

In order to quantify SAM surface composition, the differences in secondary ion yield observed for each thiol must be taken into consideration when calculating surface thiol content from molecular ion cluster peak intensity. As discussed in Section 4.3.1, a sensitivity factor must be calculated for each thiol. For both the $COOH/CH_3$ and OH/CH_3 SAM systems, the normalized molecular ion cluster intensity of the polar thiol was lower than that of the CH_3 thiol. Thus, the normalized molecular ion cluster intensity of the polar thiol was adjusted by a sensitivity factor to account for differences in secondary ion yield between the polar and nonpolar components of the binary SAM. The sensitivity factor was calculated as the ratio of the normalized molecular ion cluster intensity for the CH_3 thiol to the normalized molecular ion cluster intensity for the polar thiol at the thiol solution ratio known (from XPS) to result in a 50%/50% surface composition. SAM surface composition was then determined from the ratio of the normalized intensity of the $Au_2(M\text{-}H)^-$ peak for the polar thiol to the sum of the normalized intensities of the $Au_2(M\text{-}H)^-$ peaks for the polar and CH_3 thiols for the same spot on the same sample. In this calculation, $Au_2(M\text{-}H)^-$ peak intensities for the polar thiols were corrected for any oxygen signal measured on the homogeneous CH_3 terminated monolayer.

The relationships between thiol solution composition and binary SAM surface composition as determined by TOF-SIMS for the $COOH/CH_3$ and OH/CH_3 SAM systems are presented in Figures 5.5 and 5.6 respectively. As observed in Figure 5.1, the surface composition of the binary SAM differs significantly from the composition of the thiols in the adsorbing solution. In both systems, adsorption of the CH_3 thiol is favored over adsorption of the polar thiol yielding surfaces which are methyl-rich at low polar component solution fraction values. Excess polar thiol in the adsorbing solution is required to achieve a 50/50 surface composition for both systems. For the $COOH/CH_3$ system, a 75% COOH/25% CH_3 adsorbing solution results in a 50/50 SAM surface

composition, while a 50/50 surface composition is achieved at a 65% OH/35% CH_3 solution composition for the OH/CH_3 system. As discussed in Section 5.3.1, while adsorption of the CH_3 thiol is significantly higher than adsorption of the polar thiol in both SAM systems, adsorption of the OH thiol appears to be higher than that of the COOH thiol at an equivalent polar thiol solution concentration.

The surface composition determined by TOF-SIMS can be compared to XPS-determined surface composition to evaluate the congruence between surface analysis techniques in determining binary SAM surface composition. Figures 5.7 and 5.8 show cross-plots of the surface fraction of polar thiol as determined by TOF-SIMS (Figures 5.5 and 5.6) and polar thiol surface fraction as determined by XPS (Figure 5.1) for the COOH/CH_3 and OH/CH_3 systems, respectively. For both SAM systems, there is an excellent correlation (R^2>0.994) between surface composition determined by XPS and TOF-SIMS. The standard deviation in surface composition determined by TOF-SIMS is significantly lower than the deviation in surface composition determined by XPS. In determining surface composition by TOF-SIMS, two spots on duplicate samples were evaluated. The sample-to-sample and spot-to-spot variability for surface composition as determined from the molecular ion cluster peak intensities measured by TOF-SIMS was very low (typically < 5%). For determination of surface composition by XPS (Figure 5.1), data obtained during analysis of duplicate spots on triplicate samples obtained both by UW and Battelle was used to calculate the average surface composition. As a result, a the standard deviations of XPS-determined surface compositions were typically larger than for TOF-SIMS determined surface composition (analysis performed at UW only). The standard deviation of the surface composition determined from the combined XPS data was lower for the COOH/CH_3 system (Figure 5.7) than for the OH/CH_3 system (Figure 5.8). The increased error in XPS-determined surface composition (particularly at 60% and 70% OH surface fraction) may result from factors such as differences in

sample oxidation during surface analysis, incomplete rinsing of sample prior to analysis, etc. For the majority of surface compositions evaluated, there was excellent agreement between XPS and TOF-SIMS determined surface composition and the error was reasonable.

5.3.3 XPS and TOF-SIMS Analysis of COOH/OH SAMs

The elemental surface composition determined by XPS for a series of 7 surface compositions of COOH/OH binary SAMs is presented in Table 5.3. Elemental surface compositions for the COOH/OH SAMs are consistent with the theoretical elemental compositions predicted from the chemical compositions of the thiols used to form the binary SAMs. As expected, oxygen content decreased slightly with increasing solution concentration of OH thiol.

Quantification of $COOH/CH_3$ and OH/CH_3 SAM surface composition by XPS is facilitated by the presence of a chemically unique heteroatom in the thiol terminal functionality. The COOH/OH binary SAM system does not contain a unique chemical species and therefore, elemental surface composition determined by XPS is not sufficient to quantify binary SAM surface composition. As discussed in Section 4.3.1, since molecular ions can be observed by TOF-SIMS, no distinct chemical functionality is required for quantification of surface composition. Therefore, surface composition of the COOH/OH binary SAMs was quantified by TOF-SIMS. TOF-SIMS is ideally suited for surface analysis of a system such as the COOH/OH SAM.

Seven COOH/OH SAM surfaces were evaluated by TOF-SIMS to determine the surface composition resulting from each adsorbing thiol solution ratio. The relative intensity of the thiol molecular ion cluster ($Au_2(M\text{-}H)^-$) for each thiol measured by negative-ion TOF-SIMS for the COOH/OH binary SAMs was evaluated as a function of thiol solution composition. Figure 5.9 shows the normalized intensity of the

$HS(CH_2)_{15}CH_2OH$ molecular ion cluster (667 m/z) and the $HS(CH_2)_{15}COOH$ molecular ion cluster (681 m/z) as a function of the adsorbing thiol solution composition (solution fraction of COOH thiol). A decrease in intensity of the $HS(CH_2)_{15}CH_2OH$ molecular ion cluster (667 m/z) and an increase in intensity of the $HS(CH_2)_{15}COOH$ molecular ion cluster (681 m/z) is observed with increasing COOH thiol solution fraction. As observed in Section 5.3.2, the intensity of the 667 m/z molecular ion cluster (CH_2OH) is generally higher than that of the 681 m/z MIC (COOH). Again, the COOH molecular ion cluster was relatively low over the range of solution ratios tested.

To quantify SAM surface composition, the differences in thiol secondary ion intensity must considered when calculating surface thiol content from molecular ion cluster peak intensity. For the COOH/OH SAM system, the normalized molecular ion cluster intensity of the COOH thiol was lower than that of the OH thiol therefore, the normalized molecular ion cluster intensity of the COOH thiol was adjusted by a sensitivity factor. The sensitivity factor was calculated as the ratio of the normalized molecular ion cluster intensity for the homogeneous OH thiol to the normalized molecular ion cluster intensity for the homogeneous COOH thiol. SAM surface composition was determined from the ratio of the normalized intensity of the $Au_2(M\text{-}H)^-$ peak for the OH or COOH thiol to the sum of the normalized intensities of the $Au_2(M\text{-}H)^-$ peaks for the OH and COOH thiols for the same spot on the same sample.

The relationship between binary SAM surface composition and solution composition as determined by TOF-SIMS for the COOH/OH binary SAM system is shown in Figure 5.10. If the OH and COOH thiols had equal affinity for the gold substrate, a 1:1 relationship between surface composition and solution composition would be expected. The data shown in Figure 5.10 deviates from a 1:1 relationship. For example, a 50/50 surface composition is achieved from a COOH thiol solution fraction of approximately 0.6 rather than 0.5. At low COOH thiol solution fractions,

surface composition is essentially equivalent to solution composition as expected. However, at high COOH thiol solution fractions, COOH surface composition deviates more significantly from solution composition. In particular, at COOH thiol solution fraction values of 0.8 and 0.9, the corresponding COOH thiol surface fractions are 10% lower than expected (i.e., 70% and 80% surface COOH content rather than 80% and 90% respectively).

These results suggest that the relative affinity of the OH thiol is slightly higher than that of the COOH thiol. For the COOH/CH_3 and OH/CH_3 SAM systems, we similarly observed that at an equivalent polar thiol solution concentration, the surface fraction of OH thiol was higher than that of the COOH thiol (see Figures 5.1, 5.5 and 5.6) suggesting preferential adsorption of the OH thiol relative to the COOH thiol. For the COOH/OH SAMs, this difference in thiol affinity must be considered when preparing COOH/OH SAMs of a particular surface composition.

5.3.4 Surface Structure of COOH/OH, COOH/CH_3, and OH/CH_3 SAMs

In this section, we investigated the ability of TOF-SIMS to investigate the surface structure, specifically functional group surface dispersion, of the thiol components in the COOH/OH, COOH/CH_3, and OH/CH_3 SAM systems. While many studies have been conducted using chemically heterogeneous monolayers, in only a few cases has the arrangement of functional groups been determined. Phase separation has been previously demonstrated for OH/CH_3 and CO_2CH_3/CH_3 binary SAM systems [93,94]. It was anticipated that phase separation would occur in the COOH/CH_3 system since this functional group pair was expected to have stronger intermolecular interactions than the CO_2CH_3/CH_3 pair.

TOF-SIMS has been developed as a method for evaluating the structures of binary mixtures of mixtures of C_{16} thiols containing CH_3, CH_2CN, and CH_2OH [95]. In

studies by Atre and Allara, the relative intensity of dual species clusters (MAuM') where M and M' refer to the thiolate species in the monolayer were evaluated [95]. The intensity of the mixed cluster species was compared to the intensities for the pure cluster species as a measurement of phase segregation, with more mixed cluster species indicating more random mixing.

Canry and Vickerman evaluated the deviation of a binary SAM from a randomly mixed surface structure by determining the distribution of the dual cluster species, MAuM', containing both of the adsorbate molecules. Theoretically, the distribution of the MAuM' species generated from a randomly mixed SAM is predicted as shown in Figure 5.11 [96]. As shown in Figure 5.11, the dual species cluster intensity obtained from a randomly mixed SAM would be expected to reach a maximum at a SAM surface composition of 50%. The predicted dual species cluster intensity curve is symmetrical about the midpoint an reaches zero for the homogeneous compositions located at 0 and 100% surface compositions.

The relative intensity of the dual species cluster (MAuM') for the OH/CH_3, $COOH/CH_3$, and COOH/OH binary SAM systems as a function of binary SAM surface composition is shown in Figures 5.12 and 5.13. The experimental distribution of the dual species cluster obtained from the OH/CH_3 SAMs (m/z 727) shown in Figure 5.12 deviates from the theoretically determined distribution calculated on basis of randomly mixed SAM shown in Figure 5.11. The experimental curve for the m/z 727 dual species cluster is not symmetrically distributed about the midpoint, rather it is shifted towards the left of the midpoint and reaches a maximum at a lower OH surface fraction. The highest yield of the mixed cluster species (m/z 727) for the OH/CH_3 is obtained at a OH surface fraction of approximately 32% rather than 50% as would be expected for a randomly mixed SAM surface. These results suggest that the OH/CH_3 SAM surface does not exist

as a random mixture, rather there is likely a clustering of CH_3 and the OH thiols within the OH/CH_3 mixed SAM surface.

The experimental distributions of the dual species cluster obtained from the $COOH/CH_3$ SAMs (m/z 741) and the COOH/OH SAMs (m/z 757) are shown in Figure 5.13. The experimentally determined curve for the $COOH/CH_3$ mixed cluster species, m/z 741, exhibits a highly asymmetric distribution with a pronounced shift in maximum to the left of the midpoint line. While the highest yield of the m/z 741 mixed cluster species occurs at a 36% COOH surface fraction, high yields of the m/z 741 species are also obtained at COOH surface compositions as low as 10% and 20% COOH. As observed for the OH/CH_3 SAM systems, the pronounced deviation of the 741 mixed cluster species curve from the theoretically predicted curve for a randomly distributed SAM (Figure 5.11) suggests that the $COOH/CH_3$ SAMs also do not exist in a random mixture.

In contrast, the experimental distribution of the dual species cluster obtained from the COOH/OH SAM surfaces (m/z 757) is relatively symmetric with a slight shift of the maximum to the left of the midpoint line. The highest yield of the m/z 757 mixed cluster species is obtained at a COOH surface fraction of 42%. Of the three binary SAM series evaluated, the COOH/OH dual species cluster experimental distribution most closely approximates the theoretically determined distribution predicted for a randomly mixed SAM. These data suggest that the COOH/OH SAMs most likely exist in a randomly mixed configuration while the $COOH/CH_3$ and OH/CH_3 SAMs exist in a clustered configuration.

5.4 Conclusions

Three binary SAM systems were analyzed in surface characterization studies: 1) a series of mixtures of $HS(CH_2)_{15}COOH$ and $HS(CH_2)_{15}CH_2OH$, 2) a series of mixtures

of $HS(CH_2)_{15}COOH$ and $HS(CH_2)_{15}CH_3$ and, 3) a series of mixtures of $HS(CH_2)_{15}OH$ and $HS(CH_2)_{15}CH_3$. The chemically heterogeneous SAMs were analyzed by ellipsometry, contact angle, XPS and TOF-SIMS. Surface composition/solution composition relationships were determined for SAMs prepared from thiol solutions ranging in composition from 0-100% by evaluating surface composition determined by XPS and/or TOF-SIMS as a function of thiol solution composition. The surface composition/solution ratio relationships (Figures 5.1, 5.5, 5.6, and 5.10) were used to prepare SAMs of a desired surface composition for use in cell growth and protein adsorption studies described in Chapters 6 and 7.

For binary SAM systems containing a unique heteroatom in the thiol terminal functionality, SAM surface composition was quantified using XPS elemental surface compositions. SAM surface composition was determined from the intensity of the photoelectron signal from the heteroatom in the tail group, normalized to the intensity from the monolayer composed only of the thiol with a polar tail group.

Binary SAM surface composition was also quantified by TOF-SIMS. The strongest molecular ion signal observed for the binary composition SAMs was obtained for the thiol molecule with the loss of a proton and the adduct of two gold atoms, $Au_2(M-H)^-$. SAM surface composition was determined from the ratio of the normalized intensity of the $Au_2(M-H)^-$ peak for one thiol to the sum of the normalized intensities of the $Au_2(M-H)^-$ peaks for each thiol. The normalized intensity of the $Au_2(M-H)^-$ peak for each thiol was adjusted by a sensitivity factor to account for differences in secondary ion yield intensity observed for the different thiols. TOF-SIMS provides information regarding the surface content of each thiol and is particularly useful for binary SAMs which do not contain a unique heteroatom in the terminal functionality (i.e., COOH/OH SAMs).

XPS, contact angle, and TOF-SIMS analysis of the $COOH/CH_3$ and OH/CH_3 SAM systems demonstrated that SAM surface composition differed significantly from

the solution concentration of the adsorbing thiol solution. For the COOH/CH_3 and OH/CH_3 systems, adsorption of the nonpolar thiol (CH_3-terminated thiol) was favored over adsorption of the polar thiol (OH or COOH-terminated thiol) resulting in binary SAM surfaces which were methyl rich at low polar component solution fraction values. For both systems, an excess of polar thiol was required in the adsorbing solution in order to obtain a binary SAM surface composition of 50%/50%. Comparing the COOH/CH_3 and OH/CH_3 SAM systems, adsorption of the OH thiol was observed to be greater than adsorption of the COOH thiol given the same solution fraction of the polar thiol. For the COOH/CH_3 and OH/CH_3 systems, an excellent correlation was obtained between surface composition determined by XPS and surface composition determined by TOF-SIMS.

TOF-SIMS analysis was used to determine the surface composition/solution composition relationship for the COOH/OH SAM system. COOH/OH surface composition deviated from a 1:1 relationship between surface composition and solution composition. At low COOH thiol solution fractions, surface composition was essentially equivalent to solution composition. However, at COOH thiol solution fractions greater than 50%, adsorption of the OH-terminated thiol was favored slightly over that of the COOH-terminated thiol yielding surfaces which were rich in OH thiol. TOF-SIMS is ideally suited for surface analysis of a SAM system such as the COOH/OH system because it allows for quantification of surface composition without the requirement of a distinct chemical functionality.

TOF-SIMS analysis was also used to probe the surface dispersion of thiol components in the COOH/OH, COOH/CH_3 and OH/CH_3 SAM systems. To assess the deviation of a binary SAM from a randomly mixed surface structure, the distribution of the dual species molecular ion cluster intensity (MAuM') was evaluated. The experimentally-determined relationship between the dual species molecular ion cluster

intensity and SAM surface composition was compared to the relationship between dual species molecular cluster intensity and SAM surface composition predicted theoretically for a randomly mixed binary SAM. The experimental distribution of the dual species cluster curves showed evidence of thiol clustering for the $COOH/CH_3$ and OH/CH_3 SAM systems. In contrast, the experimental distribution of the dual species cluster curve for the COOH/OH system most closely approximated the theoretical curve for a randomly mixed surface suggesting that the COOH/OH SAM surfaces exist in a randomly mixed configuration.

Table 5.1

Elemental Composition Determined by XPS of Binary Composition SAMs of $HS(CH_2)_{15}COOH$ and $HS(CH_2)_{15}CH_3$

	Elemental Composition (atom percent)				
Thiol Soln. Composition	***C***	***Au***	***S***	***O***	***Number of Samples[1]***
0% COOH	68.8 ± 2.7	28.7 ± 1.9	1.7 ± 0.3	0.8 ± 0.6	11
10% COOH	68.2 ± 1.4	28.4 ± 1.0	2.4 ± 0.4	0.9 ± 0.1	6
20% COOH	68.2 ± 0.8	27.8 ± 0.7	2.3 ± 0.2	1.7 ± 0.3	9
30% COOH	67.4 ± 1.3	28.2 ± 1.3	2.0 ± 0.1	2.5 ± 0.2	6
40% COOH	66.8 ± 1.2	28.1 ± 1.0	2.0 ± 0.3	3.1 ± 0.6	6
50% COOH	67.8 ± 1.0	25.7 ± 1.4	1.7 ± 0.3	4.7 ± 0.8	6
60% COOH	67.0 ± 0.8	26.2 ± 1.0	1.7 ± 0.2	5.2 ± 0.3	6
70% COOH	66.7 ± 2.0	24.3 ± 2.1	1.6 ± 0.3	7.4 ± 0.5	6
80% COOH	67.2 ± 2.2	22.7 ± 2.7	1.5 ± 0.2	8.6 ± 0.8	3
90% COOH	65.0 ± 1.2	23.7 ± 1.4	1.4 ± 0.3	9.8 ± 0.6	10
100% COOH	64.2 ± 1.0	21.9 ± 1.5	1.4 ± 0.2	12.5 ± 0.7	10

[1] Data represent the average ± standard deviation for analysis performed at UW .

Table 5.2

Elemental Composition Determined by XPS of Binary Composition SAMs of $HS(CH_2)_{15}CH_2OH$ and $HS(CH_2)_{15}CH_3$

	Elemental Composition (atom percent)				
Thiol Soln. Composition	***C***	***Au***	***S***	***O***	***Number of Samples[1]***
0% CH_2OH	68.8 ± 2.7	28.7 ± 1.9	1.7 ± 0.3	0.8 ± 0.6	11
10% CH_2OH	67.4 ± 1.2	28.8 ± 1.2	1.9 ± 0.3	2.0 ± 0.3	6
20% CH_2OH	68.5 ± 2.0	27.7 ± 1.0	1.8 ± 0.5	2.0 ± 0.9	10
30% CH_2OH	60.6 ± 1.8	33.8 ± 1.5	2.6 ± 0.3	3.0 ± 0.2	6
40% CH_2OH	66.3 ± 2.3	28.9 ± 1.7	1.8 ± 0.3	3.0 ± 0.7	6
50% CH_2OH	65.7 ± 2.0	28.9 ± 1.3	2.0 ± 0.4	3.4 ± 0.5	6
60% CH_2OH	64.5 ± 3.4	29.1 ± 2.5	2.0 ± 0.4	4.4 ± 0.6	6
70% CH_2OH	65.4 ± 1.4	28.1 ± 1.8	1.9 ± 0.3	4.6 ± 0.3	6
80% CH_2OH	60.8 ± 1.3	31.1 ± 1.0	2.2 ± 0.4	5.9 ± 0.4	6
90% CH_2OH	62.0 ± 2.0	28.8 ± 1.8	1.8 ± 0.2	7.4 ± 1.0	6
100% CH_2OH	63.1 ± 2.5	26.9 ± 1.8	1.7 ± 0.5	8.4 ± 1.9	10

[1] Data represent the average ± standard deviation for analysis performed at UW.

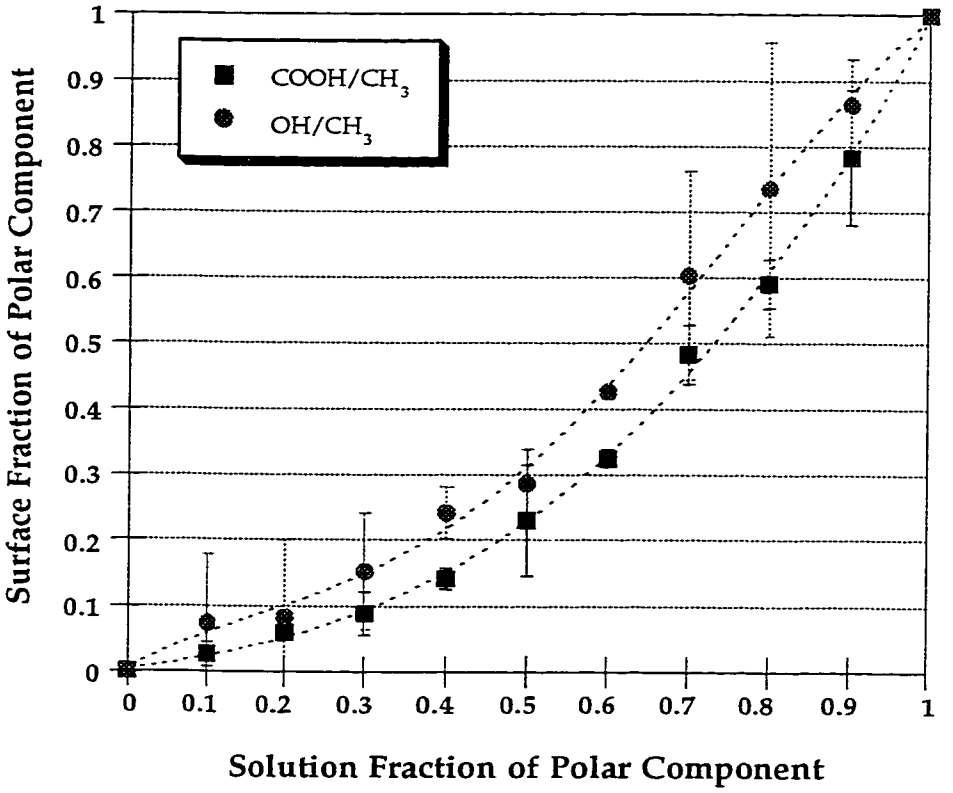

Figure 5.1 Composition of binary SAMs adsorbed from ethanolic mixtures of $HS(CH_2)_{15}COOH$ and $HS(CH_2)_{15}CH_3$ (squares) and mixtures of $HS(CH_2)_{15}CH_2OH$ and $HS(CH_2)_{15}CH_3$ (circles) onto gold substrates. The solution fraction of polar component represents the mole fraction of the COOH or OH-terminated thiol in the adsorbing thiol solution. The surface fraction of polar component represents the fraction of the COOH-terminated or OH-terminated thiol on the binary SAM surface as calculated from the ratio of the XPS O(1s) photoelectron intensity to the intensity of the Au(4f7/2) photoelectrons normalized to the O/Au ratio for the 100% COOH or 100% OH SAM. Data represent the average ± standard deviation of combined data collected at UW and Battelle.

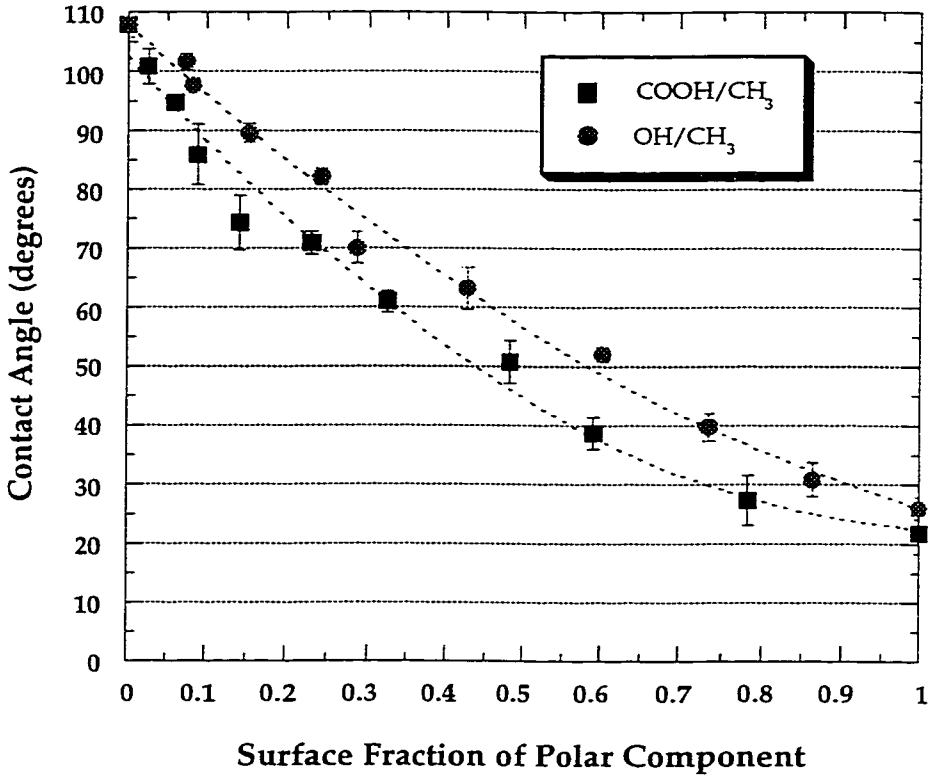

Figure 5.2 Advancing contact angles of water on binary SAMs adsorbed from ethanolic mixtures of $HS(CH_2)_{15}COOH$ and $HS(CH_2)_{15}CH_3$ (squares) and mixtures of $HS(CH_2)_{15}CH_2OH$ and $HS(CH_2)_{15}CH_3$ (circles) onto gold substrates as a function of binary SAM surface composition. The surface fraction of polar component represents the fraction of the COOH-terminated or OH-terminated thiol on the binary SAM surface as determined by XPS. Data represent the average ± standard deviation of triplicate samples.

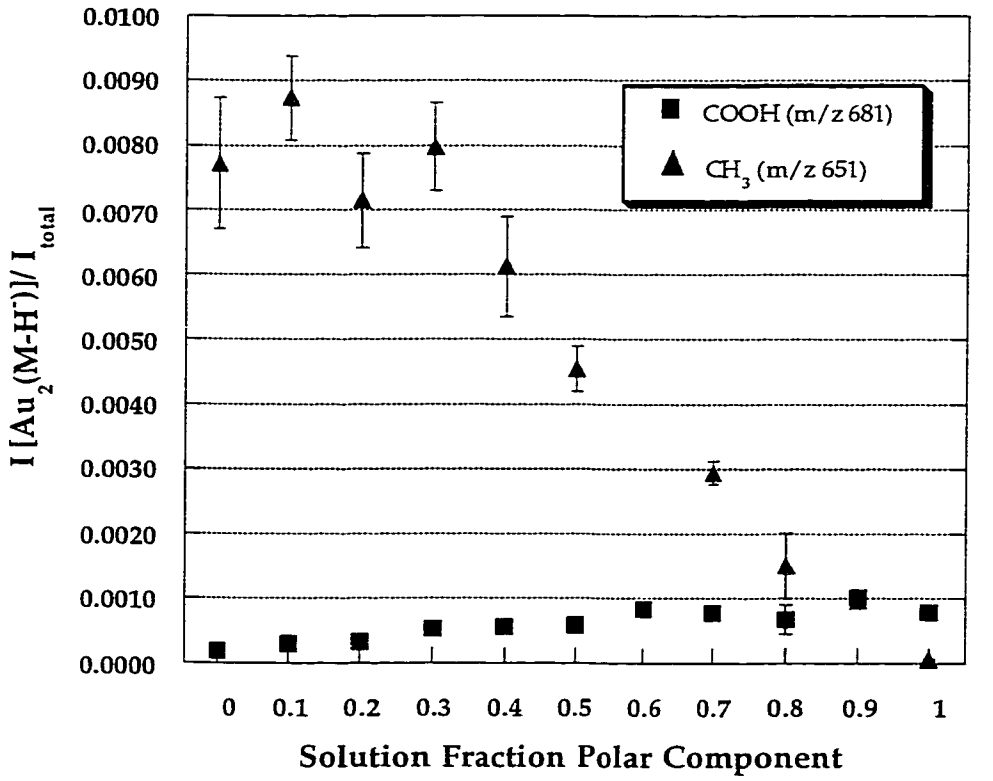

Figure 5.3 Normalized molecular ion cluster ($Au_2(M-H)^-$) peak intensity for the $HS(CH_2)_{15}COOH$ (681 m/z) and $HS(CH_2)_{15}CH_3$ (651 m/z) molecular ions obtained from the static SIMS spectra of binary composition SAMs of $HS(CH_2)_{15}COOH$ and $HS(CH_2)_{15}CH_3$ as a function of binary SAM solution composition. The solution fraction of polar component represents the mole fraction of the COOH-terminated thiol in the adsorbing thiol solution. Molecular ion cluster peak intensity was normalized to sample total ion intensity. Data represent the average ± standard deviation for two spots measured on duplicate samples.

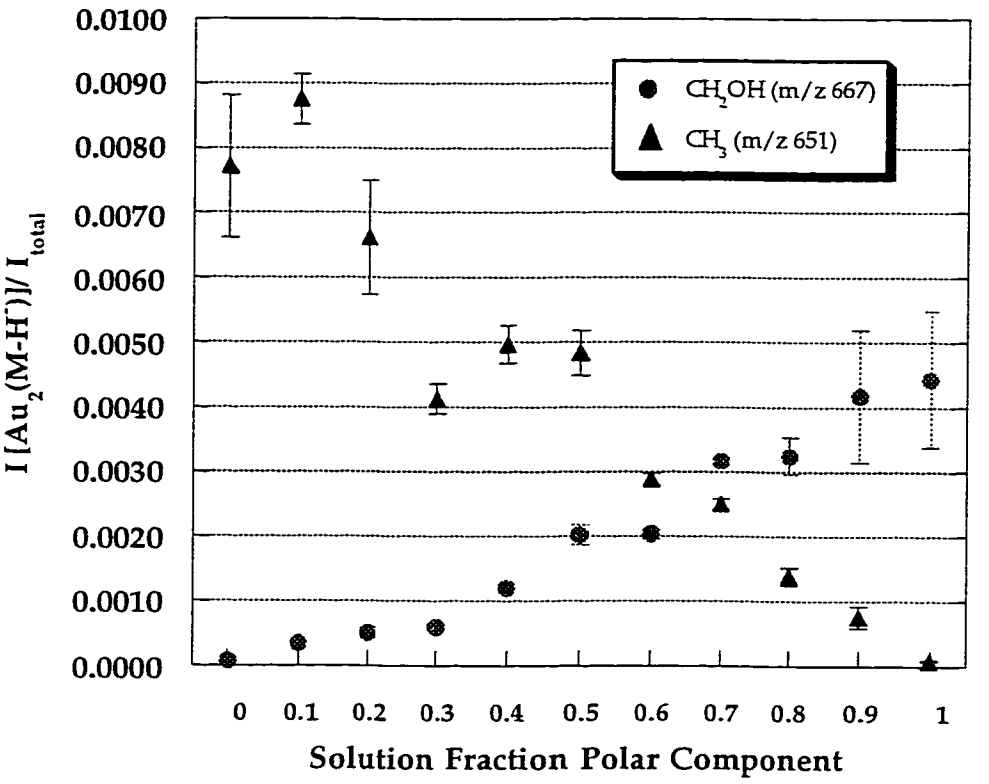

Figure 5.4 Normalized molecular ion cluster ($Au_2(M\text{-}H)^-$) peak intensity for the $HS(CH_2)_{15}CH_2OH$ (667 m/z) and $HS(CH_2)_{15}CH_3$ (651 m/z) molecular ions obtained from the static SIMS spectra of binary composition SAMs of $HS(CH_2)_{15}CH_2OH$ and $HS(CH_2)_{15}CH_3$ as a function of binary SAM solution composition. The solution fraction of polar component represents the mole fraction of the OH-terminated thiol in the adsorbing thiol solution. Molecular ion cluster peak intensity was normalized to sample total ion intensity. Data represent the average ± standard deviation for two spots measured on duplicate samples.

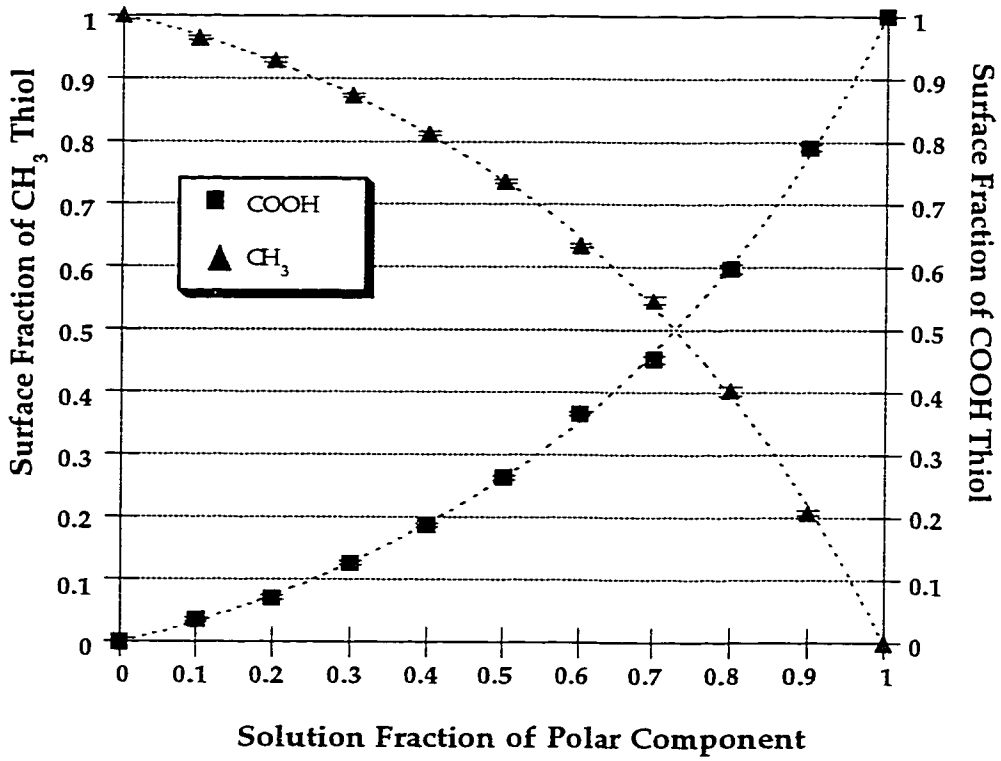

Figure 5.5 TOF-SIMS determined surface composition of binary SAMs adsorbed from ethanolic mixtures of $HS(CH_2)_{15}COOH$ and $HS(CH_2)_{15}CH_3$. The solution fraction of polar component represents the mole fraction of the COOH-terminated thiol in the adsorbing thiol solution. The surface fraction of CH_3 or COOH thiol component was calculated from the ratio of the normalized intensity of the $HS(CH_2)_{15}COOH$ or $HS(CH_2)_{15}CH_3$ molecular ion cluster to the sum of the normalized intensities of the $HS(CH_2)_{15}COOH$ and $HS(CH_2)_{15}CH_3$ molecular ion clusters for each sample as determined by TOF-SIMS. Data represent the average ± standard deviation of duplicate spots on duplicate samples.

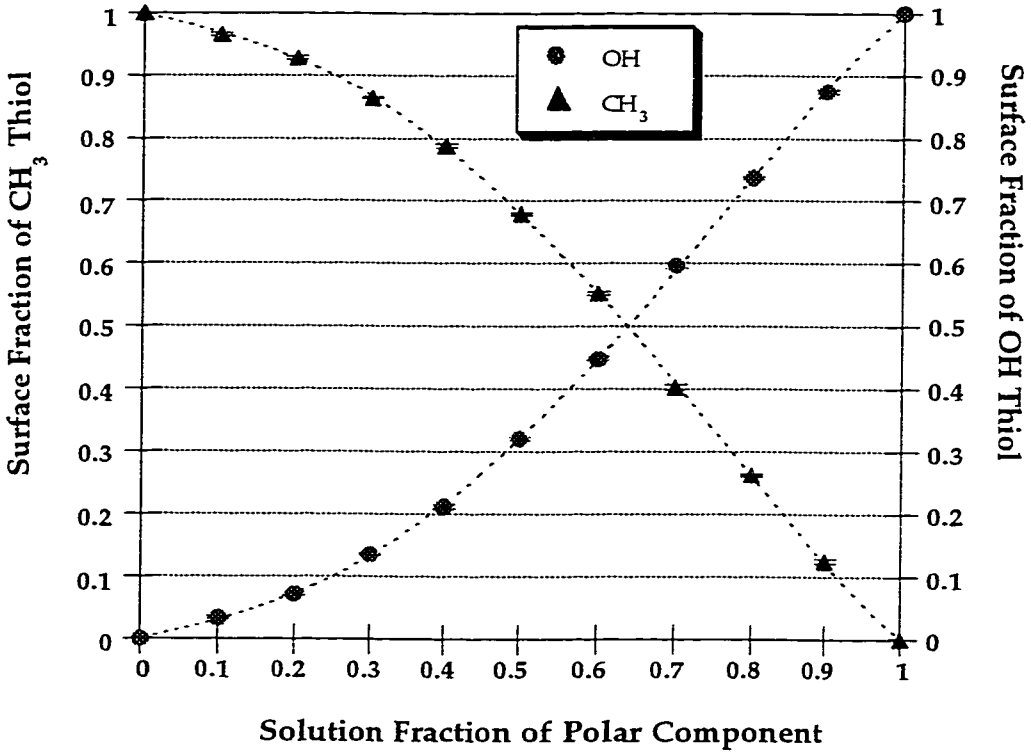

Figure 5.6 TOF-SIMS determined surface composition of binary SAMs adsorbed from ethanolic mixtures of $HS(CH_2)_{15}CH_2OH$ and $HS(CH_2)_{15}CH_3$. The solution fraction of polar component represents the mole fraction of OH-terminated thiol in the adsorbing thiol solution. The surface fraction of CH_3 or OH thiol component was calculated from the ratio of the normalized intensity of the $HS(CH_2)_{15}CH_2OH$ or $HS(CH_2)_{15}CH_3$ molecular ion cluster to the sum of the normalized intensities of the $HS(CH_2)_{15}CH_2OH$ and $HS(CH_2)_{15}CH_3$ molecular ion clusters for each sample as determined by TOF-SIMS. Data represent the average ± standard deviation of duplicate spots on duplicate samples.

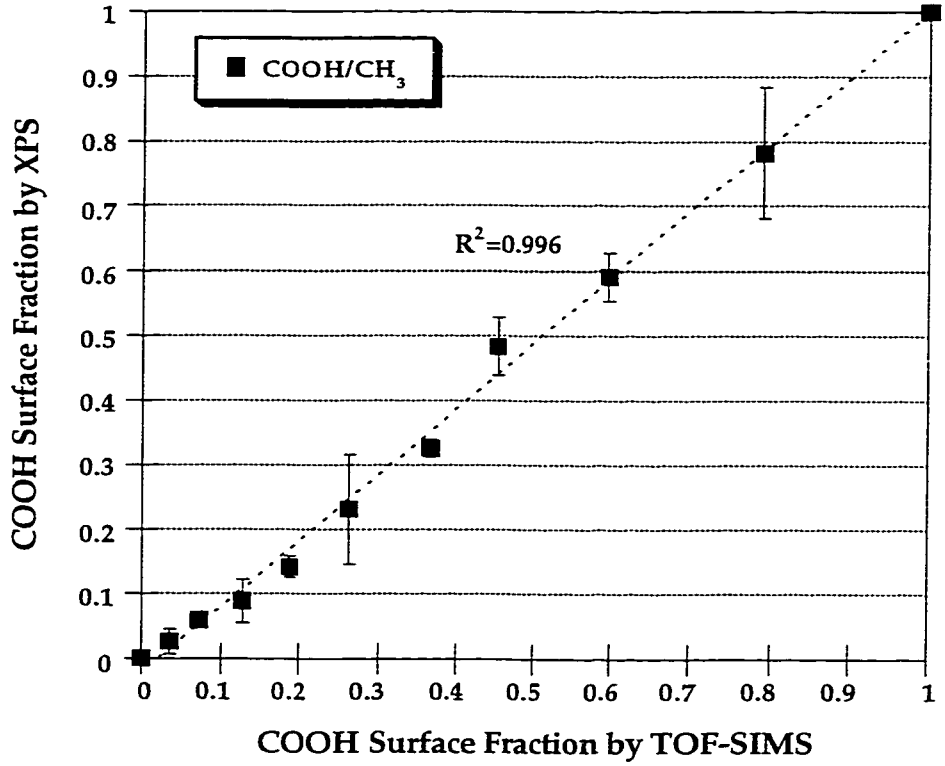

Figure 5.7 Relationship between the surface composition of binary SAMs of $HS(CH_2)_{15}COOH$ and $HS(CH_2)_{15}CH_3$ determined by XPS (reference Figure 5.1) and TOF-SIMS (reference Figures 5.1 and 5.7 respectively for description of surface composition calculations). Data represent the average ± standard deviation for duplicate spots on triplicate samples (XPS) and for duplicate spots on duplicate samples (TOF-SIMS).

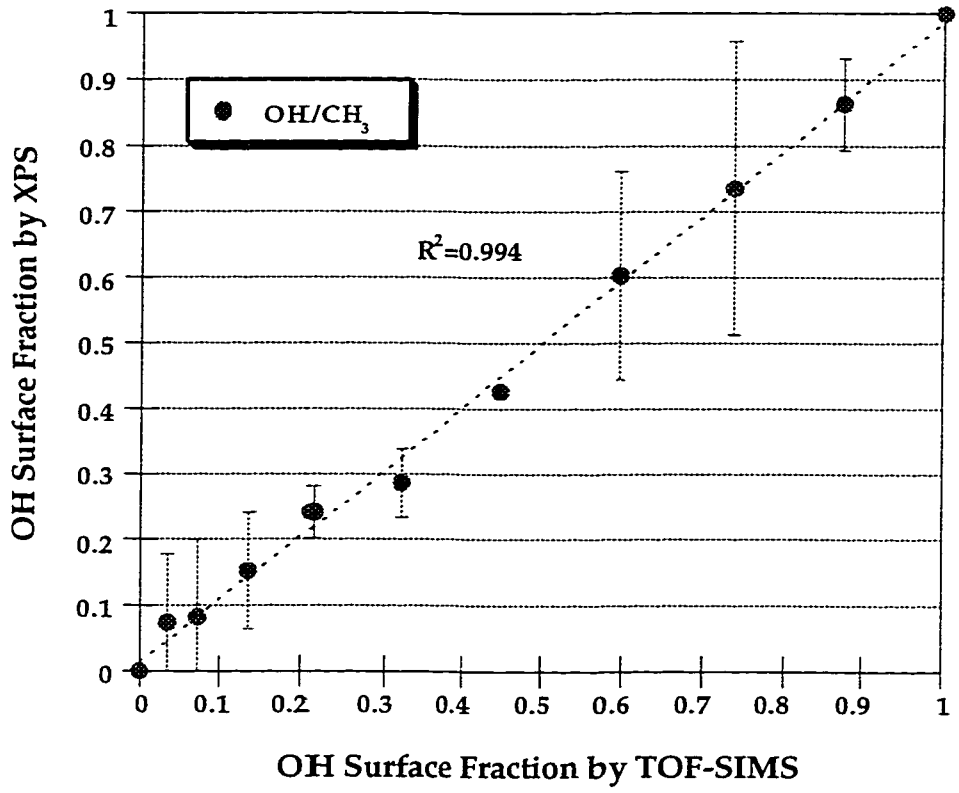

Figure 5.8 Relationship between the surface composition of binary SAMs of $HS(CH_2)_{15}CH_2OH$ and $HS(CH_2)_{15}CH_3$ determined by XPS and TOF-SIMS (reference Figures 5.1 and 5.8 respectively for description of surface composition calculations). Data represent the average ± standard deviation for duplicate spots on triplicate samples (XPS) and for duplicate spots on duplicate samples (TOF-SIMS).

Table 5.3

Elemental Composition Determined by XPS of Binary Composition SAMs of $HS(CH_2)_{15}COOH$ and $HS(CH_2)_{15}CH_2OH$

	Elemental Composition (atom percent)				
Thiol Soln. Composition	***C***	***Au***	***S***	***O***	***Number of Samples***[1]
0% OH	64.8 ± 1.4	21.3 ± 1.4	1.4 ± 0.2	12.6 ± 0.7	13
20% OH	67.0 ± 0.4	19.1 ± 0.9	1.2 ± 0.3	12.7 ± 1.0	4
40% OH	66.2 ± 0.1	21.9 ± 0.3	1.3 ± 0.4	10.6 ± 0.0	3
60% OH	66.7 ± 1.0	23.0 ± 0.4	1.6 ± 0.3	8.8 ± 0.3	4
80% OH	67.2 ± 0.4	23.3 ± 0.4	1.4 ± 0.1	8.1 ± 0.1	3
100% OH	64.0 ± 2.9	26.3 ± 2.1	1.6 ± 0.4	8.1 ± 1.7	13

[1] Data represent the average ± standard deviation for analysis performed at UW.

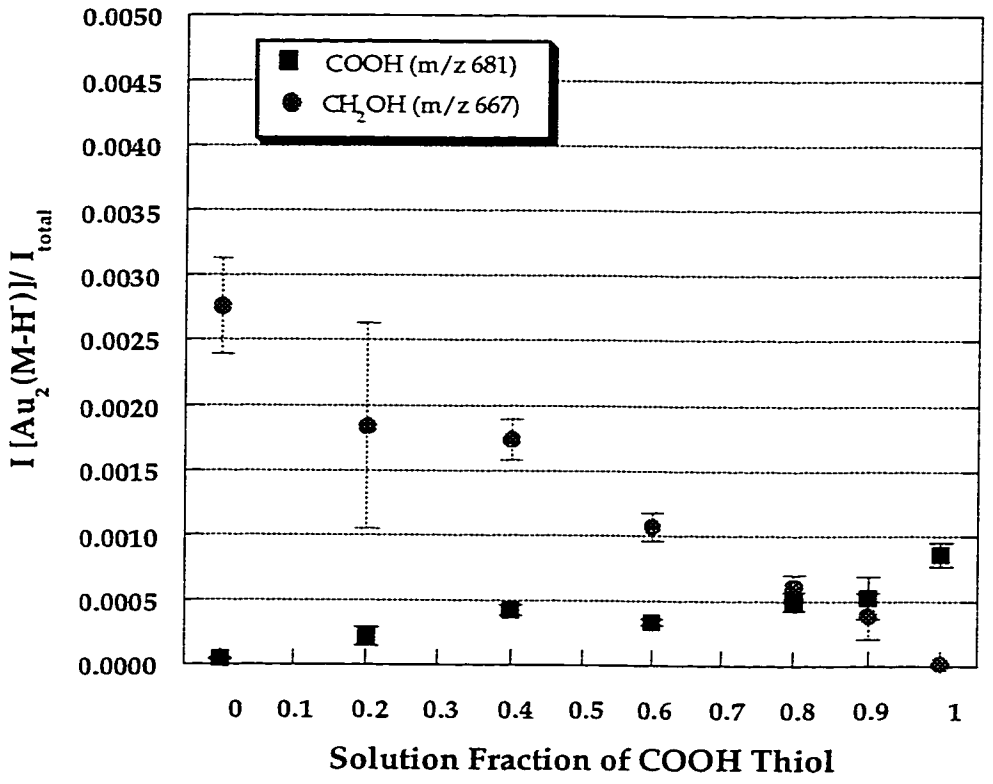

Figure 5.9 Normalized molecular ion cluster ($Au_2(M-H)^-$) peak intensity for the $HS(CH_2)_{15}COOH$ (681 m/z) and $HS(CH_2)_{15}CH_2OH$ (667 m/z) molecular ions obtained from the static SIMS spectra of binary composition SAMs of $HS(CH_2)_{15}COOH$ and $HS(CH_2)_{15}CH_2OH$ as a function of binary SAM solution composition (solution fraction of COOH thiol). Molecular ion cluster peak intensity was normalized to sample total ion intensity. Data represent the average ± standard deviation for two spots measured on duplicate samples.

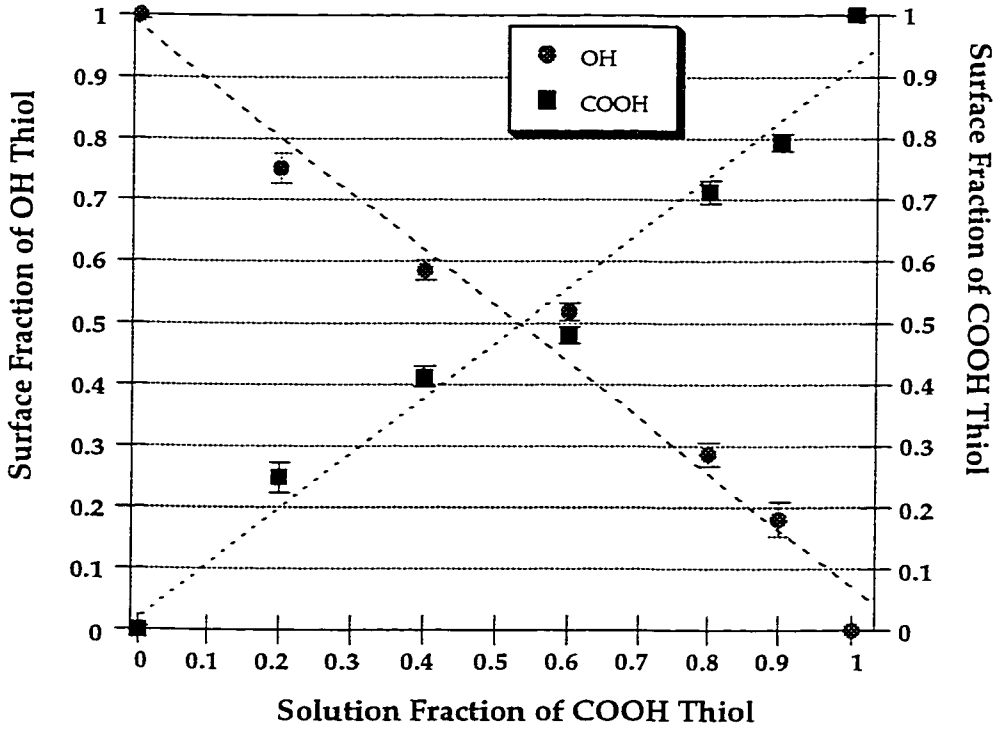

Figure 5.10 TOF-SIMS determined surface composition of binary SAMs adsorbed from ethanolic mixtures of $HS(CH_2)_{15}COOH$ and $HS(CH_2)_{15}CH_2OH$ as a function of COOH thiol solution fraction. The surface fraction of OH or COOH thiol component was calculated from the ratio of the normalized intensity of the $HS(CH_2)_{15}COOH$ or $HS(CH_2)_{15}CH_2OH$ molecular ion cluster to the sum of the normalized intensities of the $HS(CH_2)_{15}COOH$ and $HS(CH_2)_{15}CH_2OH$ molecular ion clusters for each sample as determined by TOF-SIMS. Data represent the average ± standard deviation of duplicate spots on duplicate samples.

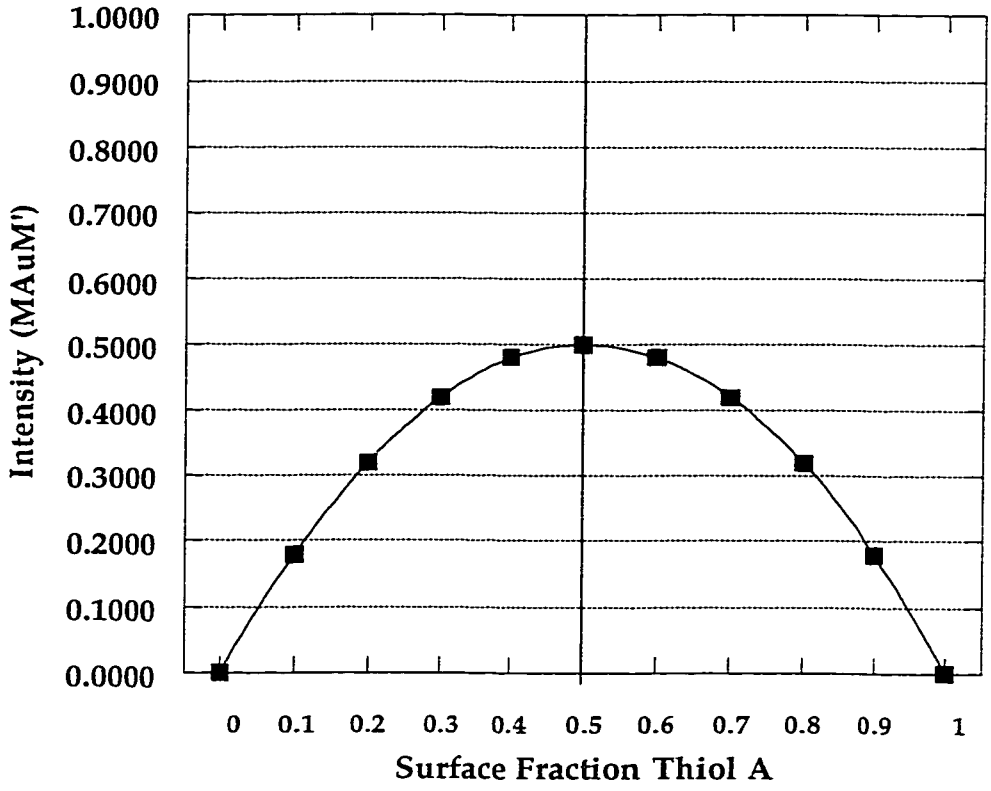

Figure 5.11 Theoretical distribution of the peak intensity of the dual species cluster (MAuM') generated from a binary component SAM as a function of surface composition of one thiol component (i.e., thiol A).

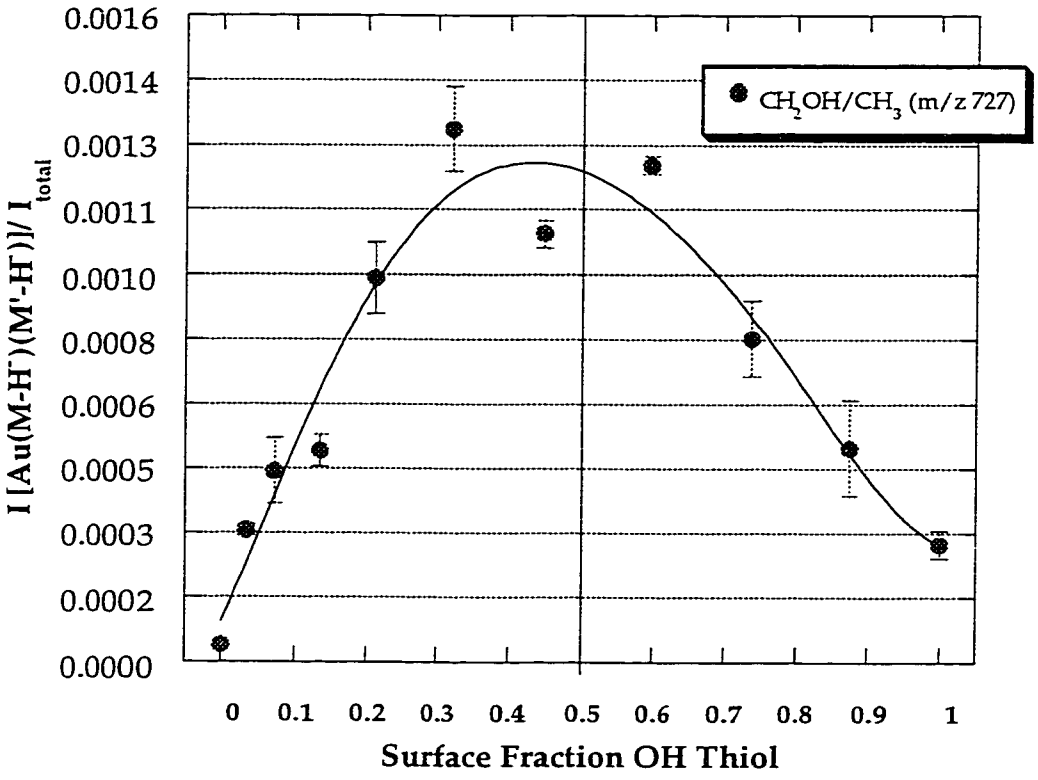

Figure 5.12 Normalized peak intensity of the dual species cluster (MAuM') obtained from the static SIMS spectra of binary composition SAMs of $HS(CH_2)_{15}CH_3$ and $HS(CH_2)_{15}CH_2OH$ as a function of binary SAM surface composition.

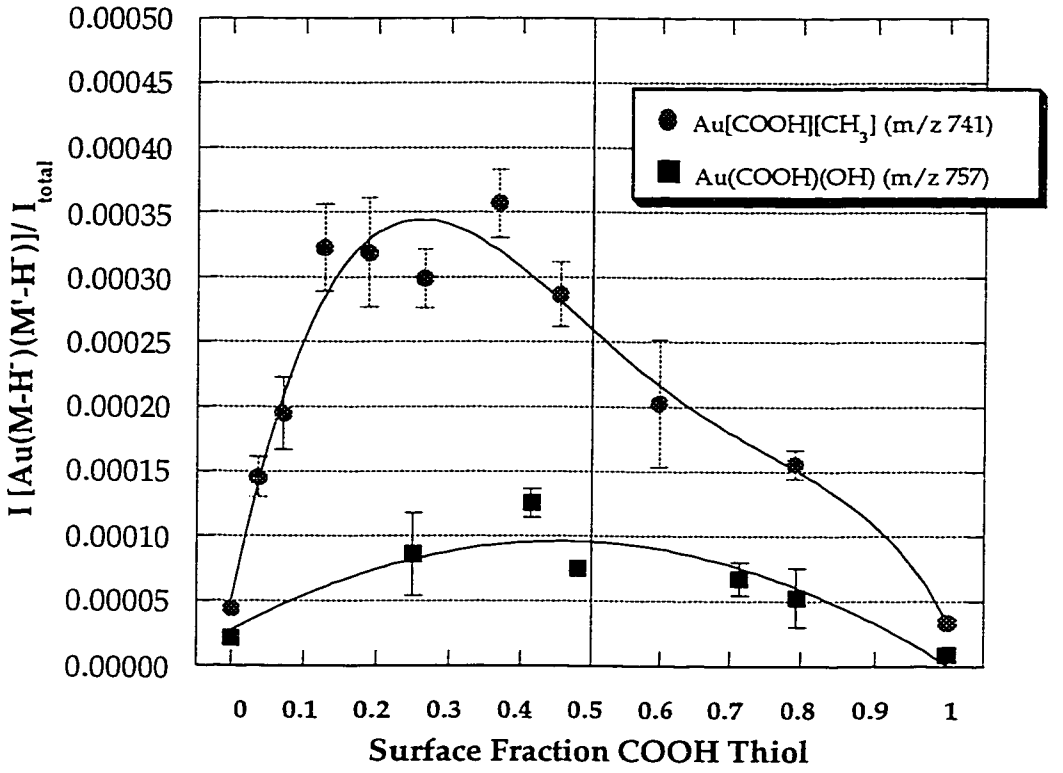

Figure 5.13 Normalized peak intensity of the dual species cluster (MAuM') obtained from the static SIMS spectra of binary composition SAMs of $HS(CH_2)_{15}COOH$ and $HS(CH_2)_{15}CH_2OH$ (squares) and binary composition SAMs of $HS(CH_2)_{15}COOH$ and $HS(CH_2)_{15}CH_3$ (circles) as a function of binary SAM surface composition.

Chapter 6

Endothelial Cell Interactions with Chemically Heterogeneous SAMs: Effect of Functional Group Concentration and Spatial Arrangement

6.1 Introduction

In preliminary studies of homogeneous and chemically heterogeneous SAMs (Chapters 3 and 4), the successful use of SAMs as model systems to investigate the effect of surface properties on protein and cellular interactions was demonstrated and several important results were obtained which provide information regarding the influence of surface chemical functionalities on cell growth. We observed significant variations in BAEC growth in response to surface chemical functionality on homogeneous SAM surfaces. Surface COOH groups were observed to promote BAEC spreading and growth to a significantly greater extent than did CH_3, CO_2CH_3 or OH groups. Preliminary studies of chemically heterogeneous SAMs demonstrated variations in cell growth in response to surface functional group concentration. However, only three target surface concentration ratios for two functional group pairs (COOH/OH and COOH/CH_3) were examined in the preliminary studies. Therefore, a more extensive evaluation the effect of functional group type and concentration on cell growth was performed. Our goal was to characterize the relationship between surface chemical functional group concentration and cell growth and consequently determine minimum surface concentrations of surface groups in binary mixtures which would result in the promotion or inhibition of growth.

Preliminary studies of chemically heterogeneous SAMs also demonstrated a possible effect of functional group spatial arrangement on cell growth and the adsorbed protein layer. Cell culture surfaces such as TCPS are typically heterogeneous with complex distributions of functional groups. While chemically complex surfaces such as

TCPS may be characterized with respect to types of surface functionalities present, the spatial arrangement and density of surface functional groups is typically not characterized. Consequently, the effect of functional group arrangement and density on cell growth is not well understood. In studies described in Chapter 4, we observed decreased cell growth for the COOH/CH_3 series compared with the COOH/OH series at the same surface COOH concentration. These results may suggest an effect of functional group arrangement in addition to concentration. Domain formation or functional group phase segregation may be occurring on the COOH/CH_3 series while a random distribution of functional groups would be expected on the COOH/OH series. To further investigate this finding, we proposed to compare cell growth on randomly mixed and phase segregated binary SAM systems.

In preliminary studies (Chapter 4), several COOH-containing binary SAM surfaces demonstrated cell growth levels which appeared to exceed growth on the homogeneous COOH surface suggesting that cell growth may be enhanced on chemically complex substrates compared with chemically homogeneous substrates. Other groups have proposed that cellular responses may be promoted on chemically and structurally complex substrates [23]. While biological surfaces are generally quite complex with local variations in structure and chemistry, most synthetic implant surfaces are in contrast, chemically and structurally uniform. In this chapter, we performed a quantitative evaluation of endothelial cell growth on homogeneous and chemically heterogeneous SAMs to assess the effect of increasing chemical complexity on biological interactions.

One limitation of the preliminary studies described in Chapters 3 and 4, was the lack of quantitative data from high seeding density studies. Therefore, for the studies described in Chapters 6 and 8, an assay that allows for quantitative evaluation of cell proliferation was utilized to measure cell number. Following a review of assay methods

available for measuring cell proliferation, the MTT assay was chosen for use. The MTT assay is a colorimetric method for determining the number of viable cells in a proliferation experiment and is described in further detail in Section 2.5.2.

The studies described in this chapter were designed to address three primary issues: 1) the effect of functional group concentration on cell growth, 2) the effect of functional group spatial arrangement on cell growth, and 3) an investigation of the cell growth characteristics of chemically heterogeneous surfaces compared with chemically homogeneous surfaces. We hypothesized that cell growth would be dependent upon the type, concentration and spatial arrangement of chemical functionalities on the substrate. Further, we hypothesized that cell growth on chemically heterogeneous surfaces would differ significantly from that on chemically homogeneous surfaces.

To investigate the effect of surface functional group content on cell growth, heterogeneous SAMs comprised of mixtures of alkanethiols terminated with growth-promoting (COOH) and growth-inhibiting functional groups (CH_3 and OH) were prepared to obtain substrates exhibiting systematic variations in functional group concentration. Two binary SAM series were evaluated: 1) a series of mixtures of $HS(CH_2)_{15}COOH$ and $HS(CH_2)_{15}CH_2OH$, and 2) a series of mixtures of $HS(CH_2)_{15}COOH$ and $HS(CH_2)_{15}CH_3$. In these binary SAM series, a growth-promoting functional group was paired with a growth-inhibiting group with the goal of achieving a gradient in cellular response.

To investigate the effect of functional group spatial arrangement, cell growth on the COOH/OH series was compared with cell growth on the COOH/CH_3 series. In Chapter 5, TOF-SIMS analysis provided evidence that the COOH/OH SAMs exist in a randomly mixed surface configuration while the COOH/CH_3 SAMs exist in a clustered, or phase-segregated configuration.

The third chemically heterogeneous SAM series evaluated in this chapter was a series of mixtures of $HS(CH_2)_{15}CH_2OH$ and $HS(CH_2)_{15}CH_3$. Since this system pairs two growth-inhibiting groups, it was used to determine if cell growth on chemically heterogeneous surfaces was improved over growth on chemically homogeneous surfaces.

6.2 Materials and Methods

6.2.1 Preparation of Chemically Heterogeneous SAMs

Three binary SAM systems were prepared as described in Section 2.2: 1) a series of mixtures of $HS(CH_2)_{15}COOH$ and $HS(CH_2)_{15}CH_2OH$, 2) a series of mixtures of $HS(CH_2)_{15}COOH$ and $HS(CH_2)_{15}CH_3$ and, 3) a series of mixtures of $HS(CH_2)_{15}OH$ and $HS(CH_2)_{15}CH_3$. The solution composition/surface composition relationships determined from surface analysis studies (Chapter 5, Figures 5.1, 5.7, 5.8, and 5.13), were used to select the appropriate thiol solution ratio required to achieve the desired surface composition. The binary SAM surface compositions prepared for evaluation in cell interactions studies are listed in Table 6.1.

6.2.2 Surface Analysis of Chemically Heterogeneous SAMs

For each binary SAM series evaluated in cell interaction studies, 4 additional samples of each surface composition were evaluated to verify SAM surface composition. 2 of the 4 samples were characterized by ellipsometry and contact angle at Battelle PNL immediately following SAM formation. The remaining 2 samples were analyzed by XPS and TOF-SIMS at the University of Washington (as described in Section 2.3 and Chapter 5) prior to performing the cell interaction studies. Binary SAM surface compositions for each series (data not presented) were verified by comparison with

surface analysis results presented in Chapter 5 to ensure that the desired surface compositions had been achieved.

6.2.3 Endothelial Cell Attachment and Growth

BAE culture was performed as described in Section 2.4. Cell growth experiments were performed using the binary SAMs listed in Table 6.1. Cell growth experiments were performed using four replicates of each binary SAM surface composition. SAM substrates were prepared for cell growth experiments as described in Section 2.5.2. TCPS was used as a control surface. Cells were seeded at a density of 5 x 10^4 cells/sample and cultured for up to 3 days. Cell number was measured using the MTT assay system as described in Section 2.5.2 after 3 culture time periods: 4 hours, 1 day, and 3 days. Cell morphology was evaluated throughout the culture period using light microscopy.

It is important to note that cell density or cell number observed qualitatively by light microscopy may differ in some instances from cell number determined quantitatively by the MTT procedure. The MTT assay procedure requires the removal of media in contact with the sample prior to the addition of the acidic isopropanol which causes cell lysis and allows for quantitation of formazan production. If any cells are weakly attached or loosely adherent (i.e., after the 4 hour culture period), removal of the media results in removal of weakly adherent cells. Therefore, while such loosely adherent cells may be visualized during light microscopy, it is possible that they would be removed and therefore not contribute to the MTT assay signal. Since the purpose of the MTT assay is to measure the number of metabolically active, adherent cells, removal of the media including non-adherent or weakly adherent cells is important to obtain an accurate measure of cell number.

In Chapter 2, the relationship between formazan solution absorbance and BAE cell number for the MTT assay (i.e., calibration curves) was illustrated in Figures 2.1 and 2.2. In addition to the calibration curves developed in Chapter 2, a calibration curve was developed in conjunction with the cell interaction experiments performed in this chapter. For each cell growth experiment performed, calibration data was developed by preparing a series of BAE cell suspensions (varying in cell concentration) using the BAE cell suspension which was applied to the binary SAM substrates for the cell growth experiment. Calibration data (i.e. formazan solution absorbance versus cell number on TCPS) was obtained for each experiment in a manner similar to that described in Section 2.5. The calibration data obtained for each cell growth experiment was combined to generate the curve shown in Figure 6.1. This curve was used to convert formazan solution absorbance values (measured during cell growth studies on the binary SAMs) to cell number.

6.3 Results and Discussion

6.3.1 BAEC Attachment and Growth on $COOH/CH_3$ Binary SAMs: Effect of Surface Composition

The effect of surface functional group content on BAE cell growth was evaluated for seven $COOH/CH_3$ SAMs following cell culture periods of 4 hours, 1 day, and 3 days. BAE cell number, as measured by the MTT assay procedure, on $COOH/CH_3$ surfaces and TCPS as a function of culture time is shown in Figure 6.2 for each surface composition. Figure 6.3 illustrates the BAE cell number measured at each culture time point on the $COOH/CH_3$ binary SAMs as a function of surface fraction of COOH thiol. The cell number measured on TCPS is also shown in Figure 6.3 for reference. In Figures 6.4, 6.5, and 6.6, the BAE cell number measured on the binary SAM normalized to the BAE cell number measured on the TCPS control surface is presented as a function

of surface COOH fraction for the 4 hour, 1 day, and 3 day culture time periods respectively.

Figure 6.2 indicates that all binary SAM surfaces showed an increase in cell number with increasing culture time however, significant differences in the rate of cell growth were observed in response to binary SAM surface composition. Cell number on the 0% COOH and 10% COOH surfaces exhibited only a 3-fold increase between the 4 hour time point and the 3 day time point. The 20% COOH and 40% COOH SAMs showed a 4-fold and 7-fold increase, respectively, in cell number over the 3 day culture period. The 60% COOH and 80% COOH surfaces demonstrated an 11-fold increase in cell number, while cell number on the 100% COOH surface increased by a factor of 9. Cell number on the TCPS control surface after 3 days of culture was lower than that on the 60%, 80%, and 100% SAMs however, a 10-fold increase in cell number was measured on TCPS over the 3 day culture period. These results clearly demonstrate an effect of SAM surface composition on cell growth.

The cell number measured at each time point for the COOH/CH_3 SAMs can be compared to cell number determined for the TCPS control surface in Figure 6.3. After the 4 hour culture period, cell numbers on the binary SAMs are essentially equivalent to cell number on TCPS. After a 1 day culture period, cell numbers on the 0%, 10%, 20% and 40% COOH surfaces are lower than on TCPS while cell numbers on the 60%, 80%, and 100% COOH surfaces are slightly higher than on TCPS. Cell number on the 0%, 10%, and 20% COOH surfaces are significantly lower than on TCPS after a 3 day culture period. The 40% COOH surface shows slightly lower cell number than TCPS. Again, the 60%, 80%, and 100% COOH surfaces demonstrate cell numbers after 3 days of culture which exceed the cell number observed on TCPS.

To specifically assess the effect of surface COOH content on cell number, SAM cell number normalized to cell number measured on TCPS is plotted as a function of

COOH surface fraction in Figures 6.4-6.6. In Figures 6.4-6.6, values greater than 1 indicate SAM cell numbers greater than values measured on TCPS, while values less than 1 indicate SAM cell numbers less than on TCPS. The doubling time for the BAE cell is typically 22 hours therefore, the measurement of cell number after a 4 hour period of culture can be considered a measurement of cell attachment (Figure 6.4) whereas the measurement of cell number after 1 and 3 days of culture is a measure of cell growth (Figures 6.5 and 6.6).

Normalized cell numbers on COOH/CH_3 SAMs after a 4 hour culture period do not differ significantly with COOH surface fraction (Figure 6.4). Cell number is lowest on the 0% COOH (100% CH_3) surface and highest on the 100% COOH SAM however, the differences are not statistically significant. These results indicate that BAE cell attachment is not dependent upon SAM surface composition. In addition, cell attachment on the COOH/CH_3 SAMs is slightly higher than cell attachment on TCPS since normalized cell numbers for all SAM compositions are slightly greater than 1.

Normalized cell numbers measured on the COOH/CH_3 SAMs after a 1 day culture period are shown in Figure 6.5. Cell numbers were lowest on the 0% and 10% COOH surfaces. Cell number increased with increasing surface COOH content for surface compositions of 10% COOH to 60% COOH. The greatest increase in cell number occurred between 40% and 60% surface COOH content (75% increase). Cell number was highest on the 60% COOH surface and decreased slightly for the 80% and 100% COOH surfaces. The 60%, 80%, and 100% COOH SAMs demonstrated cell numbers higher than cell numbers on TCPS (normalized cell numbers >1). The increases in cell number for the 60% and 80% SAMs relative to TCPS are statistically significant however, the difference in cell number between the 100% SAM and TCPS is not statistically significant.

A similar cell growth pattern was observed for the $COOH/CH_3$ SAMs following the 3 day culture period (Figure 6.6). Cell numbers were lowest on the 0% COOH and 10% COOH surfaces and increased with increasing COOH surface fraction between 10% and 60% COOH. Statistically significant increases in cell number were measured for all surface compositions between 10-60% COOH. As was observed for the 1 day culture period, cell number was highest for the 60% COOH surface and decreased slightly for the 80% and 100% COOH surfaces. Again, the 60%, 80%, and 100% COOH surfaces exhibited cell numbers higher (approximately 20% higher) than the cell number measured on TCPS. The increases in cell number for the 60%, 80%, and 100% COOH surfaces relative to TCPS are statistically significant.

BAEC density and morphology on the $COOH/CH_3$ SAMs and TCPS was also evaluated qualitatively after 4 hour, 1 day and 3 day culture periods in a series of light micrographs shown in Figures 6.7, 6.8, and 6.9. Figure 6.7 illustrates cell morphology after 4 hours of culture. Consistent with results shown in Figure 6.4, all SAM surfaces exhibited similar cell densities. Large numbers of weakly adherent, rounded cells are observed for all surfaces. For all SAM surfaces, the majority of cells are rounded in appearance however, some evidence of cell spreading is observed on the 40-100% COOH surfaces, particularly on the 60%, 80% and 100% COOH surfaces. Cell spreading is also evident on the TCPS surface.

Significant differences in both cell density and morphology are observed for the $COOH/CH_3$ SAMs after 1 and 3 day culture periods (Figures 6.8 and 6.9). After 1 day of culture, the 0% COOH (100% CH_3) and the 10% COOH surfaces show clusters of rounded cells with very few spread cells evident. Cell density was higher on the 20% COOH surface and a greater fraction of cells were spread. Cell density increased on the 40% COOH surface and the surface was uniformly covered with well spread cells. A significant increase in cell density occurred for the 60% COOH surface. This surface

exhibited a nearly confluent cell monolayer. The 80% and 100% COOH surfaces were similar appearance to the 60% surface. Similarly, a nearly confluent monolayer of cells was observed on the TCPS surface. Cell densities appeared higher on the 60-100% COOH surfaces than on TCPS due to the presence of several areas of large senescent cells observed on the TCPS surface. After 3 days of culture, similar patterns in cell density and morphology are observed. The 0% and 10% COOH surfaces show low cell densities with few cells exhibiting spreading. Cell density increased for the 20% and 40% COOH surfaces and was maximal for 60-100% COOH surfaces. The 60-100% COOH surfaces exhibited confluent cell monolayers. TCPS also exhibited a confluent monolayer with areas of large senescent cells as observed in Figure 6.8. Qualitative evaluations of the $COOH/CH_3$ SAMs are consistent with quantitative evaluations of cell number via the MTT assay.

Qualitative and quantitative evaluations of BAE interactions with a series of $COOH/CH_3$ binary SAMs demonstrate several important results. Cell number after the 4 hour culture period, a measure of cell attachment, was independent of binary SAM surface composition. High levels of cell attachment are not predictive of the cell growth potential of a surface. For example, the 10% and 80% COOH surfaces supported equivalent levels of cell attachment, yet significant differences in cell growth were noted with poor growth observed on the 10% COOH surface and excellent growth observed on the 80% COOH surface. While high levels of cell attachment do not necessarily result in the promotion of cell growth by a surface, it is certainly true that a surface cannot support cell growth unless there is cell attachment.

Results of the 1 and 3 day growth studies demonstrated significant differences in cell growth in response to SAM surface composition, specifically surface COOH content. Cell growth increased significantly with increasing surface fraction of COOH for surface compositions ranging from 10-60% COOH. A surface COOH content of 40% was

required to result in a significant increase in cell growth level relative to the 0% COOH (100% CH_3) surface. As surface COOH content increased above 60%, no significant increases in cell growth were observed. Instead, cell growth decreased slightly for surface compositions ranging from 60-100%. It appears that the optimal density of surface COOH groups required to promote cell growth is achieved at 60% surface COOH. Evaluation of the adsorbed protein layers is required to understand the significance of the 60% COOH surface in terms of its ability to promote maximal cell growth (reference Chapter 7 for summary of protein adsorption studies).

The significant increases in cell growth observed on the 60%, 80%, and 100% COOH surfaces relative to cell growth on TCPS is an important finding. In previous qualitative studies of COOH/CH_3 SAMs (in Chapter 4), we observed that cell density on 50% COOH and 75% COOH surfaces appeared to approach or exceed cell growth observed on TCPS. The results shown in Figures 6.2-6.6 provide quantitative evidence which supports the previous qualitative observations. These findings are significant since cell growth levels on the majority of synthetic biomaterial surfaces are typically lower than cell growth levels on TPCS which is considered an optimal cell culture surface. The ability to create a cell growth substrate of well-defined chemistry which promotes cell growth to levels in excess of that on TCPS may prove to be very beneficial.

6.3.2 BAEC Attachment and Growth on COOH/OH Binary SAMs: Effect of Surface Composition

The effect of surface composition on BAEC attachment and growth was evaluated for seven COOH/OH SAMs following cell culture periods of 4 hours, 1 day, and 3 days. Figure 6.10 shows BAE cell number measured on the COOH/OH SAMs and TCPS as a function of culture time. Figure 6.11 illustrates the cell number measured at each culture

time point on the COOH/OH binary SAMs as a function of COOH surface fraction. The cell number measured on TCPS is also shown in Figure 6.11 for reference. Figures 6.12, 6.13, and 6.14 illustrate BAE cell numbers measured on the COOH/OH SAMs normalized to the BAE cell number measured on the TCPS control surface as a function of surface COOH fraction for the 4 hour, 1 day, and 3 day culture time periods respectively.

All COOH/OH surfaces showed an increase in cell number with increasing culture time, however significant differences in the rate of growth were observed in response to SAM surface composition (Figure 6.10). The 0% COOH surface exhibited the lowest increase in cell number between the 4 hour and 3 day time points (4-fold increase) while the 20% COOH surface exhibited a slightly higher increase in cell number (10-fold increase). A significantly higher increase in cell number was observed for the 40-100% COOH surfaces and for TCPS. The 40-100% COOH surfaces demonstrated approximately a 20-fold increase in cell number between the 4 hour and 3 day culture time points. Cell number on the TCPS control surface after 3 days of culture was lower than on the 50%, 70%, 80% and 100% COOH surfaces however, a 22-fold increase in cell number was measured on TCPS over the 3 day culture period. These results demonstrate the effect of surface COOH content on the growth of BAE cells.

Figure 6.11 illustrates the cell number measured on the COOH/OH SAMs and on TPCS at each culture time point. After the 4 hour culture period, cell numbers on the binary SAMs are essentially equivalent to cell number on TCPS. After 1 day of culture, cell numbers on the 0% and 20% COOH surfaces are lower than on TCPS while surfaces containing 40-100% COOH show cell numbers higher than on TCPS. After 3 days of culture, cell numbers on the 0% and 20% COOH surfaces were significantly lower than on TCPS. The 40% COOH surface exhibited a slightly lower cell number than on

TCPS. Cell numbers on the 50%, 70%, 80% and 100% COOH surfaces were higher than on TCPS.

Normalized cell numbers measured on the COOH/OH SAMs after 4 hours of culture are shown in Figure 6.12. Cell attachment was highest on the 0% COOH (100% OH) surface and lowest on the 20% COOH surface. Cell attachment decreased from 0% to 20% COOH, increased between 20% and 70% COOH, decreased from 70 to 80% COOH and was equivalent for 80% and 100% COOH concentrations. There does not appear to be a consistent relationship between cell attachment and surface COOH content. All COOH/OH surfaces showed cell attachment levels higher than on TCPS with a significantly higher cell number measured on the 0% COOH surface compared with TPCS.

Figure 6.13 illustrates the normalized cell number measured on the COOH/OH SAMs after a 1 day culture period. Cell number was lowest on the 0% COOH surface and increased with increasing surface COOH fraction between 0% COOH and 50% COOH. A statistically significant increase in cell number occurred with only a 20% COOH surface fraction. The greatest increase in cell number occurred between 20% COOH and 40% COOH (85% increase). Cell number increased slightly (9%) from 40% COOH to 50% COOH and was highest on the 50% COOH surface. Cell number decreased from 50% COOH to 70% COOH (15%) and decreased slightly for surface COOH concentrations above 70%. The 40%, 50%, and 70% COOH/OH surfaces demonstrated a significantly higher cell number than the 100% COOH surface. The 40%, 50%, 70%, 80% and 100% COOH SAMs demonstrated cell numbers higher than on TPCS (normalized cell numbers >1). The increases in cell number between the 40%, 50%, and 70% surfaces relative to TCPS were statistically significant.

The COOH/OH SAMs exhibited a similar cell growth pattern following a 3 day culture period (Figure 6.14). Cell number was lowest on the 0% COOH surface and

increased with increasing COOH surface fraction from 0% to 50% COOH. A significant increase in cell number occurred at a 20% COOH content. Cell number increased by 90% between 20% and 40% COOH. Cell number increased between the 40% and 50% COOH surfaces (20%) and reached a maximum value on the 50% COOH surface. Cell number decreased 9% between 50% and 70% COOH and remained relatively constant for COOH concentrations greater than 70% COOH. Cell numbers on the 50-100% COOH surfaces were higher than on TCPS. The increase in cell number on the 50% COOH surface relative to TCPS was statistically significant.

BAEC density and morphology on the COOH/OH SAMs and TCPS was evaluated qualitatively after 4 hour, 1 day and 3 day culture periods in a series of light micrographs shown in Figures 6.15, 6.16, and 6.17. Figure 6.15 illustrates cell morphology after 4 hours of culture. Consistent with results shown in Figure 6.12, the 0% COOH (100% OH) surface exhibited the highest cell density. Cell density on the 20%-100% COOH surfaces was equivalent. The majority of cells on the SAM surfaces were rounded however, some cell spreading was observed on the 20-100% COOH surfaces and on TCPS.

Significant differences in both cell density and morphology are observed for the COOH/OH SAMs after 1 and 3 day culture periods (Figures 6.16 and 6.17). After 1 day of culture, the 0% COOH surface (100% OH) surface showed clusters of rounded cells with no evidence of cell spreading. Cell density increased on the 20% COOH surface and the majority of cells were well spread. Cell density increased significantly on the 40% COOH surface. The 50% COOH surface exhibited a nearly confluent monolayer of cells. Cell density decreased slightly on the 70% COOH surface. The 70%-100% COOH surfaces were similar in cell density and were essentially equivalent in appearance to the TCPS surface.

Similar patterns are observed for the COOH/OH surfaces after 3 days of culture (Figure 18). Few clusters of cells are present on the 0% COOH surface. The 20% COOH surface demonstrates dense areas of spread cells interspersed with areas containing very few cells. The 40% COOH surface shows a nearly confluent monolayer while a very dense, confluent cell monolayer is observed on the 50% COOH surface. The 70-100% COOH surfaces also exhibited confluent cell monolayers. The TCPS surface similarly exhibited a confluent monolayer and contained several large senescent cells as observed previously.

Evaluation of the COOH/OH SAMs in qualitative and quantitative studies provided several important results regarding the effects of surface composition on cell attachment and growth. As observed for the COOH/CH_3 binary SAM system, cell number after 4 hours of culture did not vary predictably with COOH surface concentration. Higher levels of cell attachment did not correlate with higher cell growth levels. The 0% COOH (100% OH) surface demonstrated the highest cell attachment level of all binary SAMs tested, yet this surface was a very poor supporter of cell growth as we have observed previously (Chapters 4 and 5).

Evaluation of cell growth after 1 and 3 day culture periods demonstrated significant differences in cell growth in response to SAM surface composition. Cell number was very low on the 0% COOH (100% OH) surface and increased significantly for a surface COOH content of only 20%. In Chapter 5, we observed similar increases in cell growth for a COOH surface content of 25% and proposed that a COOH surface fraction lower than 25% might support cell growth. It appears that a surface COOH content of as low as 20% is sufficient to promote cell growth. Cell growth increased dramatically as surface COOH content increased from 20% to 40%. Cell number was maximal for the 50% COOH/OH surface. While cell growth peaked at 50%, the cell growth levels on the 40% COOH/OH surface were close to cell numbers on the 50%

surface. Above 70% COOH, cell growth did not vary significantly with surface composition. The optimal density of surface COOH groups providing maximal promotion of cell growth is achieved at 50% surface COOH.

In Chapter 5, we observed in qualitative studies that cell density on 50% and 75% COOH SAMs appeared to approach or exceed the cell density on TCPS and on the 100% COOH SAM. The results shown in Figures 6.13 and 6.14 support the previous qualitative observations. Cell growth on surfaces containing 40% or more COOH demonstrated cell growth levels greater than or equal to cell growth on TCPS.

6.3.3 Comparison of BAE Attachment and Growth on COOH/CH_3 SAMs and COOH/OH SAMs: Effect of Surface Functional Group Arrangement

To investigate the effect of functional group spatial arrangement on the growth of endothelial cells, cell growth on the COOH/OH binary SAM series (described in Section 6.3.2) was compared with cell growth on the COOH/CH_3 series (Section 6.3.1). TOF-SIMS analysis of the COOH/OH and COOH/CH_3 systems (Chapter 5) provided evidence which suggested differences in the dispersion of surface functional groups for these SAM systems. The COOH/OH system demonstrated a pattern indicative of a randomly mixed surface configuration while the COOH/CH_3 system demonstrated a pattern indicative of a clustered, phase-segregated arrangement of surface functionalities. The CH_3 and OH functionalities are considered essentially equivalent in their ability to support cell growth (i.e., both are poor supports of growth). Therefore, we can compare cell growth on the COOH/OH SAMs and the COOH/CH_3 SAMs at a given surface COOH fraction to assess the effect of surface functional group arrangement.

Figure 6.18, 6.19, and 6.20 present the normalized cell numbers measured for the COOH/OH and the COOH/CH_3 SAMs after 4 hour, 1 day and 3 day culture periods as a function of surface COOH content. Cell numbers measured on the SAM surfaces

are normalized to cell number measured on the TCPS control used in the same experiment. By normalizing cell numbers in this manner, comparisons can be made between the different SAM series for experiments performed at different times.

After the 4 hour culture period, normalized cell numbers (a measure of cell attachment) did not differ significantly between the COOH/OH and COOH/CH_3 SAM systems for surface COOH concentrations between 10% and 100% COOH (Figure 6.18). At 0% COOH, cell attachment on the COOH/OH surface (100% OH) was significantly higher than that on the COOH/CH_3 surface (100% CH_3). This finding is consistent with previous studies which have demonstrated an enhanced cell adhesion or attachment on hydroxyl-containing surfaces [11, 29, also see Chapter 1, Section 2 for further discussion].

Figure 6.19 shows normalized cell number on the COOH/OH and COOH/CH_3 SAMs following a 1 day growth period. Cell growth on the 0% COOH (the 100% OH and 100% CH_3) surfaces is equivalent. However, as surface COOH content increased from 10% to 60%, significant differences in cell number were observed between the SAM systems. Cell growth on the COOH/OH surfaces was significantly higher than on the COOH/CH_3 surfaces at an equivalent surface COOH fraction. The difference is most significant at a surface COOH content of 40%. For surface COOH contents greater than 60%, the differences between the two binary systems are not significant. Cell number on the COOH/CH_3 surfaces were slightly higher than on the COOH/OH surfaces for surface COOH contents from 60% to 100%. Cell numbers on the 100% COOH surfaces measured in the separate experiments did not differ significantly.

As shown in Figures 6.5 and 6.13, maximal cell growth is measured at 50% COOH for the COOH/OH surfaces, and at 60% for the COOH/CH_3 surfaces. The COOH/OH cell number curve shown in Figure 6.19 increases more rapidly with increasing COOH content and peaks at 50% COOH. The COOH/CH_3 surfaces show a

more gradual increase in cell number with increasing surface COOH content and a peak in cell number was reached at a higher surface COOH content of 60%. Both curves show a gradual decrease in cell number with increasing surface COOH content above 70%. The results shown in Figure 6.19 suggest that for certain surface compositions, cell growth on the COOH/OH and COOH/CH_3 surfaces is affected by the spatial arrangement of the surface COOH groups. Between 0%-60%, cell numbers on the COOH/CH_3 system are lower than on the COOH/OH system at the same surface composition. At 40% COOH, the cell number on the COOH/OH surface is 80% higher than on the COOH/CH_3 surface. Cell growth on the 40% COOH/60% OH surface is higher than on the 100% COOH surface and 20% higher than on TCPS. In contrast, cell growth on the 40% COOH/60% CH_3 surface was 30% lower than on TCPS.

It appears that for COOH surface fractions less than 60%, the clustered arrangement of the COOH/CH_3 surface results in a decreased level of cell growth given the same surface COOH content. The growth inhibitory effect of the poor growth component of the binary SAM (i.e. CH_3 or OH) is more pronounced when it exists in clusters on the SAM surface. When the same concentration of the poor growth component is randomly mixed on the SAM surface, its negative effect on cell growth is diminished. The clusters of poor growth component probably influence protein adsorption and/or the deposition of cell derived proteins in a manner which depresses cell growth. At higher COOH surface fractions (i.e., lower surface fraction of poor growth component), there does not appear to be an effect of surface functional group segregation on cell growth. At these compositions, the clusters of the poor growth component are probably small enough that their effect on protein adsorption relative to adsorption on a randomly mixed surface is minimal.

After a 3 day cell growth period, cell growth patterns on the COOH/OH and COOH/CH_3 systems are very similar (Figure 6.20). Again, cell number on the 100%

OH and 100% CH_3 surfaces (0% COOH) are equivalent. Cell numbers are equivalent for the two systems between 0% and 30% COOH. From 30% to 50% COOH, cell numbers are higher on the COOH/OH surfaces than on the COOH/CH_3 surfaces however, the differences are not significant. Cell growth reaches a peak at 50% on the COOH/OH surfaces and at a higher COOH content of 60% on the COOH/CH_3 surfaces. Above the point of maximum cell number, cell growth on both systems levels off or decreases slightly with increasing surface COOH content. Cell numbers are slightly higher on the COOH/CH_3 system between 60%-100% COOH however, the differences are not significant.

After a 3 day growth period, the arrangement of surface functional groups on the binary SAM surfaces appears to have a much lower effect on cell growth compared to the effects observed after 1 day of growth. While cell number on the COOH/OH surfaces is 10% higher than on the COOH/CH_3 surfaces between 40%-50% COOH, the differences are not significant. Surface functional group dispersion appears to have an effect on cell growth in the early phase of cell growth but the effect diminishes with increasing cell culture time. In the early phase of cell interactions with a substrate (i.e. 0-24 hours of culture), surface functional group dispersion may have a more significant influence on the adsorbed protein layer composition and configuration, and consequently on cell growth. Once cell proliferation on a surface is well established, and the conditioning of the surface with cell-derived proteins is underway, the effect of surface functional group dispersion may be minimized.

6.3.4 BAEC Attachment and Growth on OH/CH_3 Binary SAMs: Effect of Surface Chemical Heterogeneity

To determine the effect of surface chemical heterogeneity on cell growth, cell growth on OH/CH_3 binary SAMs was compared with cell growth on the homogeneous

CH_3 and OH SAMs. The BAE cell number measured on the OH/CH_3 surfaces and TCPS as a function of culture time is shown in Figure 6.21 for each surface composition. Figure 6.22 shows the cell number measured on the OH/CH_3 surfaces at each culture time point as a function of OH surface fraction. In Figures 6.23, 6.24, and 6.25, the BAE cell number measured on the binary SAM normalized to the BAE cell number measured on the TCPS control surface is presented as a function of surface OH fraction for the 4 hour, 1 day, and 3 day culture time periods respectively.

All OH/CH_3 surfaces showed an increase in cell number with increasing culture time, however the rates of growth for all OH/CH_3 surfaces were very low compared with other binary SAM systems (Section 6.3.1 and 6.3.2) and compared with TCPS. Cell number on the TCPS control surface showed a 18-fold increase between the 4 hour and 3 day time points. In contrast, significantly lower increases in cell number was observed for all of the OH/CH_3 surfaces. The OH/CH_3 surfaces demonstrated approximately a 3-4 fold increase in cell number over the 3 day culture period.

Figure 6.22 illustrates the cell numbers measured on the OH/CH_3 SAMs and on TCPS at each culture time point. After 4 hours of culture, cell numbers on the OH/CH_3 surfaces are equivalent and slightly higher than on TCPS. After 1 and 3 days of culture, cell numbers on all OH/CH_3 surfaces are significantly lower than on TCPS. This difference is most pronounced at the 3 day time point.

The normalized cell numbers measured on the OH/CH_3 SAMs after 4 hours of culture are shown in Figure 6.23. Cell number (cell attachment) was highest on the 80% OH surface and lowest on the 40% OH surface. Cell attachment did not vary in a consistent manner with surface OH content. Cell attachment on the homogeneous surfaces (0% and 100% OH) did not differ significantly from cell attachment on the OH/CH_3 surfaces. Cell attachment on all OH/CH_3 surfaces was 28-49% higher than cell attachment on TCPS.

After a 1 day culture period, cell numbers on the OH/CH_3 surfaces did not differ significantly with surface OH fraction (Figure 6.24). Cell numbers on the homogeneous surfaces did not differ significantly from cell number measured on the OH/CH_3 surfaces. More importantly, cell number on all OH/CH_3 surfaces was significantly lower (approximately 50%) than TCPS cell number. A similar result is obtained after the 3 day culture period (Figure 6.25). Cell numbers on all OH/CH_3 surfaces were low. Cell number was higher on the 20% OH surface than any other OH/CH_3 surface however, the difference was not statistically significant. Cell numbers on the OH/CH_3 surfaces were significantly lower than on TCPS (approximately 75%).

BAEC density and morphology on the OH/CH_3 SAMs and TCPS was evaluated qualitatively after 4 hour, 1 day, and 3 day culture periods as shown in Figures 6.26, 6.27 and 6.28. Figure 6.26 illustrates cell morphology after 4 hours of culture. Consistent with results shown in Figure 6.23, cell density was slightly higher on the 80% and 100% OH surfaces however, cell densities did not appear to differ significantly among the OH/CH_3 surfaces. The majority of cells on all SAM surfaces appeared rounded however, some cell spreading was observed on the 0-40% OH surfaces and on TCPS.

After 1 and 3 days of culture, cell densities and morphology did not show significant differences as a function of surface OH concentration (Figure 6.27 and 6.28). After 1 day of culture, cells on the SAM surfaces were typically rounded and grouped in clusters with very few cells progressing to a spread configuration. Some areas containing groups of a few spread cells were observed, particularly on the 20% and 40% OH surfaces. These areas were unusual in appearance as there were long, "fingerlike" lines (consisting of 1-2 cells in width) which connected the clusters or groups of cells. In contrast, the TCPS surface was uniformly covered with spread cells.

Similar patterns are observed for the OH/CH_3 surfaces after 3 days of culture (Figure 28). Clusters of rounded cells are observed on the 60-100% OH surfaces. Some "lines" of spread cells are observed on the 0%, 20% and 40% OH surfaces and larger areas of spread cells were observed on the 20% OH surface. In contrast, a confluent monolayer of cells was present on the TCPS surface.

For the 20% OH surface, a difference was observed between the quantitative measurement of cell number by MTT and the qualitative observation of cell density. Cell number on the 20% OH surface, as measured by the MTT assay (Figure 6.25), was higher than the other SAM surfaces however, the difference was not significant. As discussed in Section 6.2.3, this difference arises from the fact that during the MTT assay procedure, the cell culture media (in contact with the sample) is removed prior to addition of the acidic isopropanol which causes cell lysis. If cells attached to the SAM surfaces are very weakly attached, the cells are removed with the media. In the case of the 20% OH surface, many of the areas of spread cells seen in Figure 6.28 were very loosely adherent and were therefore removed prior to the actual assay.

The qualitative and quantitative studies of OH/CH_3 SAMs demonstrated that a heterogeneous surface comprised of two components which are poor supports of cell growth results in a binary surface which poorly supports cell growth independent of surface composition. These results demonstrated that the chemically heterogeneous OH/CH_3 surfaces were as poorly supportive of cell growth as were the chemically homogeneous (100% OH and 100% CH_3) surfaces. In studies described in sections 6.3.1 and 6.3.2, cell growth on homogeneous SAMs can also be compared to cell growth on chemically heterogeneous SAMs. As shown in Figures 6.5 and 6.6, cell growth on the heterogeneous 10% COOH/90% CH_3 surface was equal to or slightly less than growth on the homogeneous CH_3 surface (0% COOH). Conversely, Figure 6.5 and 6.6 also show that growth on the heterogeneous 60% and 80% COOH surfaces was

slightly higher than cell number on the homogeneous 100% COOH surface but the difference was not significant. These results demonstrate that chemically complex, heterogeneous surfaces do not always support cell growth to a greater extent than do chemically homogeneous surfaces. Many heterogeneous surfaces demonstrated cell growth greater than that on homogeneous surfaces however, this occurred only for certain surface compositions of COOH-containing heterogeneous SAMs.

6.4 Conclusions

The studies described in this chapter were designed to address three primary issues: 1) the effect of functional group concentration on cell growth, 2) the effect of functional group spatial arrangement on cell growth, and 3) an investigation of the cell growth characteristics of chemically heterogeneous surfaces compared with chemically homogeneous surfaces. The effects of SAM surface composition, spatial arrangement, and surface chemical heterogeneity on BAEC attachment and growth were assessed quantitatively using the MTT cell proliferation assay, and qualitatively using light microscopy.

The effect of surface functional group content on cell attachment and growth was evaluated for two binary SAM systems: COOH/OH binary SAMs and COOH/CH_3 binary SAMs. For both SAM systems, cell attachment (cell number after 4 hours of culture) did not differ significantly with surface functional group content. Furthermore, it was observed that surfaces demonstrating equivalent levels of cell attachment often demonstrated significant differences in cell growth after longer cell culture periods. Surfaces demonstrating high levels of cell attachment will not necessarily support cell growth however some level of cell attachment is required for cell growth to occur.

Evaluation of cell growth on the COOH/OH and COOH/CH_3 binary SAMs after 1 and 3 day culture periods showed significant differences in cell growth in response to

binary SAM surface composition. For the $COOH/CH_3$ surfaces, cell growth increased significantly with increasing surface fraction of COOH for surface compositions ranging from 10-60% COOH and reached a maximum value at 60% COOH. As surface COOH content increased above 60%, no significant increases in cell growth were observed, rather cell growth decreased slightly for surface compositions ranging from 60-100%. A similar cell growth pattern was observed for the COOH/OH surfaces. Cell growth increased significantly with increasing surface fraction of COOH for surface compositions ranging from 0-50% COOH and reached a maximum value at 50% COOH. As surface COOH content increased above 50%, cell growth decreased for surface compositions ranging from 50-100%.

Several $COOH/CH_3$ and COOH/OH surface compositions demonstrated cell growth levels greater than or equal to cell growth measured on TCPS. These results provide quantitative evidence which supports the previous qualitative observations of increased cell growth on several heterogeneous SAM surfaces relative to TCPS (Chapter 4). This finding is significant since it demonstrates the ability to create a cell growth substrate of well-defined chemistry which promotes cell growth to levels in excess of that on TCPS.

The effect of functional group spatial arrangement on endothelial cell growth was evaluated by comparing cell growth on the COOH/OH binary SAM series to cell growth on the $COOH/CH_3$ binary SAM series. Cell growth patterns after a 1 day culture period differed between the two systems suggesting that cell growth on the COOH/OH and $COOH/CH_3$ surfaces was affected by the spatial arrangement of the surface COOH groups. Between 0%-60% surface COOH, cell growth on the COOH/OH surfaces was significantly higher than on the $COOH/CH_3$ surfaces at an equivalent surface COOH fraction. The clustered arrangement of the $COOH/CH_3$ surface appeared to result in a decreased level of cell growth given the same surface COOH content. The growth

inhibitory effect of the poor growth component of the binary SAM (i.e. CH_3 or OH) was observed to be more pronounced when existing in a clustered configuration. After a 3 day cell growth period, cell growth patterns on the COOH/OH and COOH/CH_3 systems were very similar. The effect of surface functional group dispersion on cell growth was significant in the early phase of cell growth but the effect diminished with increasing cell culture time.

The effect of surface chemical heterogeneity on cell growth was evaluated for a series of OH/CH_3 binary SAMs. Low levels of cell growth were obtained on all OH/CH_3 surface compositions and cell number was independent of surface OH content. It was our hypothesis that chemically complex, heterogeneous surfaces would support cell growth to a greater extent than chemically homogeneous surfaces. This hypothesis is true only if one of the components of the heterogeneous surface is a growth promoting functional group (i.e. COOH) and for certain surface compositions of binary SAMs containing a growth-promoting functionality. Chemical heterogeneity alone does not ensure enhanced cell growth relative to a homogeneous surface. To obtain improved cell growth, a chemically heterogeneous surface must contain an adequate surface content of a growth-promoting functional group.

Table 6.1

Surface Composition of Binary SAMs Evaluated in Cell Interaction Studies

Thiol A	*Thiol B*	*Surface Fraction Thiol A*	*Surface Fraction Thiol B*
$HS(CH_2)_{15}COOH$	$HS(CH_2)_{15}CH_3$	0%	100%
$HS(CH_2)_{15}COOH$	$HS(CH_2)_{15}CH_3$	10%	90%
$HS(CH_2)_{15}COOH$	$HS(CH_2)_{15}CH_3$	20%	80%
$HS(CH_2)_{15}COOH$	$HS(CH_2)_{15}CH_3$	40%	60%
$HS(CH_2)_{15}COOH$	$HS(CH_2)_{15}CH_3$	60%	40%
$HS(CH_2)_{15}COOH$	$HS(CH_2)_{15}CH_3$	80%	20%
$HS(CH_2)_{15}COOH$	$HS(CH_2)_{15}CH_3$	100%	0%
$HS(CH_2)_{15}COOH$	$HS(CH_2)_{15}CH_2OH$	0%	100%
$HS(CH_2)_{15}COOH$	$HS(CH_2)_{15}CH_2OH$	20%	80%
$HS(CH_2)_{15}COOH$	$HS(CH_2)_{15}CH_2OH$	40%	60%
$HS(CH_2)_{15}COOH$	$HS(CH_2)_{15}CH_2OH$	50%	50%
$HS(CH_2)_{15}COOH$	$HS(CH_2)_{15}CH_2OH$	70%	30%
$HS(CH_2)_{15}COOH$	$HS(CH_2)_{15}CH_2OH$	80%	20%
$HS(CH_2)_{15}COOH$	$HS(CH_2)_{15}CH_2OH$	100%	0%
$HS(CH_2)_{15}CH_2OH$	$HS(CH_2)_{15}CH_3$	0%	100%
$HS(CH_2)_{15}CH_2OH$	$HS(CH_2)_{15}CH_3$	20%	80%
$HS(CH_2)_{15}CH_2OH$	$HS(CH_2)_{15}CH_3$	40%	60%
$HS(CH_2)_{15}CH_2OH$	$HS(CH_2)_{15}CH_3$	60%	40%
$HS(CH_2)_{15}CH_2OH$	$HS(CH_2)_{15}CH_3$	80%	20%
$HS(CH_2)_{15}CH_2OH$	$HS(CH_2)_{15}CH_3$	100%	0%

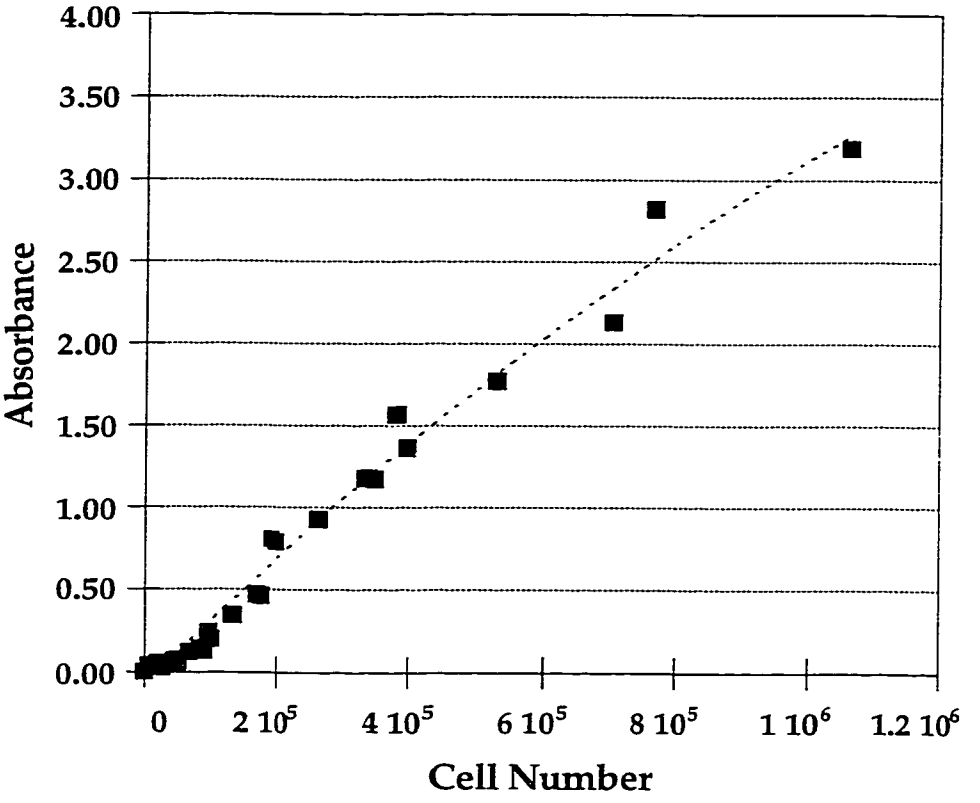

Figure 6.1 MTT conversion by BAEC on TCPS after a 3 hour incubation period. Cells were plated onto substrates in 10% bovine serum growth medium and allowed to adhere for 2 hours prior to addition of the MTT solution. Absorbance measurements were made with 100 µl sample volumes. Data represent the mean ± standard deviation for quadruplicate samples in five separate experiments.

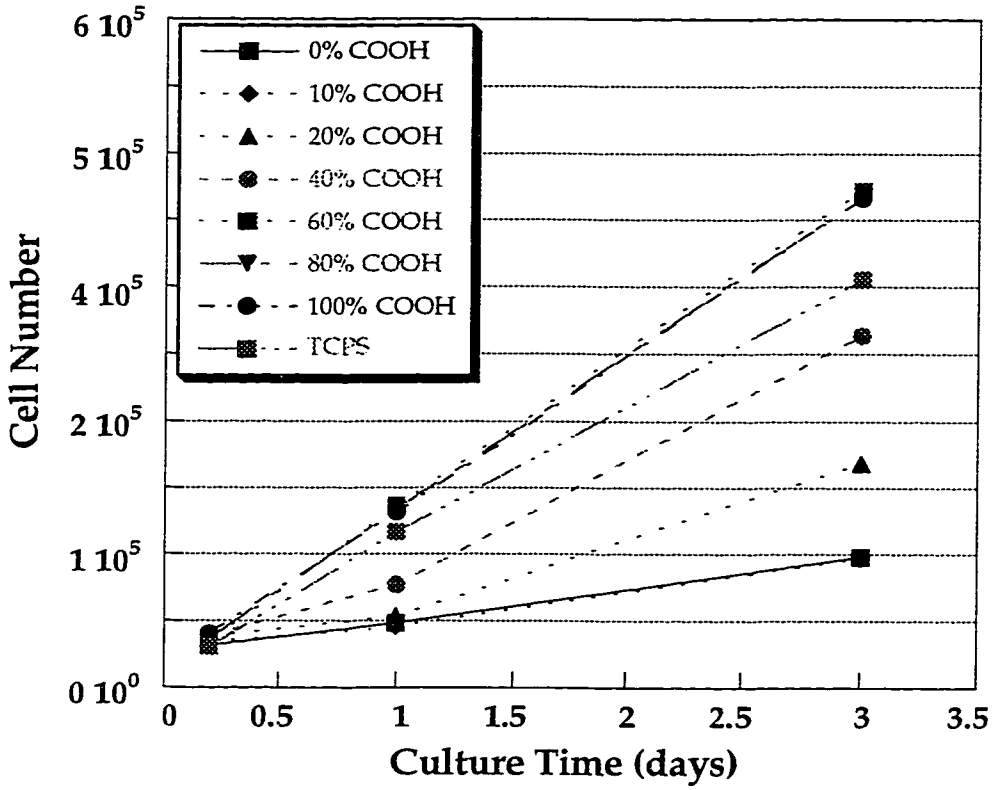

Figure 6.2 BAEC number determined on binary composition SAMs adsorbed from ethanolic mixtures of $HS(CH_2)_{15}COOH$ and $HS(CH_2)_{15}CH_3$ as a function of cell culture time. Cells were cultured for 4 hours, 1 day, and 3 days in medium containing 10% bovine serum. Cell number was determined from Figure 6.1 using absorbance values measured by MTT assay for each 15 mm diameter sample (surface area = 1.81 cm^2). Data represent the mean ± standard deviation for quadruplicate samples.

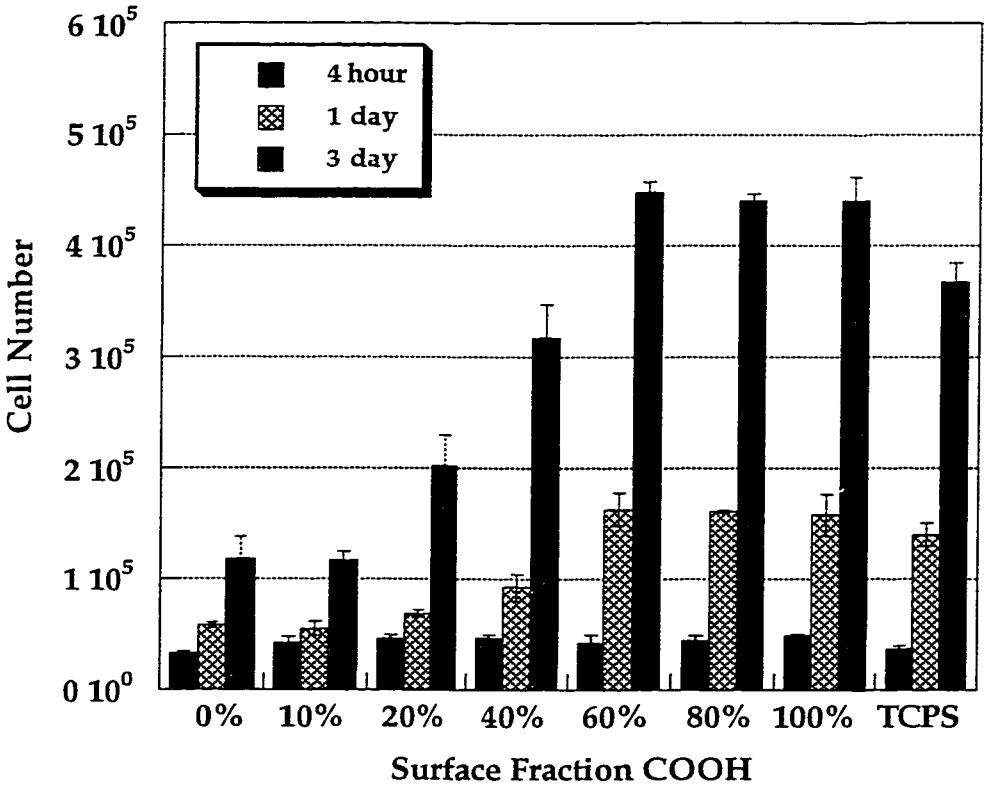

Figure 6.3 BAEC number determined on binary composition SAMs adsorbed from ethanolic mixtures of $HS(CH_2)_{15}COOH$ and $HS(CH_2)_{15}CH_3$ as a function of surface COOH content, and on TCPS. Cells were cultured for 4 hours, 1 day, and 3 days in medium containing 10% bovine serum. Cell number was determined from Figure 6.1 using absorbance values measured by MTT assay for each 15 mm diameter sample (surface area = 1.81 cm^2). Data represent the mean ± standard deviation for quadruplicate samples.

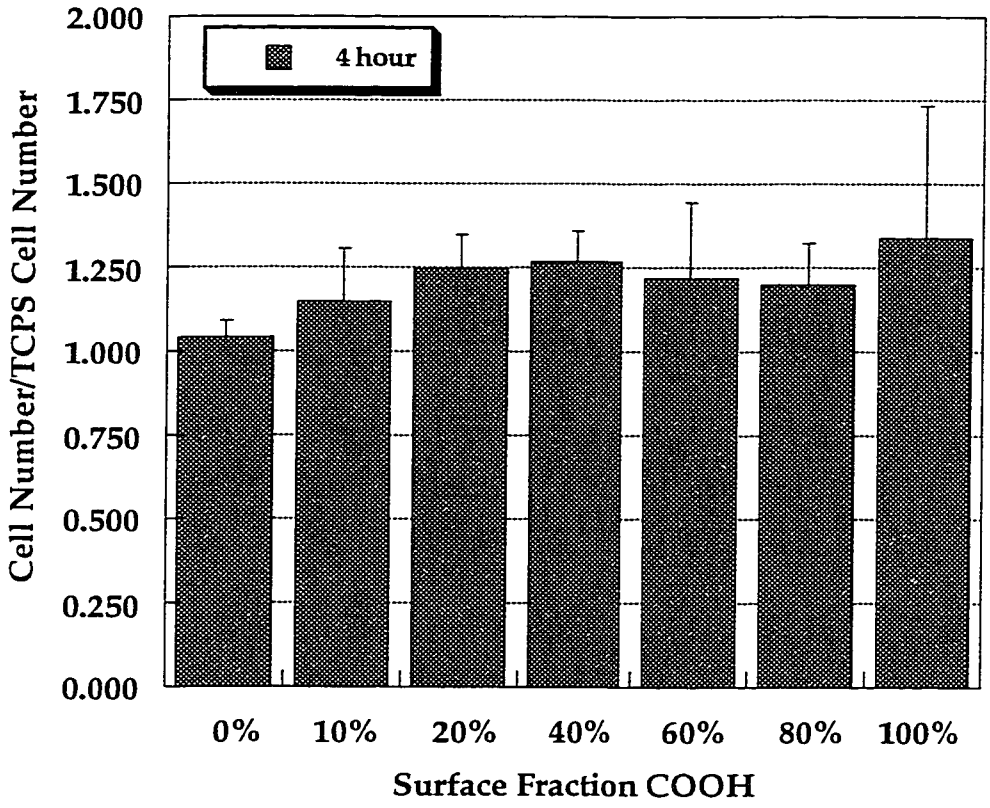

Figure 6.4 Normalized BAEC number determined on binary composition SAMs adsorbed from ethanolic mixtures of $HS(CH_2)_{15}COOH$ and $HS(CH_2)_{15}CH_3$ as a function of surface COOH content. Cells were cultured for 4 hours in medium containing 10% bovine serum. Normalized cell number was determined as the ratio of the cell number measured on the SAM surface to cell number measured on the TCPS control surface (reference Figure 6.3). Data represent the mean ± standard deviation for quadruplicate samples.

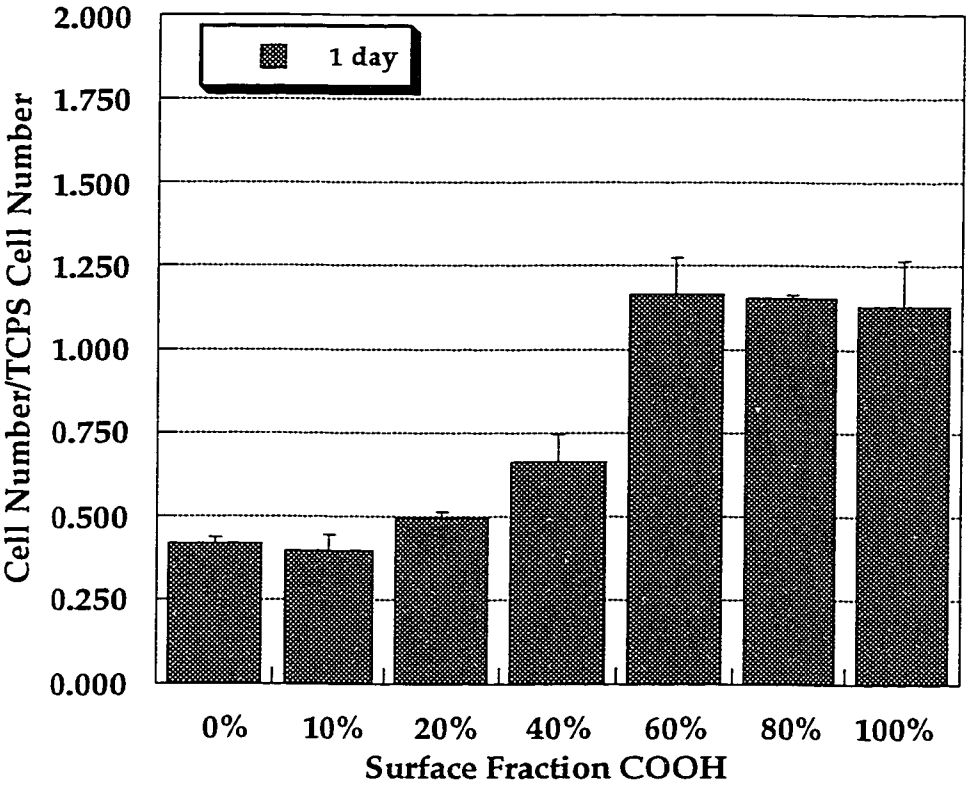

Figure 6.5 Normalized BAEC number determined on binary composition SAMs adsorbed from ethanolic mixtures of $HS(CH_2)_{15}COOH$ and $HS(CH_2)_{15}CH_3$ as a function of surface COOH content. Cells were cultured for 1 day in medium containing 10% bovine serum. Normalized cell number was determined as the ratio of the cell number measured on the SAM surface to cell number measured on the TCPS control surface (reference Figure 6.3). Data represent the mean ± standard deviation for quadruplicate samples.

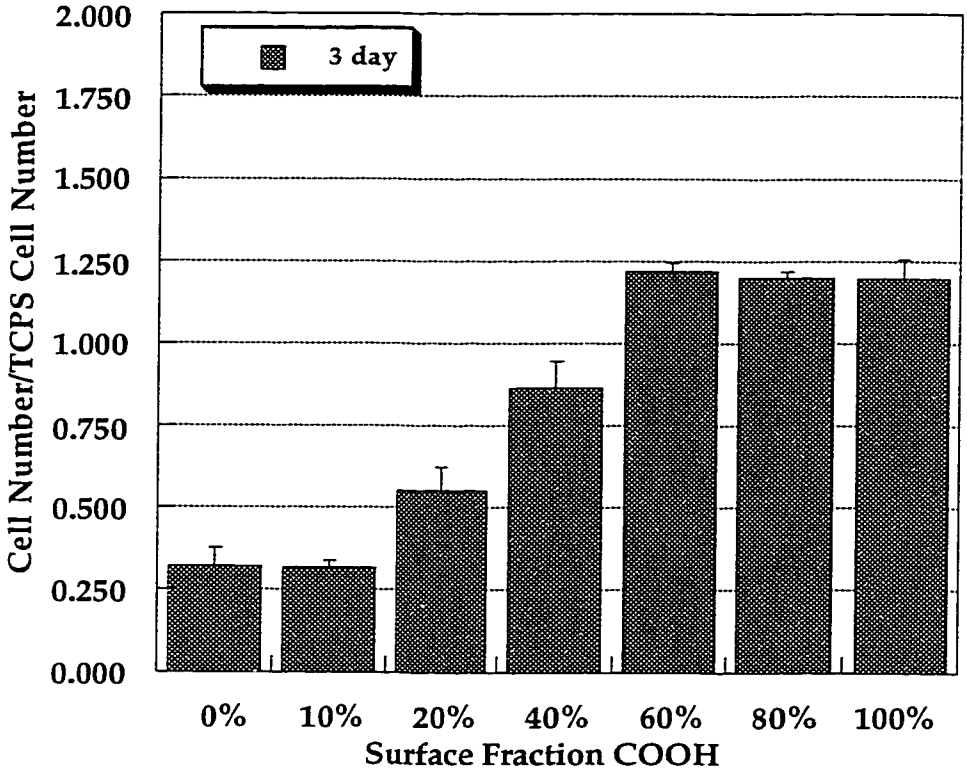

Figure 6.6 Normalized BAEC number determined on binary composition SAMs adsorbed from ethanolic mixtures of $HS(CH_2)_{15}COOH$ and $HS(CH_2)_{15}CH_3$ as a function of surface COOH content. Cells were cultured for 3 days in medium containing 10% bovine serum. Normalized cell number was determined as the ratio of the cell number measured on the SAM surface to cell number measured on the TCPS control surface (reference Figure 6.3). Data represent the mean ± standard deviation for quadruplicate samples.

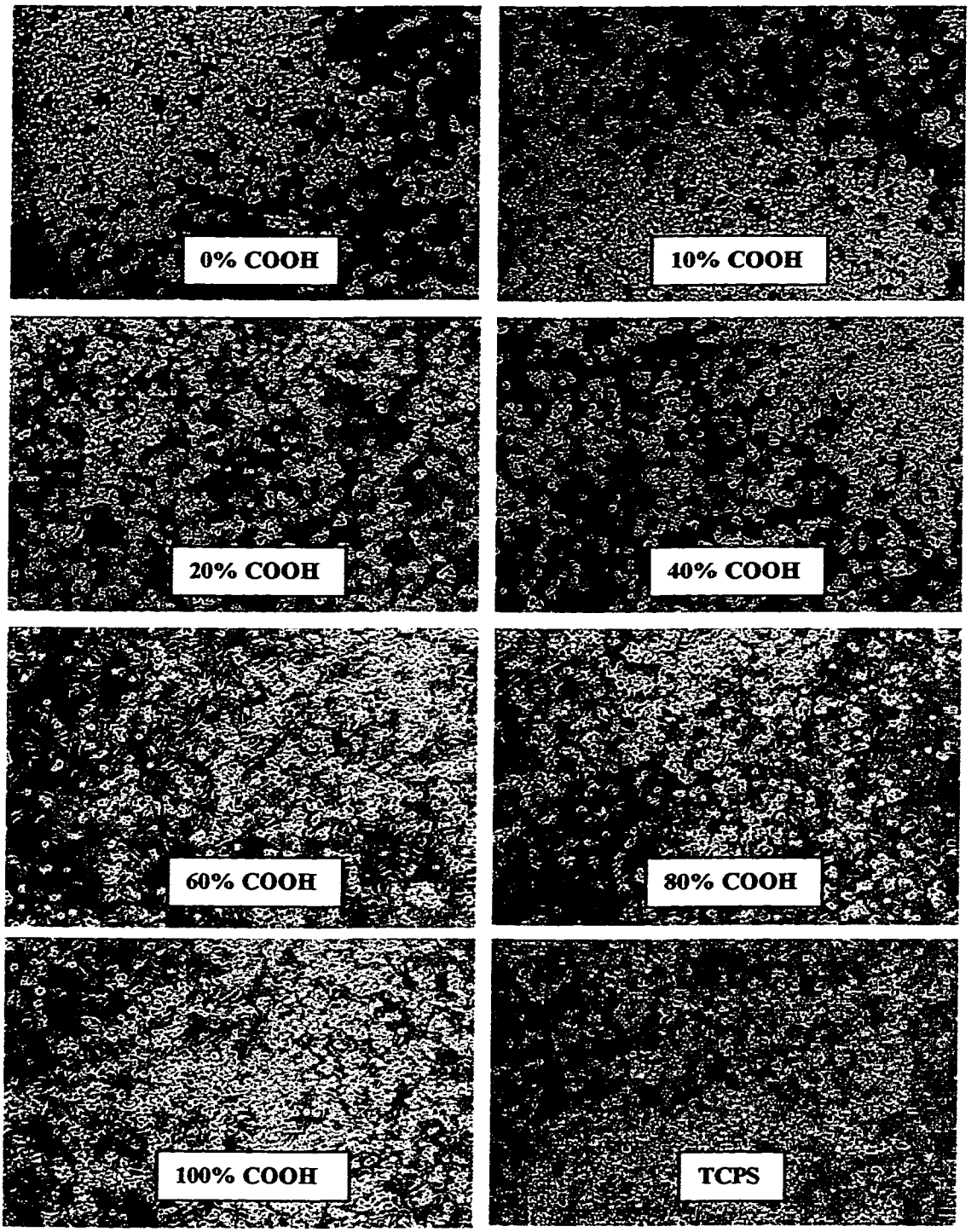

Figure 6.7 BAEC on binary composition SAMs of $HS(CH_2)_{15}COOH$ and $HS(CH_2)_{15}CH_3$ for surface compositions of 0%, 10%, 20%, 40%, 60%, 80% and 100% COOH, and on TCPS. Cells were cultured in 10% bovine serum for 4 hours.

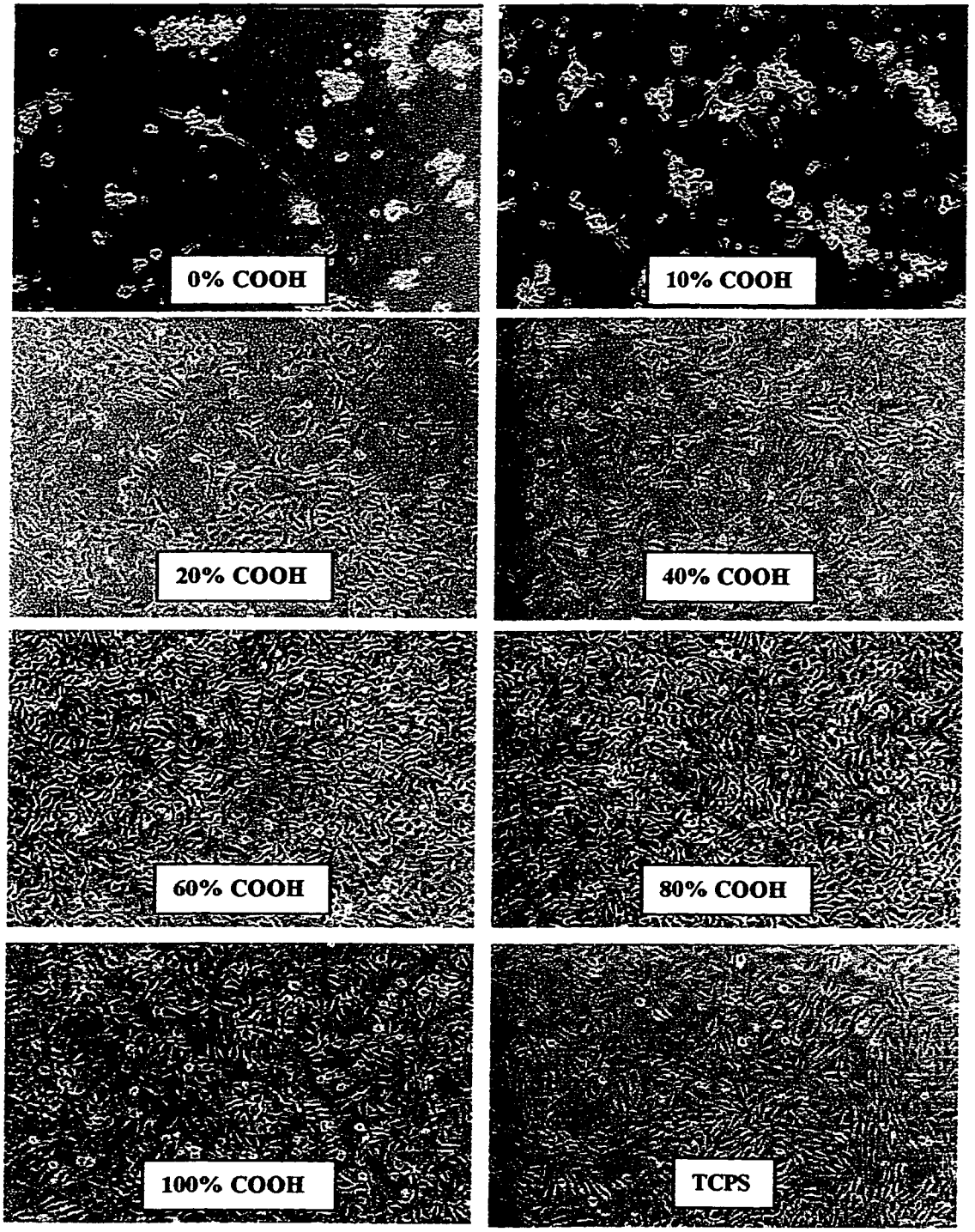

Figure 6.8 BAEC on binary composition SAMs of $HS(CH_2)_{15}COOH$ and $HS(CH_2)_{15}CH_3$ for surface compositions of 0%, 10%, 20%, 40%, 60%, 80%, and 100% COOH, and on TCPS. Cells were cultured in 10% bovine serum for 1 day.

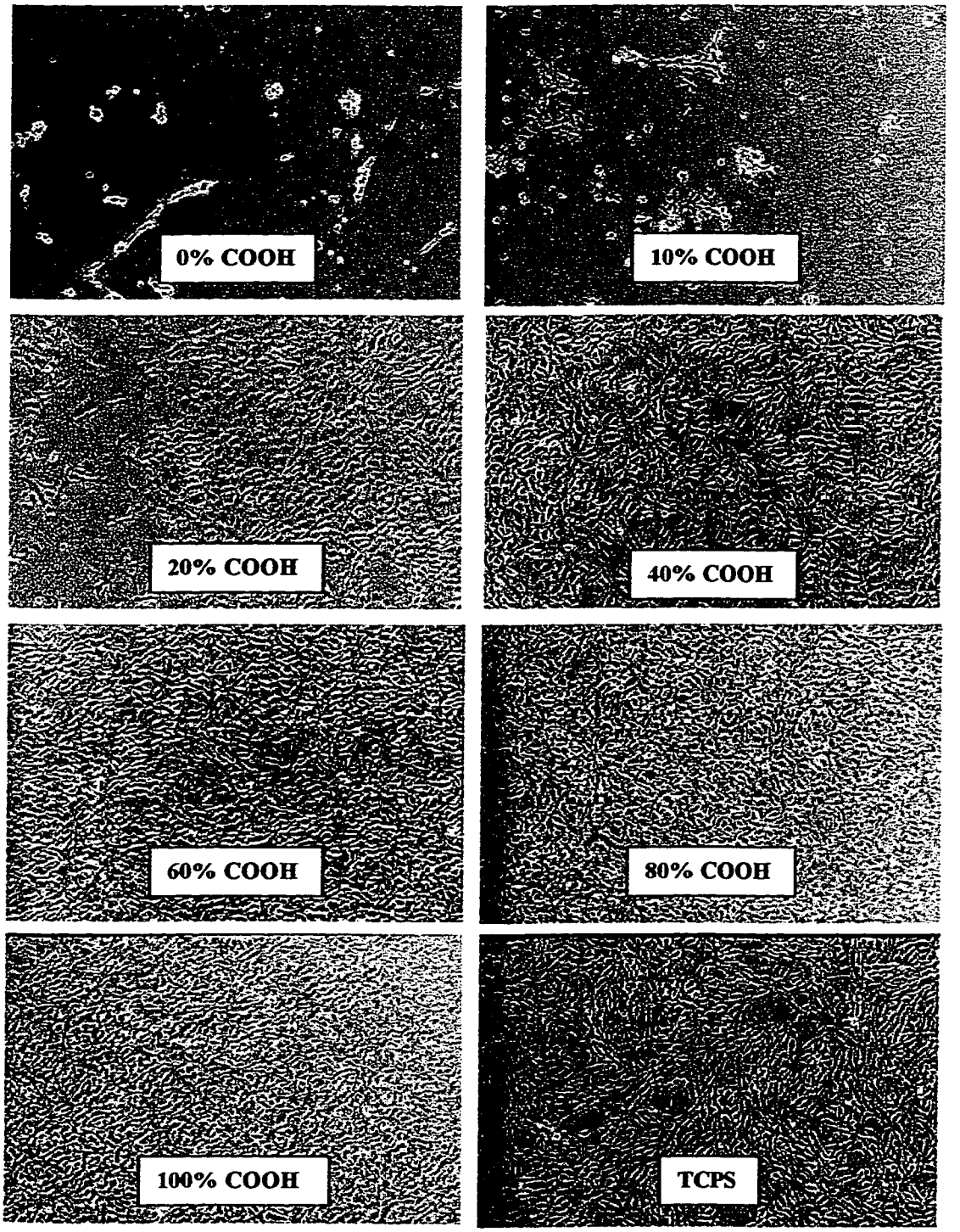

Figure 6.9 BAEC on binary composition SAMs of $HS(CH_2)_{15}COOH$ and $HS(CH_2)_{15}CH_3$ for surface compositions of 0%, 10%, 20%, 40%, 60%, 80%, and 100% COOH, and on TCPS. Cells were cultured in 10% bovine serum for 3 days.

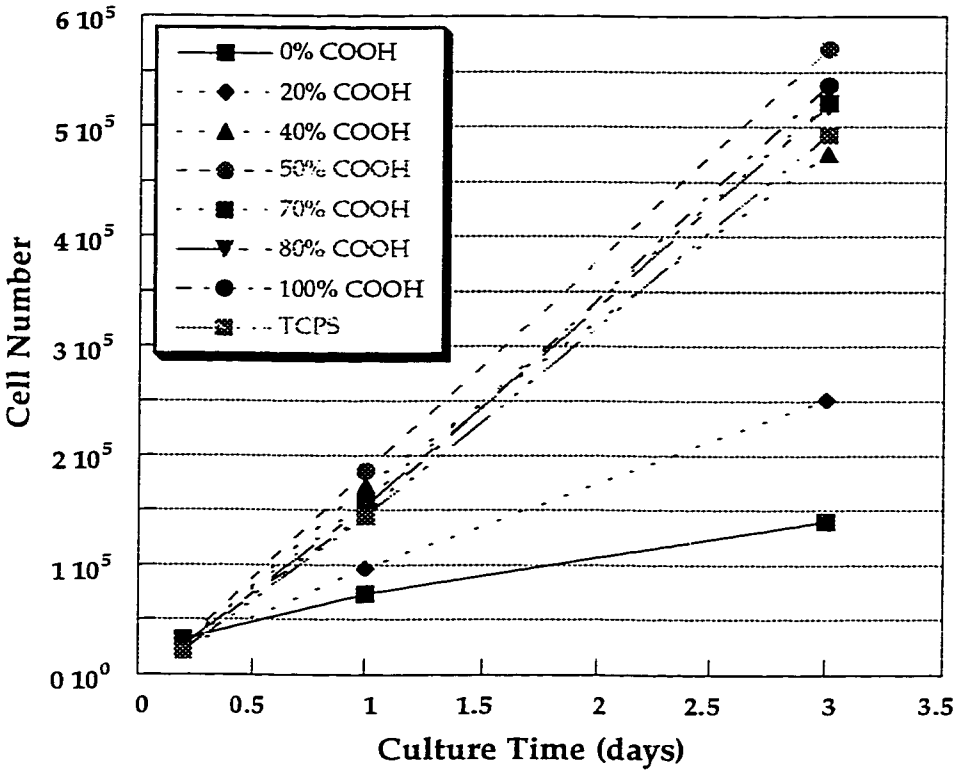

Figure 6.10 BAEC number determined on binary composition SAMs adsorbed from ethanolic mixtures of $HS(CH_2)_{15}COOH$ and $HS(CH_2)_{15}CH_2OH$ as a function of cell culture time. Cells were cultured for 4 hours, 1 day, and 3 days in medium containing 10% bovine serum. Cell number was determined from Figure 6.1 using absorbance values measured by MTT assay for each 15 mm diameter sample (surface area = 1.81 cm^2). Data represent the mean ± standard deviation for quadruplicate samples.

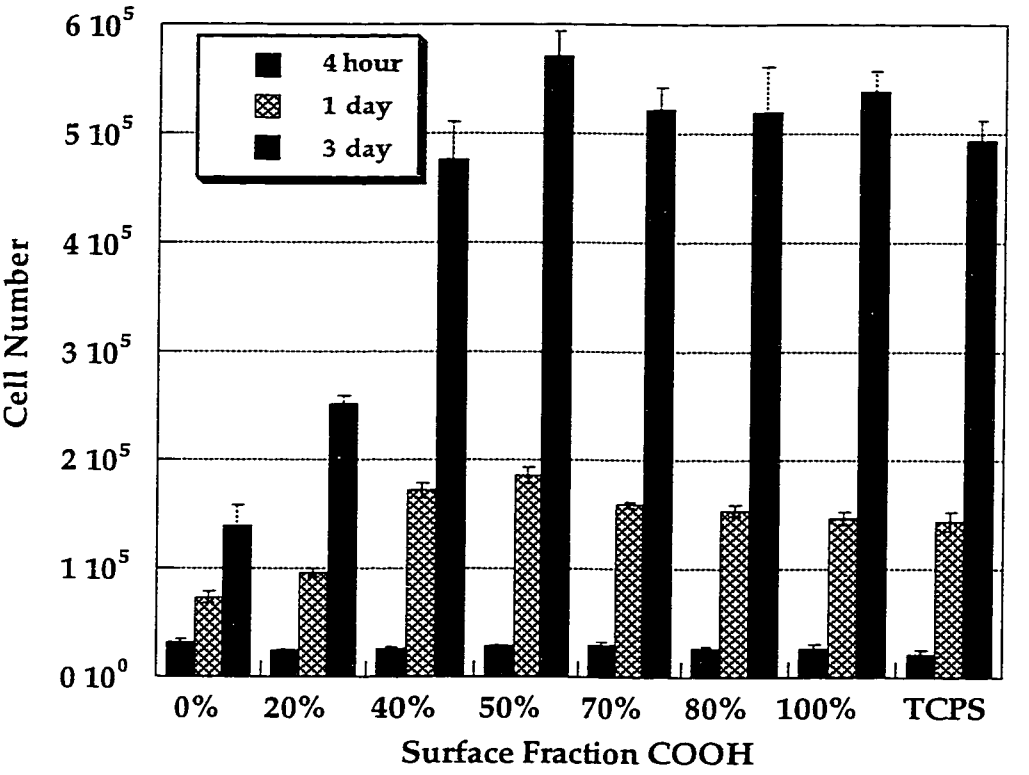

Figure 6.11 BAEC number determined on binary composition SAMs adsorbed from ethanolic mixtures of $HS(CH_2)_{15}COOH$ and $HS(CH_2)_{15}$ CH_2OH as a function of surface COOH content, and on TCPS. Cells were cultured for 4 hours, 1 day, and 3 days in medium containing 10% bovine serum. Cell number was determined from Figure 6.1 using absorbance values measured by MTT assay for each 15 mm diameter sample (surface area = 1.81 cm^2). Data represent the mean ± standard deviation for quadruplicate samples.

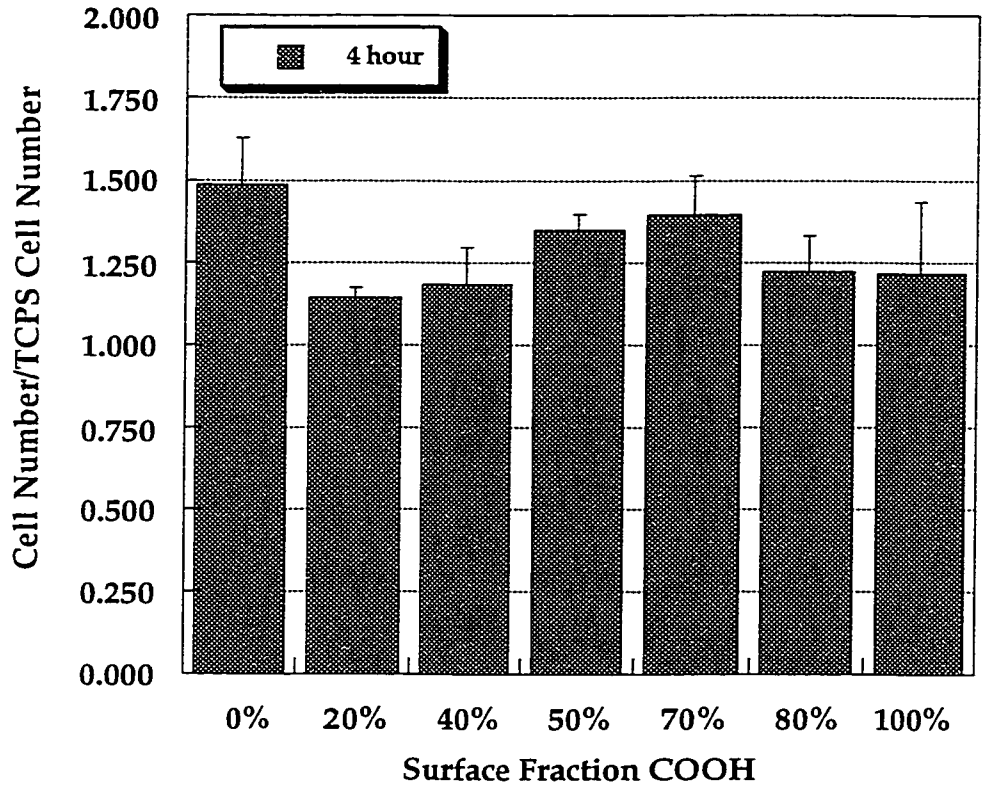

Figure 6.12 Normalized BAEC number determined on binary composition SAMs adsorbed from ethanolic mixtures of $HS(CH_2)_{15}COOH$ and $HS(CH_2)_{15}CH_2OH$ as a function of surface COOH content. Cells were cultured for 4 hours in medium containing 10% bovine serum. Normalized cell number was determined as the ratio of the cell number measured on the SAM surface to cell number measured on the TCPS control surface (reference Figure 6.11). Data represent the mean ± standard deviation for quadruplicate samples.

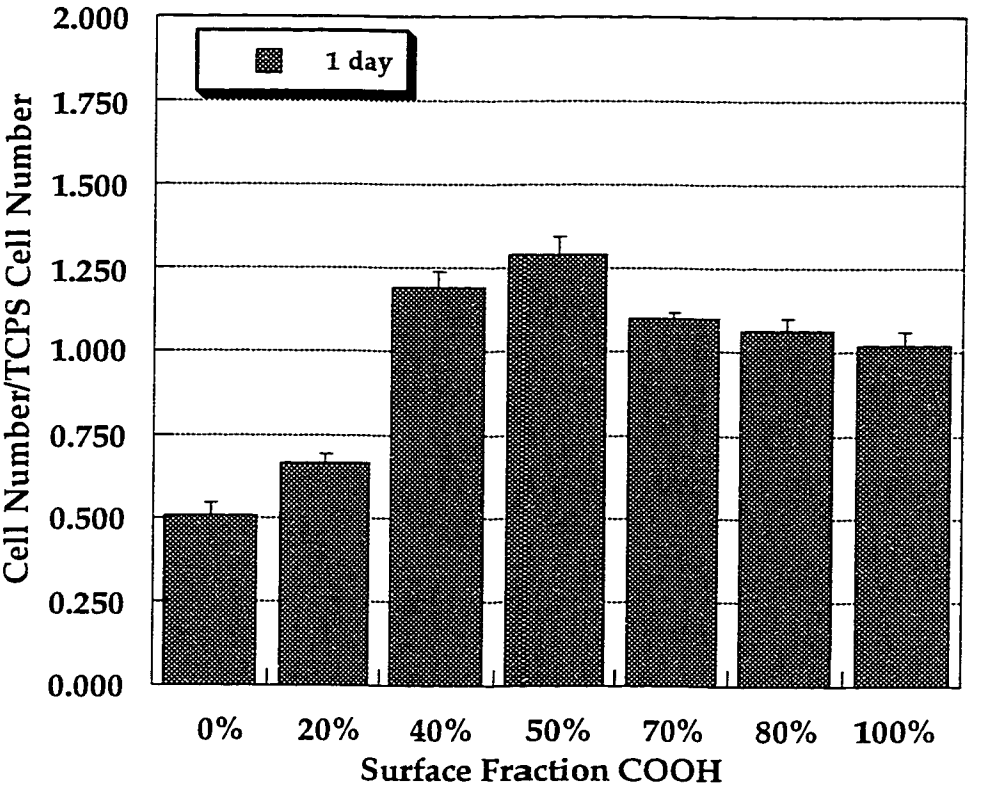

Figure 6.13 Normalized BAEC number determined on binary composition SAMs adsorbed from ethanolic mixtures of $HS(CH_2)_{15}COOH$ and $HS(CH_2)_{15}CH_2OH$ as a function of surface COOH content. Cells were cultured for 1 day in medium containing 10% bovine serum. Normalized cell number was determined as the ratio of the cell number measured on the SAM surface to cell number measured on the TCPS control surface (reference Figure 6.11). Data represent the mean ± standard deviation for quadruplicate samples.

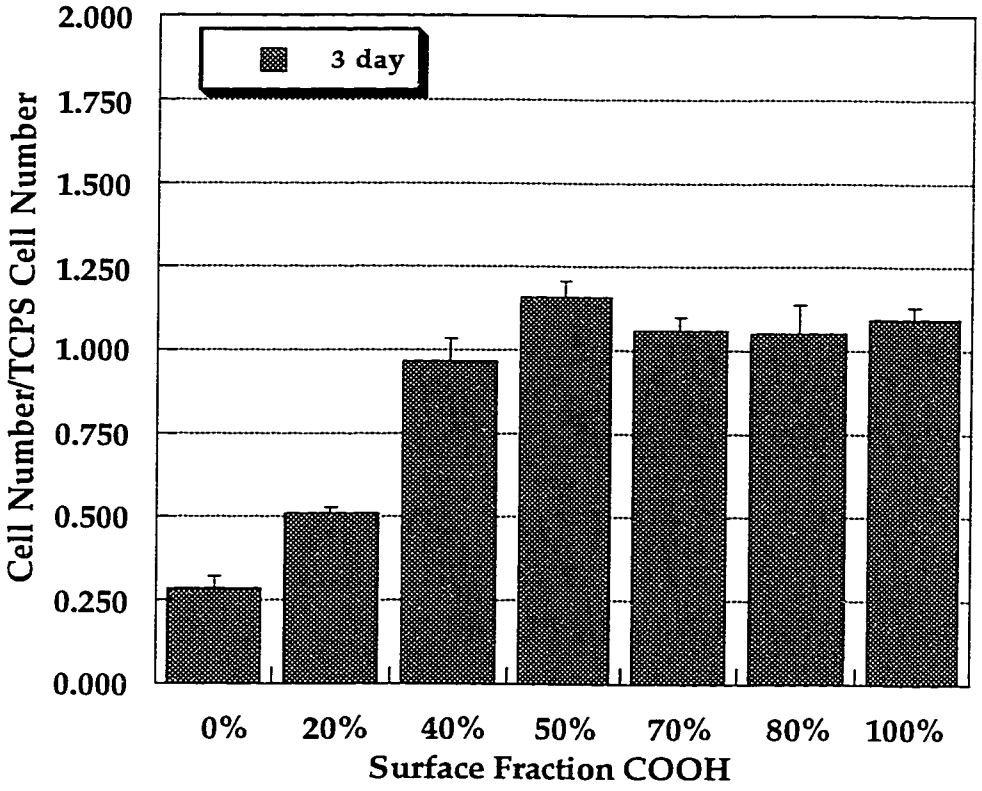

Figure 6.14 Normalized BAEC number determined on binary composition SAMs adsorbed from ethanolic mixtures of $HS(CH_2)_{15}COOH$ and $HS(CH_2)_{15}CH_2OH$ as a function of surface COOH content. Cells were cultured for 3 days in medium containing 10% bovine serum. Normalized cell number was determined as the ratio of the cell number measured on the SAM surface to cell number measured on the TCPS control surface (reference Figure 6.11). Data represent the mean ± standard deviation for quadruplicate samples.

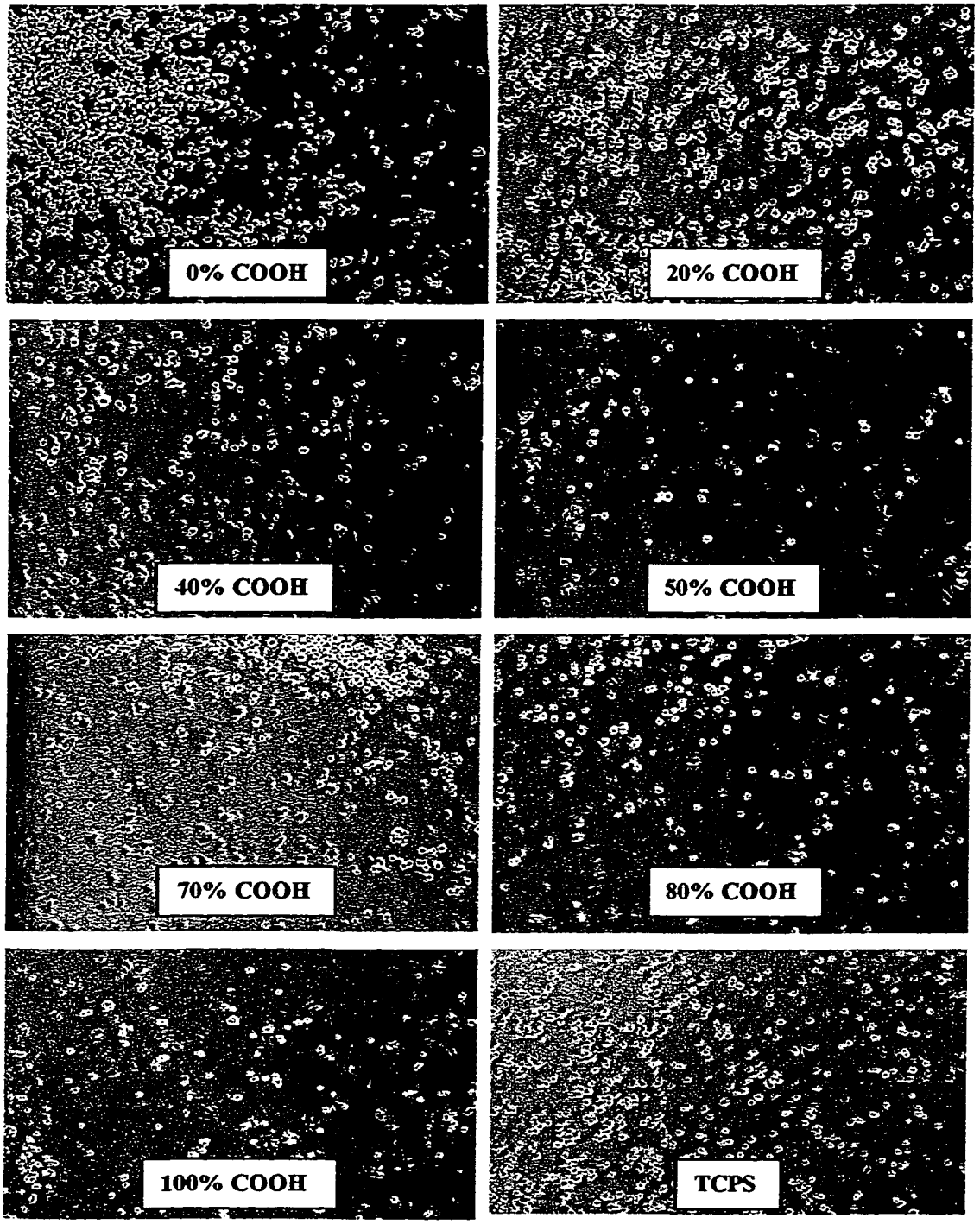

Figure 6.15 BAEC on binary composition SAMs of $HS(CH_2)_{15}COOH$ and $HS(CH_2)_{15}CH_2OH$ for surface compositions of 0%, 20%, 40%, 50%, 70%, 80%, and 100% COOH, and TCPS. Cells were cultured for 4 hours.

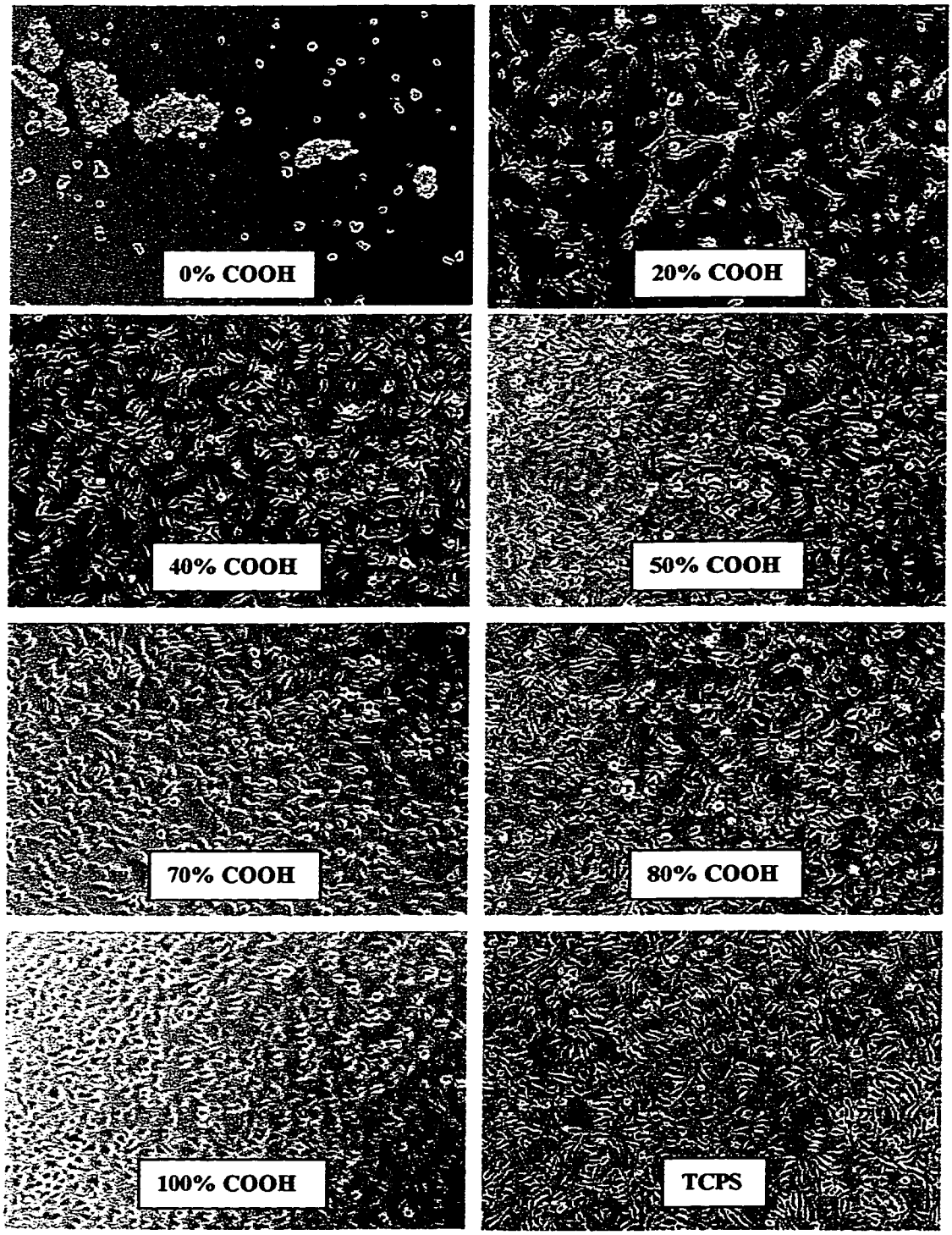

Figure 6.16 BAEC on binary composition SAMs of $HS(CH_2)_{15}COOH$ and $HS(CH_2)_{15}CH_2OH$ for surface compositions of 0%, 20%, 40%, 50%, 70%, 80%, and 100% COOH, and TCPS. Cells were cultured for 1 day.

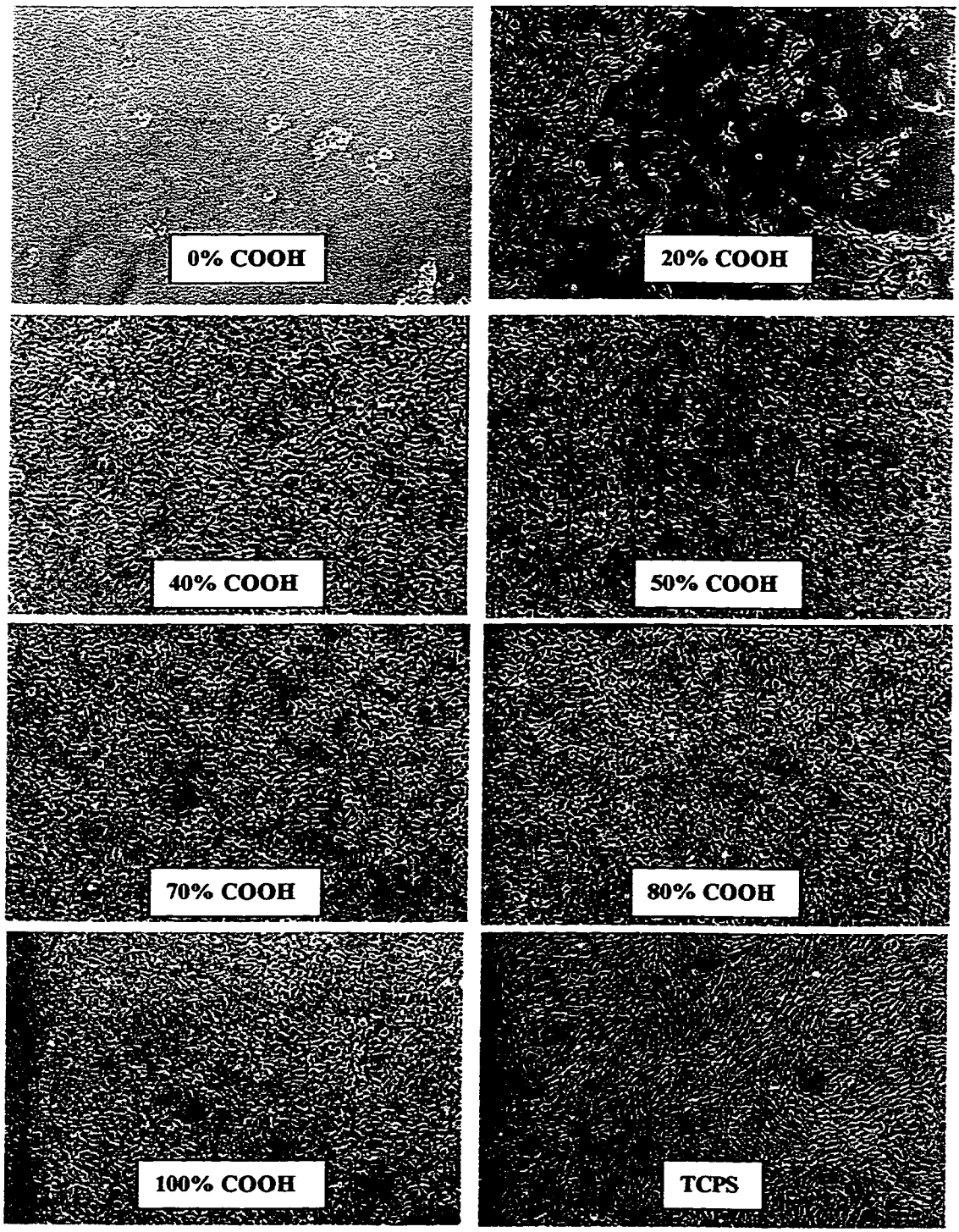

Figure 6.17 BAEC on binary composition SAMs of $HS(CH_2)_{15}COOH$ and $HS(CH_2)_{15}CH_2OH$ for surface compositions of 0%, 20%, 40%, 50%, 70%, 80%, and 100% COOH, and TCPS. Cells were cultured for 3 days.

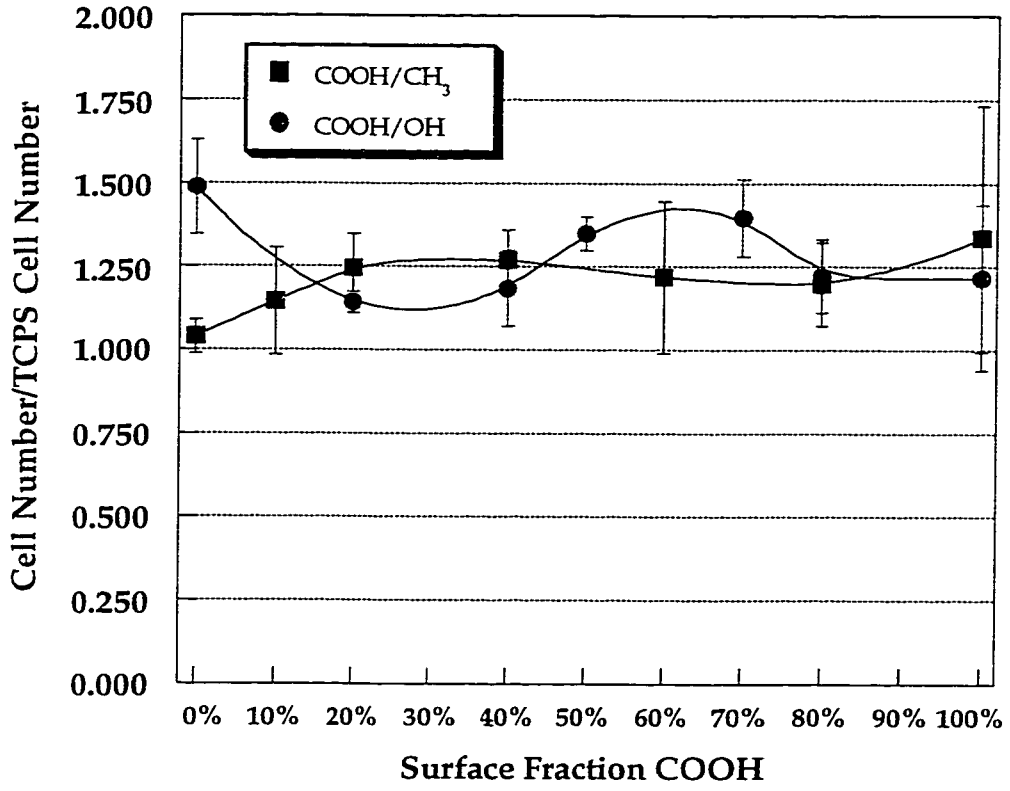

Figure 6.18 Normalized BAEC number determined on binary composition SAMs adsorbed from ethanolic mixtures of $HS(CH_2)_{15}COOH$ and $HS(CH_2)_{15}CH_2OH$ (circles) and mixtures of $HS(CH_2)_{15}COOH$ and $HS(CH_2)_{15}CH_3$ (squares) as a function of surface COOH content. Cells were cultured for 4 hours in medium containing 10% bovine serum. Data represent the mean ± standard deviation for quadruplicate samples.

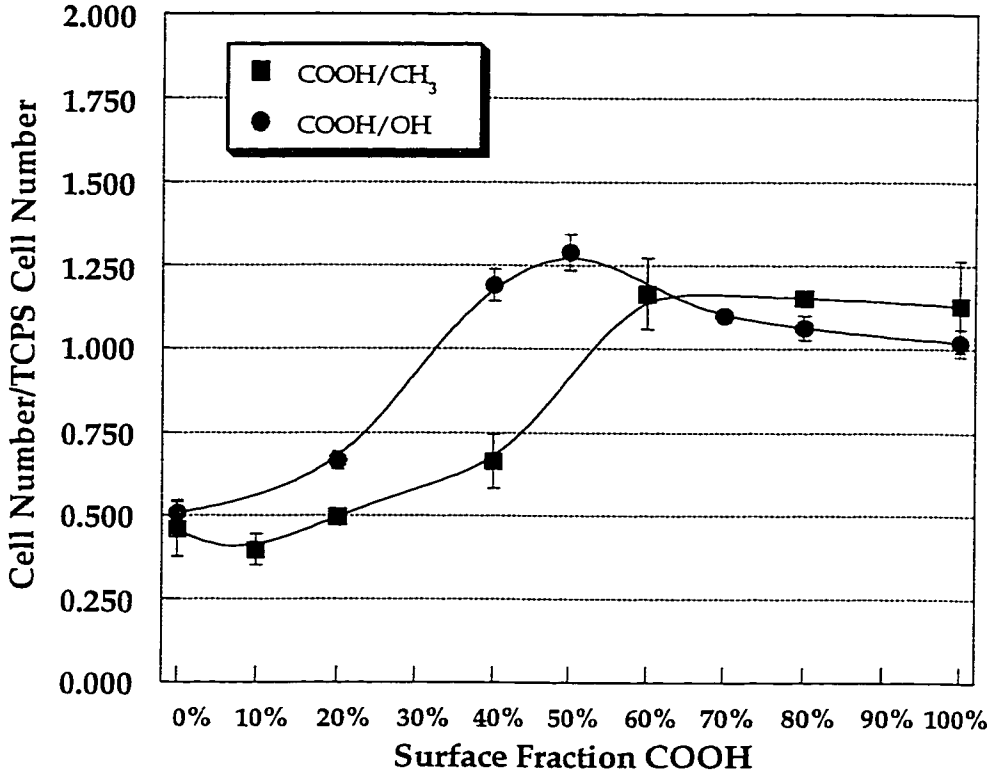

Figure 6.19 Normalized BAEC number determined on binary composition SAMs adsorbed from ethanolic mixtures of $HS(CH_2)_{15}COOH$ and $HS(CH_2)_{15}CH_2OH$ (circles) and mixtures of $HS(CH_2)_{15}COOH$ and $HS(CH_2)_{15}CH_3$ (squares) as a function of surface COOH content. Cells were cultured for 1 day in medium containing 10% bovine serum. Data represent the mean ± standard deviation for quadruplicate samples.

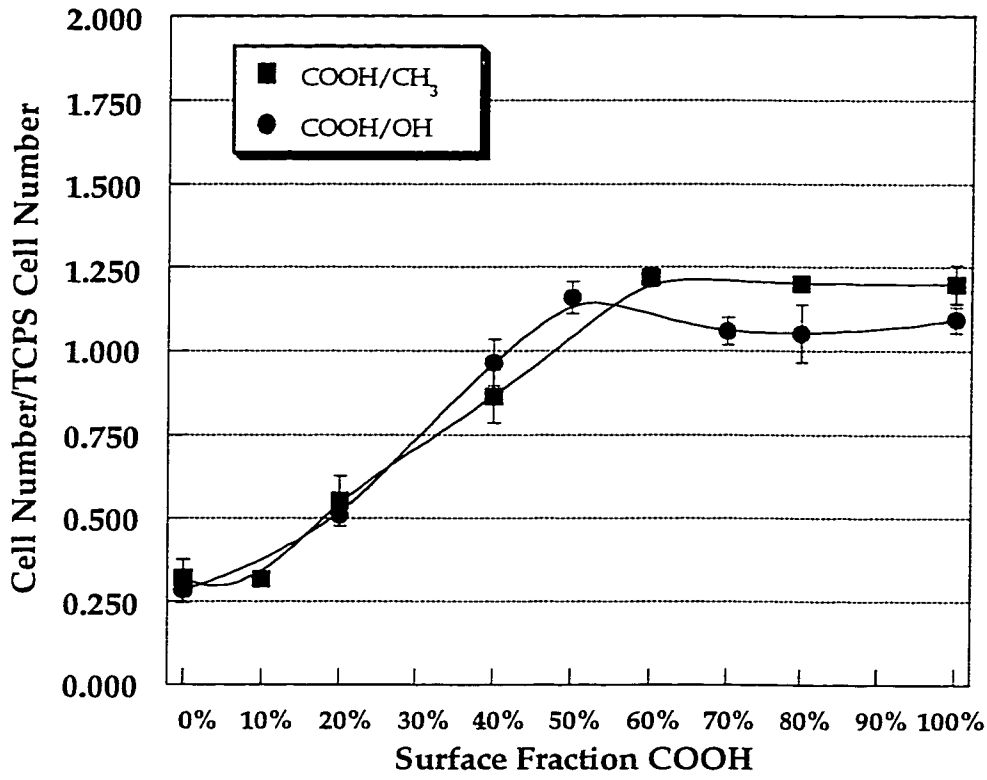

Figure 6.20 Normalized BAEC number determined on binary composition SAMs adsorbed from ethanolic mixtures of $HS(CH_2)_{15}COOH$ and $HS(CH_2)_{15}CH_2OH$ (circles) and mixtures of $HS(CH_2)_{15}COOH$ and $HS(CH_2)_{15}CH_3$ (squares) as a function of surface COOH content. Cells were cultured for 3 days in medium containing 10% bovine serum. Data represent the mean ± standard deviation for quadruplicate samples.

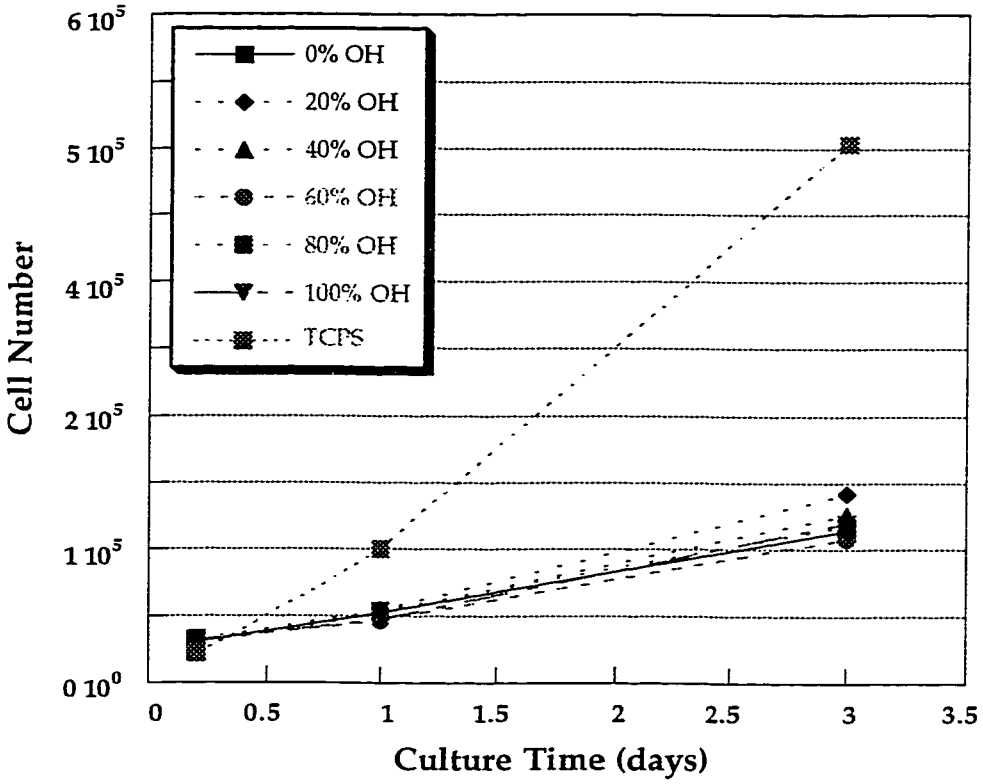

Figure 6.21 BAEC number determined on binary composition SAMs adsorbed from ethanolic mixtures of $HS(CH_2)_{15}CH_2OH$ and $HS(CH_2)_{15}CH_3$ as a function of cell culture time. Cells were cultured for 4 hours, 1 day, and 3 days in medium containing 10% bovine serum. Cell number was determined from Figure 6.1 using absorbance values measured by MTT assay for each 15 mm diameter sample (surface area = 1.81 cm^2). Data represent the mean ± standard deviation for quadruplicate samples.

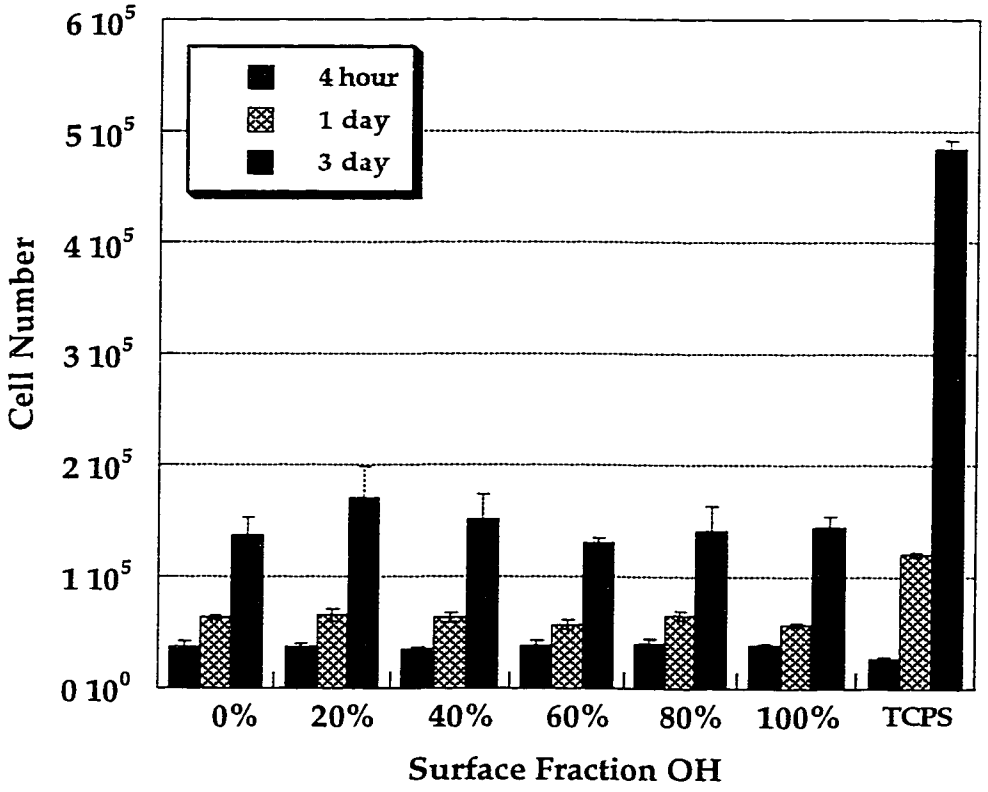

Figure 6.22 BAEC number determined on binary composition SAMs adsorbed from ethanolic mixtures of $HS(CH_2)_{15}CH_2OH$ and $HS(CH_2)_{15}CH_3$ as a function of surface OH content, and on TCPS. Cells were cultured for 4 hours, 1 day, and 3 days in medium containing 10% bovine serum. Cell number was determined from Figure 6.1 using absorbance values measured by MTT assay for each 15 mm diameter sample (surface area = 1.81 cm^2). Data represent the mean ± standard deviation for quadruplicate samples.

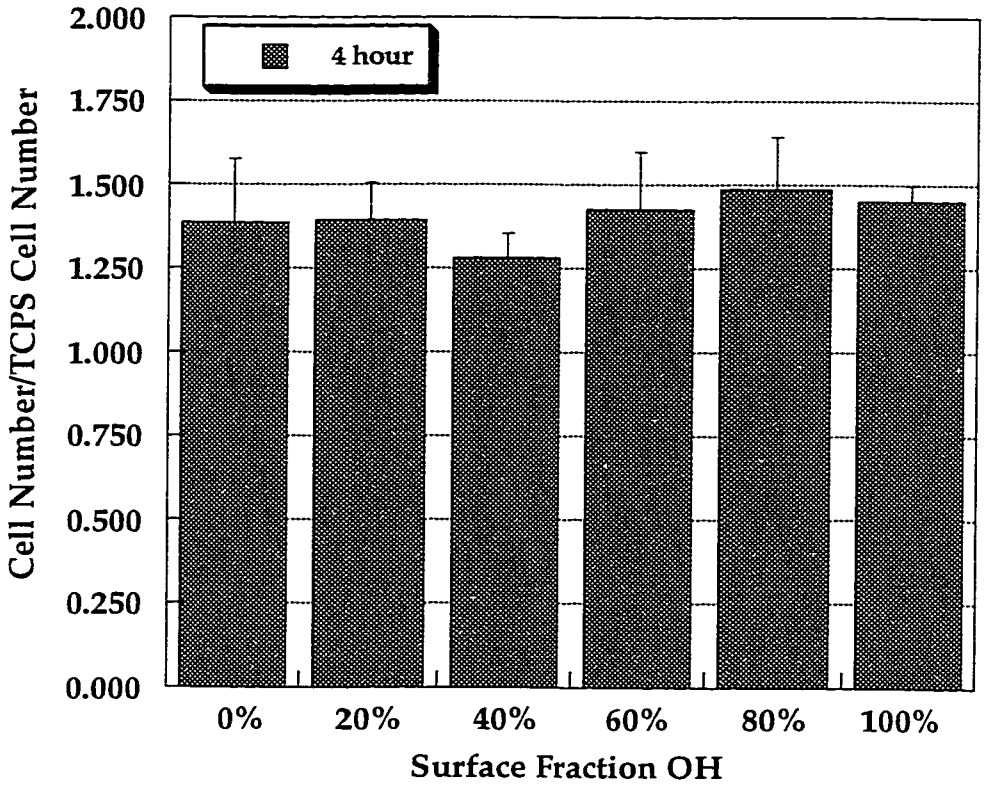

Figure 6.23 Normalized BAEC number determined on binary composition SAMs adsorbed from ethanolic mixtures of $HS(CH_2)_{15}CH_2OH$ and $HS(CH_2)_{15}CH_3$ as a function of surface OH content. Cells were cultured for 4 hours in medium containing 10% bovine serum. Normalized cell number was determined as the ratio of the cell number measured on the SAM surface to cell number measured on the TCPS control surface (reference Figure 6.22). Data represent the mean ± standard deviation for quadruplicate samples.

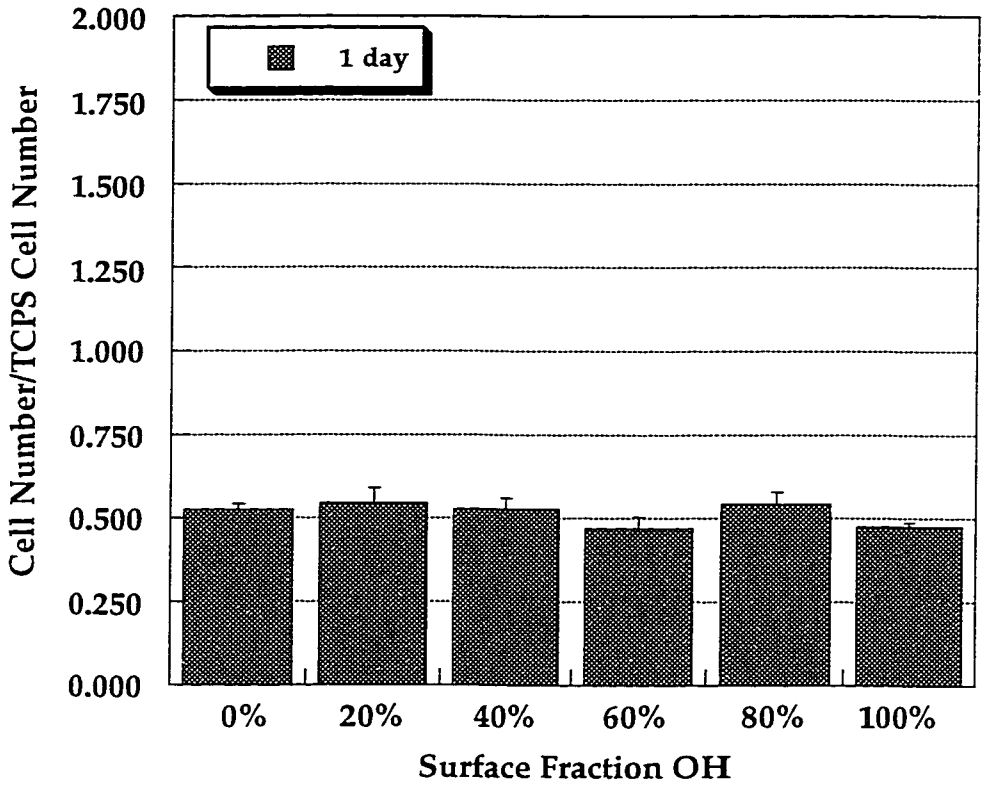

Figure 6.24 Normalized BAEC number determined on binary composition SAMs adsorbed from ethanolic mixtures of $HS(CH_2)_{15}CH_2OH$ and $HS(CH_2)_{15}CH_3$ as a function of surface OH content. Cells were cultured for 1 day in medium containing 10% bovine serum. Normalized cell number was determined as the ratio of the cell number measured on the SAM surface to cell number measured on the TCPS control surface (reference Figure 6.22). Data represent the mean ± standard deviation for quadruplicate samples.

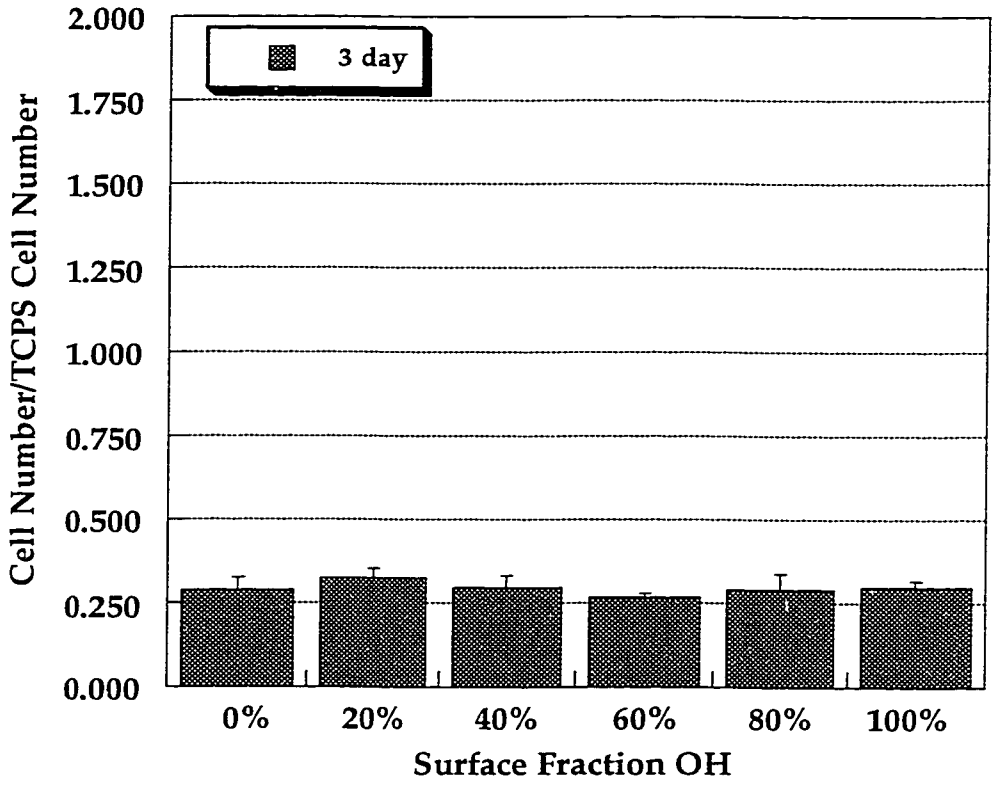

Figure 6.25 Normalized BAEC number determined on binary composition SAMs adsorbed from ethanolic mixtures of $HS(CH_2)_{15}CH_2OH$ and $HS(CH_2)_{15}CH_3$ as a function of surface OH content. Cells were cultured for 3 days in medium containing 10% bovine serum. Normalized cell number was determined as the ratio of the cell number measured on the SAM surface to cell number measured on the TCPS control surface (reference Figure 6.22). Data represent the mean ± standard deviation for quadruplicate samples.

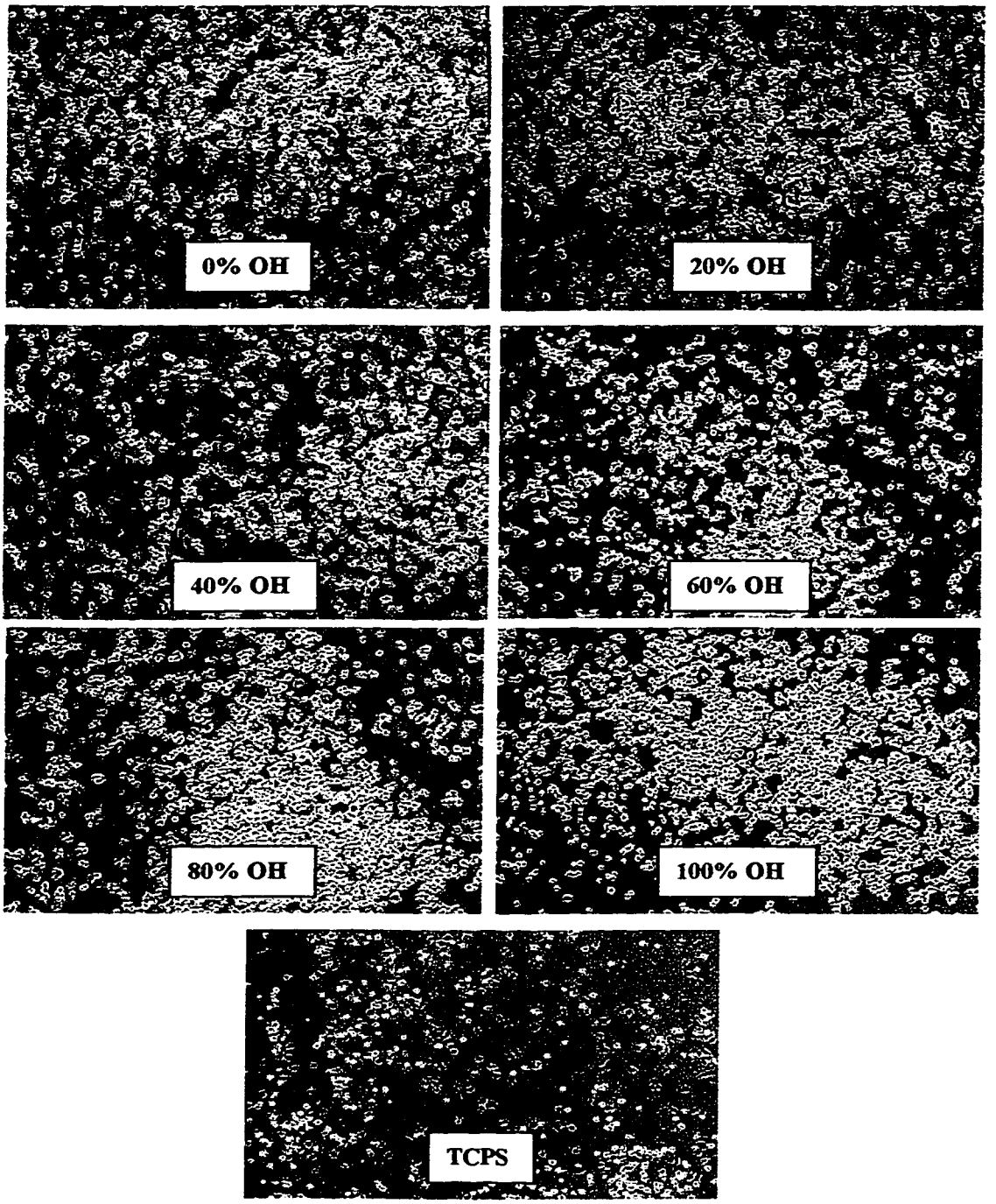

Figure 6.26 BAEC on binary composition SAMs of $HS(CH_2)_{15}CH_2OH$ and $HS(CH_2)_{15}CH_3$ for surface compositions of 0%, 20%, 40%, 60%, 80%, and 100% OH, and TCPS. Cells were cultured for 4 hours.

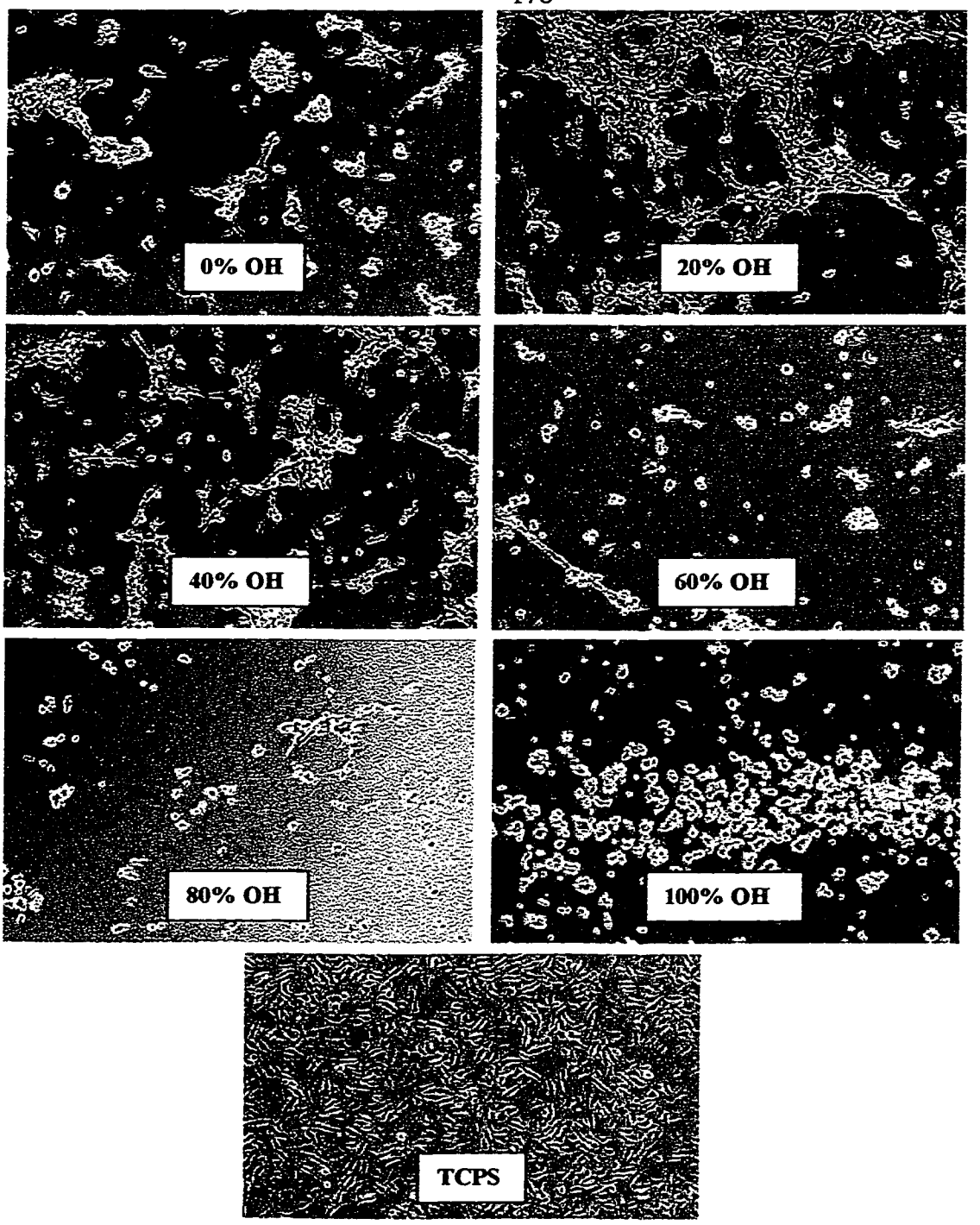

Figure 6.27 BAEC on binary composition SAMs of $HS(CH_2)_{15}CH_2OH$ and $HS(CH_2)_{15}CH_3$ for surface compositions of 0%, 20%, 40%, 60%, 80%, and 100% OH, and TCPS. Cells were cultured for 1 day.

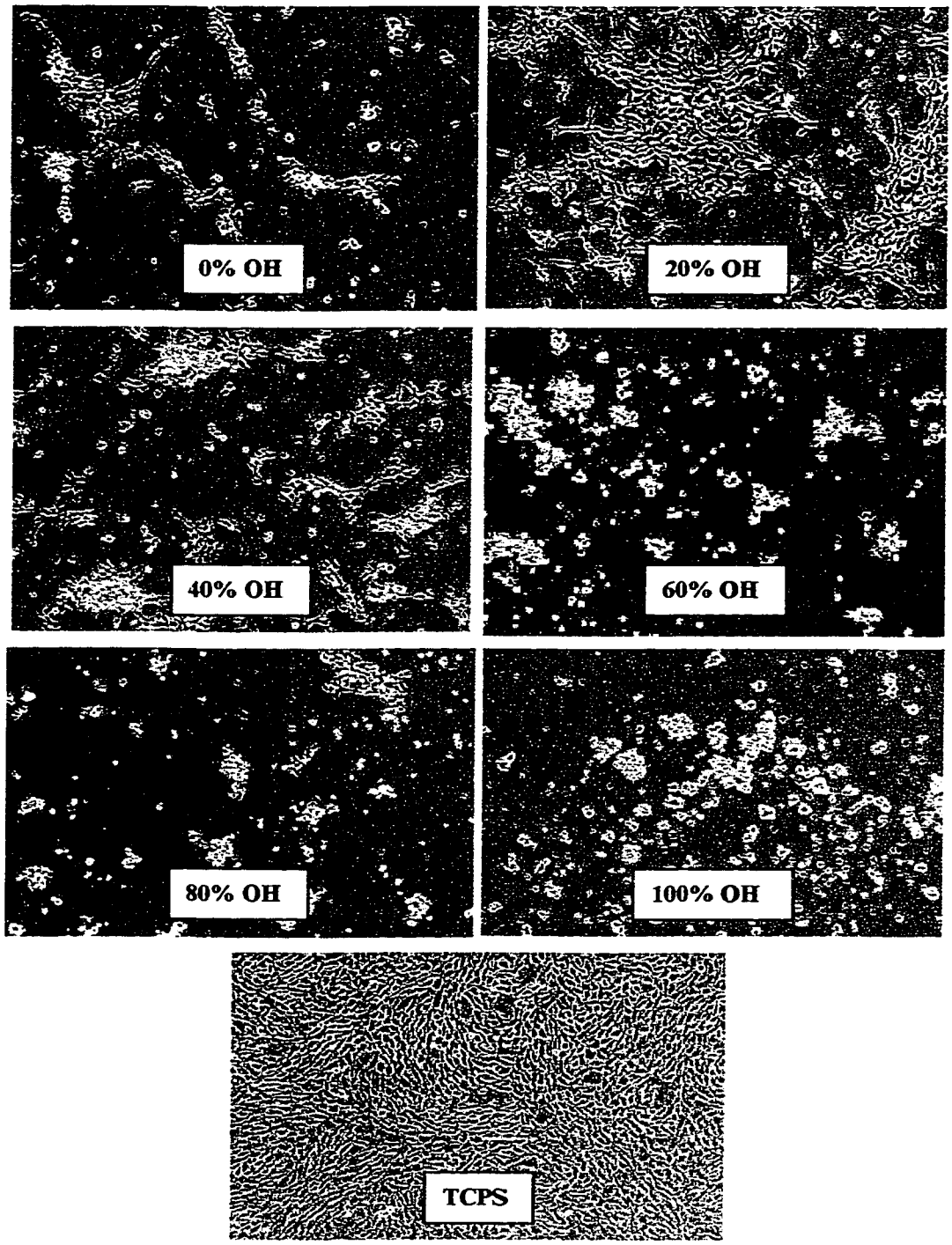

Figure 6.28 BAEC on binary composition SAMs of $HS(CH_2)_{15}CH_2OH$ and $HS(CH_2)_{15}CH_3$ for surface compositions of 0%, 20%, 40%, 60%, 80%, and 100% OH, and TCPS. Cells were cultured for 3 days.

Chapter 7

Endothelial Cell Interactions with Structurally Heterogeneous SAMs: Effect of Surface Mobility

7.1 Introduction

While the effects of surface chemistry on the biointeraction characteristics, or reactivity, of polymeric materials have been studied extensively, the role of surface molecular motions in protein adsorption, cell growth, or other cellular interactions (i.e., platelet adhesion) has received limited attention. The effect of surface mobility on biointeractions has been investigated in a limited number of studies using polymer systems which exhibit varying degrees of surface molecular motions such as irradiated block copolymers, HEMA/EMA copolymers, and polymers containing varying amounts of crosslinker. As discussed in Section 1.3, these studies suggest a significant effect of surface mobility on thrombotic events, protein adsorption, platelet adhesion, and cell growth however, the results obtained to date are somewhat contradictory. Few of these studies have been able to isolate the effects of surface molecular motions from other factors influencing the bioresponse (i.e., surface reorientation, surface chemistry, bound water, etc.) primarily because of an inability to systematically control and vary polymer substrate surface mobility.

It is generally observed that the adsorption of proteins from blood and serum is suppressed as surface mobility is increased [41,43,44]. Similarly, a decrease in platelet adhesion has been reported with increasing surface mobility [41]. In contrast, a significant decrease in platelet adhesion and thrombus formation was observed with increased restriction of side chain motions in irradiated polymer systems [34-36]. The effects of surface molecular motions on cell attachment and growth are not well understood. Fibroblast growth was observed to be low on HEMA/EMA copolymer

surfaces containing a significant fraction of mobile HEMA component. Cell growth increased with increasing surface fraction of the more rigid EMA component [39]. Certainly, for anchorage-dependent cells such as endothelial cells, the ability of cells to attach, spread and proliferate will be dependent upon the ability of adhesive serum proteins to adsorb to the substrate in the appropriate conformation and allow for cell membrane receptor interactions to occur. If surface molecular motions prevent the adsorption of sufficient quantities of adhesive proteins, cell growth will be prevented as well.

Biological surfaces are structurally and chemically complex, and interact with their complementary molecules in a fluid, mobile, dynamic manner. Cell surface receptors, enzymes, and other molecules interact with their complementary molecules using mobile, adaptive processes. Ratner suggests that rigid surfaces may require too much geometric precision and too precise of a molecular orientation for rapid reactions to occur. If mobility is incorporated into a substrate surface, surface sites and molecules interacting with these sites can more easily adapt to each other thus reducing the degree of precision required in a completely rigid system [50]. It is possible that the incorporation of a moderate degree of mobility into a substrate surface may result in the enhancement of molecular specificity, recognition, and reaction rates.

In this chapter, the effect of surface mobility, or surface molecular motions, on endothelial cell attachment and growth was investigated. We hypothesized that endothelial cell growth will be dependent upon the degree of surface molecular mobility and that cell growth on structurally complex, mobile surfaces would differ significantly from that on structurally homogeneous, ordered, immobile surfaces.

To investigate this hypothesis, surfaces exhibiting variations in surface mobility were prepared using binary SAMs composed of alkanethiols which differ in alkyl chain length (structurally heterogeneous) to obtain substrates which exhibit molecular mobility

at the interface (see reference [67] and Section 1.6 for additional discussion of binary (mixed length) SAMs). By varying the relative concentration of short chain and long chain thiol components in the adsorbing solution used to prepare the binary SAMs, the surface concentration of chains capable of movement at the interface (i.e., the long chain component) was controlled. For example, a SAM comprised of 100% C_{12} alkanethiol or 100% C_{18} alkanethiol would be expected to be highly crystalline and rigid while a binary SAM comprised of 50% C_{12} alkanethiol and 50% C_{18} alkanethiol would demonstrate mobility for the outermost six carbons of each C_{18} alkanethiol chain. Surface composition and surface molecular mobility were evaluated by several surface characterization techniques including contact angle, FTIR, and XPS. Endothelial cell attachment and growth on structurally heterogeneous SAMs were assessed using imaging and assay techniques.

7.2 Materials and Methods

7.2.1 Preparation of Structurally Heterogeneous SAMs

Two binary SAM systems were prepared: 1) a series of mixtures of $HS(CH_2)_{18}CH_3$ and $HS(CH_2)_{12}CH_3$ and, 2) a series of mixtures of $HS(CH_2)_{15}COOH$ and $HS(CH_2)_9COOH$. The C_{12}/C_{18} CH3-terminated series was prepared for a preliminary study of the relationship between surface composition and thiol solution ratio. Mixed-length methyl-terminated SAMs were prepared from eight thiol solution mixtures ($[C_{12}]/[C_{18}]$ solution ratios = 0, 1, 3, 5, 7, 10, 30, ∞) as described in section 2.2. The solution ratios were chosen to achieve a range in surface composition in accordance with previously published values [67].

The C_{10}/C_{16} COOH-terminated series was prepared for evaluation in cell growth studies since the COOH surface demonstrated the highest level of cell growth promotion in previous cell growth studies (Chapters 3, 4, and 6). Mixed-length SAMs consisting

of a short-chain underlying surface containing flexible long chains were prepared with mixtures of C_{10} and C_{16} terminally functionalized thiols to obtain a random distribution of long and short chain components. The chain length of the two thiols was chosen in accordance with studies performed by Atre et al. which demonstrated that mixtures of C_{16} and C_{10} chains resulted in randomly mixed binary surfaces [93]. Atre investigated the chain length dependence of structure and wetting properties in binary composition monolayers comprised of equimolar amounts of two alkanethiol components, $HOCH_2(CH_2)_{15}S^-$ and $H_3C(CH_2)_{(15+m)}S^-$ for which m was varied systematically from -6 to +6. It was observed that the contact angles of the non-polar liquids hexadecane and dicyclohexyl exhibited a sharp change from complete wetting to strong oleophobicity as m increased through the region of -4 to 0. This wetting data was interpreted to describe a surface structure which, at low m values, consisted of randomly mixed, protruding OH-terminated chains, while at high m values, consisted of protruding CH_3-terminated chains organized in clusters which extended away from the underlying surface. At low m values (i.e., C_{10}-CH_3/C_{16}-OH) the mixed length monolayers were randomly mixed with flexible, disordered OH-terminated chains. At high m values (i.e., C_{22}-CH_3/C_{16}-OH) the monolayers consisted of phase-segregated CH_3-terminated chains. Shorter chain pairs resulted in randomly mixed surfaces containing flexible chains while longer chain pairs resulted in phase-segregated domains.

In accordance with the results of the studies by Arte and Allara, heterogeneous SAMs which varied in concentration of chains exhibiting molecular mobility were prepared as described in Section 2.2 using mixtures of $HS(CH_2)_{15}COOH$ and $HS(CH_2)_9COOH$ with targeted surface compositions of 0%, 25%, 50% and 100% of the long chain thiol component. The solution composition/surface composition relationships determined from surface characterization of the C_{12}/C_{18} CH_3-terminated SAMs were used

to select the appropriate solution ratio of the $HS(CH_2)_{15}COOH$ and $HS(CH_2)_9COOH$ thiols required to achieve the desired surface composition.

7.2.2 Surface Analysis of Structurally Heterogeneous SAMs

Binary SAMs were characterized by ellipsometry (Battelle PNL), contact angle (Battelle PNL), and XPS (Battelle and UW) as described in section 2.3. Triplicates of each surface composition were analyzed by ellipsometry and contact angle. A minimum of two replicates of each surface composition were analyzed by XPS (analysis on 2 spots per sample).

The molecular mobility or surface disorder of the structurally heterogeneous SAMs was evaluated by contact angle and FTIR. To demonstrate the presence of the disordered, mobile outer phase in the structurally heterogeneous SAMs, advancing and receding contact angles of water were measured as described in section 2.3. The structurally heterogeneous SAMs were also characterized by FTIR as described in section 2.3 to evaluate film structure.

7.2.3 Endothelial Cell Attachment and Growth

BAE culture was performed as described in Section 2.4. The effect of surface mobility on endothelial cell attachment and growth was evaluated using binary SAMs prepared and characterized as described in Sections 7.2.1. Cell growth experiments were performed using four replicates of each type of SAM. SAM substrates were prepared for cell growth experiments as described in Section 2.5.2. TCPS was used as a control surface. Cells were seeded at a density of 5×10^4 cells/samples and cultured for up to 3 days. Cell number was measured using the MTT assay system as described in Section 2.5.2 after 3 culture time periods: 4 hours, 1 day, and 3 days. Cell morphology was evaluated throughout the culture period using light microscopy.

7.3 Results and Discussion

7.3.1 Surface Analysis of C_{12}/C_{18} CH_3-terminated Binary SAMs

For structurally heterogeneous SAMs, the relationship between thiol solution ratio and surface composition is more complex than for chemically heterogeneous SAMs of the same alkanethiol chain length. Since adsorption of the longer chain thiol is favored over adsorption of the shorter chain thiol, a significant excess of short chain component is needed to achieve a 1:1 surface composition of each component. Equation 1 predicts the relationship between an experimentally measured property of the mixed SAM (P_{SAM}) and the thiol solution ratio (R_{Soln}) [97]:

$$\text{Equation 1} \qquad P_{SAM} = P_{short} + (P_{long} - P_{short})\,(AR_{Soln}/(1+AR_{Soln})) \tag{1}$$

Equation 1 is derived from simple thermodynamic equilibrium or kinetic models for formation of the binary SAMs. In Equation 1, P_{SAM} is the experimentally measured property of the binary SAM, P_{short} and P_{long} are the properties of the SAM formed from the homogeneous short and long chain alkanethiols, respectively. In the thermodynamic equilibrium model, $A=\exp(-\alpha/RT)$ where α is the difference in free energies of adsorption of the two components. In the kinetic model, $A=(k'1/k'2)$, the relative rate of adsorption of the competing adsorbates. If P_{SAM} is plotted against the log R_{Soln}, P_{SAM} has the form of a symmetric sigmoid with midpoint centered at $R_{Soln}=1/A$.

This relationship can be used to determine the position of the monolayer property transition midpoint for a binary SAM system by fitting experimental data with a function described by Equation 1. The property transition midpoint is the value of the thiol solution ratio (R_{soln}) at which the experimental properties of the SAM lie midway between those found for the homogeneous long chain SAM and the homogeneous short

chain SAM. If the measured properties are linearly related to monolayer composition, the property transition midpoint indicates the solution ratio needed to give a ratio of thiol components on the SAM surface of 1 (Rsam =1).

A preliminary study was performed to investigate the relationship between thiol solution ratio and surface composition for a binary mixed length SAMs composed of octadecyl mercaptan ($HS(CH_2)_{17}CH_3$) and dodecanethiol ($HS(CH_2)_{11}CH_3$). Figure 7.1 shows XPS C/Au ratios obtained for a series of mixed length C_{12}/C_{18} SAMs as a function of thiol solution ratio. Experimental data were fit to equation 1 using the general curve fit function in KalidaGraph. The relationship between thiol solution ratio and surface composition (C/Au ratio determined by XPS) for the C_{12}/C_{18} mixtures is described by a sigmoidal curve. For the C_{12}/C_{18} mixed length SAMs, the property transition midpoint (the point at which the C_{12}/C_{18} ratio on the SAM surface is 1:1) was determined to occur at a C_{12}/C_{18} thiol solution ratio of 5:1 for experiment #1 and at 5.9:1 for experiment #2. Experimental data fit the theoretically predicted relationship with a correlation of 1.0 and 0.996 respectively. Figure 7.2 demonstrates the surface composition of the C_{12}/C_{18} mixed length SAMs (as determined by XPS) as a function of the thiol solution ratio. Figures 7.1 and 7.2 emphasize the importance of obtaining accurate thiol solution ratio versus surface composition curves for mixed length SAM systems in order to correctly select thiol solution ratios that will yield the desired surface concentration. Using the data obtained for the C_{12}/C_{18} series, thiol solution ratios were chosen to yield target surface compositions for the C_{10}/C_{16}-COOH-terminated binary SAM series.

7.3.2 Surface Analysis of C_{10}/C_{16} COOH-terminated Binary SAMs

To demonstrate the presence of the disordered, mobile outer phase in the mixed length SAMs, advancing and receding contact angles of water were measured. Contact

angles can provide structural information about the surface of the SAM [bain]. Hysteresis in the contact angle also provides structural information about the surface of the monolayer. Hysteresis in the contact angle is typically expressed as the difference between the minimum receding contact angle and the advancing contact angle expressed as cosines: $\cos \theta_R - \cos \theta_A$ [67,75].

Table 7.1 shows the advancing and receding contact angles of water measured for the C_{10}/C_{16} binary SAMs. Advancing water contact angles ranged from 17° on the 100% C_{16} surface to 61° on the 25% C_{16} surface. Advancing water contact angles were similar on the 25% C_{16} and 50% C_{16} surfaces (61° and 60°C respectively) and slightly lower on the 75% C_{16} surface (50°). The advancing contact angle on the 0% C_{16} (100% C_{10}) surface was much higher than expected (60°).

In a binary SAM composed of mixtures of a long chain and a short chain thiol, the randomly mixed, mobile chains of the longer chain component in the outer phase of the mixed length SAM should expose nonpolar methylene groups at the surface during measurement of an advancing contact angle [67]. The exposed methylene groups would cause an increase in the contact angle of water relative to a homogeneous COOH-terminated monolayer. Homogeneous monolayers of COOH-terminated SAMs typically demonstrate wetting or near wetting behavior with water ($\theta(H_2O)$ approximately 17°). Increased advancing water contact angles on mixed length SAMs was demonstrated by Bain et al. who measured advancing water contact angles of approximately 10° on pure monolayers of $HS(CH_2)_{11}OH$ and $HS(CH_2)_{19}OH$ and a water contact angle of approximately 40° for a 1:1 mixed monolayer of $HS(CH_2)_{11}OH$ and $HS(CH_2)_{19}OH$. Water contact angles varied with thiol solution ratio (i.e., surface composition) and were determined to be indicative of the disordered, mobile outer phase in the mixed monolayers [67].

The results shown in Table 7.1 suggest that the 25%, 50% and 75% C_{16} surfaces are disordered relative to the 100% C_{16} surface. The large increase in advancing water contact angles for the mixed length SAM surfaces is due to exposure of the nonpolar methylene groups exposed by the mobile, longer chains of the C_{16} thiol. The high water contact angle of the 0% C_{16} surface is an unexpected finding and perhaps reflects surface contamination or incomplete surface assembly of the thiol molecules in this SAM.

As discussed in Section 3.3, to minimize interfacial free energy, mobile hydrophilic or hydrophobic surface groups or segments can reorient at the aqueous interface and cause hysteresis in the contact angle. For the mixed length COOH-terminated SAMs, reorientation of the mobile, hydrophilic surface groups are expected to result in significant differences between the advancing and receding contact angles. The advancing contact angle would be measured on the surface with the longer chain component "splayed" and screening the shorter chain components therefore exposing the nonpolar methylene groups at the surface. The hydrophilic terminal group of the long chain component would likely be directed towards the surface of the SAM. During contact with water, the hydrophilic terminal group of the long chain component would reorient to the water phase. Therefore, we would expect a decrease in the receding contact angle due to this reorientation. Reorientation of surface groups is only possible if the molecules are mobile therefore, hysteresis in the contact angle allows for an indirect evaluation of mixed length SAM surface mobility.

Table 7.1 lists the receding water contact angle measured as a function of C_{16} thiol surface content. The receding contact angle ranged from 11° on the 100% C_{16} SAM to 52° on the 25% C_{16} SAM. The difference in the advancing and receding contact angle, or the contact angle hysteresis can also be used to evaluate surface disorder. Table 7.1 lists the contact angle hysteresis calculated from the advancing and receding contact angles. Hysteresis values ranged from 0.03 for the 100% C_{16} surface to a high of 0.15

for the 50% C_{16} SAM surface. Surface disorder is therefore maximum on the 50% C_{16} surface as anticipated. Surface disorder is slightly less on the 25% and 75% C_{16} surfaces and is much higher than anticipated on the 0% C_{16} surface. The 0% C_{16} surface should exhibit minimal hysteresis if it is a correctly assembled surface. The high hysteresis observed for this surface suggests that monolayer formation on this surface was incomplete.

IR can provide additional information regarding the mobile, disordered outer phase. Changes in the C-H stretching mode peaks as a function of binary SAM surface composition can be evaluated. Atre et. al, observed changes in the shapes, areas and positions of the four main C-H stretching mode peaks (2849.8, 2876.8, 2917.3, and 2963.9 cm^{-1}) as a function of the differential chain-length, m, for 1:1 binary monolayers of $HOCH_2(CH_2)_{15}S^-$ and $H_3C(CH_2)_{(15+m)}S^-$ (described above in 7.2.1) [93]. Differences in the C-H stretching mode peaks reflected changes in mixed length SAM surface structure resulting from the presence of the protruding, conformationally disordered chain segments. In particular, a shift in the CH_2 asymmetric stretch peak at 2918 cm^{-1} to higher values was strongly indicative of the presence of conformationally disordered, protruding long chain segments in a mixed length SAM.

The 0% and 50% C_{16} SAMs were characterized by IR as described in Section 2.3 to evaluate film structure. Table 7.1 lists the shift in the CH_2 asymmetric stretch peak normally located at 2918 cm^{-1} for an ordered SAM. The 100% C16 SAMs exhibited no shift in the location of the CH_2 asymmetric stretch peak demonstrating order in this surface. The 50% C_{16} SAM showed a significant shift in the CH_2 asymmetric stretch peak to 2929 cm^{-1}. These results are consistent with contact angle hysteresis values and confirm the presence of conformationally disordered, protruding long chain segments in the 50% C_{16} SAM.

7.3.3 Endothelial Cell Growth on C_{10}/C_{16} COOH-terminated Binary SAMs: Effect of Surface Molecular Mobility

The effect of surface disorder or surface molecular mobility on BAEC attachment and growth was evaluated for five C_{10}/C_{16} COOH-terminated binary SAMs and for TCPS after cell culture periods of 4 hours, 1 day, and 3 days. BAE cell number measured on the C_{10}/C_{16} SAMs as a function of cell culture time is shown in Figure 7.3. Figure 7.4 illustrates the cell number measured at each culture time point on the C_{10}/C_{16} binary SAMs as a function of surface fraction of the C_{16}-COOH thiol. Figures 7.5, 7.6, and 7.7 illustrate BAE cell numbers measured on the C_{10}/C_{16} SAMs normalized to the BAE cell number measured on the TCPS control surface as a function of surface C_{16}-COOH fraction for the 4 hour, 1 day, and 3 day culture time periods respectively.

All C_{10}/C_{16} SAMs showed an increase in cell number with increasing culture time. Between the 4 hour and the 1 day time period, the rate of growth was essentially equivalent for the five SAMs (Figure 7.3). All surfaces, including TCPS, exhibited similar increases in cell number between the 4 hour and 3 day time points (11-12-fold increase) as well. Figure 7.4 illustrates the cell number measured at each culture time point. After the 4 hour culture period, cell numbers on the binary SAMs are essentially equivalent to cell number on TCPS. After 1 day of culture, cell numbers on the 0%, 25%, 75% and 100% C_{16} surfaces are similar to TCPS. Cell number on the 50% C_{16} surface was higher than on TCPS. After 3 days of culture, cell numbers on the 0-75% C_{16} surfaces were lower than on TCPS while the 100% C_{16} surface showed cell number higher than on TPCS.

Normalized cell numbers measured on the C_{10}/C_{16} SAMs after 4 hours of culture are shown in Figure 7.5. Cell attachment was highest on the 100% C_{16} surface and lowest on the 0% C_{16} surface. Cell attachment increased slightly with increasing surface

fraction of C_{16}-COOH thiol however, the differences in cell number between the C_{16} surfaces was not significant.

Figure 7.6 illustrates the normalized cell number measured on the C_{10}/C_{16} SAMs after a 1 day culture period. Cell number was 12% higher on the 50% C_{16} surface than on the 100% C_{16} surface, a difference which was significant. Cell numbers on the 0%, 25% and 75% C_{16} SAMs did not differ significantly from each other or from that on the 100% C_{16} surface and were approximately equivalent to cell number on TCPS.

After a 3 day culture period, the growth pattern differs somewhat from that observed after a 1 day culture period. In general, the cell growth patterns as a function of C_{16} surface content are not consistent for the 1 day and 3 day growth periods. Cell number was highest on the 100% C_{16} surface and lowest on the 25% C_{16} surface (20% lower). Cell number increased slightly as surface C_{16} content increased from 25% to 100%. The 50% C_{16} surface was 15% lower in cell number than the 100% C_{16} surface. Cell numbers on the 0% and 75% C_{16} surfaces were approximately equivalent and slightly lower (~10%) than the 100% C_{16} surface. Differences between the 25% and 50% C_{16} surface and the 100% C_{16} surface were statistically significant however, differences between the 0%, 25%, 50%, and 75% C_{16} surfaces were not significant.

BAEC density and morphology on the C_{10}/C_{16} SAMs and TCPS was evaluated qualitatively after 4 hour, 1 day and 3 day culture periods in a series of light micrographs shown in Figures 7.8, 7.9, 7.10. Figure 7.8 illustrates cell morphology after 4 hours of culture. Consistent with results shown in Figure 7.5, cell density was slightly higher on the 50%, 75% and 100% C_{16} surfaces than on the 0% and 25% C_{16} surfaces. The majority of cells on the SAM surfaces were rounded however, cell spreading was observed on the 50-100% C_{16} surfaces and on TCPS.

After 1 day of culture, the 0%, 25% and 100% C_{16} surfaces were very similar in terms of cell density and morphology and were equivalent in appearance to TCPS (Figure

7.9). Cell density appeared higher on the 50% and 75% surfaces relative to the other SAM surfaces.

After 3 days of culture, cell density on the C_{10}/C_{16} SAMs and on TCPS were essentially equivalent (Figure 7.10). All surfaces demonstrated a confluent cell monolayer. Some differences in cell morphology were observed however, between the SAM surfaces. The 25% and 50% C_{16} SAMs demonstrated several large senescent cells. These types of cells were also observed on TCPS and have been observed on TCPS in previous cell growth studies (Chapter 6). There large cells were not observed on the 100% C_{16} surface. These areas of large cells are most likely the cause of the decreased cell density measured for the 25% and 50% C_{16} SAMs relative to the 100% C_{16} SAM (Figure 7.7).

To evaluate the effects of surface disorder or surface molecular mobility on cell growth, qualitative and quantitative evaluations of cell growth can be considered in conjunction with data obtained from contact angle studies. Hysteresis on the 25% and 75% C_{16} surfaces was equivalent ($\Delta\cos\Theta = 0.136$) and slightly lower than on the 50% C_{16} surface ($\Delta\cos\Theta = 0.150$). Hysteresis on the 100% C_{16} surface was significantly lower ($\Delta\cos\Theta = 0.03$). Results shown in Figures 7.6 and 7.9 demonstrated a statistically significant increase (~12%) in cell density for the most disordered surface, the 50% C_{16} surface, relative to the immobile 100% C_{16} surface. However, the 25% and 75% C_{16} surfaces, which also exhibited surface disorder, did not differ significantly in cell density from the immobile 100% C_{16} surface. These results suggest that surface disorder has a limited effect (if any) on cell growth.

After 3 days of culture, cell density on the 25% and 50% C_{16} surfaces was lower (~15%) than on the 75% and 100% C_{16} surfaces as measured by the MTT assay, however all surfaces demonstrated a confluent cell monolayer. The 25% and 50% C_{16} surfaces differed in that they exhibited areas of large, senescent cells which most likely

resulted in the decrease in cell density measured by MTT. The effect of surface disorder on cell growth appears to be negligible after the 3 day culture period since the disordered 75% C_{16} surface exhibited a cell density which did not differ significantly from that on the immobile 100% C_{16} surface. The disordered 25% and 50% C_{16} surfaces demonstrated lower cell densities than did the 100% C_{16} surface in quantitative studies but qualitative studies showed similar cell densities with the exception of the large senescent cells on the disordered SAMs.

7.4 Conclusions

The effect of surface mobility, or surface molecular motions, on endothelial cell attachment and growth was investigated in this chapter. The hypothesis investigated in these studies was that endothelial cell growth would be dependent upon the degree of surface molecular mobility and that cell growth on structurally complex, mobile surfaces would differ significantly from that on structurally homogeneous, ordered, immobile surfaces.

Two mixed length binary SAMs systems were evaluated. A series of mixtures of $HS(CH_2)_{18}CH_3$ and $HS(CH_2)_{12}CH_3$ were evaluated in a preliminary surface characterization study to determine the relationship between surface composition and thiol solution ratio. A series of mixtures of $HS(CH_2)_{15}COOH$ and $HS(CH_2)_9COOH$ were evaluated in cell growth studies. Five C_{10}/C_{16} binary SAMs were prepared using the solution composition/solution ratio relationship developed for the C_{12}/C_{18} binary SAMs.

The C_{10}/C_{16} SAMs were characterized by XPS, ellipsometry, contact angle and FTIR. Surface disorder or surface mobility was assessed by advancing water contact angle, contact angle hysteresis, and changes in the C-H stretching mode peaks as

measured by FTIR. Surface disorder was maximal on the 50% C_{16} surface and lowest on the 100% C_{16} surface.

Endothelial cell attachment and growth was evaluated on the C_{10}/C_{16} binary SAMs using imaging and the MTT assay system. In general, the effects of surface disorder or surface mobility on cell growth were limited. After 4 hours of culture, no significant differences in cell number were observed in response to differences in surface disorder. After 1 day of culture, a significant increase in cell number was observed for the most disordered surface, the 50% C_{16} surface, relative to the immobile 100% C_{16} surface however, the 25% and 75% surfaces which also exhibited surface mobility, did not differ in cell number from the immobile 100% C_{16} surface. After the 3 day culture period, all C_{10}/C_{16} surfaces exhibited confluent monolayers. The 25% C_{16} and 50% C_{16} surfaces demonstrated significantly lower cell numbers than the 100% C_{16} surface however, this decrease was attributed to the presence of large, senescent cells on these surfaces. After 3 days of culture, the effects of surface disorder on cell growth were negligible.

Contrary to the hypothesis posed in the beginning of this chapter, the effects of surface disorder or surface mobility on cell growth appears to be limited. Any effects of surface mobility on cell growth also appear to be limited to the early phases of cell interactions with a surface (i.e., 1 day) as opposed to later times in the cell growth process. There may be a transitory effect of surface mobility on the adsorption of adhesive proteins which promote cell growth or the deposition of cell-derived proteins. Certainly the differences observed in cell growth in response to surface chemistry (functional group content) as described in Chapter 6 are far more significant than the effects of surface mobility on cell growth. Since the COOH surface is such an effective promoter of cell growth, it is possible that any effect of surface mobility was overshadowed by the tremendous cell growth potential of the COOH surface.

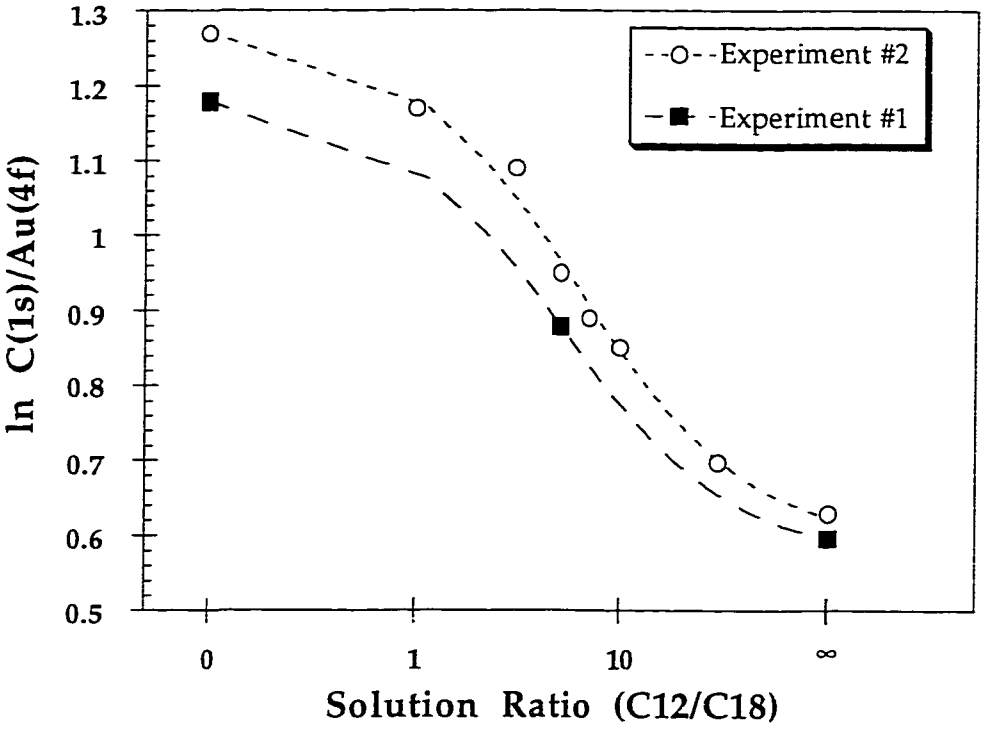

Figure 7.1 Ratio of C(1s) to Au (4f) peak areas in XPS for monolayers adsorbed onto gold from binary solutions of octadecyl mercaptan and dodecanethiol in ethanol. Data represent mean of triplicate samples. The position of the monolayer property transition midpoint is determined by fitting experimental data with a function that describes the relationship between C/Au ratio and the solution ratio. Experimental data were fit to equation 1 using the general curve fit function in KalidaGraph (dashed lines). Transition midpoints were calculated at a solution ratio equal to 5.0 for experiment #1 and at 5.9 for experiment #2. Experimental data fit the theoretically predicted relationship with a correlation of 1.0 and 0.996 respectively.

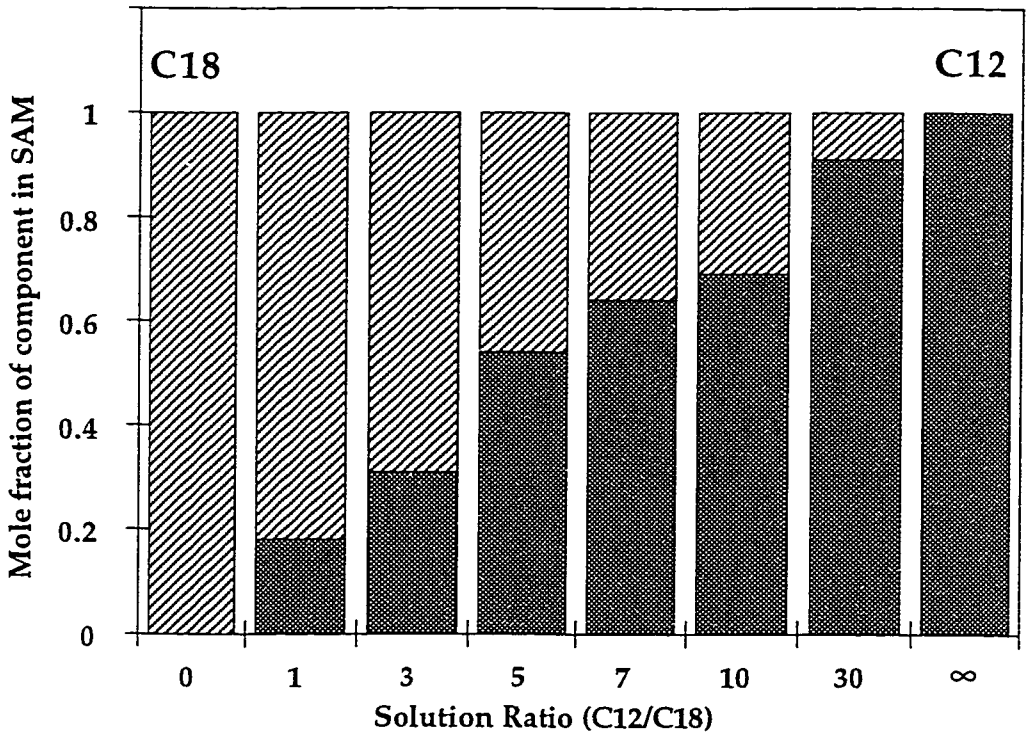

Figure 7.2 Surface composition (determined by XPS) of mixed monolayers of octadecyl mercaptan and dodecanethiol adsorbed onto gold from ethanol as a function of thiol concentration ratio in solution. Data represent mean of triplicate samples.

Table 7.1

Surface Characterization of C_{10}/C_{16} Binary SAMs by Contact Angle and FTIR

SAM Surface Composition	$\Theta_{Advancing}$	$\Theta_{Receding}$	$\Delta \cos \Theta$	*CH_2 Peak Position (cm^{-1})*
0% C_{16}/100% C_{10}	60.4 ± 2.2	51.2 ± 1.2	0.14	
25% C_{16}/75% C_{10}	61.1 ± 3.5	51.6 ± 1.2	0.136	
50% C_{16}/50% C_{10}	59.8 ± 2.3	49.2 ± 2.0	0.150	2929
75% C_{16}/25% C_{10}	49.9 ± 1.2	38.4 ± 1.5	0.138	
100% C_{16}/0% C_{10}	17.3 ± 2.3	10.5 ± 1.8	0.03	2918

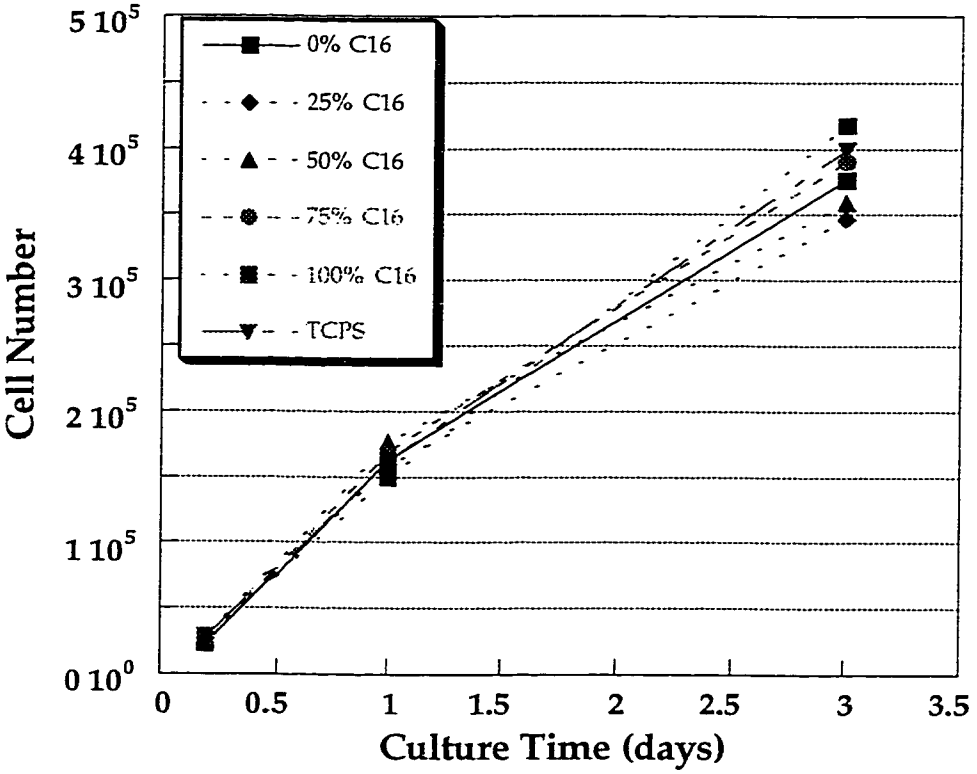

Figure 7.3 BAEC number determined on binary composition SAMs adsorbed from ethanolic mixtures of $HS(CH_2)_9COOH$ and $HS(CH_2)_{15}COOH$ as a function of cell culture time. Cells were cultured for 4 hours, 1 day, and 3 days in medium containing 10% bovine serum. Cell number was determined from Figure 6.1 using absorbance values measured by MTT assay for each 15 mm diameter sample (surface area = 1.81 cm^2). Data represent the mean ± standard deviation for quadruplicate samples.

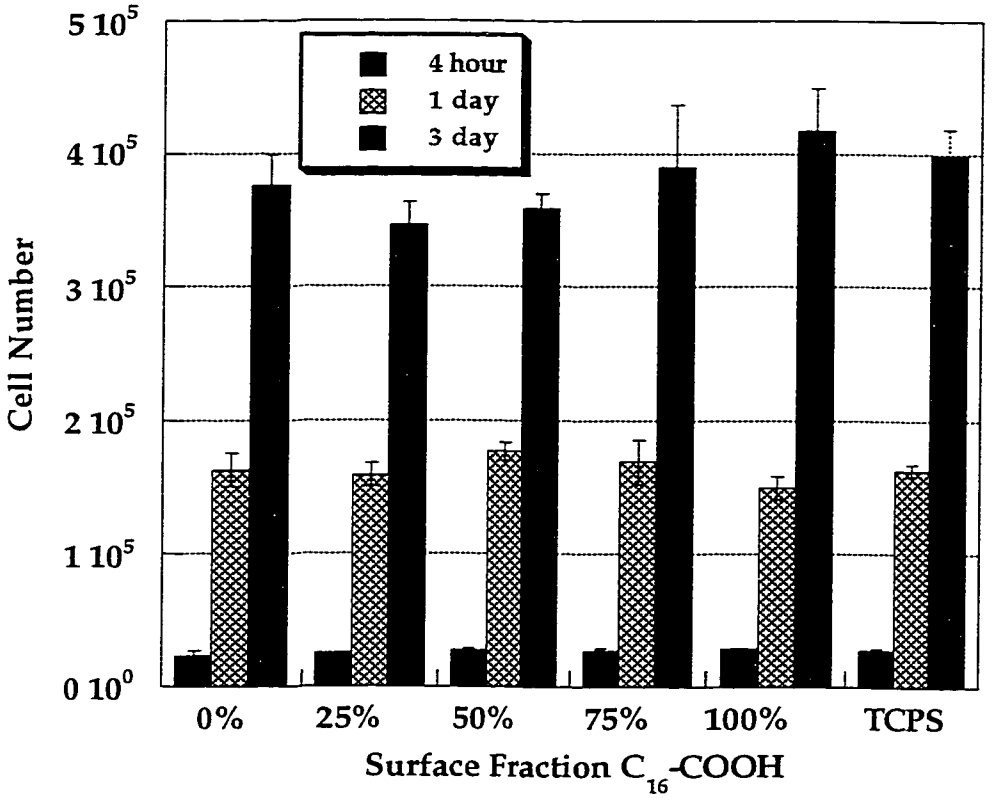

Figure 7.4 BAEC number determined on binary composition SAMs adsorbed from ethanolic mixtures of $HS(CH_2)_9COOH$ and $HS(CH_2)_{15}COOH$ as a function of surface $HS(CH_2)_{15}COOH$ thiol content, and on TCPS. Cells were cultured for 4 hours, 1 day, and 3 days in medium containing 10% bovine serum. Cell number was determined from Figure 6.1 using absorbance values measured by MTT assay for each 15 mm diameter sample (surface area = 1.81 cm^2). Data represent the mean ± standard deviation for quadruplicate samples.

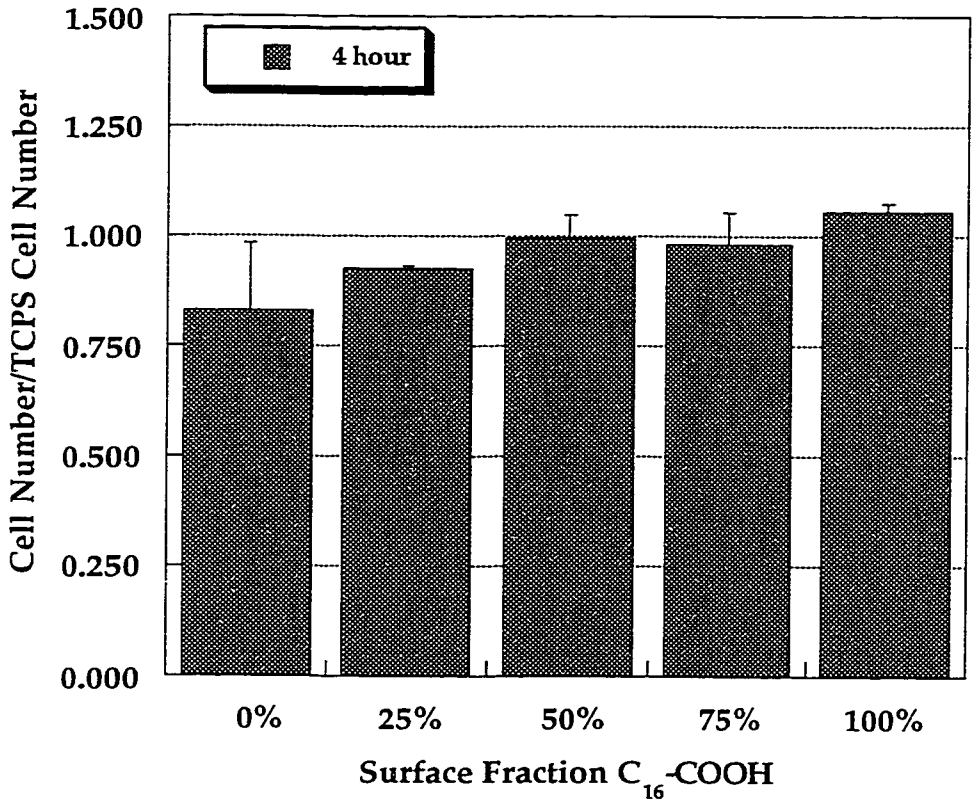

Figure 7.5 Normalized BAEC number determined on binary composition SAMs adsorbed from ethanolic mixtures of $HS(CH_2)_9COOH$ and $HS(CH_2)_{15}COOH$ as a function of surface $HS(CH_2)_{15}COOH$ thiol content. Cells were cultured for 4 hours in medium containing 10% bovine serum. Normalized cell number was determined as the ratio of the cell number measured on the SAM surface to cell number measured on the TCPS control surface (reference Figure 7.4). Data represent the mean ± standard deviation for quadruplicate samples.

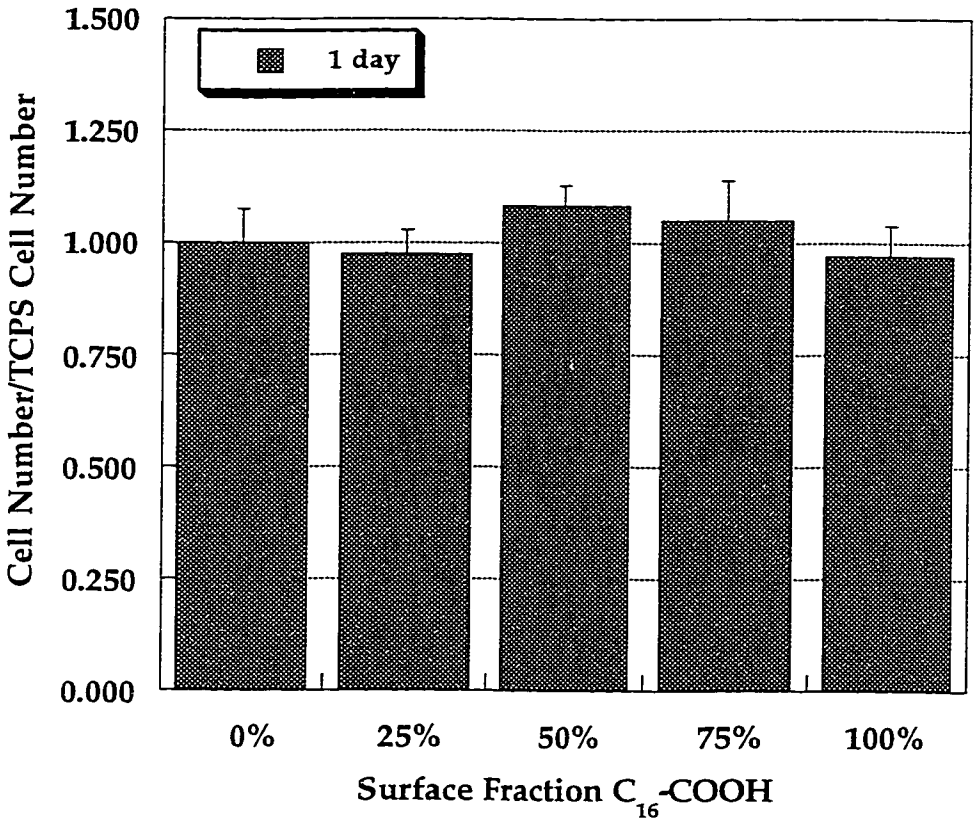

Figure 7.6 Normalized BAEC number determined on binary composition SAMs adsorbed from ethanolic mixtures of $HS(CH_2)_9COOH$ and $HS(CH_2)_{15}COOH$ as a function of surface $HS(CH_2)_{15}COOH$ thiol content. Cells were cultured for 1 day in medium containing 10% bovine serum. Normalized cell number was determined as the ratio of the cell number measured on the SAM surface to cell number measured on the TCPS control surface (reference Figure 7.4). Data represent the mean ± standard deviation for quadruplicate samples.

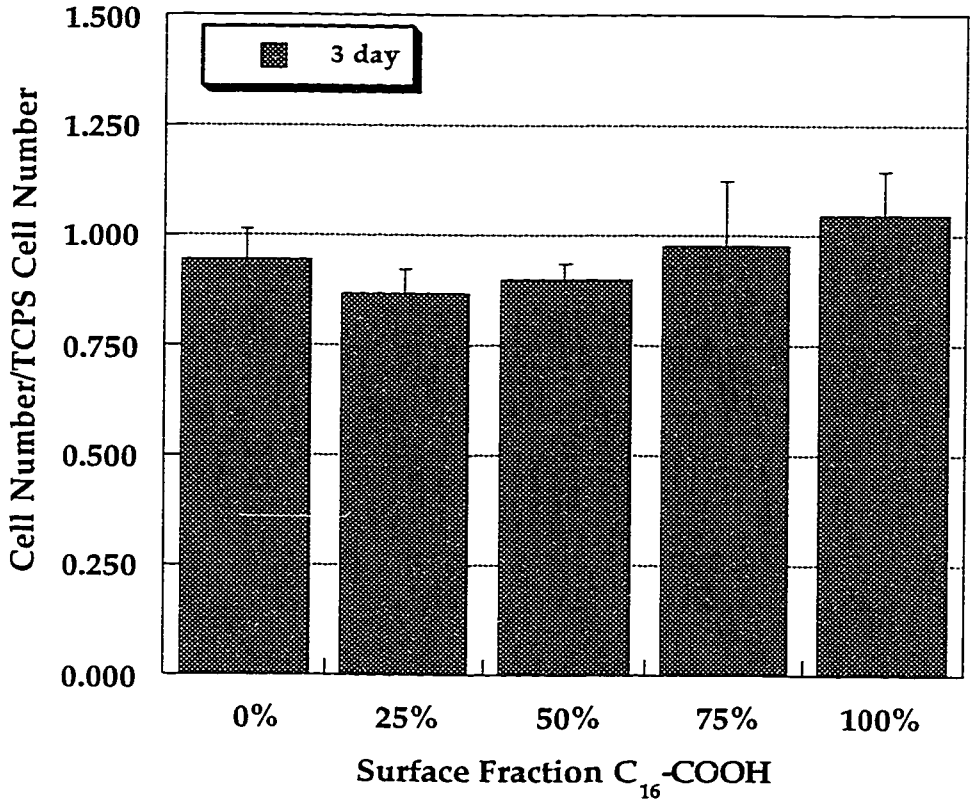

Figure 7.7 Normalized BAEC number determined on binary composition SAMs adsorbed from ethanolic mixtures of $HS(CH_2)_9COOH$ and $HS(CH_2)_{15}COOH$ as a function of surface $HS(CH_2)_{15}COOH$ thiol content. Cells were cultured for 3 days in medium containing 10% bovine serum. Normalized cell number was determined as the ratio of the cell number measured on the SAM surface to cell number measured on the TCPS control surface (reference Figure 7.4). Data represent the mean ± standard deviation for quadruplicate samples.

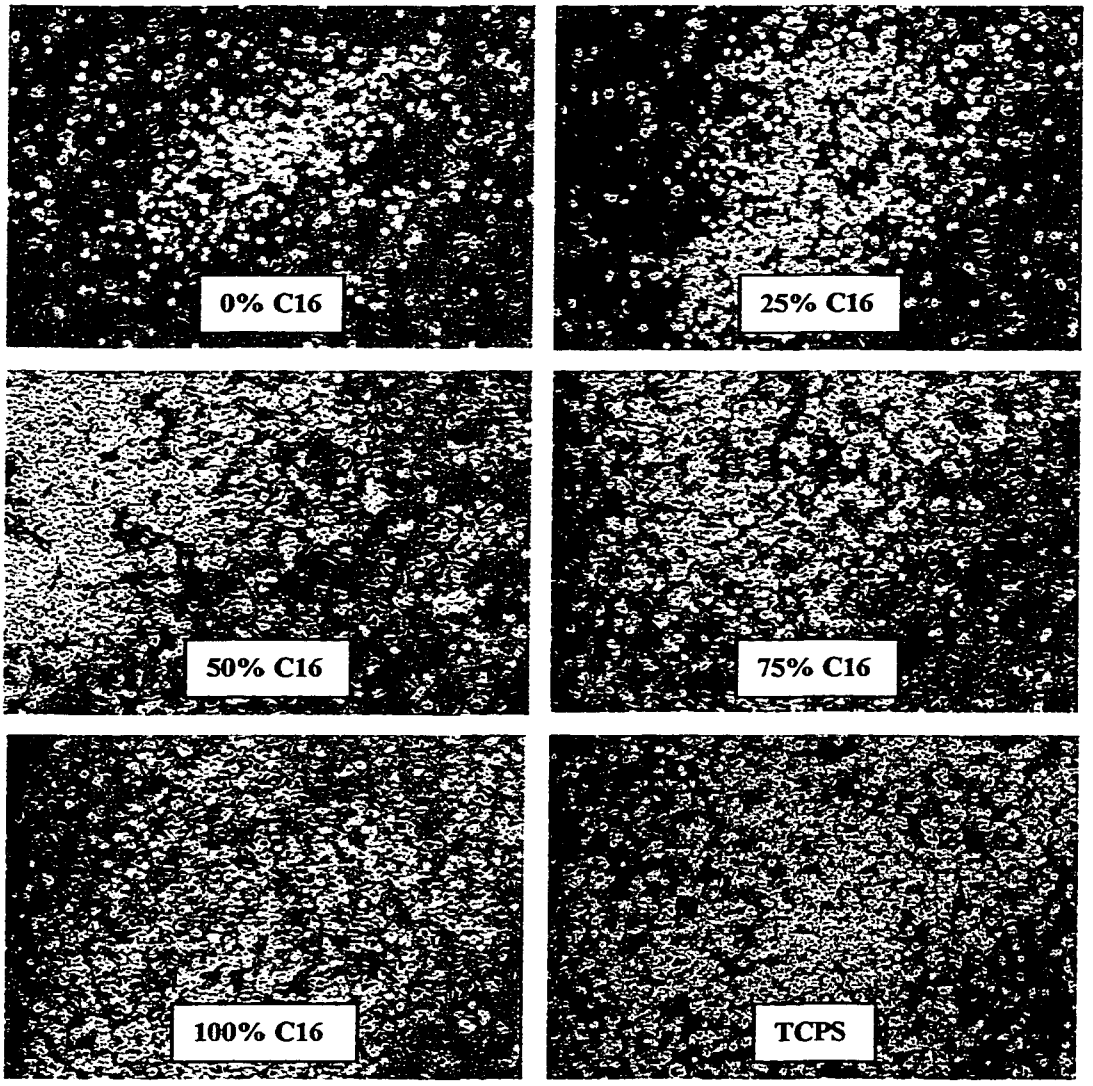

Figure 7.8 BAEC on binary composition SAMs of $HS(CH_2)_9COOH$ and $HS(CH_2)_{15}COOH$ for surface compositions of 0% C_{16}-COOH, 25% C_{16}-COOH, 50% C_{16}-COOH, 75% C_{16}-COOH, 100% C_{16}-COOH, and on TCPS. Cells were cultured in 10% bovine serum for 4 hours.

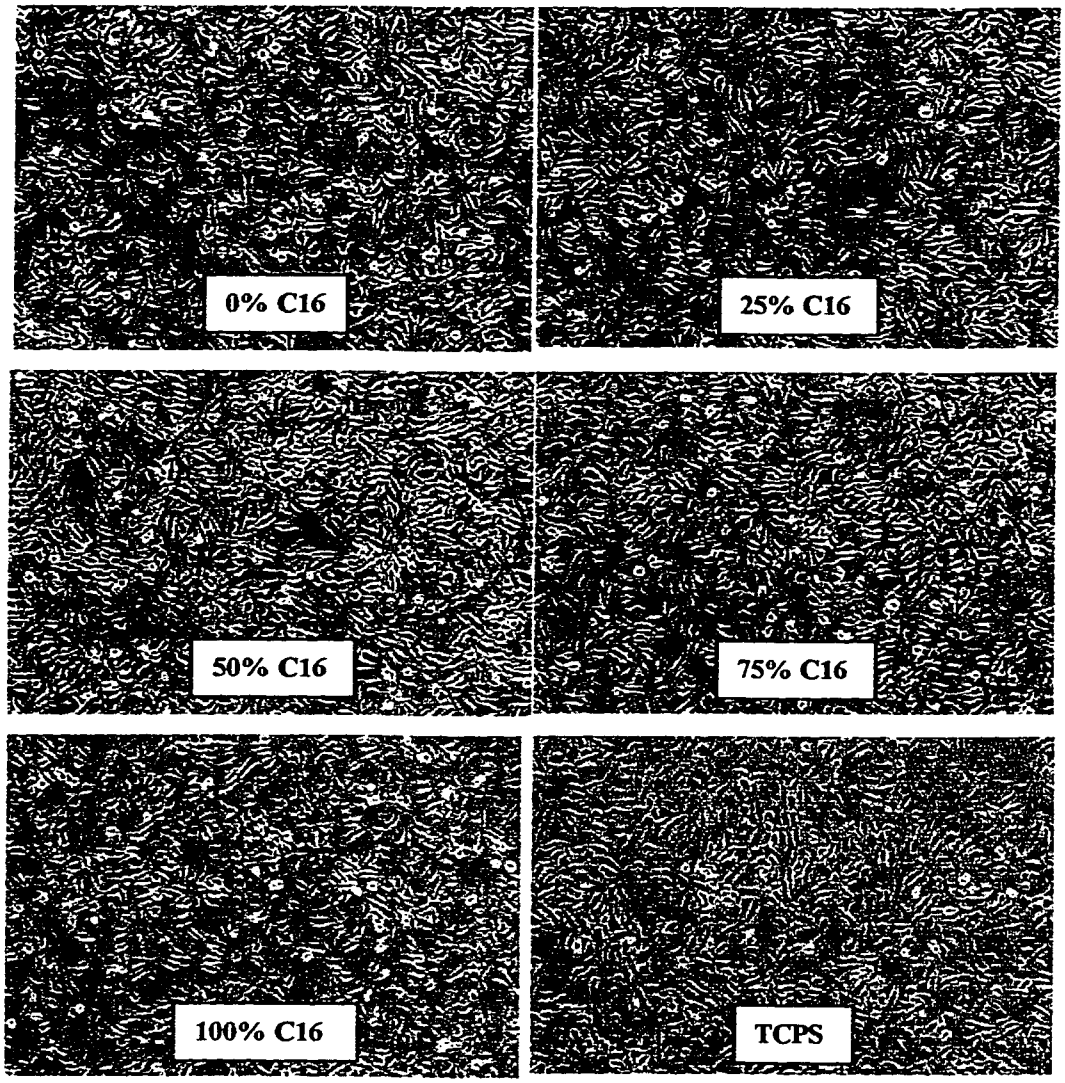

Figure 7.9 BAEC on binary composition SAMs of $HS(CH_2)_9COOH$ and $HS(CH_2)_{15}COOH$ for surface compositions of 0% C_{16}-COOH, 25% C_{16}-COOH, 50% C_{16}-COOH, 75% C_{16}-COOH, 100% C_{16}-COOH, and on TCPS. Cells were cultured in 10% bovine serum for 1 day.

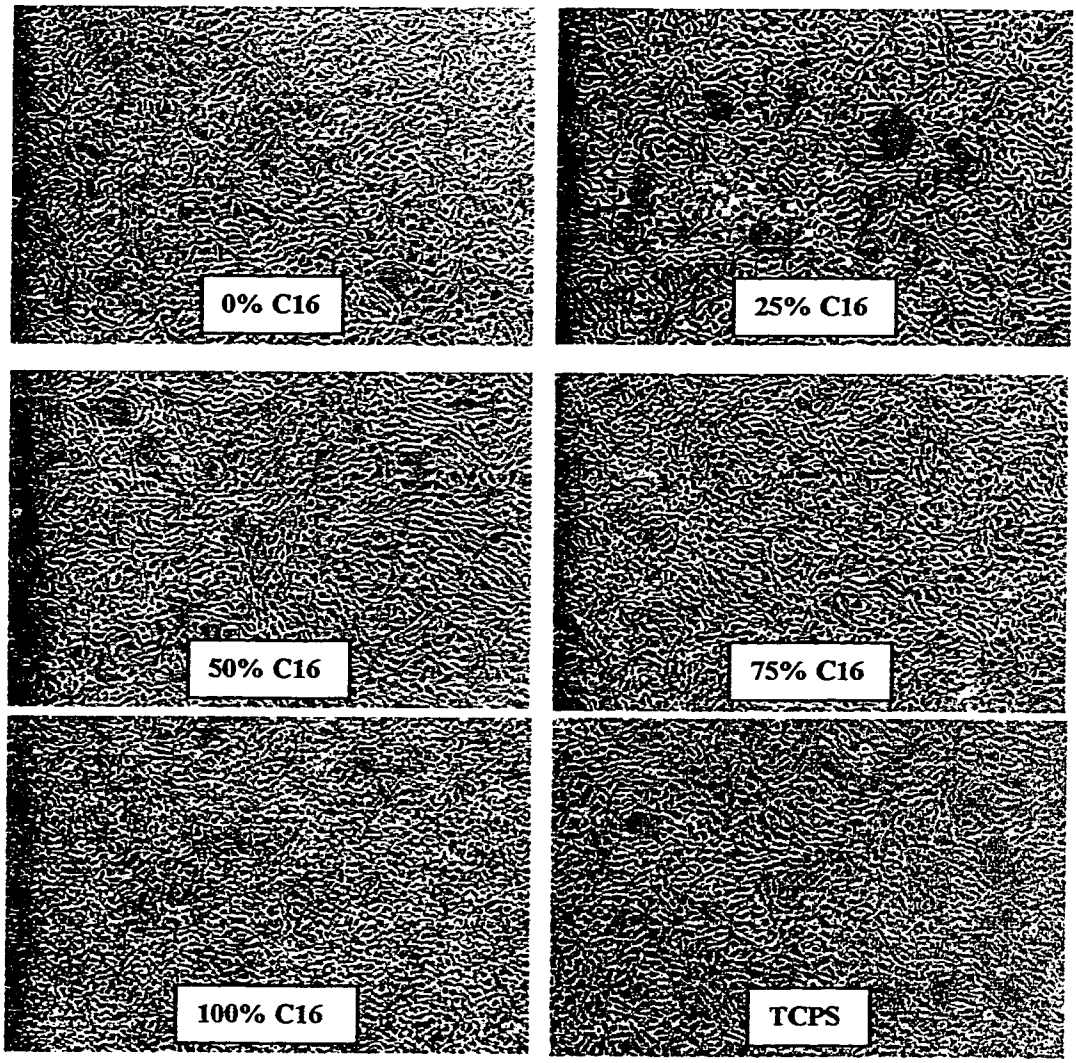

Figure 7.10 BAEC on binary composition SAMs of $HS(CH_2)_9COOH$ and $HS(CH_2)_{15}COOH$ for surface compositions of 0% C_{16}-COOH, 25% C_{16}-COOH, 50% C_{16}-COOH, 75% C_{16}-COOH, 100% C_{16}-COOH, and on TCPS. Cells were cultured in 10% bovine serum for 3 days.

Chapter 8

Characterization of Protein Layers Adsorbed to Binary SAMs: Effect of Surface Properties and Influence on Endothelial Cell Growth

8.1 Introduction

The studies described in this chapter were designed to address several important issues. First, while many studies have provided evidence that substrate chemistry directly affects the adsorption behavior of proteins (as discussed in Section 3.1), relatively few studies have been performed to systematically investigate the effect of specific surface chemical functionalities on the adsorbed protein layer. This issue has been difficult to address primarily because of the difficulty in preparing substrates which vary systematically in functional group type and concentration. Our preliminary studies of homogeneous SAMs (Chapter 3) have demonstrated an effect of surface chemical functionality on the adsorption and SDS elutability of Fn and Alb from serum. Preliminary studies of protein adsorption and elution from a limited series of COOH/OH SAMs (Chapter 4) also demonstrated variations in Alb and Fn adsorption and elutability in response to SAM surface composition. However, the adsorption of only two proteins to only three binary SAM surface compositions were examined in these studies. Therefore, a more extensive evaluation of the effect of functional group type and concentration on the composition and binding strength of three key serum proteins (albumin, fibronectin, and vitronectin) in the adsorbed protein layer was performed.

The most significant issue addressed in this chapter is the influence of the adsorbed protein layer on cell growth. Many studies have been directed at understanding various aspects of this complex issue (see Chapter 1). Among the factors influencing cell attachment and growth is the composition of the adsorbed protein layer as discussed

in Section 1.5. Sufficient quantities of adhesive molecules must be present in the appropriate conformations to facilitate cell adhesion, spreading and growth. Nonadhesive molecules such as albumin can also influence growth by affecting the conformation of adsorbed adhesive molecules. The initially adsorbed protein layer is dynamic in nature and undergoes compositional changes with time as other serum proteins displace proteins in the adsorbed layer. Cellular attachment and spreading is a time-dependent process during which there are cellular interactions with the adsorbed proteins which involve cell membrane receptor interactions with the various adsorbed adhesive proteins [19].

Another factor which may have greater impact on cell-substrate interactions than adsorbed protein layer composition is the biological activity of the adsorbed proteins as discussed in Section 1.5. Variations in the biological activity of adsorbed proteins can be related to differences in protein conformation and/or orientation, or alternately, differences in the binding strength of the adsorbed protein. Variations in protein binding strength can affect the ability of a cell to interact with an adsorbed adhesive protein or the ability of an adsorbed protein to be displaced by other serum proteins [19]. Therefore, the binding strength the adsorbed protein layer is of considerable importance in its influence on cell attachment, spreading and growth.

In preliminary protein interaction studies described in Chapters 3 and 4, the effects of the adsorbed protein layer composition and binding strength on cell growth were investigated by measuring protein adsorption (Alb and Fn) and cell growth on homogeneous SAMs and a limited series of binary SAMs. We observed relationships between cell growth and characteristics of the adsorbed protein layers. Surface promoting cell growth demonstrated moderate to high Alb elutabilities and higher levels of Fn adsorption than did substrates inhibiting cell growth. It was observed that the

amount of Alb adsorbed to a surface did not correlate with, and more importantly, did not negatively affect cell growth.

To more thoroughly evaluate relationships between adsorbed protein layer characteristics and cell growth, 2 of the 3 binary SAM series evaluated in cell growth studies described in Chapter 6 were investigated in the protein adsorption studies described in this chapter. By examining the effects of substrate properties on cell growth (Chapter 6) and by subsequently evaluating the effects of the same substrate properties on the adsorbed protein layer (using substrates with a well-defined, carefully controlled chemistry and structure) we were able to systematically investigate the influence of various aspects of the adsorbed protein layer on endothelial cell growth.

In protein interaction studies described in Chapters 3 and 4, the adsorption and elutability of Alb and Fn were measured. In this chapter, we also investigated the effects of surface composition on Fn and Alb adsorption from serum by measuring protein layer characteristics as a function of surface functional group content. However, we additionally investigated the effects of surface composition on the adsorption of vitronectin, another key adhesive serum protein. As discussed in Section 1.5, several studies suggest that Vn is the key adhesive protein mediating cell attachment and growth on oxygen-containing surfaces [20,58,98,99]. The majority of cell attachment activity in cell culture media containing bovine or human serum is due to Vn and to a lesser extent, Fn. This is due in part to a 20-40 fold higher adsorption of Vn from plasma or serum to tissue culture dishes compared to Fn [100]. Since Vn adsorption from plasma or serum onto a substrate is generally significantly higher than Fn adsorption, Vn was expected to have a significant effect on cell attachment and growth on SAMs. Evaluating the effect of substrate properties on Vn adsorption and the influence of the adsorbed Vn on cell

attachment and growth is of critical importance in understanding factors which influence endothelial cell growth.

To investigate the effect of surface composition on the adsorbed protein layer and to evaluate the influence of the adsorbed protein layer on endothelial cell growth, two binary SAM series were investigated: 1) a series of mixtures of $HS(CH_2)_{15}COOH$ and $HS(CH_2)_{15}CH_2OH$, and 2) a series of mixtures of $HS(CH_2)_{15}COOH$ and $HS(CH_2)_{15}CH_3$. These binary SAM surfaces had demonstrated a gradient in cellular response in cell interactions studies described in Chapter 6 and therefore were selected for evaluation in protein interaction studies. The OH/CH_3 SAM series was excluded from protein adsorption studies due to its poor performance in cell growth studies.

Several important characteristics of the adsorbed protein layers were evaluated including composition and binding strength. The adsorption of three serum proteins (Alb, Fn, and Vn) to the binary SAMs from the complex solution used to conduct cell proliferation studies (10% bovine serum containing media) was measured and the composition of the adsorbed protein layer was determined. The SDS elutability of each of the serum proteins was assessed to evaluate the effect of substrate properties on the protein-substrate binding or interaction strength. Information obtained in cell growth studies (Chapter 6) was compared with results obtained in protein interaction studies with to evaluate possible relationships between substrate properties, properties of the adsorbed protein layer, and cell growth. We hypothesized that surfaces which demonstrate an increased affinity for adhesive proteins (Fn, Vn) and permit the subsequent adsorption of cell-derived ECM proteins or other serum proteins which promote cell spreading and growth onto, or after displacement of, the initially adsorbed protein layer (i.e., permit sufficient displacement of nonadhesive proteins (Alb)) would promote endothelial cell growth.

8.2 Materials and Methods

8.2.1 Preparation of Chemically Heterogeneous SAMs

Two binary SAM systems were prepared as described in Section 2.2: 1) a series of mixtures of $HS(CH_2)_{15}COOH$ and $HS(CH_2)_{15}CH_2OH$, and, 2) a series of mixtures of $HS(CH_2)_{15}COOH$ and $HS(CH_2)_{15}CH_3$. The solution composition/surface composition relationships determined from surface analysis studies (Chapter 5, Figures 5.1, 5.7, 5.8, and 5.13), were used to select the appropriate thiol solution ratio required to achieve the desired surface composition. The binary SAM surface compositions prepared for evaluation in protein interactions studies are listed in Table 8.1.

8.2.2 Surface Analysis of Chemically Heterogeneous SAMs

For each binary SAM series evaluated in protein interaction studies, 4 additional samples of each surface composition were evaluated to verify SAM surface composition. 2 of the 4 samples were characterized by ellipsometry and contact angle at Battelle PNL immediately following SAM formation. The remaining samples were analyzed by XPS and TOF-SIMS at the University of Washington (as described in Section 2.3 and Chapter 5) prior to performing the protein interaction studies. Binary SAM surface compositions for each series (data not presented) were verified by comparison with surface analysis results presented in Chapter 5 to ensure that the desired surface compositions had been achieved.

8.2.3 Protein Radiolabeling

The adsorption of three radiolabeled serum proteins was investigated in protein adsorption studies. ^{125}I labeled bovine fibronectin was purchased from ICN (see Section 2.6.1). Bovine albumin and bovine vitronectin were radiolabeled with ^{125}I using the

iodine monochloride method as described in Section 2.6. Radiolabeled protein solutions were stored at -70°C and used within 2 weeks of preparation. A small volume of the ^{125}I labeled protein solution was added to the bovine serum solution to obtain a specific activity of 10^7 cpm/mg for Fn and Vn, and 10^6 cpm/mg for Alb.

8.2.4 Protein Adsorption and SDS Elutability

The adsorption of ^{125}I labeled Alb, Fn, and Vn from 10% bovine serum solution to binary SAMs was evaluated as described in Section 2.7 using triplicate samples of the surface compositions listed in Table 8.1. The SDS elutability of Alb, Fn, and Vn adsorbed to the binary SAM surfaces was evaluated to determine the strength of protein-surface interactions. SDS elutability studies were conducted as described in Section 2.8 using triplicate samples of each surface composition. The percent elutability (the percent of adsorbed protein which is removed by SDS) for each protein as a function of adsorption time was determined.

8.3 Results and Discussion

8.3.1 Albumin, Fibronectin, and Vitronectin Adsorption to COOH/CH_3 SAMs: Effect of Surface Composition

The amounts of albumin, vitronectin, and fibronectin adsorbed from 10% serum to six COOH/CH_3 surfaces are shown in Figure 8.1. Albumin adsorption ranged from 42 ng/cm^2 on the 0% COOH surface to 14 ng/cm^2 on the 60% COOH surface. Albumin adsorption differed with COOH surface content. Albumin adsorption decreased as surface COOH content increased from 0% to 60% COOH, and increased for surface COOH contents above 60%.

Vitronectin adsorption to the SAM surfaces was lowest on the 0% COOH surface (18 ng/cm^2) and highest on the 40% COOH surface (38 ng/cm^2). Vitronectin adsorption increased between 0% COOH and 40% COOH, then decreased by 15% for the 60% COOH surface. Vitronectin adsorption did not differ significantly between 60% COOH and 100% COOH. In contrast, fibronectin adsorption to the SAM surfaces was significantly lower than albumin or vitronectin adsorption levels. Fibronectin adsorption ranged from 1.2 ng/cm^2 on the 0% COOH surface to 2.69 ng/cm^2 on the 80% COOH surface. Fibronectin adsorption was higher on the 80% COOH and 100% COOH SAMs than on SAMs containing 0-60% COOH.

Figure 8.1 highlights the dramatic differences in protein adsorption which occur when adsorption is conducted from a complex mixture such as 10% serum. It has been demonstrated that Fn adsorption is significantly decreased or completely blocked by other serum components such as Vn or Alb at serum concentrations greater than 1% [20,51,52,53]. The low levels of fibronectin adsorption measured in this study and in studies described in Chapter 3 and 4 are consistent with these findings.

The concentration ranges of Vn (0.2-0.4 mg/ml) and Fn (0.2-0.6 mg/ml) in serum are approximately equivalent [101-103] yet, significant differences in the relative amounts of adsorption are observed for the two proteins. The extent of Fn adsorption has been shown to depend on the plasma or serum concentration from which it is adsorbed (the Vroman effect) with maximum adsorption occurring at low plasma or serum concentrations [103]. Vn adsorption does not exhibit a Vroman peak and increases with increasing plasma concentration therefore, Vn adsorption to surfaces at serum concentrations greater than 1% is typically higher than Fn adsorption [20, 21, 58, 104].

On average, the ratio of vitronectin to fibronectin adsorbed to the SAM surfaces as shown in Figure 8.1 was 20:1. These results are consistent with a similar evaluation

of Vn and Fn adsorption to TCPS which demonstrated a 28-fold increase in adsorbed Vn compared with adsorbed Fn [20]. These findings suggest that while the serum concentrations of Fn and Vn are equivalent, the competitive effectiveness of Vn for adsorption to the SAM substrates is significantly higher than that of Fn. Similarly, the concentrations of Alb and Vn in serum differ significantly (40 mg/ml for Alb and 0.2-0.4 mg/ml for Vn), yet Alb adsorption to the $COOH/CH_3$ SAMs was slightly lower than or equal to Vn adsorption. Since serum contains a 100-fold excess of Alb compared with Vn, the results shown in Figure 8.1 indicate that the competitive effectiveness of Alb for adsorption to the SAM substrates is significantly lower than that of Vn. Fabrizius-Homan et al. investigated the competitive effectiveness of Vn against Alb, Fn, and fibrinogen from binary mixtures and similarly observed that Alb and Fn were far less effective in inhibiting Vn adsorption [62].

To evaluate the effect of surface composition on the relative differences in the adsorption levels of each protein, the surface fraction of each protein relative to the total amount of protein adsorbed on a surface was determined. Figure 8.2 shows the fractional amount of each protein in the adsorbed layer calculated as a ratio of the amount of protein in the adsorbed phase to the total adsorption of the three proteins. In this way, the composition of the adsorbed protein layer can be evaluated and the relative affinity of each protein as a function of surface composition can be determined.

The surface fraction of each protein as a function of surface composition is shown in Figure 8.2. Figure 8.3 shows the relationship between surface composition and albumin surface fraction. Figure 8.4 shows the surface fraction of Vn and Fn combined as a function of surface composition. The surface fraction of Vn and Fn represents the total surface fraction of the adhesive proteins and was calculated as the ratio of the amounts of Fn and Vn in the adsorbed phase to the total adsorption of the three

proteins. Figure 8.5 is identical to Figure 8.4 however, the contribution of each protein to the combined adhesive protein surface fraction is illustrated.

Albumin surface fraction ranged from 69% on the 0% COOH surface to 31% on the 60% COOH surface (Figure 8.3). Alb surface fraction decreased between 0-60% COOH and increased from 60-100% COOH. The combined Vn and Fn surface fraction was highest on the 60% COOH surface (70%) and lowest on the 0% COOH surface (30%). The combined surface fraction increased from 0-60% COOH and decreased for 80% and 100% COOH surfaces.

These results indicate that the affinity of Fn and Vn for the COOH/CH_3 SAM surfaces is affected by COOH surface composition. The 0% COOH (100% CH_3) surface has a higher affinity for albumin relative to the other proteins than any of the SAM surfaces. The adsorbed protein layer on this surface predominantly consists of Alb. For the 20-80% COOH SAMs, the adsorbed protein layers are predominantly Vn with a smaller fraction of Fn. The adhesive protein (Vn and Fn) surface fraction increases slightly from 20% to 40% COOH (2%) and increases significantly from 40% to 60% surface COOH (13%). The adhesive protein surface fraction is 8% lower on the 80% COOH surface than on the 60% COOH surface. The 100% COOH surface shows an equal surface fraction of Alb and adhesive proteins.

These results show that surface composition, specifically functional group content, clearly affects the adsorption of serum proteins and more importantly, that the relative affinity of the 3 serum proteins is significantly influenced by surface COOH content. These differences in relative protein affinity result in significant differences in adsorbed protein layer composition which are dependent upon SAM surface composition.

8.3.2 *Albumin, Fibronectin, and Vitronectin Adsorption to COOH/OH SAMs: Effect of Surface Composition*

The amounts of Alb, Fn, and Vn adsorbed from 10% serum to six COOH/OH surfaces are illustrated in Figure 8.6, Alb adsorption ranged from 20 ng/cm^2 on the 50% COOH surface to 39 ng/cm^2 on the 0% COOH surface. Alb adsorption decreased with increasing COOH content between 0% and 50% COOH and increased for surface COOH contents above 50%. Alb adsorption on the COOH/OH SAMs was similar to that measured on the COOH/CH_3 SAMs.

Vn adsorption to the COOH/OH SAMs ranged from 15 ng/cm^2 on the 0% COOH surface to 30 ng/cm^2 on the 100% COOH surface. Vn adsorption increased significantly between 0% and 20% COOH and did not vary significantly between 20-70% COOH. In general, Vn adsorption on the COOH/OH SAMs was approximately 25% lower than on the COOH/CH_3 SAMs for surfaces of an equivalent surface COOH content. It is possible that the presence of the hydrophobic methyl component in the COOH/CH_3 SAMs results in the increased Vn adsorption since hydrophobic surfaces typically demonstrate increased levels of protein adsorption relative to hydrophilic surface [31,105,106,107]. The COOH/OH and COOH/CH_3 SAMs also differ in surface functional group spatial arrangement (Chapter 5). The clustered arrangement of the COOH/CH_3 SAMs which results in domains of hydrophobic methyl groups may promote Vn adsorption relative to the randomly mixed arrangement of groups on the COOH/OH surface.

Fn adsorption to the COOH/OH surfaces was significantly lower than Alb or Vn adsorption. Fn adsorption levels ranged from 0.8 ng/cm^2 on the 100% OH surface to 3.7 ng/cm^2 on the 50% COOH surface. Fn adsorption was higher on the 50-100%

COOH surfaces than on the 0-40% COOH surfaces. Fn adsorption on the COOH/OH SAMs was very similar to the Fn adsorption patterns seen on the COOH/CH_3 SAMs.

As observed for the COOH/CH_3 SAMs, significant differences in the relative amounts of Fn, Alb, and Vn adsorbed are obtained. On average, the ratio of Vn to Fn adsorbed was 15:1 demonstrating the increased competitive effectiveness of Vn relative to Fn. The levels of Alb and Vn adsorbed to COOH/OH SAMs were approximately equivalent. As discussed in section 8.3.1, serum levels of Alb are 100-fold that of Vn thus these results confirm the decreased competitive effectiveness of Alb relative to Vn for adsorption onto COOH/OH SAMs.

Figure 8.7 illustrates the surface fraction of Alb, Fn, and Vn as a function of surface COOH content. Figure 8.8 shows the relationship between Alb surface fraction and surface composition while Figures 8.9 and 8.10 illustrate the surface fraction of adhesive protein (Fn and Vn) as a function of surface composition.

Alb surface fraction ranged from 71% on the 0% COOH surface to 42% on the 50% COOH surface (Figure 8.8). A decrease in Alb surface fraction was observed between 0-50% COOH. Alb surface fraction was slightly higher on the 70% and 100% COOH surfaces than on the 50% COOH surface. The adhesive protein surface fraction was lowest on the 0% COOH surface (28%) and highest on the 50% surface (58%). Adhesive protein surface fraction increase between and 50% COOH and decreased from the 70% and 100% COOH surfaces (Figure 8.9). Figure 8.10 details the contribution of Fn to the adhesive protein surface fraction. The low levels of Fn adsorption result in a small contribution of Fn to the adhesive protein surface fraction. However, the 50-100% COOH surfaces show a higher surface fraction of Fn than do the 0-40% COOH surfaces and Fn surface fraction is highest on the 50% COOH surface.

The protein layer on the 0% COOH (100% OH) surface consists predominantly of Alb. The 20-100% COOH surfaces have protein layers comprised of 47-57% Vn and Fn. Adhesive protein surface fraction increases gradually from 49% to 58% for the 20%-50% COOH SAMs and is highest on the 50% COOH surface. The 70% and 100% COOH surfaces resulted in adsorbed protein layers with a 50% Alb/50% adhesive protein content. As shown in section 8.3.1 for $COOH/CH_3$ SAMs, Figure 8.6-8.10 demonstrate that SAM surface composition, specifically surface COOH content, affects protein adsorption resulting in adsorbed protein layers which differ significantly in composition. Differences in adsorbed protein layer composition are due to the differences in relative affinity of Vn, Alb, and Fn for the COOH/OH SAMs in response to variations in SAM surface composition.

8.3.3 Albumin, Fibronectin, and Vitronectin Elutability from $COOH/CH_3$ SAMs: Effect of Surface Composition

The retention of Alb, Fn, and Vn after elution by SDS for 24 hours was measured for the 6 $COOH/CH_3$ surfaces evaluated in protein adsorption studies. The amount of protein retained by each surface is shown in Figure 8.11 as a function of surface COOH content. All surfaces retained higher levels of Alb than of Vn or Fn after SDS elution. Alb retention values ranged from 18 ng/cm^2 on the 40% COOH surface to 5 ng/cm^2 on the 100% COOH surface. Alb retention differed with surface composition however, the relationship between the amount of Alb retained and surface composition was not consistent.

The amounts of Vn retained after SDS elution were significantly lower than Alb retention levels. Vn retention values were highest on the 0% COOH surface (8 ng/cm^2) and lowest on the 60% COOH surface (2.5 ng/cm^2). The amount of Vn retained

decreased as surface COOH content increased from 0% to 60% and remained constant as surface COOH content increased from 60% to 100%. The amounts of Fn retained were very low, ranging from 0.2-1.6 ng/cm^2. Fn levels were lowest on the 0% COOH surface (0.2 ng/cm^2) and were essentially equivalent for the 20-100% COOH SAMs (~1.1 ng/cm^2).

The percent elutability (the percent of adsorbed protein which is removed by SDS) for each protein was determined and is shown in Figures 8.12, 8.13, and 8.14. Alb elutability was highest on the 100% COOH surface (81%) and lowest on the 40% COOH surface (45%). Alb elutability did not vary consistently with surface COOH content. Elutability was approximately 60% on the 0% and 20% COOH surfaces and decreased to a 40% level for the 40-80% COOH surfaces. A significantly higher Alb elutability was obtained for the 100% COOH surface.

Fn elutability similarly did not vary consistently with surface COOH content (Figure 8.13). The highest level of Fn elutability was obtained on the 0% COOH surface (81%). Fn elutability was approximately 40% (range of 35-45%) for the 20-80% COOH SAMs and increased to 65% for the 100% COOH surface. The standard deviation of the Fn elutability values was relatively large due to the low levels of protein being measured.

The elutability of Vn from the COOH/CH_3 surfaces is shown in Figure 8.14. Figure 8.14 shows the Vn elution values on a scale ranging from 50-100% to better illustrate the differences observed. Vn elutability was lowest on the 0% COOH surface (55%). Elutability values for the 20-100% surfaces were significantly higher and ranged from a low of 87.5% (20% COOH) to a high of 92.3% (60% COOH surface). Vn elutability increased as surface COOH content increased from 20% to 60% COOH. Elutability decreased slightly from 60-100% COOH.

8.3.4 Albumin, Fibronectin, and Vitronectin Elutability from COOH/OH SAMs: Effect of Surface Composition

The retention of Alb, Fn, and Vn after elution by SDS for 24 hours was measured for the 6 COOH/OH SAMs. The amount of protein retained by each surface is shown in Figure 8.15 as a function of surface COOH content. All surfaces retained higher levels of Alb than of Vn or Fn after SDS elution. Alb retention values ranged from 22 ng/cm^2 on the 0% COOH surface to 5 ng/cm^2 on the 100% COOH surface. While differences in the amount of Alb retained were observed in response to variations in surface composition, the relationship between the amount of Alb retained and surface composition was not consistent.

Vn retention levels were significantly lower than Alb retention levels. The amounts of Vn retained ranged from 5.8 ng/cm^2 on the 0% OH surface to 2.2 ng/cm^2 on the 50% COOH surface. The amounts of Vn retained decreased gradually from 0% to 50% surface COOH and remained constant for COOH contents above 50%. The amounts of Fn retained were low and ranged from 0.3 on the 0% COOH surface to 2.8 ng/cm^2 on the 50% COOH surface. Equivalent levels of Fn (~1 ng/cm^2) were retained on the 20%, 40%, 70%, and 100% COOH SAMs.

The elutability of Alb, Fn, and Vn are shown in Figures 8.16, 8.17, and 8.18, respectively. Alb elutability was lowest on the 0% COOH (100% OH) surface and highest on the 100% COOH surface. Equivalent Alb elutabilities were obtained for the 20% and 70% COOH surfaces (~62%). As observed for the COOH/CH_3 SAMs, Alb elutability did not vary consistently with surface COOH content. Fn elutability also did not vary consistently with surface COOH content (Figure 8.17). Fn elutability was highest on the 0% COOH surface (65%) and slightly lower on the 40% and 100% COOH surfaces. Fn elutability was lowest on the 50% COOH surface (25%).

The elutability of Vn from the COOH/OH SAMs is shown in Figure 8.18. Vn elutability was lowest on the 0% COOH surface (62%). Fn elutabilities for the 20-100% surfaces were significantly higher than the 0% COOH surface. Fn elutability increased between 20% and 50% COOH and ranged from 83.1% (20% COOH) to 91.2% (50% COOH surface). Vn elutability remained essentially constant from 50-100% COOH.

8.3.5 Relating Protein Adsorption and Elutability on Homogeneous Composition SAMs to Cell Growth

To evaluate relationships between adsorbed protein layer composition and cell growth, it is useful to first compare the adsorbed protein layer compositions of the homogeneous SAMs; the 100% OH, 100% COOH and 100% CH_3 SAMs. Since these three surfaces exhibited significant differences in cell growth characteristics, we can begin a search for relationships by comparing the adsorbed protein layer characteristics of the growth-promoting 100% COOH SAM with those of the growth-inhibiting 100% OH and 100% CH_3 SAMs.

Figure 8.19 shows the surface fraction of Alb and the surface fraction of the adhesive proteins (Fn and Vn) adsorbed to the homogenous SAMs. The poor growth surfaces, 100% OH and 100% CH_3, demonstrate a significantly higher surface fraction of Alb (~70%) and a lower surface fraction of adhesive proteins (~30%) than does the 100% COOH surface (51% Fn and Vn, 49% Alb). The COOH surface shows a slightly higher surface fraction of adhesive proteins than Alb. Since cell attachment, spreading, and growth are dependent upon cellular interactions with adsorbed adhesive proteins, Figure 8.19 suggests that one factor which contributes to the growth-promoting ability of the COOH surface is a sufficient surface fraction of adhesive proteins relative to the surface fraction of nonadhesive protein.

Another characteristic of the adsorbed protein layer which will influence cell growth are the binding strengths of the various adsorbed proteins. Variations in protein binding strength can affect the ability of a cell to interact with an adsorbed adhesive protein or the ability of an adsorbed protein to be displaced by other serum proteins. Figure 8.20 illustrates the elutability of Alb, Fn, and Vn from the homogeneous SAM surfaces. The elutabilities of these three proteins can be compared for the growth promoting surface (COOH) and the growth-inhibiting surfaces (CH_3 and OH). Alb elutability was lowest on the OH surface, higher on the CH_3 surface, and significantly higher on the COOH surface. Vn elutability was low on the OH and CH_3 surfaces and significantly higher on the COOH surface. Fn elutability was highest on the CH_3 surface and equivalent on the COOH and OH surfaces.

These results suggest that Fn elutability does not correlate with cell growth promotion or inhibition. Alb and Vn elutability however, appear to correlate with cell growth on the homogeneous surfaces as both growth inhibiting surfaces demonstrated lower Alb and Vn elutabilities than did the growth promoting COOH surface. As discussed in Chapter 3, a surface which allows Alb displaceability may permit the deposition of other adhesive proteins or cell-derived proteins which promote cell growth. The observation that Fn elutability does not appear to influence cell growth is not unexpected considered the extremely low levels of Fn which adsorb from 10% serum. The observation of higher Vn elutablity on the cell growth promoting surface is an interesting, unexpected finding as is discussed in section 8.3.6.

In summary, for the homogeneous SAMs, three factors were identified which appear to be associated with the promotion or inhibition of cell growth: 1) the surface fraction of adsorbed adhesive protein, 2) the elutability of Vn, and 3) the elutability of Alb.

8.3.6 Relating Protein Adsorption and Elutability on Binary Composition SAMs to Cell Growth

To investigate relationships between cell growth and adsorbed protein layer characteristics for the binary composition SAMs, we can compare trends observed in cell growth (Chapter 6) with trends observed during protein adsorption and elutability studies (Chapter 8), specifically for the factors associated with cell growth for the homogeneous SAMs. Briefly, the trends observed in cell growth studies were as follows. For the $COOH/CH_3$ SAMs, cell growth increased between 0-60% COOH and then decreased slightly from 60-100% COOH (Figure 6.5 and 6.6). For the COOH/OH SAMs, cell growth similarly increased from 0-50% COOH and decreased slightly from 50-100% COOH (Figure 6.13 and 6.14).

Figures 8.4 and 8.9 demonstrate trends in the surface fraction of adhesive protein which are similar to the trends observed for cell growth. Figures 8.14 and 8.18 also demonstrate trends in Vn elutability which are similar to the trends observed in cell growth for both binary SAM series. The trends in Alb elutability (Figures 8.12 and 8.16) however, are not consistent with the trends observed in cell growth for the binary SAMs. For the binary composition SAMs, Alb elutability does not vary consistently with surface composition and does not show a consistent relationship to cell growth. For example, cell growth on the 60% and 80% COOH surfaces in the $COOH/CH_3$ series was equivalent to cell growth on the 100% COOH surface yet the Alb elutabilities on the 60% and 80% COOH SAMs were ~40% while the Alb elutability on the 100% COOH surface was 80% (Figure 8.12). Alb elutabilities on the COOH/OH surface (Figure 8.16) also are not consistent with cell growth trends. It appears that Alb elutability, while an important factor which correlates with cell growth on homogeneous SAMs, does not have a similar correlation for the binary composition SAMs. In summary, for

the binary composition SAMs, two factors were identified which appear to be associated cell growth: 1) the surface fraction of adsorbed adhesive protein and 2) the elutability of Vn.

If we consider the binary composition SAMs separately from the homogeneous composition SAMs, cell growth trends can be specifically compared with trends in adhesive protein surface fraction and Vn elutability as a function of surface composition. Figure 8.21 illustrates the surface fraction of adhesive protein and normalized cell number (relative to TCPS) after 1 and 3 day culture periods for the $COOH/CH_3$ binary SAMs ranging from 20-80% surface fraction of COOH. Figure 8.22 illustrates the relationship between Vn elutablity and normalized cell number as a function of surface COOH content. Both the surface fraction of adhesive protein and the Vn elutability demonstrated trends similar to the 1 day and 3 day cell growth trends. The surface fraction of adhesive protein increased between 20% and 60% COOH and decreased between 60% and 80% COOH. Similarly, Vn elutability increased from 20-60% COOH and decreases slightly from 60-80% COOH.

To evaluate if correlations exist between adsorbed protein layer properties and cell number, the adsorbed protein layer property (surface fraction of adhesive protein or Vn elutability) can be plotted as a function of normalized cell number. The strength and direction of a correlation between cell growth and the adsorbed protein layer property can be evaluated by the correlation coefficient (r). In general, the strength of correlation between two variables is defined as follows: strong correlation = $r \geq 0.8$; moderate correlation = $0.5 < r < 0.8$; and weak correlation = $r \leq 0.5$.

Figures 8.23 and 8.24 illustrate the relationships between adhesive protein surface fraction and normalized cell number for 1 and 3 day culture periods respectively. The correlation coefficient (r) determined for the relationship is noted on each figure.

For the $COOH/CH_3$ SAMs (20-80% COOH), strong correlations are observed between adhesive protein surface fraction and normalized cell number (0.91 and 0.88).

Figures 8.25 and 8.26 show relationships between Vn elutablity and normalized cell number for the $COOH/CH_3$ SAMs after 1 and 3 day culture periods respectively. Vn elutability was strongly correlated with normalized cell number after 1 day of culture (0.95) and also after 3 days of culture (0.97). These results suggest a direct relationship between adhesive protein surface fraction and cell growth and also between Vn elutability and cell growth for $COOH/CH_3$ SAMs ranging in surface COOH content from 20-80%.

For the COOH/OH SAMs, we can similarly evaluate correlations between adsorbed protein layer properties and cell growth. Figures 8.27 shows the surface fraction of adsorbed adhesive protein and normalized cell number for COOH/OH SAMs ranging in surface COOH content from 20-70% COOH. The adhesive protein surface fraction increases as does cell number, from 20-50% COOH. However, between 50% and 70% COOH, the adhesive protein surface fraction decreases significantly while cell growth decreases only slightly. Figure 8.28 illustrates the Vn elutability and normalized cell number for the 20-70% COOH/OH SAMs. Vn elutability increases similar to increases in cell number between 20-50% COOH. Between 50% and 70% COOH, cell number decreases slightly while Vn elutability remains essentially constant.

The relationships between adhesive protein surface fraction and normalized cell number are shown in Figures 8.29 and 8.30. The correlations between adhesive protein surface fraction and cell number after 1 day and 3 days are moderate (0.64 and 0.52 respectively). The decreased strength of correlation is due primarily to the lower adhesive protein surface fraction measured on the 70% COOH/OH surface. If the correlation is evaluated for 20-50% COOH surface compositions only, correlations

between cell number and adhesive protein surface fraction increase significantly (0.88 for 1 day and 0.94 3 day cell number, data not shown).

Figures 8.31 and 8.32 illustrate the relationships between Vn elutability and normalized cell number for the 20-70% COOH/OH SAMs. Vn elutability was strongly correlated with cell number after 1 day of culture (0.81) and after 3 days of culture (0.94). These correlations are similar to correlations determined for the COOH/CH_3 SAMs and demonstrates a direct relationship between cell growth and elutability of Vn for COOH/OH SAMs between 20-70% COOH.

The influence of the adsorbed protein layer on cellular interactions has been well documented [14,19,20,58]. Protein adsorption occurs instantaneously with a 2-5 nm layer of protein adsorbing to a substrate surface after approximately one minute of exposure to biological media. Cells in suspension will gravitate to within 5-8 nm of the substrate in approximately 5 minutes [85]. Cellular attachment and spreading is a time-dependent process during which there are cellular interactions with the adsorbed proteins which involve cell membrane receptor interactions with the various adsorbed adhesive proteins. Human endothelial cell attachment has been reported to begin approximately 30 minutes after seeding and with full spreading (polygonal morphology) observed 2 hours after seeding [108].

In order for cell adhesion, spreading, and proliferation to occur, adequate quantities of adhesive proteins are required. As discussed in Section 1.5, Vn is the key adhesive protein mediating cell attachment and growth on oxygen-containing surfaces and has been demonstrated to have a significant effect on cell attachment and growth. The majority of cell attachment activity in cell culture media containing bovine or human serum is due to the enhanced adsorption and activity of serum Vn [21, 100,109]. It has also been demonstrated that certain anchorage-dependent cell lines attach and grow on

culture dishes only when Vn is present in the cell culture medium suggesting that Vn may affect cell growth in other ways in addition to the direct promotion of cell attachment [99,104,109,110,111]. Fn is also an adhesive protein which is involved in the attachment and growth of endothelial cells however, the low levels of Fn adsorption which occur at 10% serum result in a minor role for Fn in the promotion of cell growth.

In our protein adsorption studies, a strong correlation was observed between adhesive protein surface fraction and cell growth for the COOH/CH_3 SAMs, and a moderate correlation was observed between adhesive protein surface fraction and cell growth for the COOH/OH SAMs. Since the adhesive protein surface fraction resulted primarily from the contribution of adsorbed Vn, our results are consistent with previous studies which demonstrate the significance of Vn in the promotion of cell attachment and growth. Our results further document a direct relationship between cell growth and adhesive protein surface fraction. Vn is clearly the key adhesive protein mediating cell growth and Fn plays a minor, relatively insignificant role however, there is a contribution of Fn to the adhesive protein surface fraction and consequently to the promotion of cell growth.

Vn most likely contributes to the promotion of cell growth via direct interactions with endothelial cell membrane receptions however, adsorbed Vn may influence cell interactions in another way. In culture, bovine aortic endothelial cells produce an endogenous ECM containing Fn, laminin, types III, IV, V, and VI collagen, and proteoglycans [112-114]. The ECM produced by cells *in vivo* is an important mediator of endothelial cell functions including cell adhesion, spreading, migration, and proliferation [115]. The ability of cells to readily proliferate and express their normal phenotype in culture has been reported to be dependent upon their ability to produce and assemble an ECM [116]. Horbett has proposed that initial cell attachment and spreading

events occur in response to the initially adsorbed protein layer, while longer term spreading events are related to cellular modification of the surface [39]. The types and quantities of cell-secreted ECM molecules are dependent upon the composition of the adsorbed protein layer as influenced by substrate properties [86, 117]. Vn has been demonstrated to effect ECM secretion as different mixtures of endogenously secreted molecules are observed on substrates adsorbing different levels of Vn [86, 115]. In a study of ECM production, Underwood et al. observed that on Vn coated substrates, relatively high amounts of ECM were produced in early cell passages [115].

Considering the observation of an association between cell growth and the surface fraction of adhesive protein on binary SAM surfaces, our results may suggest that binary SAMs surfaces with higher levels of adsorbed Vn possibly promote cell growth by influencing the secretion of cell-derived ECM proteins. Conversely, SAM surfaces exhibiting lower surface fractions of adsorbed Vn may cause insufficient levels of ECM secretion which may result in the failure of cell proliferation to progress.

For both the $COOH/CH_3$ and the COOH/OH SAMs, strong correlations were obtained between Vn elutability and cell growth. The observation of higher Vn elutablity on the cell growth promoting surfaces is an interesting, unexpected finding. Since Vn is the primary adhesive protein reported to affect cell attachment, spreading and growth, its influence on cell growth is not unexpected. However, the fact that cell growth appears to be associated with an increase in Vn elutability is interesting. Several hypotheses are possible to explain this finding.

As discussed in Chapter 3, the removal or elution of adsorbed proteins by SDS was developed as a technique for examining the strength of protein-surface interactions. Adsorbed protein resistance to SDS solubilization is indicative of protein binding strength and differences in SDS elutability have been demonstrated to reflect changes in

the protein structure or the protein-polymer interaction strength [117,118]. Factors which can affect protein binding strength include protein-surface interaction strength and/or adsorbed protein conformation. Tight binding of a protein to a surface may suggest that conformational changes have occurred in the protein which would affect the ability of an adhesive protein to interact with cells via the cell-binding domain.

For Vn, the RGD sequence has been shown to mediate binding of Vn to the Vn receptor present on endothelial cells [119]. The conformation of different domains of Vn, including the cell-binding domain, responds individually to different physical and chemical stimuli. The adsorption or binding of Vn to a surface is one factor which can induce a conformational change in Vn from a folded state, to an extended form which exposes a heparin binding site, and additional sites which are cryptic in the folded molecule [109,120,121]. Studies suggest that the extended form of Vn is the preferential conformational state of the molecule present in association with the extracellular matrix [122].

Conformational changes which occur upon surface adsorption of adhesive proteins such as Fn and Vn are important factors which can influence the effectiveness of a surface for supporting cell adhesion and growth. In an investigation of the effect of surface chemistry on the biological activity of adsorbed proteins, Underwood et al. probed the conformational status of surface adsorbed Fn and Vn, specifically the conformational integrity of the Fn and Vn cell adhesion domains using monoclonal antibodies [123]. Significant differences were observed in the conformational status of Fn and Vn adsorbed on different brands of TCPS which was concluded to reflect the differences in the ability of the TCPS surfaces to support optimal growth of different cell types.

Considering the results of our studies in light of the results reported by Underwood et al. it is possible that the increased Vn elutability values measured on the growth-promoting binary SAM surfaces reflects the fact that the Vn bound to these surfaces is adsorbed in a conformation which facilitates interaction of endothelial cell membrane receptors with the adsorbed Vn. Vn adsorbed to binary SAM surfaces which do not promote cell growth is harder to elute from the surface possibly reflecting conformational changes occurring in Vn adsorbed to these surfaces. Vn bound to such surfaces may be adsorbed in a conformation which yields the endothelial cell binding domain unavailable for interaction with the endothelial cells. The Vn endothelial binding site appears to be available or accessible for cellular interactions on the SAM surfaces demonstrating higher Vn elutability than on surfaces with lower Vn elutability. SAM surfaces which do not promote cell growth may induce further conformational changes to the adsorbed Vn or adsorb the Vn in a conformation which renders the cell binding domain inaccessible.

8.4 Conclusions

In this chapter, the effects of binary SAM surface composition on the adsorbed protein layer and the influence of the adsorbed protein layer on endothelial cell growth was investigated. It was hypothesized that surfaces which demonstrate an increased affinity for adhesive proteins (Fn and Vn) and permit the subsequent adsorption of cell-derived ECM protein or other serum proteins promoting cell growth onto, or after displacement of the initially adsorbed protein layer would promote endothelial cell growth.

Two binary SAM series were investigated in protein interaction studies; a series of mixtures of $HS(CH_2)_{15}COOH$ and $HS(CH_2)_{15}CH_2OH$, and a series of mixtures of

$HS(CH_2)_{15}COOH$ and $HS(CH_2)_{15}CH_3$. The adsorption of three serum proteins, albumin, fibronectin, and vitronectin from 10% bovine serum-containing media was measured to determine the surface composition of the adsorbed protein layer. The SDS elutability of each protein was measured to indirectly assess protein-substrate binding strength.

The composition of protein layers adsorbed to the binary SAM substrates differed significantly in response to SAM surface composition. In general, Fn adsorption to the binary SAMs was very low (~1-3 ng/cm^2). The levels of Alb and Vn adsorbed to the binary SAMs were significantly higher than Fn and were approximately equivalent (~15-40 ng/cm^2). Differences in adsorbed protein layer composition were due to differences in the relative affinity of Vn, Alb, and Fn for the binary SAM surfaces in response to variations in SAM surface composition.

The elutability of Alb, Fn, and Vn adsorbed to binary SAMs was measured after exposure to SDS. The elutability of Alb and Fn did not vary consistently with surface COOH content. Vn elutability on the COOH/CH_3 and COOH/OH SAMs increased gradually as surface COOH content increased from 20-50% COOH (COOH/OH SAMs) or 20-60% (COOH/CH_3 SAMs), and then leveled off or decreased slightly for higher surface COOH contents.

Results of cell interactions studies described in Chapter 6 were compared with results obtained in protein adsorption studies to investigate relationships between cell growth and adsorbed protein layer characteristics. For the homogeneous SAMs (OH, COOH, and CH_3), three factors were identified which were associated with the promotion of cell growth; the surface fraction of adsorbed adhesive protein (vitronectin and fibronectin), the elutability of Vn, and the elutability of Alb. The 100% COOH

surface demonstrated a significantly higher adhesive protein surface fraction and higher Alb and Vn elutabilities than did the 100% OH or the 100% CH_3 surfaces.

The trends observed in cell growth studies were compared with trends observed in protein adsorption and elutability studies to investigate relationships between cell growth and adsorbed protein layer characteristics for the binary composition SAMs. Both the surface fraction of adhesive protein and Vn elutability demonstrated similar trends as a function of surface COOH content as did cell growth. The trends in Alb elutability however, were not consistent with trends observed in cell growth for the binary composition SAMs.

The relationships between adhesive protein surface fraction and normalized cell number for 1 and 3 day culture periods were evaluated and the strength of correlation was determined. For the COOH/CH_3 SAMs (20-80% COOH), strong correlations were determined between adhesive protein surface fraction normalized cell number. Similarly, strong correlations were obtained between Vn elutability and cell number. For the COOH/OH SAMs, a moderate correlation was determined between adhesive protein surface fraction and cell number. However, a strong correlation was obtained between Vn elutability and cell number. These results suggest that cell growth on binary composition, chemically heterogeneous SAMs is affected by the surface fraction of adhesive protein and the elutability of adsorbed Vn. In general, surfaces promoting endothelial cell growth demonstrated a higher surface fraction of adhesive proteins (vitronectin and fibronectin) and a higher Vn elutability than did surfaces which poorly supported cell growth.

Table 8.1

Surface Composition of Binary SAMs Evaluated in Protein Interaction Studies

Thiol A	*Thiol B*	*Surface Fraction Thiol A*	*Surface Fraction Thiol B*
$HS(CH_2)_{15}COOH$	$HS(CH_2)_{15}CH_3$	0%	100%
$HS(CH_2)_{15}COOH$	$HS(CH_2)_{15}CH_3$	20%	80%
$HS(CH_2)_{15}COOH$	$HS(CH_2)_{15}CH_3$	40%	60%
$HS(CH_2)_{15}COOH$	$HS(CH_2)_{15}CH_3$	60%	40%
$HS(CH_2)_{15}COOH$	$HS(CH_2)_{15}CH_3$	80%	20%
$HS(CH_2)_{15}COOH$	$HS(CH_2)_{15}CH_3$	100%	0%
$HS(CH_2)_{15}COOH$	$HS(CH_2)_{15}CH_2OH$	0%	100%
$HS(CH_2)_{15}COOH$	$HS(CH_2)_{15}CH_2OH$	20%	80%
$HS(CH_2)_{15}COOH$	$HS(CH_2)_{15}CH_2OH$	40%	60%
$HS(CH_2)_{15}COOH$	$HS(CH_2)_{15}CH_2OH$	50%	50%
$HS(CH_2)_{15}COOH$	$HS(CH_2)_{15}CH_2OH$	70%	30%
$HS(CH_2)_{15}COOH$	$HS(CH_2)_{15}CH_2OH$	100%	0%

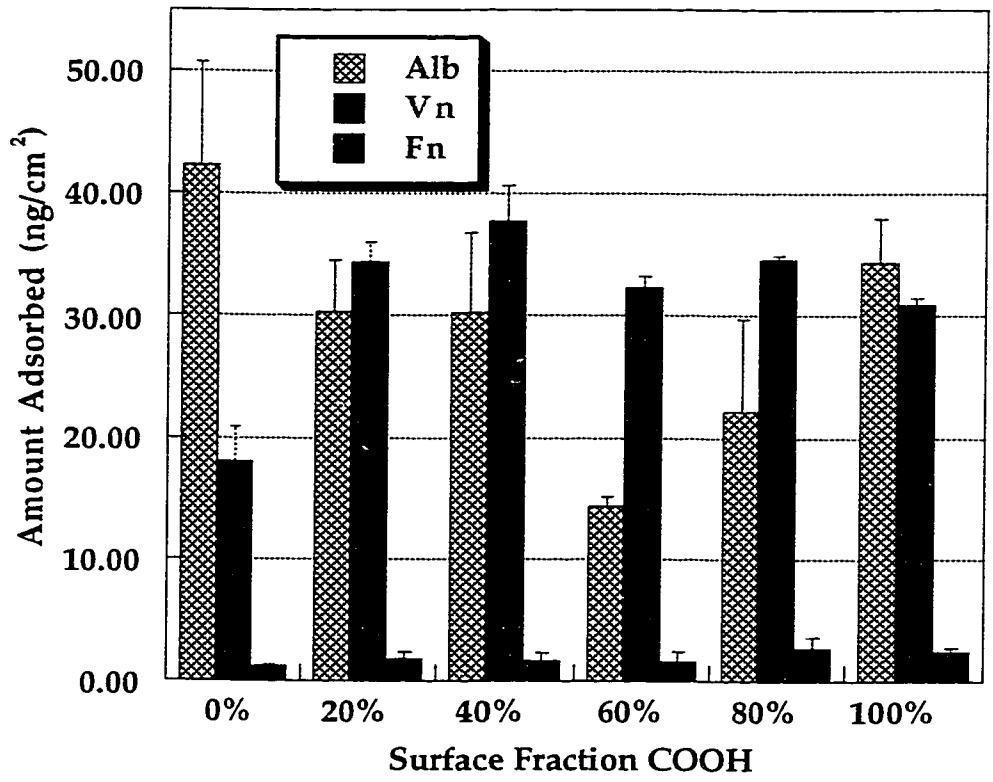

Figure 8.1 Effect of surface COOH content on Alb, Fn, and Vn adsorption to binary composition SAMs of $HS(CH_2)_{15}COOH$ and $HS(CH_2)_{15}CH_3$. Alb, Vn, and Fn were adsorbed from 10% bovine serum for 2 hours at 37°C. Data represent mean ± standard deviation for triplicate samples.

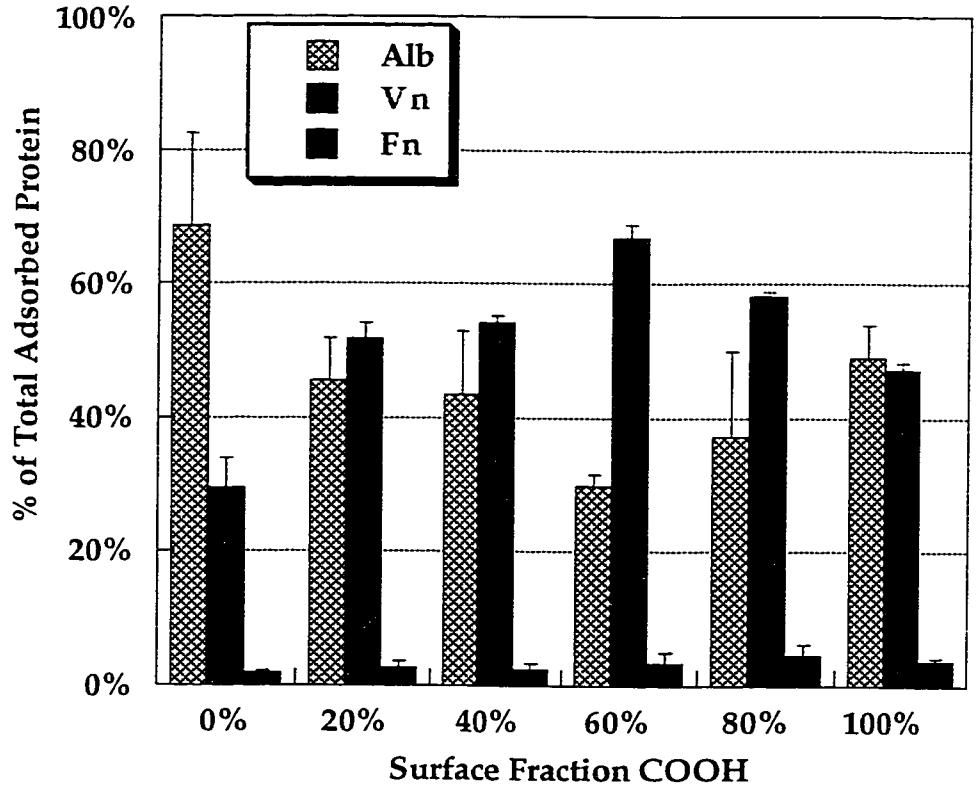

Figure 8.2 Surface fraction of Alb, Fn, and Vn in adsorbed protein layers on binary composition SAMs of $HS(CH_2)_{15}COOH$ and $HS(CH_2)_{15}CH_3$. Alb, Vn, and Fn were adsorbed from 10% bovine serum for 2 hours at 37°C. The fractional amount of each protein in the adsorbed layer was calculated as the ratio of the amount of protein in the adsorbed phase to the total adsorption of the three proteins. Data represent mean ± standard deviation for triplicate samples.

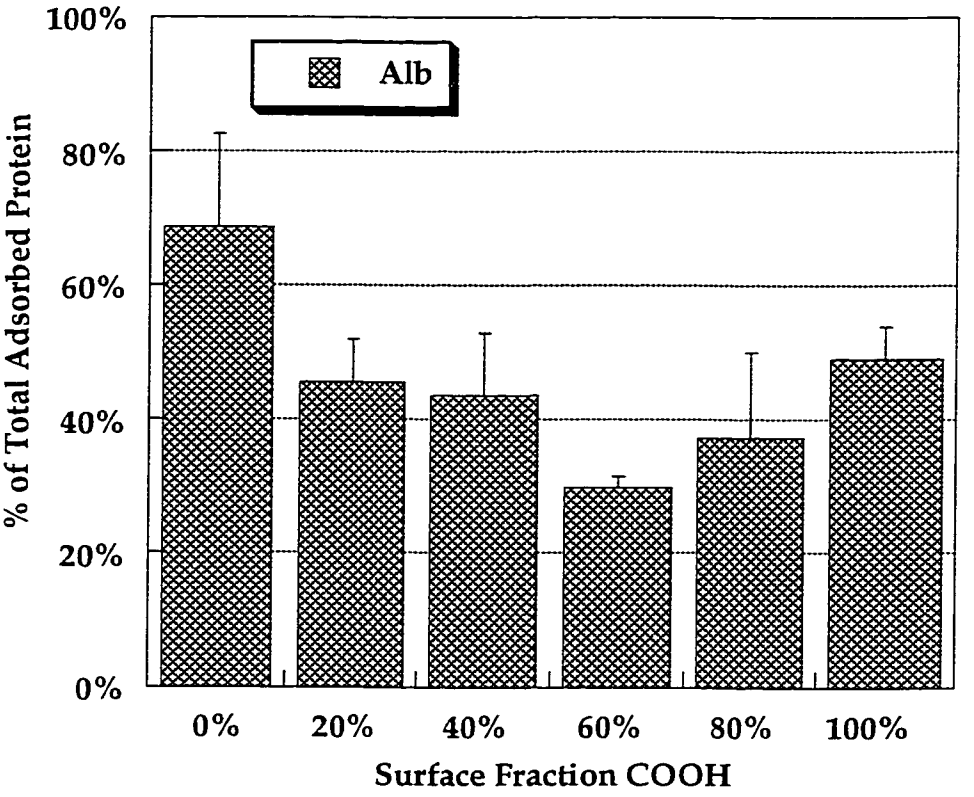

Figure 8.3 Surface fraction of albumin in adsorbed protein layers on binary composition SAMs of $HS(CH_2)_{15}COOH$ and $HS(CH_2)_{15}CH_3$. Alb was adsorbed from 10% bovine serum for 2 hours at 37°C. Data represent mean ± standard deviation for triplicate samples.

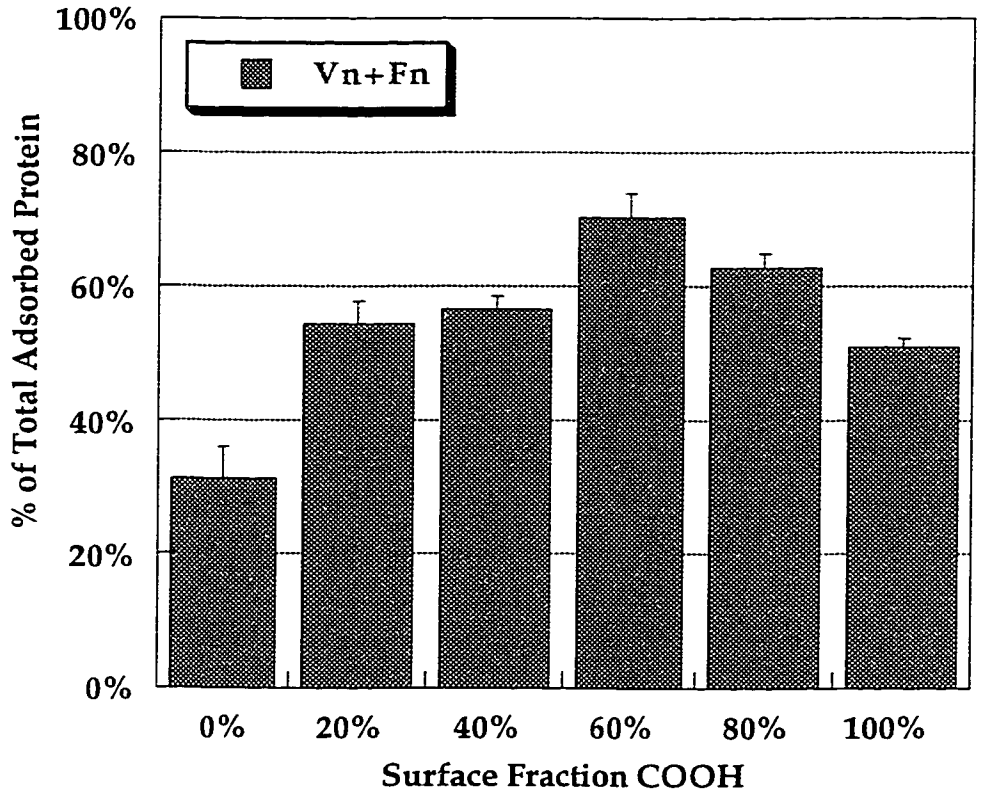

Figure 8.4 Surface fraction of vitronectin and fibronectin in adsorbed protein layers on binary composition SAMs of $HS(CH_2)_{15}COOH$ and $HS(CH_2)_{15}CH_3$. Vitronectin and fibronectin were adsorbed from 10% bovine serum for 2 hours at 37°C. The fractional amount of vitronectin and fibronectin in the adsorbed layer was calculated as the ratio of the sum of the amounts of vitronectin and fibronectin in the adsorbed phase to the total adsorption of the three proteins (Alb, Vn, and Fn). Data represent mean ± standard deviation for triplicate samples.

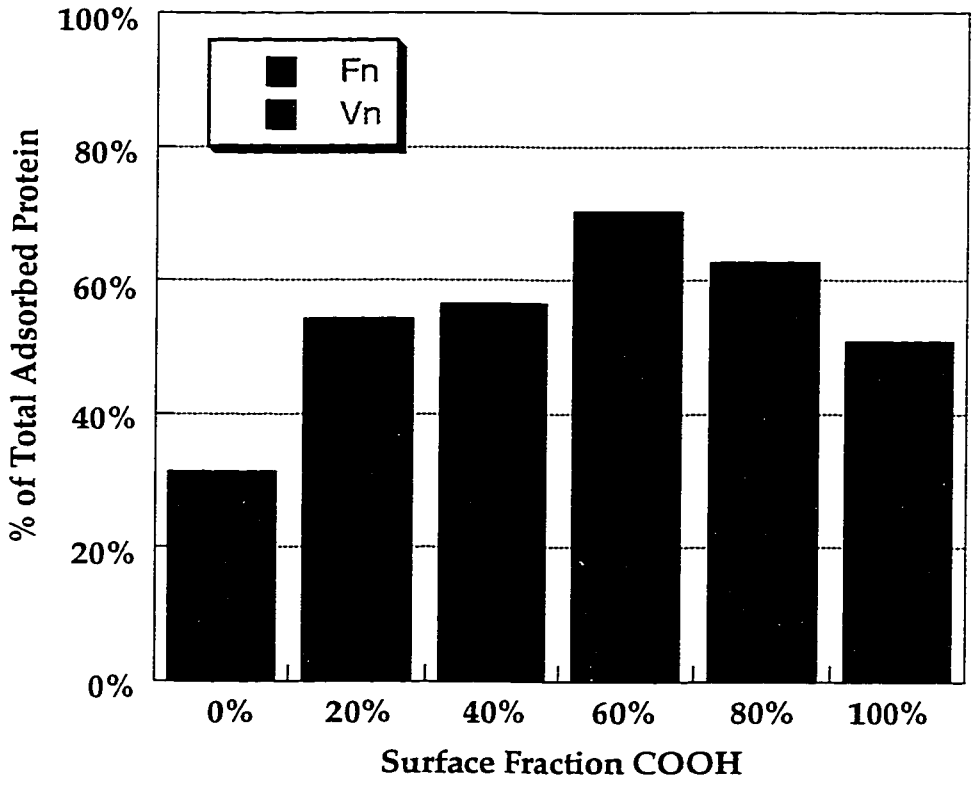

Figure 8.5 Surface fraction of vitronectin and fibronectin in adsorbed protein layers on binary composition SAMs of $HS(CH_2)_{15}COOH$ and $HS(CH_2)_{15}CH_3$. This figure is identical to Figure 8.5 however, the contribution of Fn and Vn to the combined adhesive protein surface fraction is shown. Vitronectin and fibronectin were adsorbed from 10% bovine serum for 2 hours at 37°C.

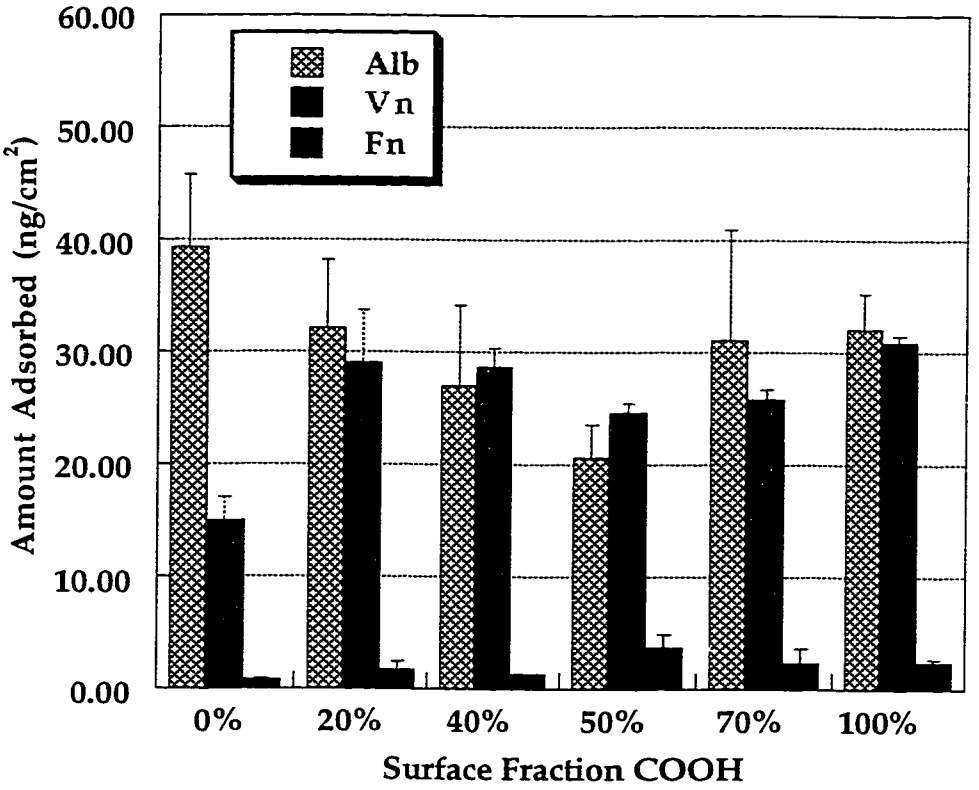

Figure 8.6 Effect of surface COOH content on Alb, Fn, and Vn adsorption to binary composition SAMs of $HS(CH_2)_{15}COOH$ and $HS(CH_2)_{15}CH_2OH$. Alb, Vn, and Fn were adsorbed from 10% bovine serum for 2 hours at 37°C. Data represent mean ± standard deviation for triplicate samples.

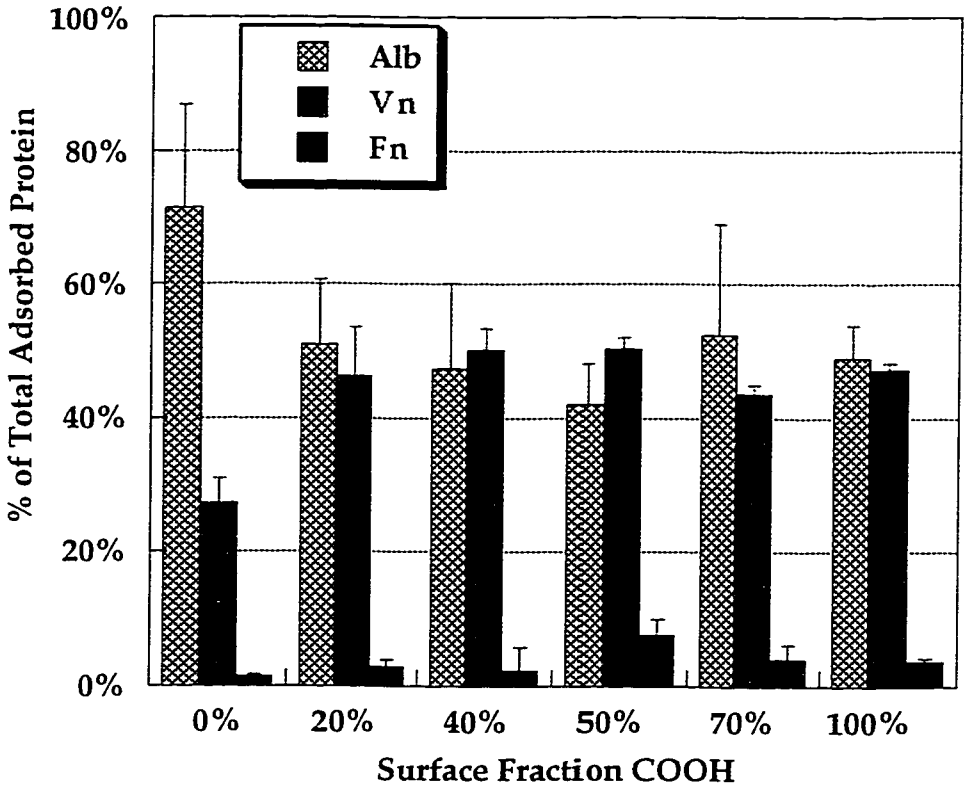

Figure 8.7 Surface fraction of Alb, Fn, and Vn in adsorbed protein layers on binary composition SAMs of $HS(CH_2)_{15}COOH$ and $HS(CH_2)_{15}CH_2OH$. Alb, Vn, and Fn were adsorbed from 10% bovine serum for 2 hours at 37°C. The fractional amount of each protein in the adsorbed layer was calculated as the ratio of the amount of protein in the adsorbed phase to the total adsorption of the three proteins. Data represent mean ± standard deviation for triplicate samples.

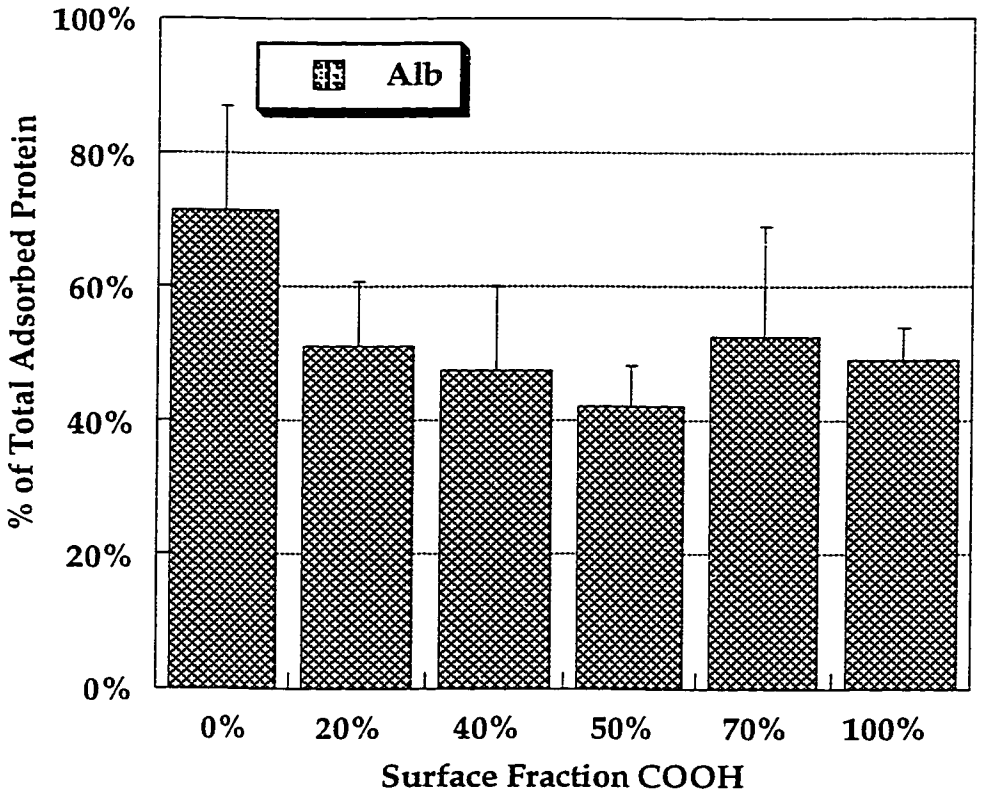

Figure 8.8 Surface fraction of albumin in adsorbed protein layers on binary composition SAMs of $HS(CH_2)_{15}COOH$ and $HS(CH_2)_{15}CH_2OH$. Alb was adsorbed from 10% bovine serum for 2 hours at 37°C. Data represent mean ± standard deviation for triplicate samples.

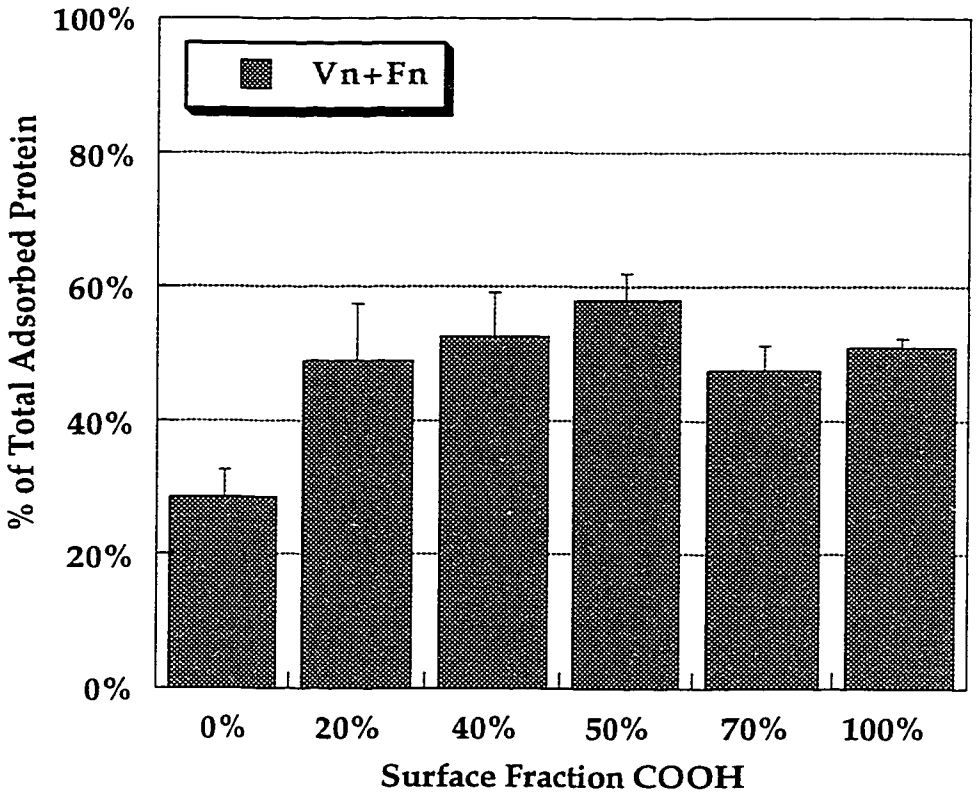

Figure 8.9 Surface fraction of vitronectin and fibronectin in adsorbed protein layers on binary composition SAMs of $HS(CH_2)_{15}COOH$ and $HS(CH_2)_{15}CH_2OH$. Vitronectin and fibronectin were adsorbed from 10% bovine serum for 2 hours at 37°C. The fractional amount of vitronectin and fibronectin in the adsorbed layer was calculated as the ratio of the sum of the amounts of vitronectin and fibronectin in the adsorbed phase to the total adsorption of the three proteins (Alb, Vn, and Fn). Data represent mean ± standard deviation for triplicate samples.

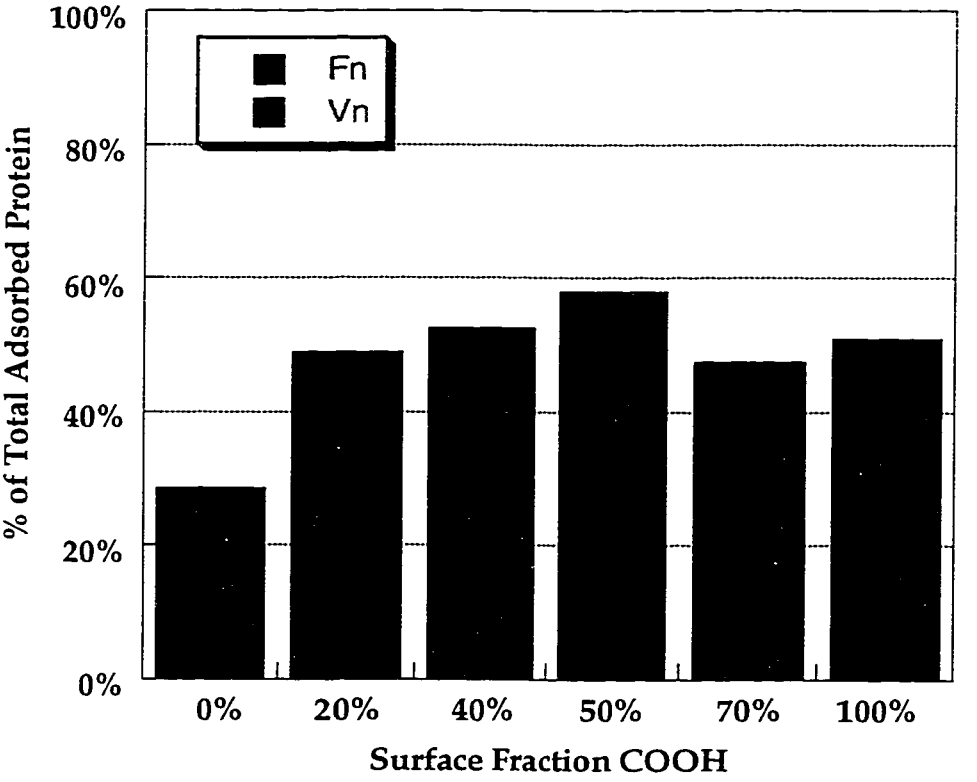

Figure 8.10 Surface fraction of vitronectin and fibronectin in adsorbed protein layers on binary composition SAMs of $HS(CH_2)_{15}COOH$ and $HS(CH_2)_{15}CH_2OH$. This figure is identical to Figure 8.9 however, the contribution of Fn and Vn to the combined adhesive protein surface fraction is shown. Vitronectin and fibronectin were adsorbed from 10% bovine serum for 2 hours at 37°C.

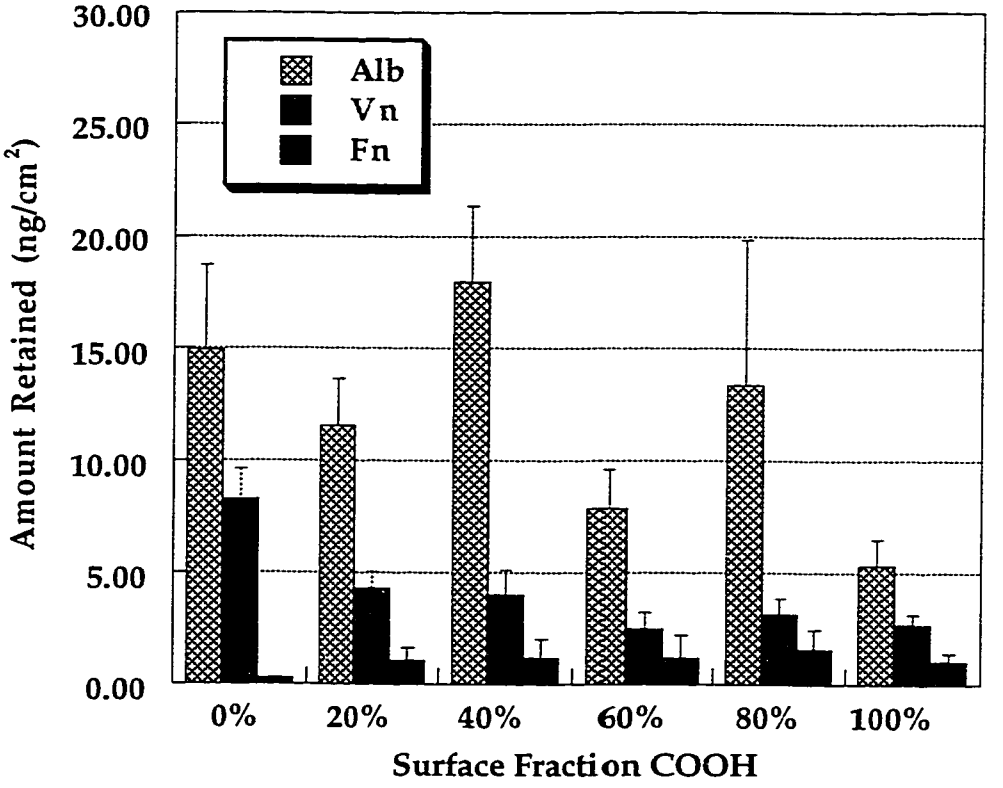

Figure 8.11 Effect of surface COOH content on Alb, Fn, and Vn retention on binary composition SAMs of $HS(CH_2)_{15}COOH$ and $HS(CH_2)_{15}CH_3$. Alb, Vn, and Fn were adsorbed from 10% bovine serum for 2 hours at 37°C. Adsorbed proteins were eluted for in a 3% SDS solution for 24 hours at 37°C. Data represent mean ± standard deviation for triplicate samples.

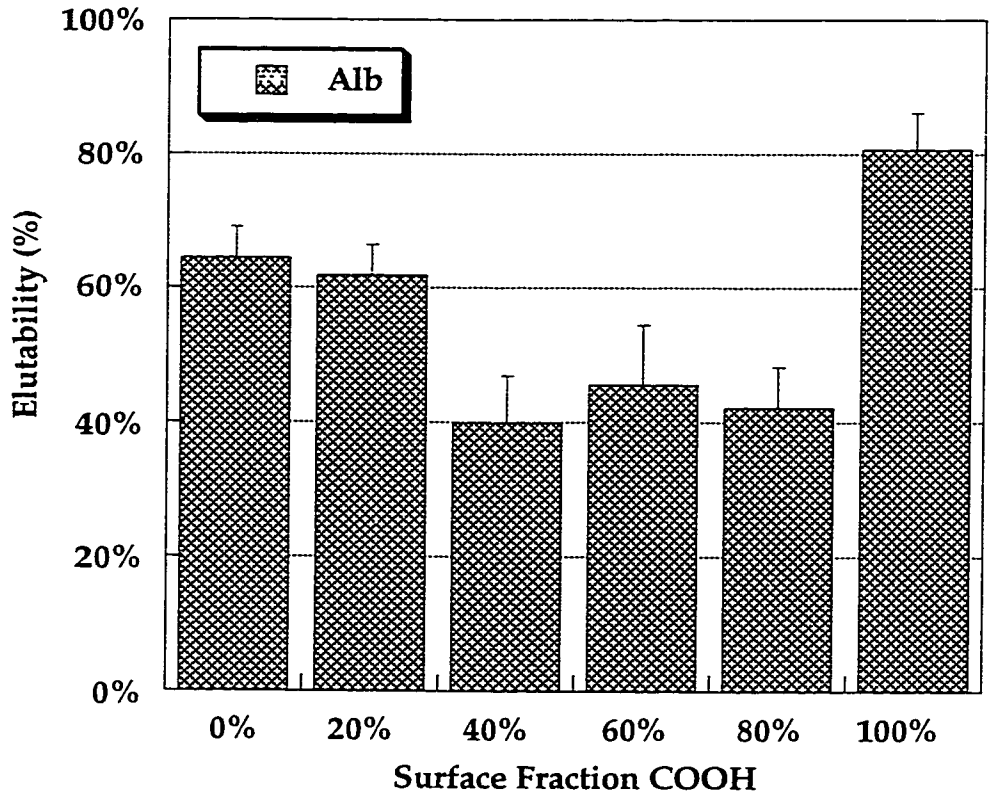

Figure 8.12 Effect of surface COOH content on Alb elutability from binary composition SAMs of $HS(CH_2)_{15}COOH$ and $HS(CH_2)_{15}CH_3$. Alb was adsorbed from 10% bovine serum for 2 hours at 37°C. Adsorbed albumin was eluted in a 3% SDS solution for 24 hours. Percent elutability is the fraction of initially adsorbed protein removed by the SDS solution. Data represent mean ± standard deviation for triplicate samples.

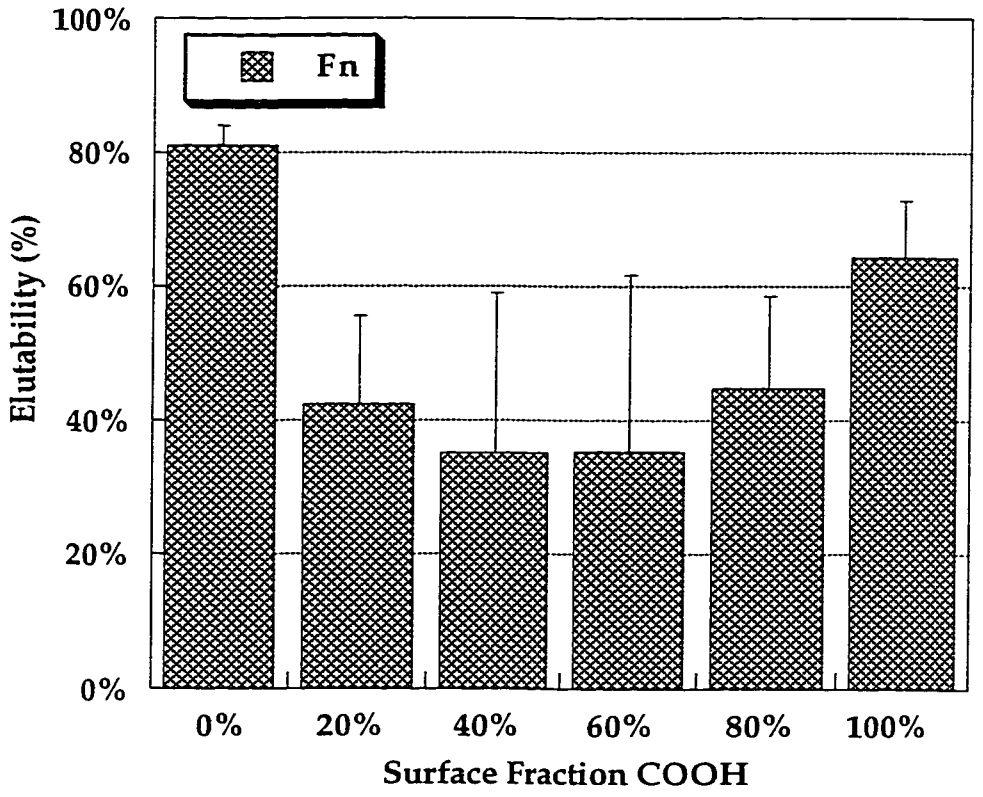

Figure 8.13 Effect of surface COOH content on Fn elutability from binary composition SAMs of $HS(CH_2)_{15}COOH$ and $HS(CH_2)_{15}CH_3$. Fn was adsorbed from 10% bovine serum for 2 hours at 37°C. Adsorbed Fn was eluted in a 3% SDS solution for 24 hours. Percent elutability is the fraction of initially adsorbed protein removed by the SDS solution. Data represent mean ± standard deviation for triplicate samples.

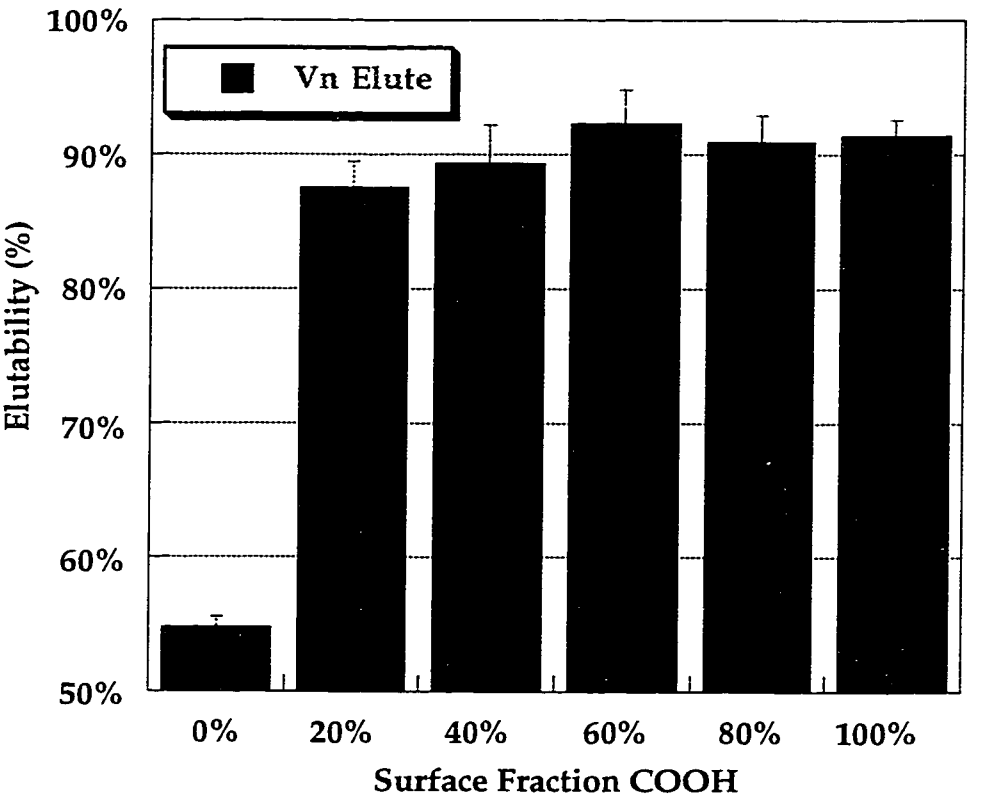

Figure 8.14 Effect of surface COOH content on Vn elutability from binary composition SAMs of $HS(CH_2)_{15}COOH$ and $HS(CH_2)_{15}CH_3$. Vn was adsorbed from 10% bovine serum for 2 hours at 37°C. Adsorbed vitronectin was eluted in a 3% SDS solution for 24 hours. Percent elutability is the fraction of initially adsorbed protein removed by the SDS solution. Data represent mean ± standard deviation for triplicate samples.

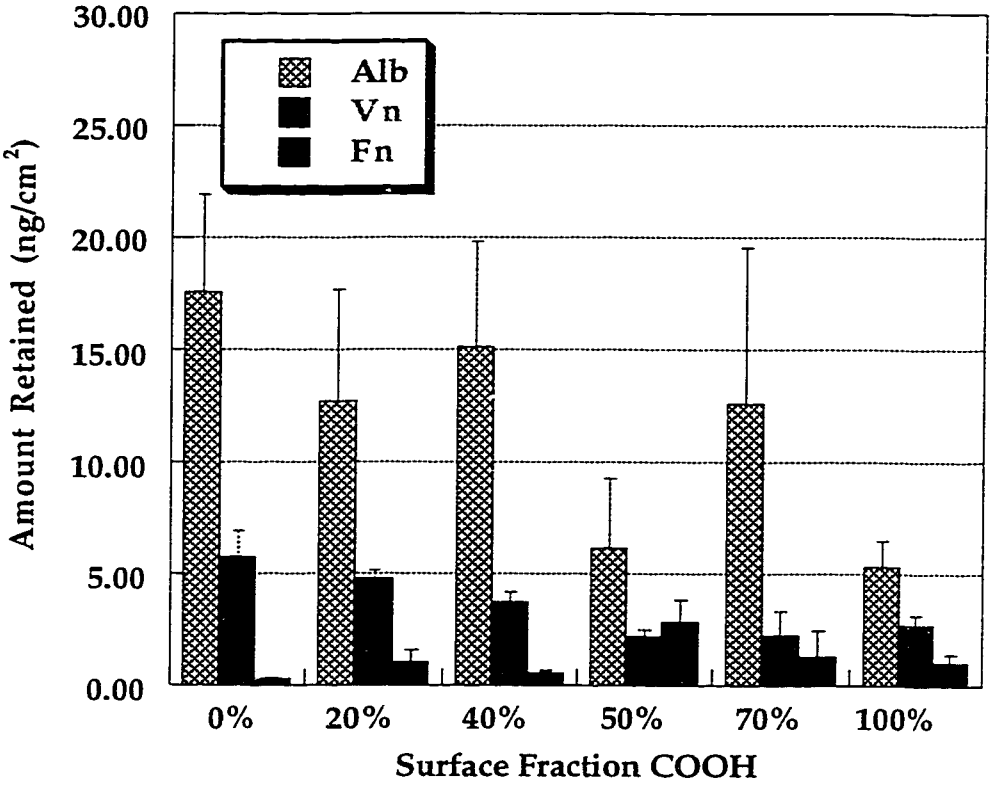

Figure 8.15 Effect of surface COOH content on Alb, Fn, and Vn retention on binary composition SAMs of $HS(CH_2)_{15}COOH$ and $HS(CH_2)_{15}CH_2OH$. Alb, Vn, and Fn were adsorbed from 10% bovine serum for 2 hours at 37°C. Adsorbed proteins were eluted for in a 3% SDS solution for 24 hours at 37°C. Data represent mean ± standard deviation for triplicate samples.

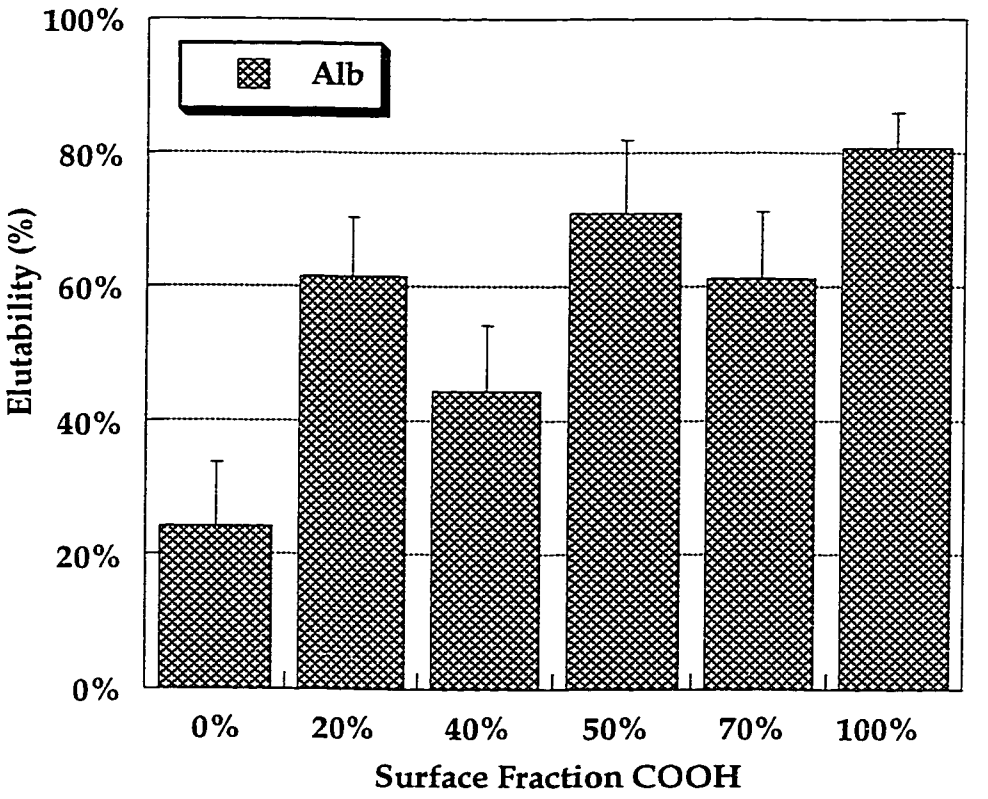

Figure 8.16 Effect of surface COOH content on Alb elutability from binary composition SAMs of $HS(CH_2)_{15}COOH$ and $HS(CH_2)_{15}CH_2OH$. Alb was adsorbed from 10% bovine serum for 2 hours at 37°C. Adsorbed albumin was eluted in a 3% SDS solution for 24 hours. Percent elutability is the fraction of initially adsorbed protein removed by the SDS solution. Data represent mean ± standard deviation for triplicate samples.

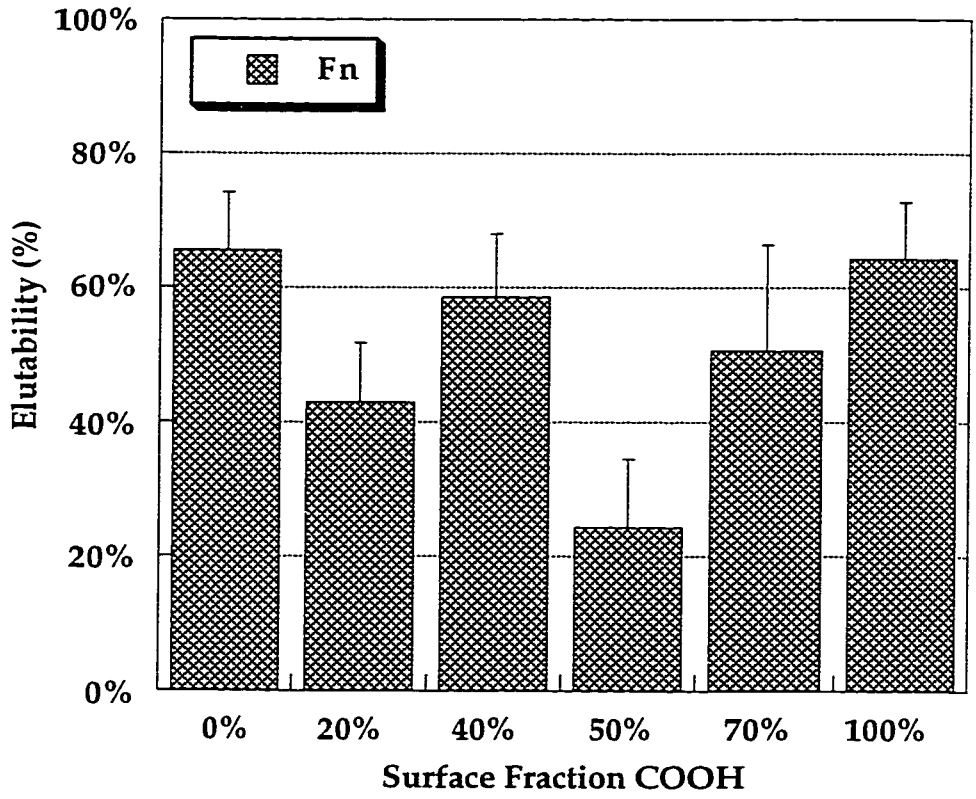

Figure 8.17 Effect of surface COOH content on Fn elutability from binary composition SAMs of $HS(CH_2)_{15}COOH$ and $HS(CH_2)_{15}CH_2OH$. Fn was adsorbed from 10% bovine serum for 2 hours at 37°C. Adsorbed Fn was eluted in a 3% SDS solution for 24 hours. Percent elutability is the fraction of initially adsorbed protein removed by the SDS solution. Data represent mean ± standard deviation for triplicate samples.

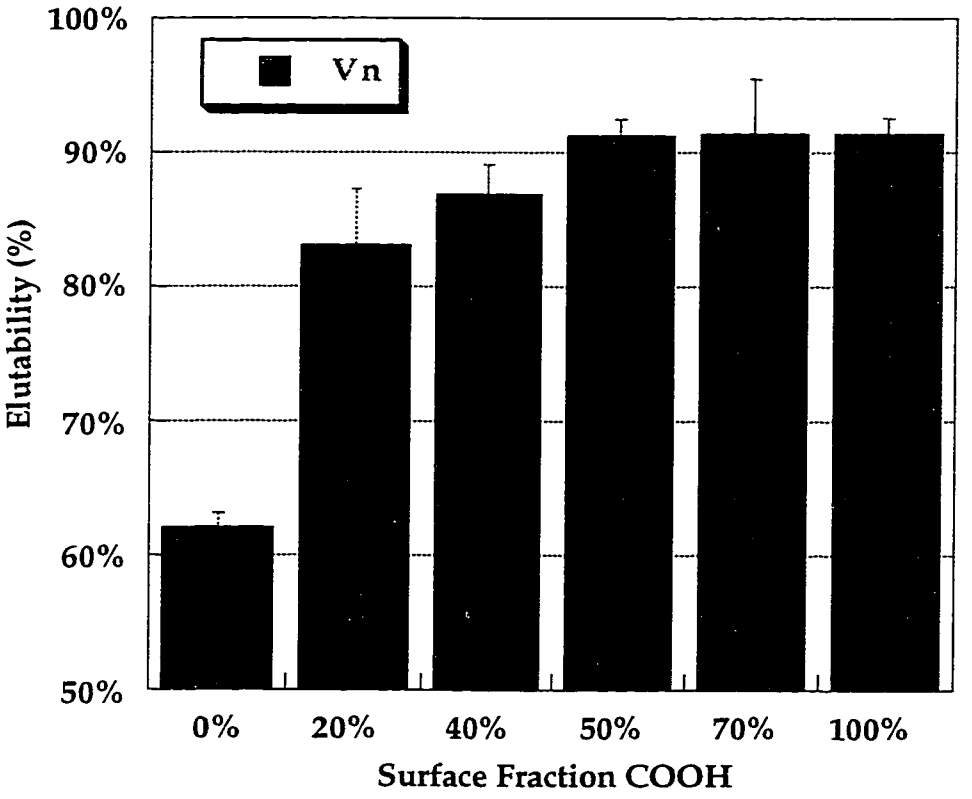

Figure 8.18 Effect of surface COOH content on Vn elutability from binary composition SAMs of $HS(CH_2)_{15}COOH$ and $HS(CH_2)_{15}CH_2OH$. Vn was adsorbed from 10% bovine serum for 2 hours at 37°C. Adsorbed vitronectin was eluted in a 3% SDS solution for 24 hours. Percent elutability is the fraction of initially adsorbed protein removed by the SDS solution. Data represent mean ± standard deviation for triplicate samples.

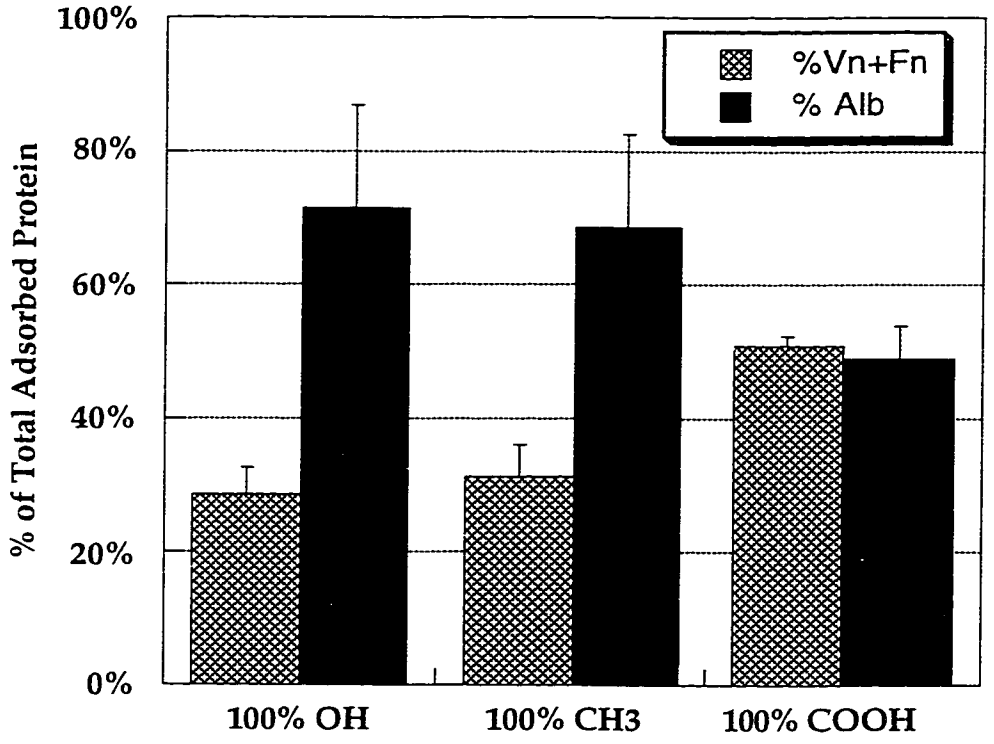

Figure 8.19 Surface fraction of adhesive protein (vitronectin and fibronectin) and albumin in adsorbed protein layers on homogeneous composition SAMs of $HS(CH_2)_{15}COOH$, $HS(CH_2)_{15}CH_3$, and $HS(CH_2)_{15}CH_2OH$. Data shown in this figure were obtained from Figures 8.3, 8.4, 8.8, and 8.9.

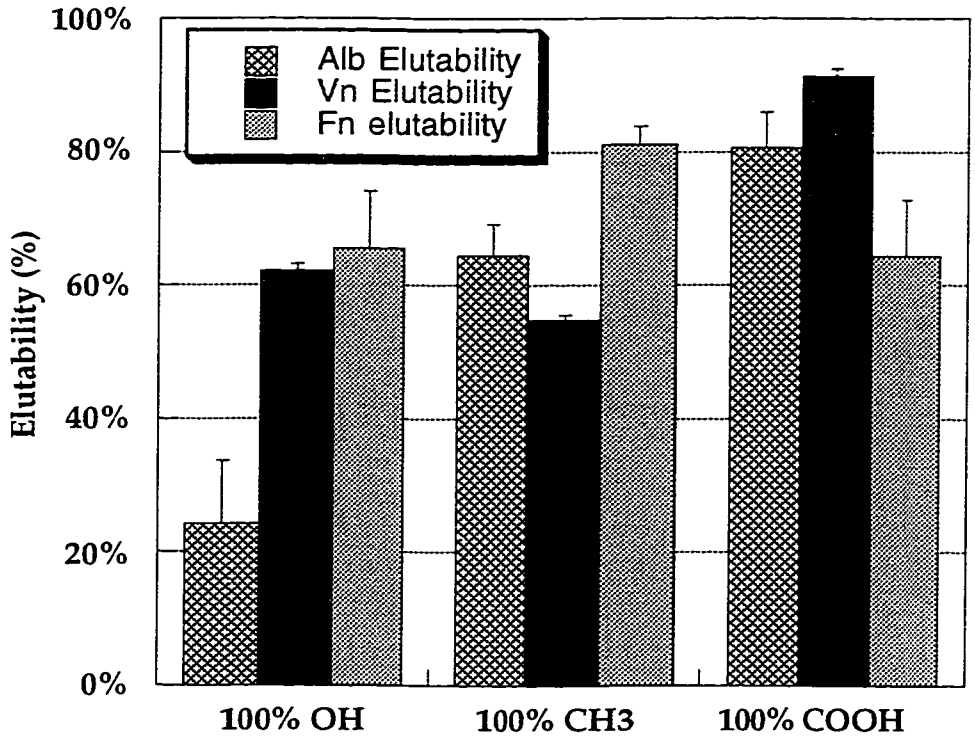

Figure 8.20 SDS elutability of Alb, Fn, and Vn adsorbed to homogeneous composition SAMs of $HS(CH_2)_{15}COOH$, $HS(CH_2)_{15}CH_3$, and $HS(CH_2)_{15}CH_2OH$. Data shown in this figure were obtained from Figures 8.12 through 8.14, and Figures 8.16 through 8.18.

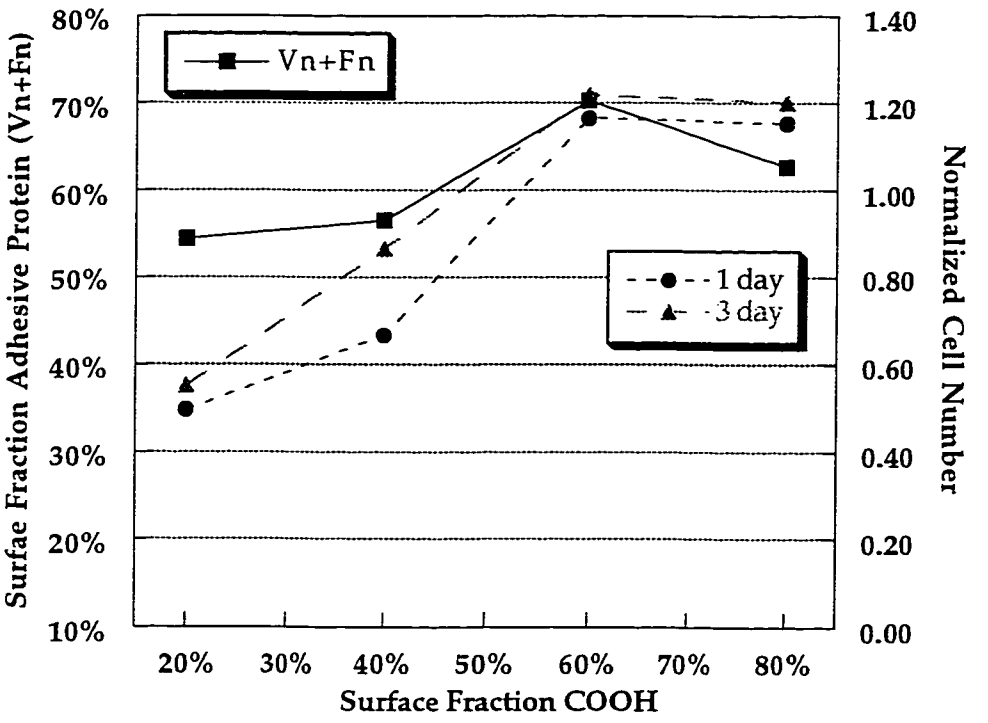

Figure 8.21 Surface fraction of vitronectin and fibronectin in adsorbed protein layers, and normalized cell number after 1 day and 3 day culture periods on binary composition SAMs of $HS(CH_2)_{15}COOH$ and $HS(CH_2)_{15}CH_3$.

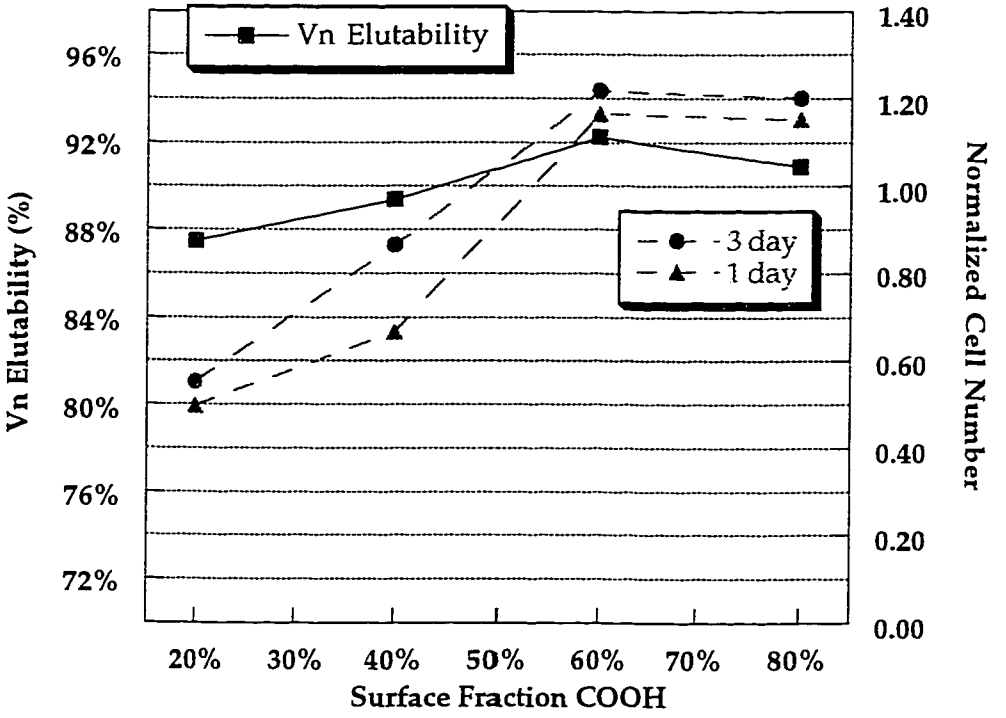

Figure 8.22 Elutability of Vn in adsorbed protein layers and normalized cell number after 1 day and 3 day culture periods on binary composition SAMs of $HS(CH_2)_{15}COOH$ and $HS(CH_2)_{15}CH_3$.

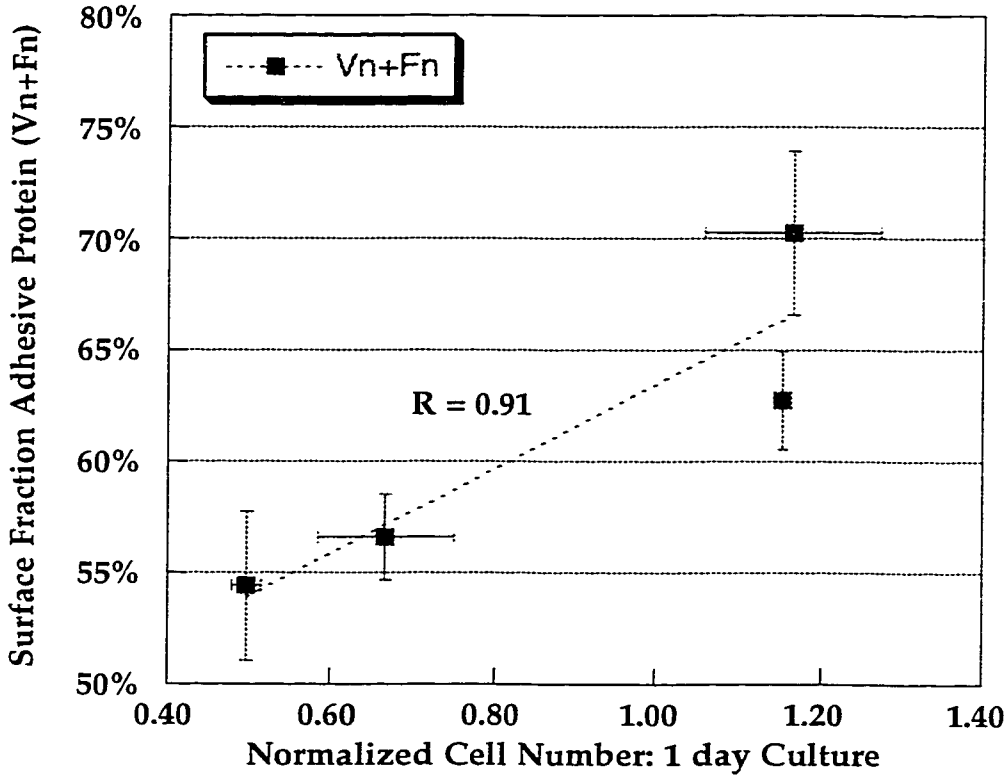

Figure 8.23 Cross-plot of adhesive protein surface fraction and normalized cell number (1 day culture period) for binary composition SAMs of $HS(CH_2)_{15}COOH$ and $HS(CH_2)_{15}CH_3$.

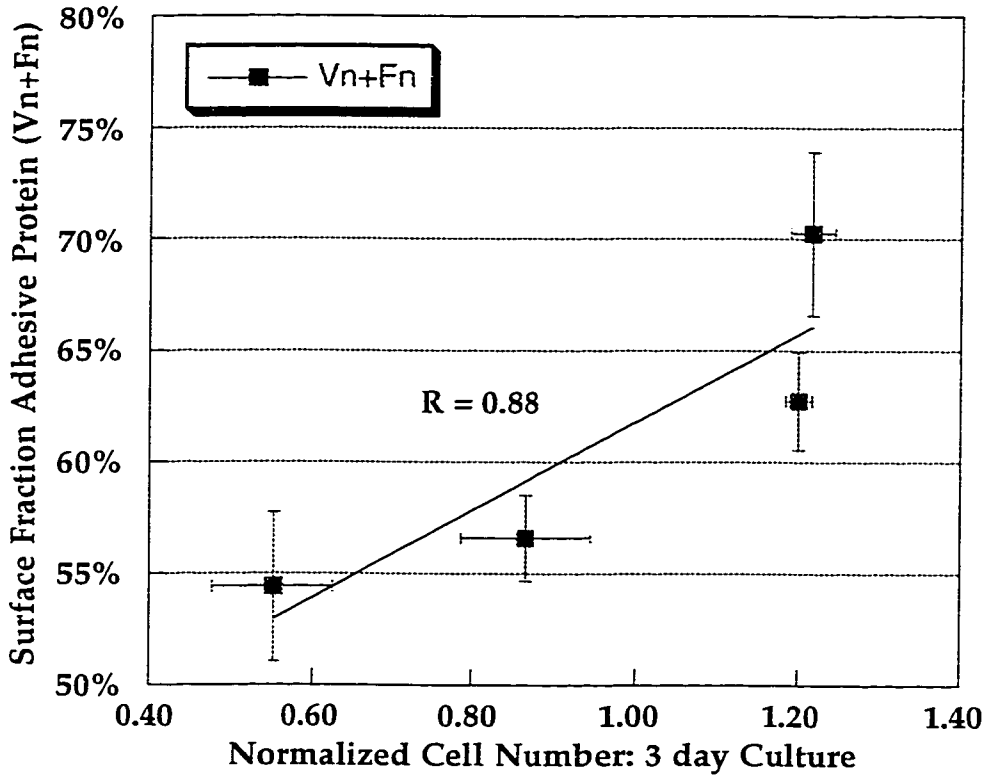

Figure 8.24 Cross-plot of adhesive protein surface fraction and normalized cell number (3 day culture period) for binary composition SAMs of $HS(CH_2)_{15}COOH$ and $HS(CH_2)_{15}CH_3$.

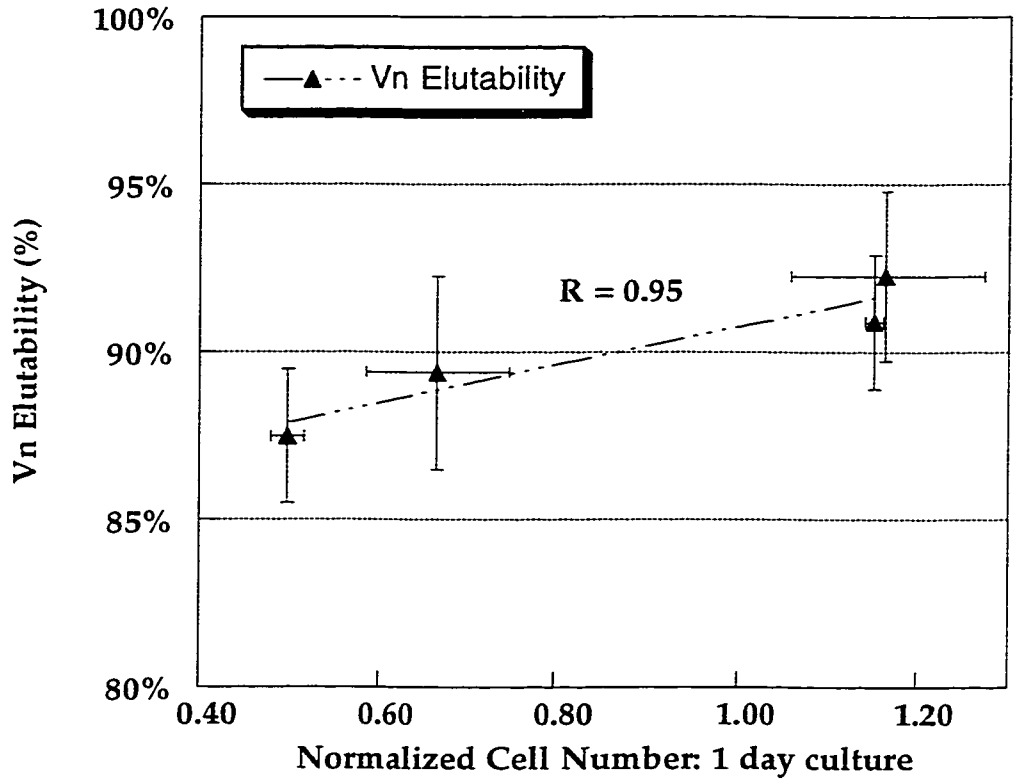

Figure 8.25 Cross-plot of Vn elutability and normalized cell number (1 day culture period) for binary composition SAMs of $HS(CH_2)_{15}COOH$ and $HS(CH_2)_{15}CH_3$.

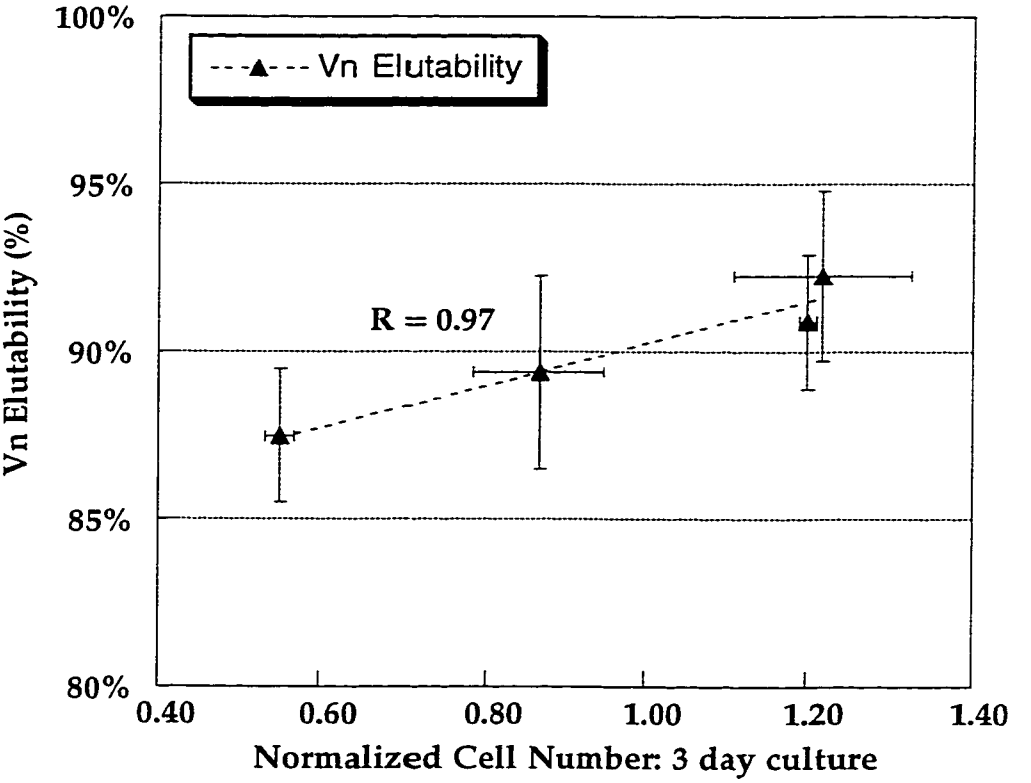

Figure 8.26 Cross-plot of Vn elutability and normalized cell number (3 day culture period) for binary composition SAMs of $HS(CH_2)_{15}COOH$ and $HS(CH_2)_{15}CH_3$.

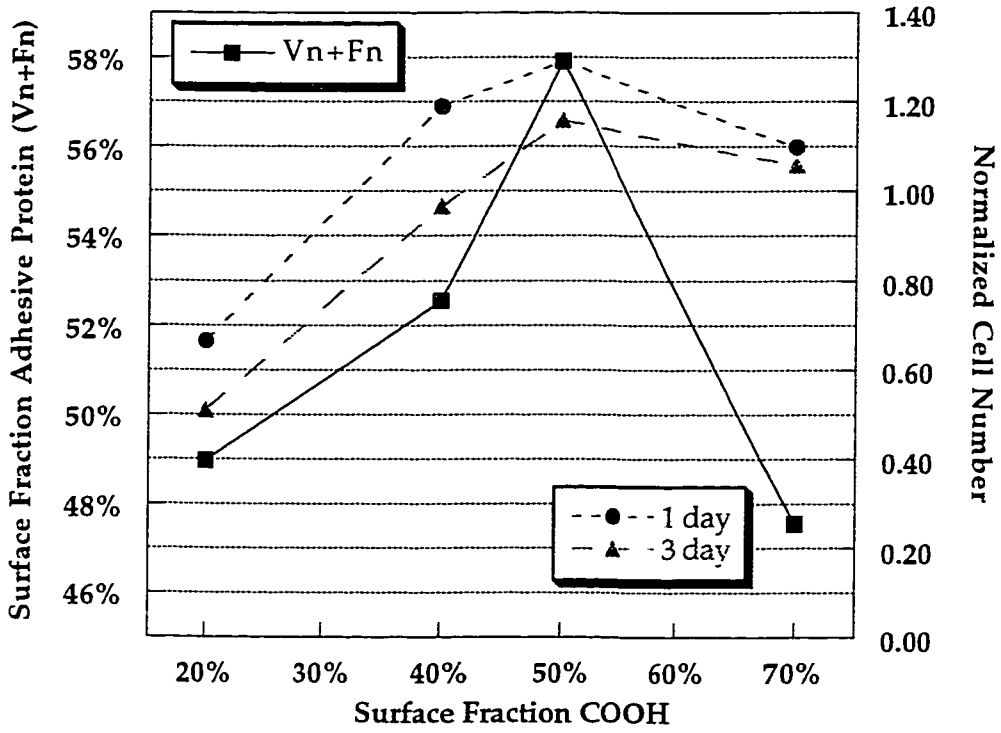

Figure 8.27 Surface fraction of vitronectin and fibronectin in adsorbed protein layers, and normalized cell number after 1 day and 3 day culture periods on binary composition SAMs of $HS(CH_2)_{15}COOH$ and $HS(CH_2)_{15}CH_2OH$.

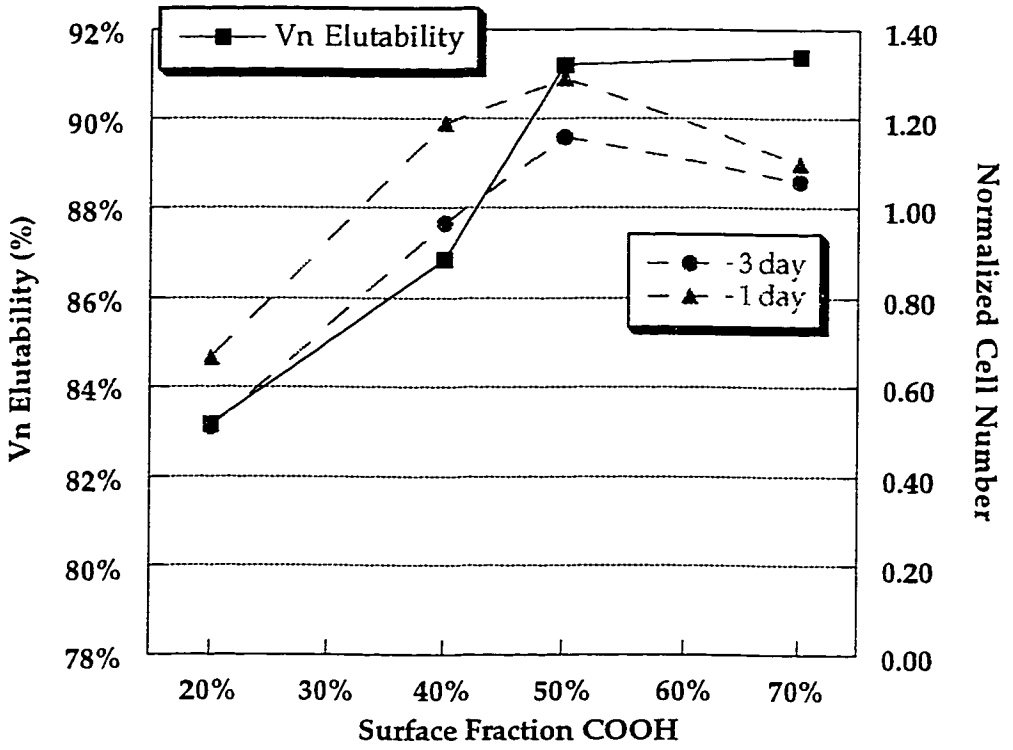

Figure 8.28 Elutability of Vn in adsorbed protein layers and normalized cell number after 1 day and 3 day culture periods on binary composition SAMs of $HS(CH_2)_{15}COOH$ and $HS(CH_2)_{15}CH_2OH$.

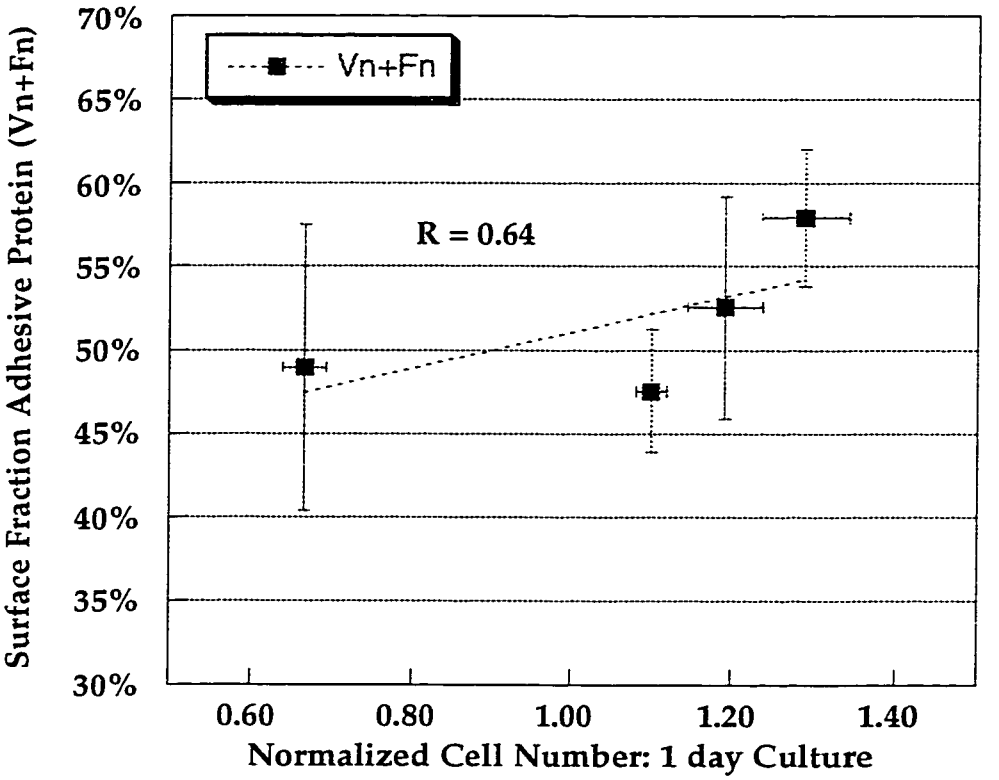

Figure 8.29 Cross-plot of adhesive protein surface fraction and normalized cell number (1 day culture period) for binary composition SAMs of $HS(CH_2)_{15}COOH$ and $HS(CH_2)_{15}CH_2OH$.

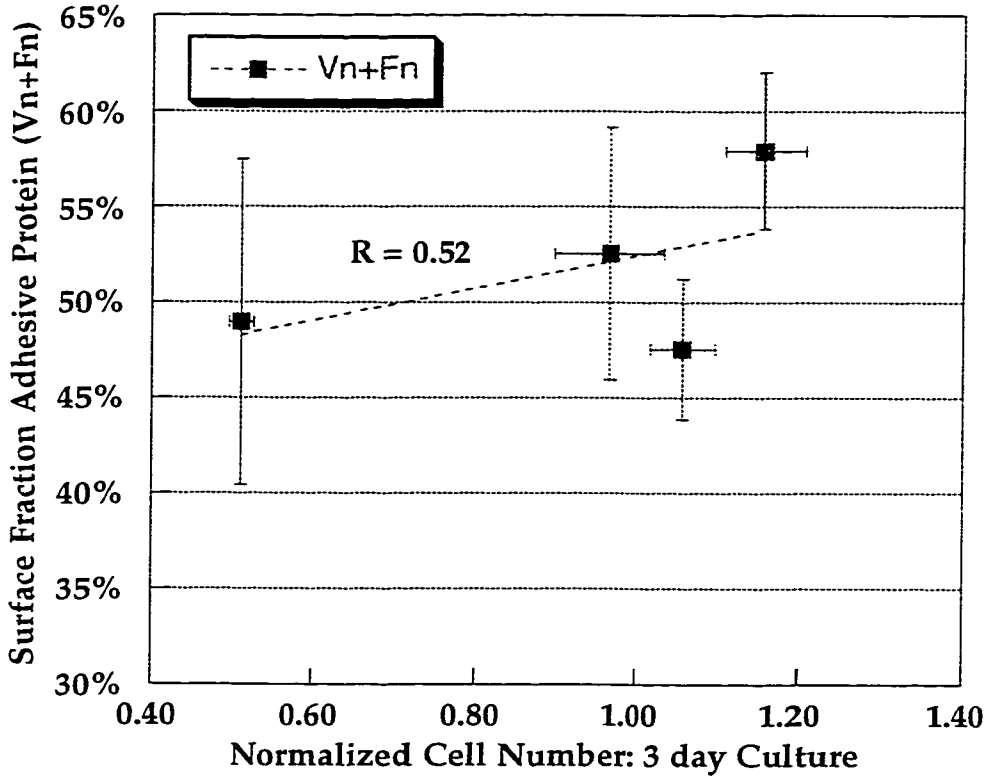

Figure 8.30 Cross-plot of adhesive protein surface fraction and normalized cell number (3 day culture period) for binary composition SAMs of $HS(CH_2)_{15}COOH$ and $HS(CH_2)_{15}CH_2OH$.

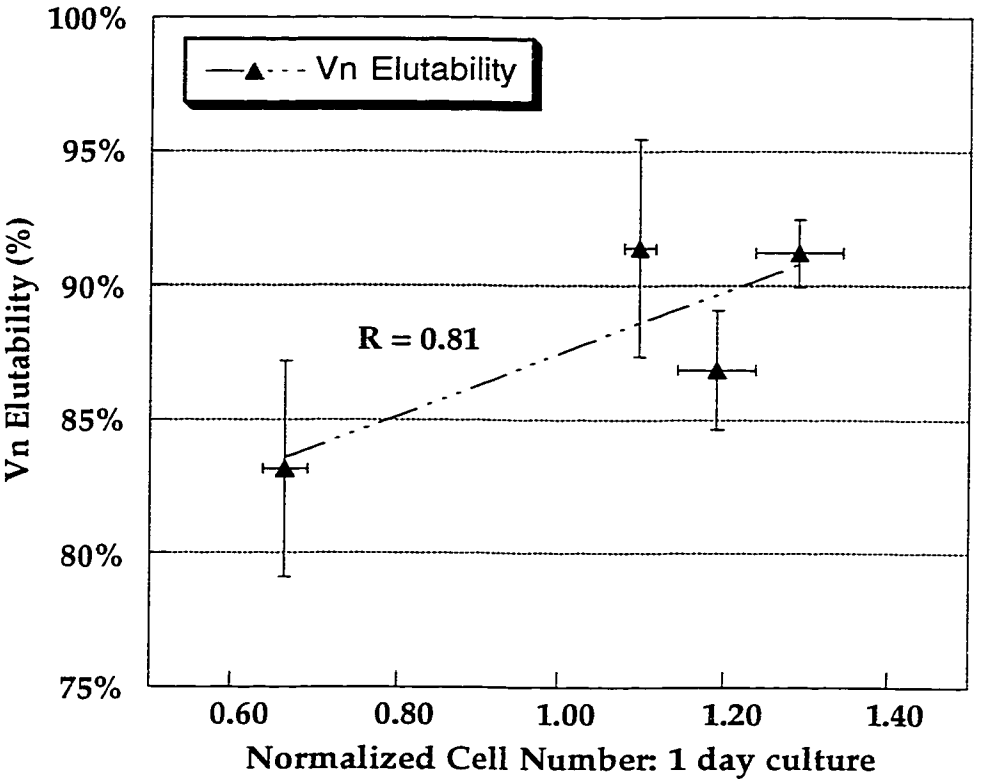

Figure 8.31 Cross-plot of Vn elutability and normalized cell number (1 day culture period) for binary composition SAMs of $HS(CH_2)_{15}COOH$ and $HS(CH_2)_{15}CH_2OH$.

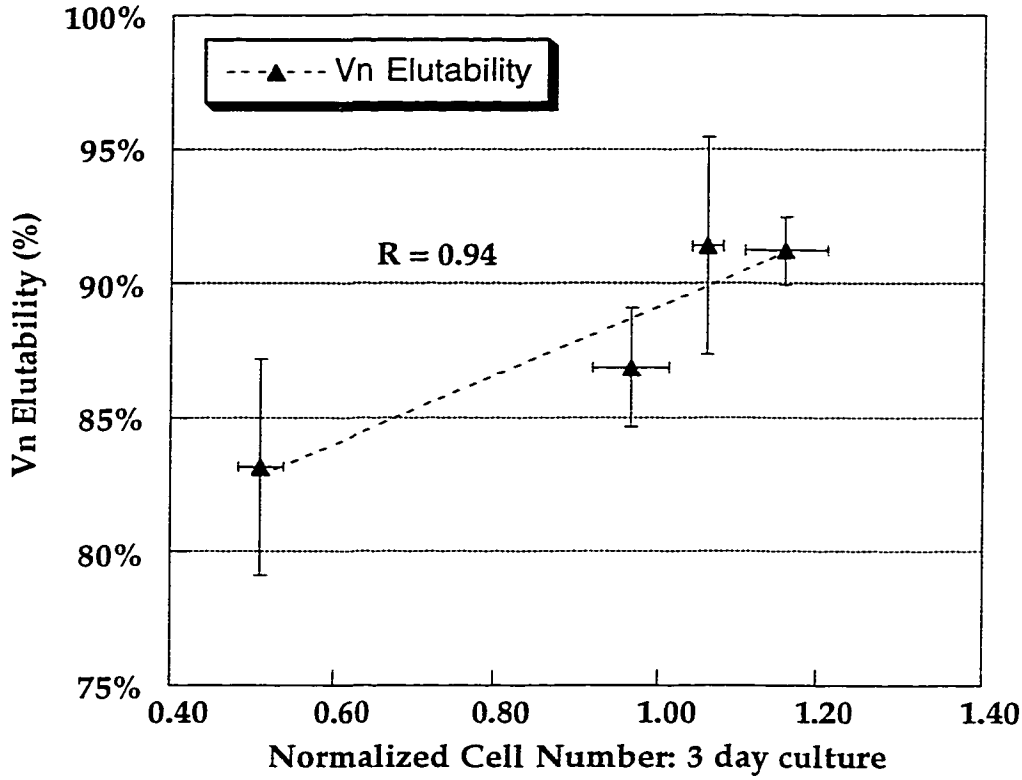

Figure 8.32 Cross-plot of Vn elutability and normalized cell number (3 day culture period) for binary composition SAMs of $HS(CH_2)_{15}COOH$ and $HS(CH_2)_{15}CH_2OH$.

Chapter 9

Conclusions and Recommendations

9.1 Summary of Conclusions

The surface of a biomaterial is well known to influence the biological response however, there is a limited understanding of the roles of many specific surface properties in controlling protein and cellular interactions with a substrate. In this study, we investigated the role of two important surface properties, surface chemistry and surface mobility, in serum protein adsorption and endothelial cell growth. The specific aims of this research were first, to investigate the effects of surface chemistry (specifically functional group concentration and spatial arrangement) and surface mobility on endothelial cell growth using homogeneous and heterogeneous composition self-assembled monolayers as model surfaces. Secondly, protein layers adsorbed on homogeneous and heterogeneous SAM surfaces were characterized to investigate the effects of surface chemistry and mobility on the composition and binding strength of adsorbed protein layers. The final goal of this study was to establish correlations between surface properties, properties of the adsorbed protein layer, and endothelial cell growth. The central hypothesis of this proposal was that endothelial cell growth on biomaterial surfaces is influenced by surface chemical composition (specifically functional group concentration and spatial arrangement) and surface molecular motions or surface mobility, as mediated by the adsorbed protein layer.

Self-assembled monolayers of alkanethiols on gold were used as model surfaces in these studies. Techniques were developed to prepare SAMs suitable for use in protein and cell interactions studies that incorporated requirements specific for biointeractions studies (i.e., double-sided samples, specific sample geometries, ability to produce many samples in one run, transparent samples, etc.). Since biointeraction studies involve the

exposure of the SAM to a variety of different solutions for varying time periods, a critical requirement for utilizing SAMs in such studies is the maintenance of SAM stability throughout the experimental procedure. Stability studies were performed to assess SAM integrity following exposure to each type of solution used in the protein adsorption/elution and cell growth studies. In all stability experiments, no changes in surface composition, film thickness, or IR spectral features indicative of SAM delamination or degradation were observed.

The role of specific chemical functionalities in endothelial cell growth was investigated using a series of chemically homogeneous SAMs terminally functionalized with hydroxyl, methyl, methyl ester and carboxyl groups (Chapter 3). Cell growth was evaluated qualitatively in a clonal growth study (low seeding density) and a quantitatively, following seeding at high density. The use of these functionalities provided a series of surfaces exhibiting a wide range in surface hydrophobicity and allowed for investigation of the role of oxygen-containing functional groups. Since cells seeded on a substrate in serum-containing culture medium interact with the adsorbed protein layer rather than with the substrate itself, the effect of chemical functionality on the adsorbed protein layer was investigated in conjunction with cell growth. The role of two serum proteins, Alb (a nonadhesive or blocking protein) and Fn (an adhesive protein), in cell growth was evaluated.

BAEC growth on homogeneous SAMs varied significantly in response surface chemical functionality. BAEC spreading and growth was significantly higher on the COOH SAM than on the CH_3, CO_2CH_3, or OH-terminated SAMs. Cell growth on the homogeneous SAMs was generally lower than cell growth on TCPS, particularly in the clonal growth study, and to a lesser extent in the high seeding density growth study. Protein interaction studies demonstrated variations in protein adsorption and elutability in response to SAM terminal functional group. Fn adsorption and Alb elutability were

significantly higher on the best cell growth substrate (COOH SAM) than on growth-inhibiting substrates (CO_2CH_3 and OH SAMs). These results led to the hypothesis that substrates adsorbing higher levels of Fn and demonstrating increased Alb elutability (i.e., the COOH SAM) may encourage cell growth by permitting the subsequent adsorption of cell-derived ECM proteins or other serum proteins which promote cell spreading and growth onto, or after displacement of, the initially adsorbed protein layer.

The observation of increased cell growth on TCPS relative to the homogenous SAM surfaces led to the hypothesis that the presence of multiple chemical functionalities in certain proportions may be desirable for the promotion of cell attachment and growth. The effect of increasing the chemical complexity of a surface on protein adsorption and cell growth, was investigated in a preliminary study utilizing two series of chemically heterogeneous or binary composition "mixed" SAMs (Chapter 4). In clonal growth studies, endothelial cell growth increased with COOH surface concentration for both the COOH/OH series and the CH_3/COOH series. In high seeding density studies (qualitative), cell density on binary SAMs with a surface COOH concentration of 50% or higher appeared to approach or exceed growth on the homogeneous COOH surfaces. These results demonstrated an effect of surface functional group concentration on cell growth and suggested that chemically heterogeneous surfaces may result in improved cell growth characteristics compared with chemically homogeneous surfaces. In these studies, unexpected differences in cell growth were observed between the COOH/OH and the CH_3/COOH series. In general, cell growth was lower on the CH_3/COOH SAMs than on the COOH/OH SAMs at the same COOH surface concentration suggesting an effect of functional group spatial arrangement and degree of phase separation on endothelial cell growth in addition to the effect of functional group concentration.

Protein interaction studies with the COOH/OH SAMs demonstrated variations in Alb and Fn adsorption and elutability in response to SAM surface composition.

Relationships between cell growth and adsorbed protein layer characteristics were observed which were similar to results obtained for homogeneous SAMs. Surfaces promoting cell growth (the COOH and the binary COOH/OH SAMs) demonstrated moderate to high albumin elutabilities and higher levels of Fn adsorption than did substrates inhibiting cell growth (the OH SAM).

In Chapter 5, surface composition/solution composition relationships were determined for three binary SAM systems (COOH/OH, COOH/CH_3, and OH/CH_3 SAMs). For many binary SAM systems, surface composition differs from the alkanethiol solution composition due to differences in relative solubility and affinities of the thiol components for the surface therefore, determination of the relationship between solution composition/surface composition relationship was crucial for obtaining binary SAMs with the desired surface functional group concentration. The chemically heterogeneous SAMs were analyzed by ellipsometry, contact angle, XPS and TOF-SIMS. Surface composition/solution composition relationships were determined for SAMs prepared from thiol solutions ranging in composition from 0-100% by evaluating surface composition determined by XPS and/or TOF-SIMS as a function of thiol solution composition. The surface composition/solution ratio relationships were used to prepare SAMs of a desired surface composition for use in cell growth and protein adsorption studies described in Chapters 6 and 8.

For binary SAM systems containing a unique heteroatom in the thiol terminal functionality, SAM surface composition was quantified using XPS elemental surface compositions. Binary SAM surface composition was also quantified by TOF-SIMS. XPS, contact angle, and TOF-SIMS analysis of the COOH/CH_3 and OH/CH_3 SAM systems demonstrated that SAM surface composition differed significantly from the solution concentration of the adsorbing thiol solution with adsorption of the nonpolar thiol favored over adsorption of the polar thiol resulting in binary SAM surfaces which

were methyl rich. TOF-SIMS analysis was used to determine the surface composition/solution composition relationship for the COOH/OH SAM system. COOH/OH surface composition deviated slightly from a 1:1 relationship between surface composition and solution composition. Since a distinct chemical functionality was not required for quantifying surface composition, TOF-SIMS was ideally suited for surface analysis of a SAM system such as the COOH/OH system.

TOF-SIMS analysis was also used to probe the surface dispersion of thiol components in the COOH/OH, COOH/CH_3 and OH/CH_3 SAM systems. The deviation of a binary SAM from a randomly mixed surface structure was assessed by evaluating the distribution of the dual species molecular ion cluster intensity. Evidence of thiol clustering was obtained for the COOH/CH_3 and OH/CH_3 SAM systems while the experimental distribution of the dual species cluster curve for the COOH/OH system most closely approximated the theoretical curve for a randomly mixed surface suggesting that a randomly mixed configuration.

To expand upon the preliminary studies of cell growth and protein adsorption on chemically heterogeneous SAMs (Chapter 4), the effects of SAM surface composition, spatial arrangement, and surface chemical heterogeneity on BAEC attachment and growth were investigated using three series of chemically heterogeneous binary SAMs (Chapter 6). Cell attachment and growth were assessed quantitatively using the MTT cell proliferation assay and qualitatively using light microscopy. The effect of surface functional group content on cell growth was investigated using two binary SAM series (COOH/OH and COOH/CH_3) which paired a growth-promoting functional group with a growth-inhibiting group to achieve a gradient in cellular response. The effect of functional group spatial arrangement was evaluated by comparing cell growth on the COOH/OH series with cell growth on the COOH/CH_3 series since TOF-SIMS analysis had demonstrated differences in functional group dispersion between these systems. To

determine if cell growth on chemically heterogeneous surfaces was improved over growth on chemically homogeneous surfaces, cell growth was evaluated on a system pairing two growth-inhibiting groups (OH/CH_3).

For the COOH/OH and $COOH/CH_3$ SAMs, cell attachment did not differ significantly with surface functional group content and it was observed that surfaces demonstrating equivalent levels of cell attachment often demonstrated significant differences in cell growth after longer cell culture periods. It was concluded that while some level of cell attachment is required for cell growth to occur, cell attachment is not necessarily predictive of cell growth since some surfaces demonstrating high levels of cell attachment did not support cell growth.

Significant differences in cell growth were observed on both the COOH/OH and $COOH/CH_3$ binary SAMs in response to binary SAM surface composition. Similar patterns in cell growth were observed for the two COOH-containing SAM systems. Cell growth increased significantly with increasing surface fraction of COOH for surface compositions ranging from 0-60% COOH for the $COOH/CH_3$ SAMs and 0-50% COOH for the COOH/OH SAMs. Cell growth reached a maximum value at 60% COOH ($COOH/CH_3$) or 50% COOH (COOH/OH). As surface COOH content increased the maximum point, no significant increases in cell growth were observed, rather cell growth decreased slightly for increasing surface fraction of COOH. These results clearly demonstrate a significant effect of surface functional group concentration on cell growth and further emphasize the growth-promoting ability of the COOH functionality. These results are significant in that we have demonstrated that endothelial cell growth on a substrate can be influenced by controlling the surface composition of growth-promoting and growth-inhibiting functional groups. Several $COOH/CH_3$ and COOH/OH surface compositions demonstrated cell growth levels which exceeded cell growth measured on TCPS. These results are significant since they demonstrate the ability to create a cell

growth substrate of well-defined chemistry which promotes cell growth to levels in excess of that on TCPS.

A comparison of cell growth on the COOH/OH and COOH/CH_3 systems after 1 day of culture suggested that cell growth was affected by the spatial arrangement of the surface COOH groups. The growth inhibitory effect of the poor growth component of the binary SAM (i.e. CH_3 or OH) was observed to be more pronounced when existing in a clustered configuration since the clustered arrangement of the COOH/CH_3 surface resulted in a decreased level of cell growth given the same surface COOH content. However, after 3 days of culture, cell growth on the COOH/OH and COOH/CH_3 systems did not differ significantly. It was concluded that the effect of surface functional group dispersion on cell growth was significant in the early phase of cell growth but diminished with increasing cell culture time.

The effect of surface chemical heterogeneity on cell growth was evaluated for a series of OH/CH_3 binary SAMs. Low levels of cell growth were obtained on all OH/CH_3 surface compositions and cell number was independent of surface OH content. These results indicated that a chemically heterogeneous surface must contain an adequate surface content of a growth-promoting functional group in order for cell growth to be improved, and that chemical heterogeneity alone does not result in enhanced cell growth relative to that on a homogeneous surface.

The effect of surface mobility, or surface molecular motions, on endothelial cell attachment and growth was investigated to test the hypothesis that endothelial cell growth would be dependent upon the degree of surface molecular mobility and that cell growth on structurally complex, mobile surfaces would differ significantly from that on structurally homogeneous, ordered, immobile surfaces (Chapter 7). Structurally heterogeneous SAMs which varied systematically in the concentration of chains

exhibiting molecular mobility at the interface were formed using mixtures of thiols differing in chain length (C_{10} and C_{16} COOH-terminated thiols).

The C_{10}/C_{16} SAMs were characterized by XPS, ellipsometry, contact angle and FTIR. Surface disorder or surface mobility was assessed by advancing water contact angle, contact angle hysteresis, and changes in the C-H stretching mode peaks as measured by FTIR. Surface disorder was maximal on the 50% C_{16} surface and lowest on the 100% C_{16} surface. Endothelial cell attachment and growth was evaluated on the C_{10}/C_{16} binary SAMs using imaging and the MTT assay system.

The effects of surface disorder or surface mobility on cell growth were limited. No significant differences in cell attachment were observed in response to differences in surface disorder. Cell number was highest on the most disordered surface (50% C_{16}) after 1 day of culture however, the 25% and 75% surfaces which also exhibited surface mobility, did not differ in cell number from the immobile 100% C_{16} surface. After the 3 day culture period, all C_{10}/C_{16} surfaces exhibited confluent monolayers and the effects of surface disorder on cell growth were negligible. These results suggest that the effects of surface mobility on cell growth are minimal and appear to be limited to early phases of cell-substrate interactions. Clearly the effects of surface chemistry on cell growth are far more significant than the effects of surface mobility.

The effects of binary SAM surface composition on the adsorbed protein layer and the influence of the adsorbed protein layer on endothelial cell growth were investigated In Chapter 8. The COOH/OH and COOH/CH_3 SAMs had demonstrated a gradient in cellular response in cell interactions studies described in Chapter 6 and were therefore selected for evaluation in protein interaction studies. The adsorption of three serum proteins, albumin, fibronectin, and vitronectin from 10% bovine serum-containing media was measured to determine the surface composition of the adsorbed protein layer. The

SDS elutability of each protein was measured to indirectly assess protein-substrate binding strength.

Significant differences in the composition of protein layers adsorbed to the binary SAM substrates were observed in response to SAM surface composition. The levels of Alb and Vn adsorbed to the binary SAMs were approximately equivalent and were significantly higher than Fn adsorption. Differences in adsorbed protein layer composition were due to differences in the relative affinity of Vn, Alb, and Fn for the binary SAM surfaces in response to variations in SAM surface composition. The competitive effectiveness of Vn for adsorption to the binary SAM surfaces was significantly higher than that of Fn or Alb.

The elutability of Alb, Fn, and Vn adsorbed to binary SAMs was measured after exposure to SDS. The elutability of Alb and Fn did not vary consistently with surface COOH content. Vn elutability on the COOH/CH_3 and COOH/OH SAMs increased gradually as surface COOH content increased from 20-50% COOH (COOH/OH SAMs) or 20-60% (COOH/CH_3 SAMs), and then leveled off or decreased slightly for higher surface COOH contents.

Relationships between cell growth and adsorbed protein layer characteristics were evaluated by comparing results of cell interaction studies (Chapter 6) with results obtained in protein interactions studies (Chapter 8). For the homogeneous SAMs (OH, COOH, and CH_3), the promotion of cell growth was associated with the surface fraction of adsorbed adhesive protein (vitronectin and fibronectin), the elutability of Vn, and the elutability of Alb. For the binary composition SAMs, both the surface fraction of adhesive protein and the elutability of Vn demonstrated similar trends in response to surface COOH content as did cell growth. For the binary composition SAMs, the trend in Alb elutability was not consistent with the trend observed in cell growth as a function of surface COOH content.

The strength and direction of correlations between adhesive protein surface fraction and normalized cell number, and Vn elutability and normalized cell number were evaluated for both binary SAM series. Adhesive protein surface fraction and Vn elutability was strongly correlated with cell growth for the COOH/CH_3 SAMs. For the COOH/OH SAMs, a moderate correlation was obtained between adhesive protein surface fraction and cell number while Vn elutability was strongly correlated with cell number. It was concluded that cell growth on binary composition, chemically heterogeneous SAMs is influenced by the surface fraction of adsorbed adhesive protein and the elutability of adsorbed Vn. Surfaces which were poor supports of cell growth demonstrated a lower surface fraction of adhesive protein and a lower Vn elutability than did surfaces which promoted cell growth.

The ultimate application of this research is to use information obtained to aid in the design of a vascular graft surface which supports endothelial cell adhesion, growth, and migration after implantation. We have identified several substrate properties and adsorbed protein layer properties which are associated with the promotion of endothelial cell growth. In this research, we have determined that the type and concentration of surface functional group can have a significant effect of endothelial cell growth. The spatial arrangement of surface functionalities can have a significant, short-term effect on cell growth however, the long-term effect is limited. Surface mobility appears to have a very limited effect on cell growth. These effects are mediated via the adsorbed protein layer. Adsorbed protein layer properties which are associated with the promotion of endothelial cell growth include the surface fraction of adsorbed Fn and Vn, and the elutability of vitronectin. It is hoped that the information gained through this research regarding factors which influence biologic processes will lead to strategies for designing materials and implant surfaces that guide a specific biologic response such as the promotion or inhibition of endothelial cell growth.

9.2 Recommendations for Future Work

Several interesting lines of research can be proposed to further test hypotheses which can be developed as a result of this research. First, while the OH, COOH, and CH_3 functionalities were primary the focus of this research, other biologically relevant functional groups should be evaluated with regard to their effects on cell growth. There is evidence which suggests that amine and sulfonate functionalities result in the promotion of cell growth [10,69] therefore, further studies of these groups may prove to be useful in identifying other growth-promoting functional groups.

In the investigation of the effect of surface mobility on cell growth, COOH groups were used as the terminal functionality on the short and long alkanethiol chains since it was anticipated that surface mobility would result in a decrease in cell growth. However, surface mobility resulted in an increase in cell number after a short culture period and had no effect after a longer culture period. The growth-promoting ability of the COOH group may have overwhelmed any effect surface mobility. To further evaluate the effect of surface mobility on cell growth, other functional groups which do not promote growth as well as the COOH group should be evaluated using the C_{10}/C_{16} binary SAM system.

In Chapter 8, a correlation between Vn elutability and cell growth was observed. As discussed in Chapter 8, it is possible that this finding may suggest that Vn or Fn adsorbed on growth-promoting surfaces differs conformationally from adhesive proteins adsorbed on surfaces which do not promote cell growth as well. We can hypothesize that adsorbed adhesive protein conformation and subsequently the accessibility/availability of the adhesive protein cell binding domain is affected by binary SAM surface chemistry. To test this hypothesis, the conformation of Fn and Vn adsorbed to binary SAMs can be investigated using a series of domain-specific monoclonal antibodies [123,124]. Underwood et al. demonstrated that using a panel of

monoclonal antibodies against Fn and Vn, including antibodies affecting biological activity, the conformational status of adsorbed protein can be determined and this information can be used to analyze the cell adhesive behavior of adsorbed proteins on different surfaces [123]. The effect of binary SAM surface chemistry on the conformational integrity of the Fn and Vn cell adhesion domains after adsorption to the SAM substrates from a complex biological mixture such as serum can be determined in this manner.

In the characterization of protein layers adsorbed to binary SAMs, a correlation between cell growth and the surface fraction of adsorbed adhesive protein was observed. As discussed in Chapter 8, it is possible that binary SAM surfaces with higher levels of adsorbed Vn may promote cell growth by influencing the secretion of cell-derived ECM proteins. To test the hypothesis that ECM production is influenced by adsorbed protein layer composition, the output of endogenous extracellular matrix molecules such as collagen, laminin, and fibronectin by endothelial cells cultured on binary SAMs could be measured. Underwood and Bennett evaluated the production of four ECM molecules, from bovine corneal endothelial cells cultured on different ECM substrates using a panel of monoclonal antibodies raised to native endothelial ECM. The effect of binary SAM surface chemistry on the production of ECM molecules from endothelial cells could be investigated in a similar manner.

Finally, the clinical goal of this research would be to use the information obtained regarding surface properties resulting in optimal endothelial cell growth to develop a vascular graft which would support an endothelial cell monolayer. To that end, it is important that endothelial cells growing on synthetic surfaces demonstrate characteristics or functions which are integral to the maintenance of a smooth, antithrombogenic surface. The morphology and function of an endothelial cell monolayer growing on a synthetic surface must be similar to that of the endothelium in the native vessel [125]. In

the native vessel, endothelial cells are not passive cells, rather they are metabolically active and interact with blood and tissues to control many processes. Therefore, the coverage of a synthetic vascular graft surface by endothelial cells is desirable if cells exhibit their normal antithrombotic properties including the production of heparin-like molecules, plasminogen activator, prostaglandins, and thrombomodulin [126-130]. Additionally, endothelial cell monolayers should not stimulate undesirable procoagulant activities such as production of coagulation components (i.e., tissue factor, factor V), the activation of procoagulant macromolecular complexes, or the production of adhesive cofactors (i.e., von Willebrand factor, thrombospondin) [131-138]. Therefore, future studies should include the characterization of endothelial cells growing on synthetic substrates developed using information gained in this research determine whether appropriate cell morphology and function are obtained.

BIBLIOGRAPHY

1. Chard, R.B.; Johnson, D.C..; Nunn, G.R.; Cartmill, T.B. *J. Thorac. Cardiovasc. Surg.* **1987**, *94(1)*, 132-134.
2. Zilla, P.; Fasol, R.; Deutsch, M.; Fischlein, T.; Minar, E.; Hammerle, A.; Krupicka, O.; Kadletz, M. *J. Vasc. Surg.* **1987**, *6(6)*, 535-541.
3. Ortenwall, P.; Wadenvick, H.; Kutti, J.; Risberg, B. *J. Vasc. Surg.* **1987**, *6(1)*, 17-25.
4. Graham, L.M.; Burkel, W.E.; Ford, J.W.; Vinter, D.W.; Kahn, R.H.; Stanley, J.C. *Surgery* **1982**, *91(5)*, 550-559.
5. Shindo, S.; Takagi, A.; Whittemore, A.D. *J. Vasc. Surg.* **1987**, *6(4)*, 325-332.
6. Joseph, J.; Sharma, C.P. *J. Biomed. Mater. Res.* **1986**, *20*, 677-682.
7. Fischer, A.M.; Mauzac, M.; Tapon-Bretaudiere, J.; Jozefonvicz, *J. Biomaterials* **1985**, *6*, 198-202.
8. van Wachem, P.B.; Beugeling, T.; Feijen, J.; Bantjes, A.; Detmers, J.P.; van Aken, W.G.*Biomaterials* **1985**, *6*, 403-408.
9. van Wachem, P.B.; Hogt, A.H.; Beugeling, T.; Feijen, J.; Bantjes, A.; Detmers, J.P.; van Aken, W.G. *Biomaterials* **1987**, *8*, 323-327.
10. Maroudas, N.G. *J. Cell. Physiol.* **1976**, *90*, 511-520.
11. Curtis, A.S.G.; Forrester, J.V.; McInnes, C.; Lawrie, F. *J. Cell Biol.* **1983**, *97*, 1500-1506.
12. van Wachem, P.B.; Vreriks, C.M.; Beugeling, T.; Feijen, J.; Bantjes, A.; Detmers, J.P.; van Aken, W.G. *J. Biomed. Mater. Res.* **1987**, *21*, 701-713.
13. Kaehler, J.; Zilla, P.; Fasol, R.; Deutsch, M.; Kadletz, M. *J. Vasc. Surg.* **1989**, *9(4)*, 535-541.

14. Horbett, T.A. In *Biomaterials: Interfacial Phenomena and Applications*; Cooper, S.L., Peppas, N.A., Eds.; ACS Symposium Series No. 199; American Chemical Society: Washington, DC, 1982; p 233.

15. Grinnell, F. In *Biocompatible Polymers, Metals and Composites*; Szycher, M., Ed.; Technomic Publishing Co.: Lancaster, 1983; p 674.

16. Lindon, J.N.; McManama, G.; Kushner, L.; Merrill, E.W. Saltzman, E.W.; *Blood* **1986**, *68*(2), 355-362.

17. Horbett, T.A. *J. Biomed. Mater. Res.* **1981**, *15*, 673-695.

18. Uniyal, S.; Brash, J.L. *Thromb. Haemostasis* **1982**, *47(3)*, 285-290.

19. Horbett, T.A. *Colloids Surf. B: Biointerfaces* **1994**, *2*, 225-240.

20. Steele, J.G.; Johnson, G.; Underwood, P.A. *J. Biomed. Mater. Res.* **1992**, *26*, 861-884.

21. Steele, J.G.; Dalton, B.A.; Johnson, G.; Underwood, P.A. *J. Biomed. Mater. Res.* **1993**, *27*, 927-940.

22. Ertel, S.I.; Chilkoti, A.; Horbett, T.A.; Ratner, B.D. *J. Biomater. Sci., Polym. Edn.* **1991**, *3*, 163-183.

23. Horbett, T.A.; Klumb, L.A. In *Interfacial Phenomena and Bioproducts*; Brash, J.L., Wojciechowski, P.W., Eds.; Marcel Dekker: New York, 1996; p. 351.

24. Ertel, S.I.; Ratner, B.D.; Horbett, T.A. *J. Biomed. Mater. Res.* **1990**, *24*, 1637-1659.

25. Ertel, S.I.; Ratner, B.D.; Horbett, T.A. *J. Colloid Interface Sci.* **1991**, *147*, 433-442.

26. Shivakumar, K.; Renuka Nair, R.R.; Jayakrishnan, A.; Thanoo, B.C.; Kartha, C.C. *In Vitro Cell. Dev. Biol.* **1989**, *25(4)*, 353-357.

27. Ramsey, W.S.; Hertl, W.; Nowlan, E.D.; Bimkowski, N.J. *In Vitro* **1984**, 20(10), 802-808.

28. McAuslan, B.R.; Johnson, G. *J. Biomed. Mater. Res.* **1987**, *21*, 921-935.

29. Brandley, B.K.; Weisz, O.A.; Schnarr, R.L. *J. Biol. Chem.* **1987**, *262(13)*, 6431-6437.

30. Lopez, G.P.; Albers, M.W.; Schrieber, S.L.; Carroll, R.; Peralta, E.; Whitesides, G.M. *J. Am. Chem. Soc.* **1993**, *115*, 5877-5878.

31. Prime, K.L.; Whitesides, G.M. *Science* **1991**, *252*, 1164-1167.

32. Wojciechowski, P.W.; Brash, J.L. *Coll. Surf. B: Biointerfaces* **1993**, *1*, 107-117.

33. Andrade, J.D. In *Polymer Surface Dynamics*; Andrade, J.D., Ed.; Plenum Press, New York, NY, **1988**; Vol. 1.

34. Barenberg, S.A.; Schultz, J.S.; Anderson, J.M.; Geil, P.H. *Trans. Am. Soc. Artif. Int. Organs* **1979**, *25*, 159-166.

35. Merrill, E.W. *Ann. N. Y. Acad. Sci.* **1977**, *282*, 6-16.

36. Reichert, W.M.; Filisko, F.E.; Barenberg, S.A. *J. Biomed. Mater. Res.* **1982**, *16*, 301-312.

37. Maroudas, N.G. *Nature* **1973**, *244*, 353-354.

38. Maroudas, N.G. *J. Theor. Biol.* **1979**, *79*, 101-116.

39. Horbett, T.A.; Schway, M.B.; Ratner, B.D. *J. Colloid Interface Sci.* **1985**, *104(1)*, 28-39.

40. Merrill, E.W.; *J. Biomater. Sci. Polymer. Edn.* **1993**, *5(1/2)*, 1-11.

41. Nagaoka, S.; Mori ,Y.; Takiuchi, H.; Yokota, K.; Tanzawa, H.; Nishiumi, S. *ACS Polym. Prepr.* **1983**, *24(1)*, 67-68.

42. Yeh, Y.S.; Iriyama, Y; Matsuzawa, Y; Hanson, S.R.; Yasuda, H. *J. Biomed. Mater. Res.* **1988**, *22*, 795-818.

43. Van Damme, H.S.; Beugeling, T; Ratering, M.T.; Feijen, J. *J. Biomater. Sci. Polymer. Edn.* **1991**, *3(1)*, 69-84.

44. Lopez, G.P.; Ratner, B.D.; Rapoza, R.J.; Horbett, T.A. *Macromolecules* **1993**, *26*, 3247-3253.

45. Andrade, J.D.; Chen, W.Y. *Surf. Interface Anal.* **1986**, *8*, 253-256.

46. Andrade, J.D.; Smith, L.M.; Gregonis, D.E. In *Surface and Interfacial Aspects of Biomedical Polymers, Surface Chemistry and Physics*; Andrade, J.D., Ed.; Plenum Press, New York, **1985**; Vol. 1, 249-292.

47. Chen, Y.L.; Helm, C.A.; Israelachivili, J.N. *J. Phys. Chem.*

48. Yokota, K.; Abe, A.; Hosaka, S.; Sakai, I.; Saito, H. *Macromolecules* **1978**, *11(1)*, 95-100.

49. Chilkoti, A.; Lopez, G.P.; Ratner, B.D.; Hearn, M.J.; Briggs, D. *Macromolecules* **1993**, *26*, 4825-4832.

50. B.D. Ratner, In *A Surface Analysis Facility for Biomedical Problems*, Competitive Renewal Application to the NIH, **1992**.

51. Horbett, T.A.; Schway, M.B. *J. Biomed. Mater. Res.* **1988**, *22*, 763-793.

52. Bentley, K.L.; Klebe, R.J. *J. Biomed. Mater. Res.* **1985**, *19*, 757-769.

53. Grinnell, F.; Feld, M.K. *J. Biol. Chem.* **1982**, 257, 4888-4893.

54. van Wachem, P.B.; Mallens, B.W.L.; Dekker, A.; Beugeling, T.; Feijen, J.; Bantjes, A.; Detmers, J.P.; van Aken, W.G. *J. Biomed. Mater. Res.* **1987**, *21*, 1317-1327.

55. Steele, J.G.; Johnson, G.; McFarland, C.; Dalton, B.A.; Gengenbach, T.R.; Chatelier, R.C.; Underwood, P.A.; Griesser, H.J. *J. Biomater. Sci., Polym. Edn.* **1994**, *6(6)*, 511-532.

56. van Wachem, P.B.; Beugeling, T.; Mallens, B.W.L.; Dekker, A.; Feijen, J.; Bantjes, A.; van Aken, W.G. *Biomaterials* **1988**, *9*, 121-123.

57. Gospodarowicz, D.; Greenburg, G.; Birdwell, C.R. *Cancer Res.* **1978**, *38*, 4155-4171.

58. Steele, J.G.; Johnson, G.; Norris, W.D.; Underwood, P.A. *Biomaterials* **1991**, *12*, 531-539.

59. Chinn, J.A.; Horbett, T.A.; Ratner, B.D.; Schway, M.B.; Haque, Y. *J.Colloid Interface Sci.* **1989**, *127(1)*, 67-87.

60. Pettit, D.K.; Horbett, T.A.; Hoffman, A.S. *J. Biomed. Mater. Res.* **1992**, *26*, 1259-1275.

61. Tamada, Y.; Ikada, Y. *J. Biomed. Mater. Res.* **1994**, *28(7)*, 783-789.

62. Fabrizius-Homan, D.J.; Cooper, S.L. *J. Biomed. Mater. Res.* **1991**, *25*, 953-971.

63. Johnson, S.D.; Anderson, J.M.; Marchant, R.E. *J. Biomed. Mater. Res.* **1992**, *26*, 915-935.

64. Grinnell, F.; Feld, M.K.; *J. Biomed. Mater. Res.* **1981**, *15(3)*, 363-381.

65. Nuzzo, R.G.; Dubois, L.H.; Allara, D.L. *J. Am. Chem. Soc.* **1990**, *112*, 558-569.

66. Dubois, L.H.; Nuzzo, R.G. *Annu. Rev. Phys. Chem.* **1992**, *43*, 437-463.

67. Bain, C.D.; Whitesides, G.W. *J. Am. Chem. Soc.* **1989**, *111*, 7164-7175.

68. Lewandowska, K.; Pergament, E.; Sukenik, C.N.; Culp, L.A. *J. Biomed. Mater. Res.* **1992**, *26*, 1343.

69. Stenger, D.A.; Georger, J.H.; Dulcey, C.S.; Hickman, J.J.; Rudolph, A.S.; Nielsen, T.B.; McCort, S.M.; Calvert, J.M. *J. Am. Chem. Soc.* **1992**, *114 (22)*, 8435-8442.

70. Stenger, D.A.; Pike, C.J.; Hickman, J.J.; Cotman, C.W. *Brain Res.* **1993**, *630*, 136-147.

71. DiMilla, P.A.; Folkers, J.P.; Biebuyck, H.A.; Harter, R.; Lopez, G.P.; Whitesides, G.P. *J. Am. Chem. Soc.* **1994**, *116*, 2225-2226.

72. Bain, C.D. Ph.D. Thesis, Harvard University, 1988.

73. Allara, D.L.; Nuzzo, R.G. *Langmuir* **1985**, *1*, 45-52.

74. Porter, M.D.; Bright, T.B.; Allara, D.L.; Chidsey, C.E.D. *J. Am. Chem. Soc.* **1987**, *109*, 3559-3568.

75. Bain, C.D.; Troughton, E.B.; Tao, Y.T.; Evall. J.; Whitesides, G.M.; Nuzzo, R.G. *J. Am. Chem. Soc.* **1989**, *111(1)*, 321-335.

76. Dilks, A; In *Electron Spectroscopy: Theory, Techniques, and Applications*; Baker, A.D., Brindle, C.R., Eds.; Academic Press, London, **1981**; Vol. 4, 277-359.

77. Kenny, G.E. In *Infectionen durch mycoplasmatales*; Gylstroff, I., Ed.; V.E.B. Gustav Fischer: Jena, 1985; p 220.

78. Jaffe, E.A.; Hayer, L.W.; Nachman, R.L. *J. Clin. Inves.* **1973**, *52(11)*, 2757-2764.

79. Voyta, J.C..; Via, D.P.; Butterfield, C.E.; Zetter, B.R. *J. Cell Biol.***1984**, *99(6)*, 2034-2040.

80. Berridge, M.V.; Tan, A.S.; McCoy, K.D.; Wang, R. *Biochemica* **1996**, *4*, 14-19.

81. MacFarlane, A. *Nature* **1959**, *182*, 53.

82. Helmkamp, R.W.; Goodland, R.L.; Bale, W.F.; Spar, I.L.: Mutschler, L.E. *Cancer Res.* **1960**, *20*, 1495-1500.

83. Konstadinidis, K.; Zhang, P.; Opila, R.L.; Allara, D.L. *Surf. Sci.* **1995**, *338*, 300-312.

84. Troughton, E.B.; Bain, C.D.; Whitesides, G.M.; Nuzzo, R.G.; Allara, D.L.; Porter, M.D. *Langmuir* **1988**, *4*, 365-385.

85. Vogler, E.A.; Bussian, R.W. *J. Biomed. Mater. Res.* **1987**, *21*, 1197-1211.

86. Steele, J.G.; Dalton, B.A.; Johnson, G.; Underwood, P.A. *Biomaterials* **1995**, *16(14)*, 1057-1067.

87. Bohnert, J.L.; Horbett, T.A. *J. Colloid Interface Sci.* **1986**, *111(2)*, 363-377.

88. Jozefonvicz, J.; Jozefowicz, M. *J. Biomater. Sci., Polm. Edn.* **1990**, *1(3),* 147-165.

89. Bain, C.D.; Evall, J; Whitesides, G.M. *J. Am. Chem. Soc.* **1989**, *111,* 7155-7164.

90. Bain, C.D.; Whitesides, G.M. *J. Am. Chem. Soc.* **1988**, 110, 6560-6561.

91. Cassie, A.B.D. *Discuss. Faraday Soc.* **1948**, 3, 11-16.

92. Bain, C.D.; Whitesides, G.M. *Angew. Chem.* **1989**, 101, 522-528.

93. Atre, S.V.; Liedberg, B., Allara, D.L. *Langmuir* **1995**, *11*, 3882-3893

94. Stranik, S.J.; Parikh, A.N.; Allara, D.L.; Weiss, P.S. *J. Phys. Chem.* **1994**, *98*, 11136.

95. Atre, S.V.; Ph.D. Thesis, Dept. of Chemistry, Pennsylvania State University, **1995**.

96. Canry, J.-C.; Vickerman, J.C. *Proceedings of ECASIA* **1995**.

97. Offord, D.A.; John, C.M.; Lindford, M.R.; Griffin, J.H. *Langmuir* **1994**, *10*, 883-889.

98. Knox, P. *J. Cell Sci.* **1984**, *71*, 51.

99. Underwood, P.A.; Bennett, F.A. *J. Cell Sci.* **1989**, *93*, 641.

100. Bale, M.D.; Wohlfahrt, L.A.; Mosher, D.F.; Tomasini, B.; Sutton, R.C. *Blood* **1989**, *74(8),* 2698-2706.

101. Shaffer, M.C.; Foley, T.P.; Barnes, D.W. *J. Lab. Clin. Med.* **1984**, *103*, 783-91.

102. Preissner, K.T.; Wassmuth, R.; Muller-Berghaus, G. *Biochem. J.* **1985**, *231*, 349-55.

103. Grinnel, F. Ann. *NY Acad. Sci.* **1987**, *516*, 280.

104. Hayman, E.G.; Pierschbacher, M.D.; Suzuki, S.; Ruoslahti, E. *Exp. Cell. Res.* **1985**, *160*, 245.

105. Horbett, T.A.; Brash, J.L. In *Proteins at Interfaces: Physicochemical and Biochemical Studies*; Brash, J.L., Horbett, T.A. Eds.; ACS Symposium Series No. 343; American Chemical Society: Washington, DC, 1987; p 1.

106. Horbett, T.A.; Ratner, B.D.; Schakenraad, J.M.; Schoen, F.J. In *Biomaterials Science*, Academic Press, 1996, p. 133.

107. Norde, W.; Lyklema, J. *J. Biomater.Sci. Polym. Edn.* **1991**, *2*, 183.

108. Dejana, E.; Colella, S.; Conforti, G.; Abbadini, M.; Gaboli, M.; Marchisio, P.C.*J. Cell Bio.* **1988**, *107*, 1215-1223.

109. Preissner, K.T.; Jenne, D. *Thromb. Haemostasis* **1991**, *66(1)*, 123-132.

110. Ruoslahti, E.; Pierschbacher, M.D. *Science*, **1987**, *238*, 491-97.

111. Edwards, J.C.; Robson, R.T.; Campbell, G. *J. Cell. Sci.* **1987**, *87*, 657-65.

112. Gospodarowicz, D.; Delgado, D.; Vlodavsky, I. *Proc. Natl. Acad. Sci. USA* **1980**, *71*, 4094-4098.

113. Gospodarowicz, D.; In *Biochemical Interactions at the Endothelium*, Cryer, A. Ed.; Elsevier, Amsterdam/NY, 1983; p. 363-403.

114. Sawada, H.; Furthmayr, H. *Exp. Cell. Res.* **1987**, *171*, 94-109.

115. Underwood, P.; Bennett, F. *Exp. Cell. Res.* **1993**, *205*, 311-319.

116. Gospodarowicz, D.; Lui, G.-M. *J. Cell. Physio.* **1981**, *109*, 69-81.

117. Ertel, S.I. Ph.D. Thesis, Dept. of Chemical Engineering, University of Washington, **1990**.

118. Rapoza, R.J.; Ph.D. Thesis, Dept. of Chemical Engineering, University of Washington, **1989**.

119. Ruoslahti, E.; Pierschbacher, M.D. *Cell* **1986**, *44*, 517-518.

120. Tomasini, B.R.; Mosher, D.F. *Blood* **1988**, *72*, 903-912.

121. Preissner, K.T. *Annu. Rev. Cell Biol.* **1991**, *7*, 275-310.

122. Preissner, K.T.; Grulich-Hemm, J.; Ehrlich, H.J.; Dederck, P.; Justus, C.; Collen, D.; Pannekoek, H.; Muller-Berghaus, G. *J. Biol. Chem.* **1990**, *265*, 3543-3548.

123. Underwood, P.A.: Steele, J.C.; Dalton, B.A. *J. Cell Sci.* **1993**, *104*, 793-803.

124. Underwood, P.A. *J. Immunol. Methods* **1990**, *127*, 91-101.

125. Jarrell, B.E.; Williams, S.K.; Hoch, J.R.; Carabasi, R.A. *Bull. N.Y. Acad. Med.* **1987**, *63 (2)*, 156-167.

126. Esmon, C.T.; Owen, W.G. *Proc. Natl. Acad. Sci. USA* **1981**, *78*, 2249-52.

127. Levine, E.G.; Loskutoff, D.J. *J. Cell Biol.* **1982**, *94*, 631-36.

128. Rosenberg, R.D.; Rosenberg, J.S.*J. Clin. Invest.* **1984**, *74*, 1-5.

129. Wesksler, B.B.; Marcus, A.J.; Jaffe, E.A. *Proc. Natl. Acad. Sci. USA* **1977**, *74*, 3922-26.

130. Kisiel, W.; Canfield, W.M.; Ericsson, L.H.: Davie, E.W. *Biochem.* **1977**, *16*, 5824-31.

131. Grinnell, F.; Billingham, R.E., Burgess, L. *J. Invest. Dermatol.* **1981**, *76*, 181-189.

132. Clark, R.A.F.; Dvorak, H.F.; Colvin, R.B.*J. Immunol.* **1981**, *126*, 787-93.

133. Johnsen, U.L.; Lyberg, H.T.; Galdal, K.S.; Prydz. H. *Thromb. Haemostas.* **1983**, *49*, 69-72.

134. Wagner, D.D.; Marder, V.J. *J. Biol. Chem.* **1983**, *258*, 2065-67.

135. Mosher, D.F.; Doyle, H.F.; Colvin, R.B. *J. Immunol.* **1981**, *126*, 787-93.

136. Brox, J.H.; Osterud, B.; Bjoklid, E.; Fenton, H.J. *Hemotology* **1984**, *57*, 239-46.

137. Cerveny, T.J.; Fass, D.N.; Mann, K.J. *Blood* **1984**, *63*, 1467-74.

138. Lynch, D.C.; Williams, R.; Zimmerman, T.S.; Kirby, E.P.; Livingston, D.M. *Proc. Natl. Acad. Sci. USA* **1983**, *80*, 2738-42.

VITA

Caren Diana Tidwell

University Of Washington

1999

Education

1999 Doctor of Philosophy, Department of Bioengineering, University of Washington, Seattle, Washington

1990 Master of Science in Engineering, Department of Bioengineering, University of Washington, Seattle, Washington

1982 Bachelor of Science in Engineering, Department of Chemical Engineering, University of California at Los Angeles, Los Angeles, California

1979 Associate in Arts, Orange Coast College, Costa Mesa, California

Professional Experience

1991-1992 Research Scientist, Department of Bioengineering, University of Washington

1982-1988 Senior Project Engineer, Cardiovascular Device Division, Shiley Inc., Irvine, California

Patents

"Surface-Modified Self-Passivating Intraocular Lenses," B.D. Ratner and C.L. Tidwell, submitted Mar. 25, 1991, allowed Dec. 15, 1992, U.S. Patent # 5,171,267.

Awards and Fellowships

Battelle Pacific Northwest Laboratory Energy Research Fellowship, 1994-1995.

NIH Cardiovascular Training Grant Fellowship, 1997-1998.

Society of Women Engineers, Department of Bioengineering, Graduate Student of the Year Award, 1998.

Publications

C.D. Tidwell, S.I. Ertel, B.D. Ratner, B. Tarasevich, S. Atre, and D. Allara, "Endothelial Cell Growth and Protein Adsorption on Terminally-Functionalized, Self-Assembled Monolayers of Alkanethiolates on Gold," Langmuir, 1997, 13, 3404-3413 (1997).

B.D. Ratner, T. Boland, E.E. Johnston, C.D. Tidwell, "Engineering Biomaterials that Exhibit Recognition and Specificity," In: Thin Films and Surfaces for Bioactivity and Biomedical Applications, (Eds.: C.M. Cotell, S.M. Gorbatkin, G. Gorbe, A.E. Meyer), Materials Research Society, Philadelphia, PA (1996).

B.D. Ratner, C.D. Tidwell, D.G. Castner, S. Golledge, K. Meyer, B. Hagenhoff, A. Benninghoven, "TOF-SIMS Studies of Adsorbed Protein Films," ACS Polym. Prepr. 37(1), 843-844 (1996).

G.P. Lopez, B.D. Ratner, C.D. Tidwell, C.L. Haycox, R.J. Rapoza, and T.A. Horbett, "Glow discharge plasma deposition of tetraethylene glycol dimethyl ether for fouling-resistant biomaterial surfaces," J. Biomed. Mater. Res. 26(4), 415-439 (1992).

C.D. Tidwell, "Development of a Surface-Modified, Self-Passivating IOL," M.S.E. Thesis, Univ. of Washington, (1990).

Abstracts

B.D. Ratner and C.D. Tidwell, "Effect of Surface Mobility on Biointeractions," pg. 143, Abstracts of the American Vacuum Society: 41st National Symposium, Denver, CO, October 24-28, 1994.

B.D. Ratner, D. Leach-Scampavia, C.D. Tidwell, T. Boland and P. Yang, "Surface Studies of Filled Silicone Elastomers," 41st National Symposium of the American Vacuum Society and NANO 3: Third International Conference on Nanometer-Scale Science and Technology, October 24-28, 1994.

B.D. Ratner, D.G. Castner, C.D. Tidwell, K. Meyer, B. Hagenhoff, and A. Benninghoven, "TOF-SIMS Studies of Adsorbed Protein Films on Metal and Fluoropolymer Surfaces," Society for Biomaterials, 21st Annual Meeting, San Francisco, CA, March 18-22, 1995.

B.D. Ratner, T. Boland, E. Johnston, and C. Tidwell, "Novel Organic-Metal Interfaces: Structures and Chemistries," Materials Research Society, San Francisco, April 17-21, 1995.

D. G. Castner, C. D. Tidwell, B. D. Ratner, K. Meyer, A. Benninghoven, "ToF Studies of Adsorbed Protein Films" 42nd National Symposium of the American Vacuum Society, Minneapolis, MN, October 1995.

B. D. Ratner, C.D. Tidwell, B. Tarasevich, and D.L. Allara, "Order and Disorder in Polymeric and Organic Surfaces: Influence on Cell and Protein Interactions," American Chemical Society, International Chemical Congress of Pacific Basin Societies, Honolulu, HI, December 17-22, 1995.

C.D. Tidwell, B.D. Ratner, B. Tarasevich, S. Atre, and D.L. Allara, "Endothelial Cell Growth and Serum Protein Adsorption: Effect of Surface Chemistry as Assessed with Self-Assembled Monolayers," Volume I, pg. 24, Society for Biomaterials, Fifth World Biomaterials Congress, May 29-June 2, 1996, Toronto, Canada.

B.D. Ratner, C.D. Tidwell, K. Meyer, D.G. Castner, S. Golledge, B. Hagenhoff, and A. Benninghoven, "Adsorbed Protein Configuration and Orientation Probed by ESCA and TOF-SIMS," Volume I, pg. 577, Society for Biomaterials, Fifth World Biomaterials Congress, May 29-June 2, 1996, Toronto, Canada.

S.L. Golledge, B.D. Ratner, D.G. Castner, M.D. Garrison, C.D. Tidwell, and A.M. Belu, "Influence of Self-Assembled Monolayer Defect Structure on Cell Growth," 43rd National Symposium of the American Vacuum Society, Philadelphia, PA, October 14-18, 1996.

C.D. Tidwell, A.M. Belu, B. Tarasevich, D.L. Allara, and B.D. Ratner, "Endothelial Cell Interactions with Model Surfaces: Effect of Surface Chemistry and the Adsorbed Protein Layer, " 43rd National Symposium of the American Vacuum Society, Philadelphia, PA, October 14-18, 1996.

A.M. Belu, C.D. Tidwell, B. Tarasevich, D.L. Allara, and B.D. Ratner, "Surface Characterization of Terminally Functionalized Alkanethiol Self-Assembled Monolayers and Mixtures," 43rd National Symposium of the American Vacuum Society, Philadelphia, PA, October 14-18, 1996.

D.G. Castner, C.D. Tidwell, B.D. Ratner, M-W. Tsao, and J.F. Rabolt, "Protein Adsorption and Cell Growth on Fluorocarbon Surfaces," The Division of Polymer Chemistry, American Chemical Society, Workshop: Molecular Engineering of Polymers: Directing Biological Response, Santa Barbara, CA, November 22-24, 1996.

B.J. Tarasevich, C.D. Tidwell, B.D. Ratner and D.L. Allara, "Endothelial Cell Growth and Protein Adsorption onto Model Self-Assembled Surfaces," 1996 Fall Meeting of the Materials Research Society, Boston, MA, December 1996.

C.D. Tidwell, A.M. Belu, B.D. Ratner, B. Tarasevich, S. Atre, and D.L. Allara, "Endothelial Cell Growth on Binary Composition Self-assembled Monolayers: Effect of Surface Chemistry and the Adsorbed Protein Layer, 23rd Annual Meeting of the Society for Biomaterials, New Orleans, Louisiana, April 30-May 4, 1997.

D.G. Castner, C.D. Tidwell, B.D. Ratner, M-W. Tsao, and J.F. Rabolt, "The Effect of Fluorocarbon Surface Structure on Endothelial Cell Growth," 23rd Annual Meeting of the Society for Biomaterials, New Orleans, Louisiana, April 30-May 4, 1997.

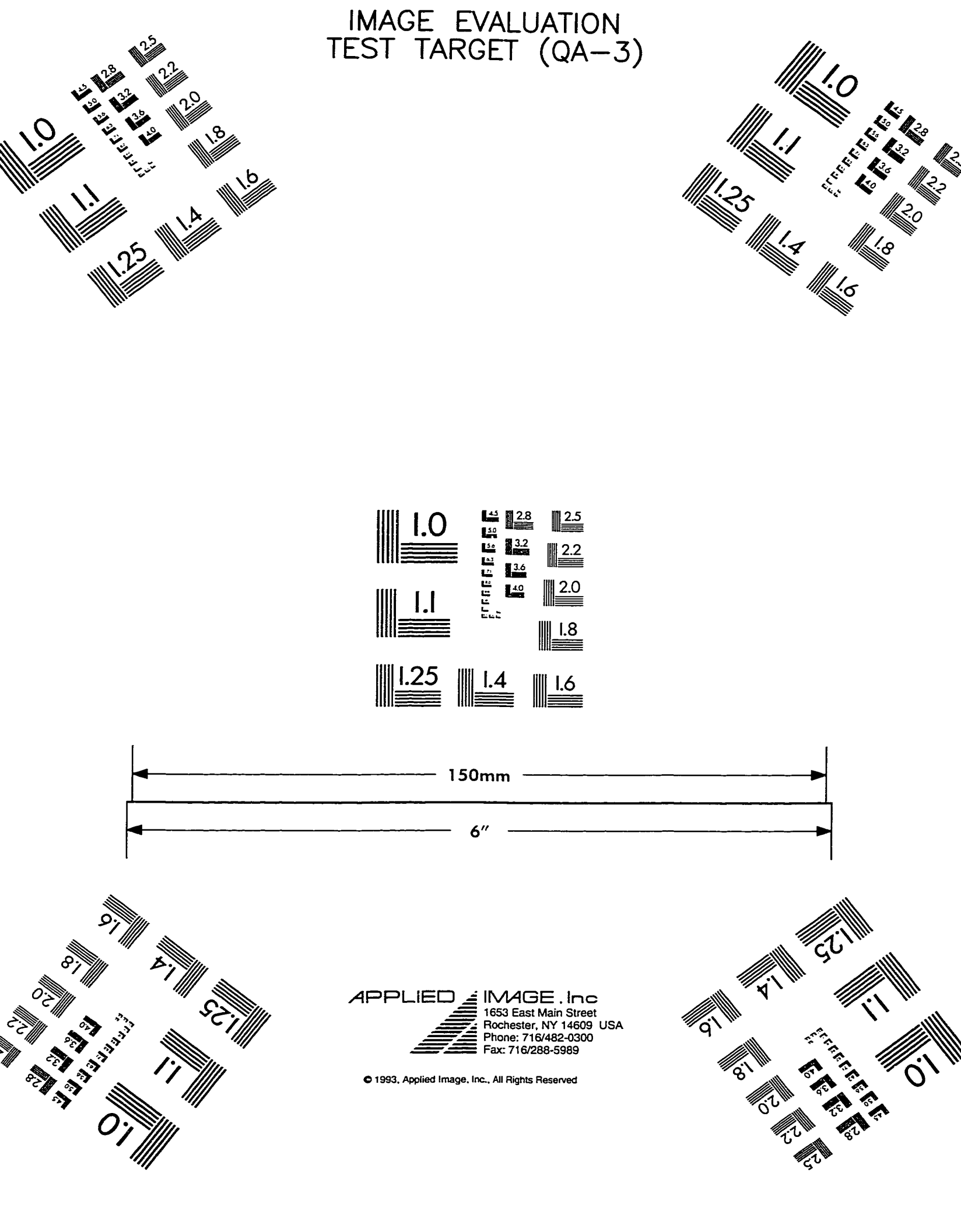
IMAGE EVALUATION
TEST TARGET (QA-3)
1.0
1.1
1.25
1.4
1.6
2.8
2.5
3.2
2.2
3.6
2.0
4.0
1.8
150mm
6"
APPLIED IMAGE, Inc
1653 East Main Street
Rochester, NY 14609 USA
Phone: 716/482-0300
Fax: 716/288-5989
© 1993, Applied Image, Inc., All Rights Reserved